Tumour targeting with macrocyde conjugates

Fiona Calder Smith

Tumour Targeting with Macrocycle Conjugates

by

Fiona Calder Smith B.Sc. (Hons.)

University of Durham

Department of Chemistry

A Thesis submitted for the degree of Doctor of Philosophy

April 1995

STATEMENT OF COPYRIGHT

DECLARATION

The work described in this thesis was carried out in the Department of Chemistry at the University of Durham between October 1991 and September 1994. All the work is my own, unless stated to the contrary, and it has not been submitted previously for a degree at this or any other University.

To my parents

and

Adrian

But Mousie, thou art no thy lane,

In proving foresight may be vain;

The best-laid schemes o'mice an' men

Gang aft agley,

An' lea'a us nought but grief an' pain,

For promis'd joy!

from 'To a Mouse' by Robert Burns

ACKNOWLEDGEMENTS

I would like to thank my supervisor Prof. David Parker for his encouragement, support and enthusiasm throughout this project. I am indebted to Alice Harrison and Louise Royle from the Radiobiology Unit at Harwell and those at Celltech and The Royal Marsden Hospital for conducting the biodistribution studies and Andrei Batsanov for the crystal structure. I would also like to thank the North of England Cancer Research Campaign for their financial support.

There are many others to whom I am grateful for help and friendship during my time in the chemistry department. Lenny Lauchlan for helping with HPLC, Mike Jones and Lara Turner for mass spectrometry, (and VG and the Swansea Mass Spectrometry Service for helping out when things got too much), Julia Say, Alan Kenwright and Ray Matthews for help with NMR, all the technical staff, Hazel, Jean and Maureen for looking after us on the day shift and Clarence, Eddy and the boys for looking after us on the night shift. A special thank you to all the boys and girls in and around lab 27, past, present and future, it's been a lot of fun. Last, but by no means least, thanks to Adrian.

ABSTRACT

TUMOUR TARGETING WITH MACROCYCLE CONJUGATES

Complexes of the radionuclides ^{67}Ga and ^{111}In, or of the paramagnetic contrast agent Gd, used in MRI, provide a means of imaging tumours. The stability of the ^{71}Ga-NOTA complex was verified by *in vivo* NMR spectroscopy. The novel phosphinic acid NOTA analogue, bearing an isopropyl substituent on phosphorus was prepared and its lipophilicity and ^{111}In biodistribution in mice determined. The crystal structure of the yttrium complex of N,N''-bis(benzylcarbamoylmethyl)diethylenetriamine-N,N',N''-triacetic acid revealed amide carbonyl ligation in a distorted mono-capped square antiprismatic structure, with one metal-bound water. The biodistribution of the analogous Gd complex was examined.

A novel series of 9N3 based ligands incorporating three further N donor atoms, carboxymethyl groups and a potentially larger cavity size were synthesised. The analogous series containing phosphinic acid groups and the 12N3 counterparts were also prepared. The former series formed complexes with Gd and the biodistribution in mice was studied. The 12N3 analogues failed to form Gd complexes.

2-Nitroimidazoles are known to selectively target hypoxic tumour tissue. Two conjugates of 2-nitroimidazole for tumour imaging were prepared, the Gd complex of a DTPA-bis(2-nitroimidazole) amide and the ^{111}In complex of a C-functionalised NOTA-nitroimidazole conjugate. The biodistribution in mice of each was studied and luminescence experiments on the Tb complex of the former revealed one metal bound water molecule.

Novel conjugates of the tetrapeptide tuftsin and a complexing agent based on the 12N4 skeleton and an N-linked NOTA derivative were synthesised. Biodistributions of the Gd and In complexes respectively are being carried out.

Acridine intercalators reversibly bind DNA, possibly enhancing the effectiveness of tumour targeting conjugates. Novel multifunctionally labelled acridines based on tris(2-aminoethyl) amine were sought. The p-nitrophenolate active ester of 9-acridine carbamoyl-2-(2-aminoethyl)-2-methyl amine was also prepared as a versatile agent for acridine labelling.

Fiona Calder Smith (April 1995)

GLOSSARY

BOPTA	Benzyloxypropionic tetraacetic acid
CT	X-ray Computerised Tomography
DCC	Dicyclohexylcarbodiimide
DCI	Desorption Chemical Ionisation
DCU	Dicyclohexylurea
DMAP	N,N-Dimethylaminopyridine
DMF	N,N-Dimethylformamide
DOTA	1,4,7,10-Tetraazacyclododecane-N,N',N'',N'''-tetraacetic acid
DPPA	Diphenylphosphoryl azide
DTPA	Diethylenetriaminepentaacetic acid
EDTA	Ethylenediaminetetraacetic acid
EOBDTPA	3,6,9-Triaza-3,6,9-tris(carboxymethyl)-4-(-ethoxybenzyl)-undecandicarboxylic acid
FAB	Fast Atom Bombardment
Fab	Fragment Antigen Binding
FTIR	Fourier Transform Infra-Red
FTNMR	Fourier Transform Nuclear Magnetic Resonance Spectroscopy
HBED	N,N'-Bis(2-hydroxybenzyl)ethylenediamine-N,N'-diacetic acid
HPLC	High Performance Liquid Chromatography
HT29	Human Colorectal Tumour
HX118	Malignant Melanoma Tumour
IgG	Immunoglobulin
IR	Infra-Red
m.p.	Melting Point
MRC	Medical Research Council
MRI	Magnetic Resonance Imaging
2-Nim	2-Nitroimidazole
NMR	Nuclear Magnetic Resonance
9N3	1,4,7-Triazacyclononane
12N3	1,5,9-Triazacyclododecane
12N4	1,4,7,10-Tetraazacylododecane
14N4	1,4,8,11-Tetraazacycltetradecane (CYCLAM)
NOTA	1,4,7-Triazacyclononane-1,4,7-triyltriacetic acid
NOTPMe	1,4,7-Triazacyclononane N,N',N'' tris[methylene(methylphosphinic)] acid
NOTPPh	1,4,7-Triazacyclononane N,N',N'' tris[methylene(phenylphosphinic)] acid

NOTPPri	1,4,7-Triazacyclononane N,N',N'' tris [methylene (isopropylphosphinic)] acid
NOTPBz	1,4,7-Triazacyclononane N,N',N'' tris[methylene(benzylphosphinic)] acid
NOTAMe	1,4,7-Tris(2'-methylcarboxymethyl)-triazacyclononane
NOTAPh	1,4,7-Tris(2'-phenylcarboxymethyl)-triazacyclononane
NOE	Nuclear Overhauser Effect
PBOP	Benzotriazol-1-yloxy-tripyrrolidinophosphonium hexafluorophosphate
PBS	Phosphate Buffered Saline
PET	Positron Emission Tomography
PLC	Preparative Thin Layer Chromatography
PLED	N,N'-Bis(2-hydroxypyridyl)ethylenediamine-N,N'-diacetic acid
R.T.	Room Temperature
SPECT	Single Photon Emission Computerised Tomography
TFA	Trifluoroacetic acid
Tf	Triflate
THF	Tetrahydrofuran
TLC	Thin Layer Chromatography
tms	Tetramethylsilane

CONTENTS ..... **page**

CHAPTER 1: INTRODUCTION

CHAPTER 2: SYNTHESIS, STRUCTURE AND BIODISTRIBUTION OF SIMPLE COMPLEXES OF Ga, In, Gd and Y

CHAPTER 3: NITROIMIDAZOLE CONJUGATES

CHAPTER 4: TUFTSIN CONJUGATES

CHAPTER 5: ACRIDINE CONJUGATES

CHAPTER 6: EXPERIMENTAL

Chapter One

Introduction

1.1 CANCER

1.1.1 INCIDENCE OF CANCER

Almost all multicellular organisms can be affected by cancer.[1] Palaeopathologists have found cancerous lesions in dinosaur bones and Egyptians wrote about human cancers in hieroglyphics on papyrus dated earlier than 1600 B.C.,[2] but it is only in this century that the general population have become acutely aware of its significance. Today in the developed world cancer accounts for one death in every five and one person in three is likely to contract the disease.

FIGURE 1.1 *Mortality Rate in the United Kingdom 1985-89[3]; Age-standardised death rate based on the world standard.[4]*

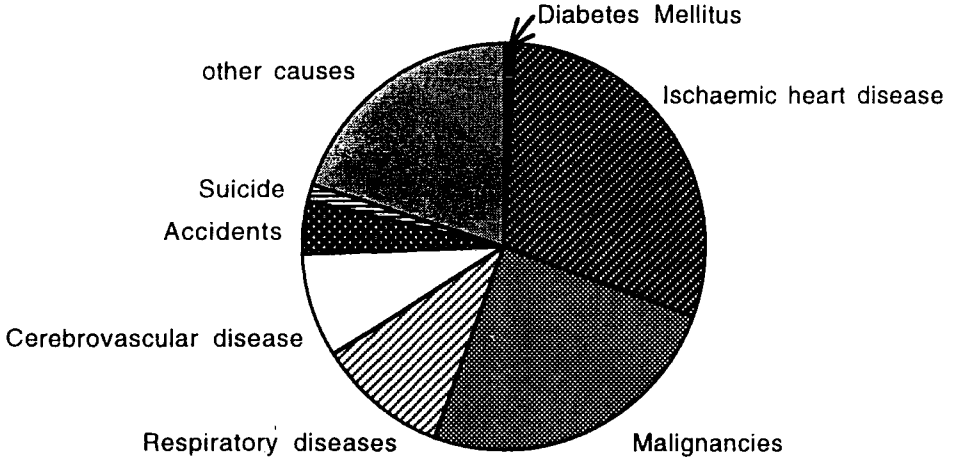

It can be seen from figure 1.1 that malignant cancers are the second greatest killers in the United Kingdom. The term cancer does not refer to a single disease but to over 200 types which vary in severity and in the age group and sex of those whom they affect. In almost every age group cancer is responsible for a higher proportion of deaths in women than men,[5] incidence among younger people is less, an exception is the skin cancer malignant melanoma which has seen an increase of 70% since 1974[6] among the under 40's.

FIGURE 1.2 *The ten most frequently diagnosed cancers by sex in 1991.*[7]

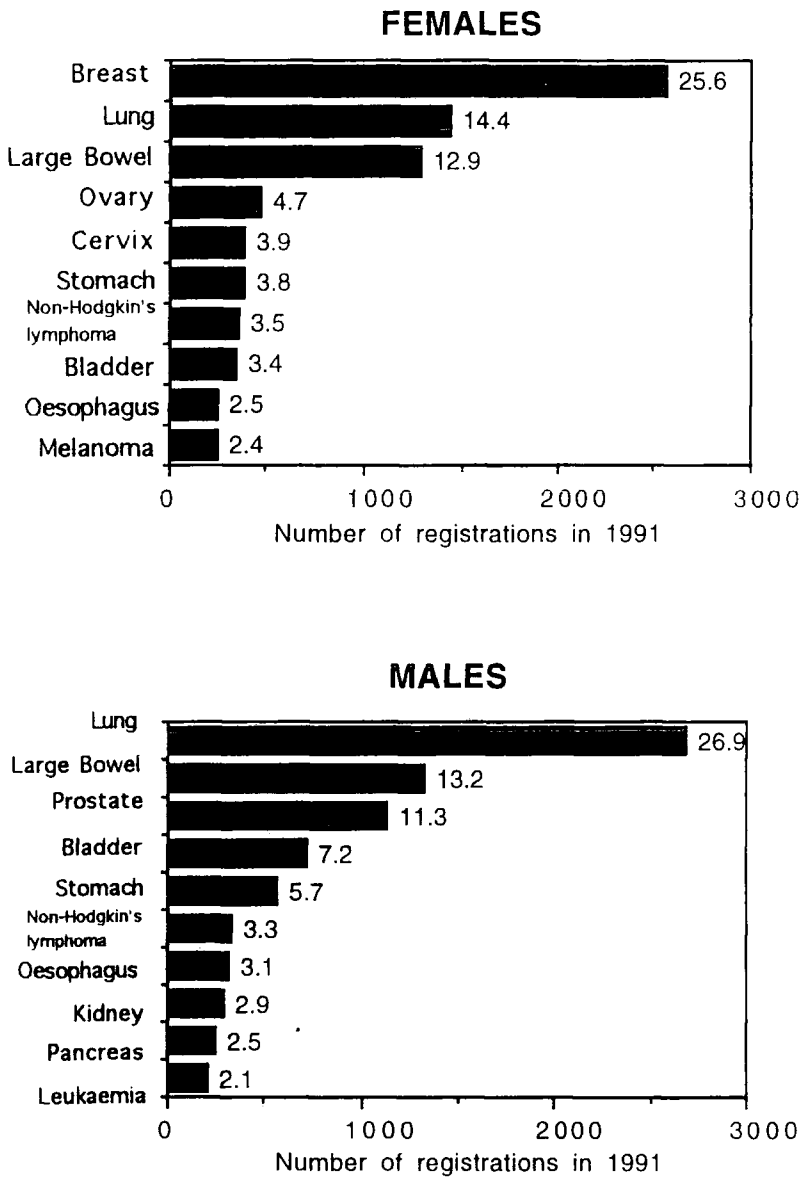

Some types of cancer are more life threatening than others; the annual relative survival rates for specific cancer sites presented in figure 1.3[8] demonstrate this. Some types can be treated if detected quickly such as cervical cancer and melanoma (where 93% survive if the tumour is found while less than 1.5mm thick) but if allowed to spread to other organs, tumours are more difficult to detect and treat and are more likely to prove fatal. This highlights the importance of finding new methods of detection, while not providing a cure in themselves they are undoubtedly of great benefit because they make the patient more curable.

FIGURE 1.3 *Annual relative survival rate for patients diagnosed in 1983-87 by site of cancer.*

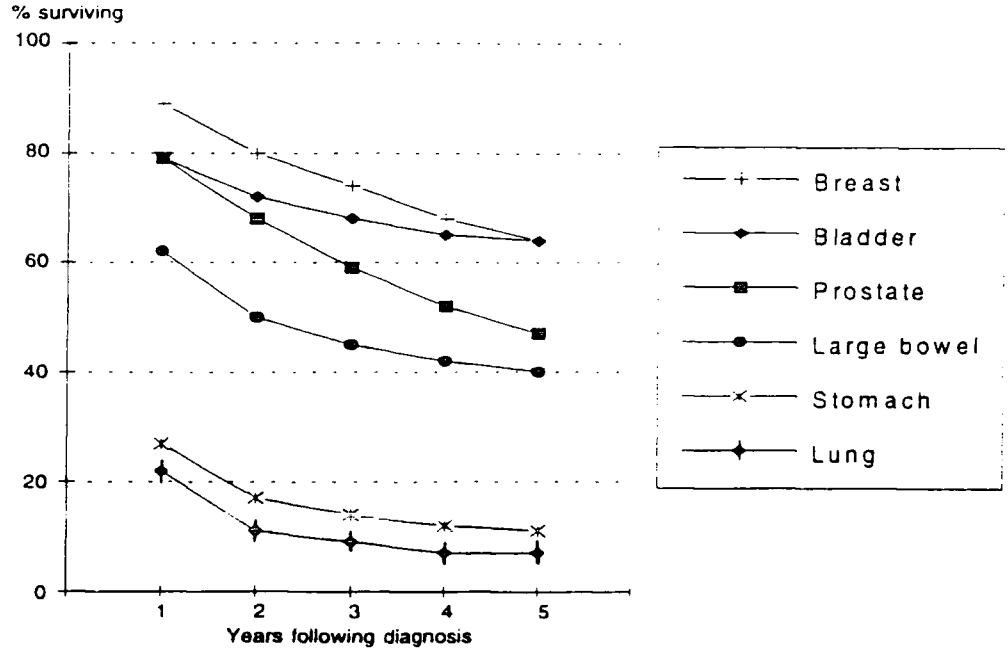

1.1.2 CARCINOGENESIS

Factors causing carcinogenesis are partly inherited, partly environmental and not well understood. Exposure to a carcinogen starts an "initiation" process in which certain genes in DNA are disrupted. Later division of initiated cells leads to a group of cells called a tumour.[9] The tumour may remain where it is (in which case it is a benign tumour) or it may fragment and spread to other tissues (in which case it is a malignant tumour). The second of these processes, metastasis is the more difficult to treat and consequently the major cause of cancer death. The process of metastasis is summarised in figure 1.4.

1.2 DIAGNOSIS OF CANCER

1.2.1 IMAGING TECHNIQUES

Since early and accurate diagnosis of cancer gives a patient a considerably greater likelihood of survival or cure, the efforts of many research groups have been directed towards the development of imaging techniques. *In vivo* imaging[10] relies upon a form of electromagnetic radiation which has minimal interaction with the biological tissues of the body, but which can interact efficiently with a detector to produce a signal. Biological tissues absorb radiation in the mid frequency range (10^{10}-10^{18} Hz), leaving the high energy and low energy ends of the spectrum for use in imaging.

FIGURE 1.4 *Metastasis: Ability of malignant tumour to invade surrounding cells.*[11]

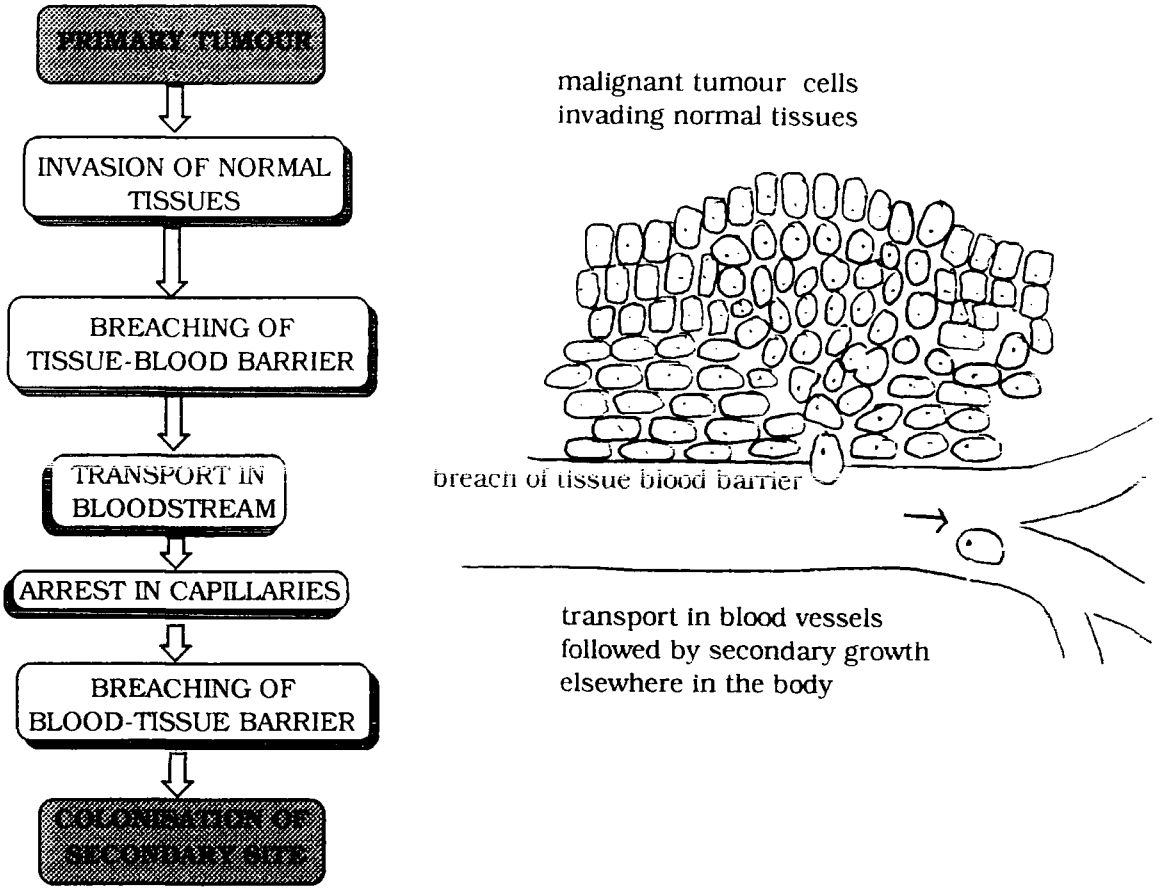

There are two main categories of techniques employed in the diagnosis of disease:
(i) those involving the interaction of photons with body tissues and organs such as X-ray computed tomography (CT), ultrasound imaging and magnetic resonance imaging (MRI) which are able to delineate anatomical features with high resolution but provide only a limited amount of information about biological function.
(ii) those involving a radiopharmaceutical, a drug containing a radionuclide; this method takes advantage of the nuclear properties of the radionuclide and the pharmacological properties of the radiopharmaceutical to allow *in vivo* monitoring of biochemical *and* physiological functions.

1.2.2 IMAGING WITH CT AND MRI

X-ray computerised tomography (CT) presented images in a way that was completely new to many clinicians and so had a considerable impact, demonstrating the advantages of medical imaging by tomographic sections through the head or body. It works on the principle that the source and the detector are aligned and data is collected in segments at many fixed angles. The absorption data are resolved into a series of digitised images

representing thin slices of tissue by solving the resultant simultaneous equations computationally.

The success of CT paved the way for the development of another tomographic technique, NMR imaging in the early 1970's.[12] The advantages of being able to view the body in three dimensional images representing slices of tissue far outweighed the disadvantages of the high cost of the technology involved in developing the NMR imaging instrument. The instrument used in magnetic resonance imaging (MRI) differs little in principle from a laboratory FTNMR spectrometer, however it does present new engineering challenges in requiring a sample chamber large enough for a human head or whole body and the addition of gradient radiofrequency coils.

Given that the body is more than 60% water, the water proton resonance is the most abundant resonance to detect *in vivo*. The gradient magnetic field which replaces the familiar static field used in laboratory FTNMR spectrometers makes the water proton resonance frequency position dependent. This provides a signal which must be decoded to give a digitised image. In a typical experiment for each volume element (with concentration of water protons = $[H_2O]$) the signal intensity depends on the longitudinal and transverse water relaxation times (T_1 and T_2) and the nature of the pulse used (e.g. using the common 'spin-echo' pulse, T_E is the echo delay time and T_R the pulse repetition rate) as shown in equation (1)[13,14] where H_v is a motion factor.

$$\text{Signal intensity} = [H_2O]H_v(\exp[-T_E / T_2])(1-\exp[-T_R / T_1]) \qquad (1)$$

Paramagnetic species catalyse the proton relaxation of aqueous solutions in which they are dissolved, a highly paramagnetic ion like Gd^{3+} or Mn^{2+} causes the relaxation time of water protons to decrease by a factor of about 10^6. As can be seen from equation (1), decreasing the relaxation times T_1 and T_2 changes the signal intensity, but the two terms have opposing effects. In practice a "T_1-weighted" image is obtained by varying T_E and T_R appropriately. Relaxivity is the term used to describe this ability of paramagnetic ions to shorten the water proton relaxation rate. Gadolinium complexes are used commonly because the Gd^{3+} ion combines a high magnetic moment with a long electronic relaxation time ($\tau_s = 10^{-9}$s in the case of Gd^{3+}), two features that ensure effective nuclear spin relaxation.[15]

MRI was originally considered to be a noninvasive radiological technique, but it now appears that contrast agents are often necessary to highlight lesions that otherwise could not have been detected. In clinical practice, paramagnetic contrast agents are now used routinely to improve the signal intensity in NMR imaging. Most of these agents are

based on Gd(III) because of its high relaxivity described above. When designing a potential new contrast agent there are some important points to note:

(1) Since the dose given to the patient is high (ca. 10g) the contrast agent must be non-toxic at these levels.
(2) The contrast agent must be soluble in water in these quantities also.
(3) It must possess an osmolality similar to that of serum lest crenation of red blood cells leads to pain on administration.[14]
(4) Relaxivity is further increased by contrast agents in which water molecules are coordinated directly to the metal ion.[16]

1.2.3 IMAGING WITH RADIOPHARMACEUTICALS

When a radioisotope is used in diagnosis (termed radioimmunoscintigraphy) a minimal interaction of radiation with the tissues of the patient is desired whilst the interaction of radiation with a detector outside the body is maximised. Gamma emitters may be suitable in this respect if they deliver photons of appropriate energy to escape from the body (>80 keV) and with sufficient density to achieve the necessary resolution for imaging.[17] They fall into two main categories:

(i) Single photon emitters where the γ emission occurs as a direct result of simple nuclear decay.

(ii) Positron emitters where the isotope emits a positron (β^+) and leads to the creation of two opposing γ rays.

1.2.3.1 GAMMA RAY SCINTIGRAPHY AND SPECT

Single photon emission (γ emission) is detected by means of an Anger camera. In view of the random direction of emission from gamma emitting isotopes a collimator is used to localise the radiation upon the detector to provide a signal which is amplified and counted as electrical pulses. The resolution obtainable is modest at 1-2 cm, coarser than that obtained using X-rays.

A three dimensional image may be obtained by mounting the Anger camera on a rotating gantry, recording multiple images at different angles. The procedure is computerised and known as Single Photon Emission Computerised Tomography (SPECT).

1.2.3.2 POSITRON EMISSION TOMOGRAPHY (PET)

If a radionuclide emits a positron (β^+) which annihilates with an electron from the surrounding tissue, two photons (511 keV) are produced which travel at 180° to each other as shown in figure 1.5.[18]

FIGURE 1.5 *Annihilation of a positron and electron.*

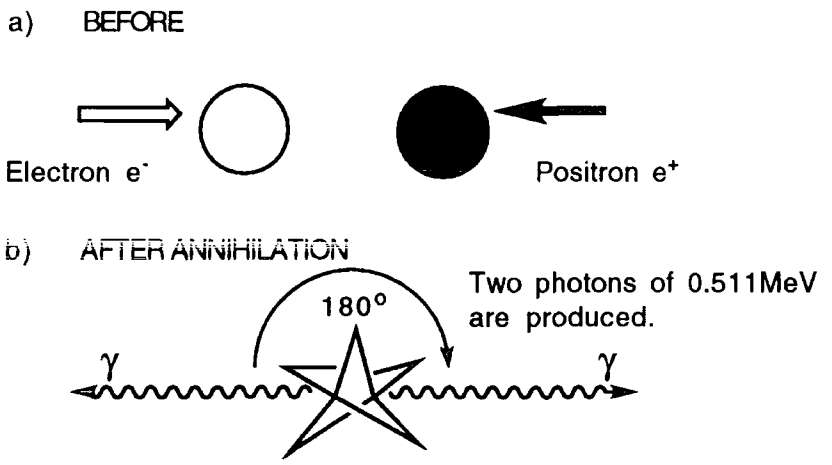

As a result of the directional nature of these emissions, tomographical information may be obtained by detecting the two gamma rays at each side of the source within the patient. This confines the annihilation event to a single line joining the two detectors. The PET scanner[19] may be a series of static or mobile Anger cameras around the patient which scan through a given volume element. Resolution is very good, of the order of 3mm, but the high cost of the PET scanner has caused its use to be much more limited than SPECT.

1.2.3.3 CHOICE OF RADIOISOTOPES FOR USE IN IMAGING

In addition to selecting the type of radiation required for the chosen tumour imaging technique there are a number of other principles to be considered when choosing the most suitable radionuclide.[20]

(1) HALF-LIFE: This should be long enough to permit transportation to the site of tumour before one half-life has elapsed, but short enough to limit the radiation dose to which the patient is exposed. (Typical $t^1/_2$ is 6 hours-8 days).

(2) GAMMA ENERGY: Between 80 and 240 keV, (in the case of positron emitters, photons have an energy of 511 keV).

(3) GAMMA ABUNDANCE: To minimise the quantity of radiopharmaceutical required, the radioisotope should be (i) 'carrier-free', that is with no 'cold'

isotopes of the same element, (ii) have a high percentage of single energy gamma emissions and (iii) very low abundance of any β or α emissions.

(4) RADIOCHEMICAL PROPERTIES: The isotope should be easily produced at low cost (preferably from a generator[21]), be readily purified from other isotopes and decay without hazardous daughter products.

FIGURE 1.6 *Gamma emitting radioisotopes used in SPECT imaging.*

Radionuclide	t 1/2 (hours)	E_{photon} (keV, %)	source
^{99m}Tc	6.02	141 (89)	generator
^{111}In	68	171 (88)	cyclotron
		247 (94)	
^{67}Ga	78	184 (24)	cyclotron
^{131}I	193	364 (82)	reactor
^{123}I	13.2	159	cyclotron

FIGURE 1.7 *Positron emitters used in PET.*

Radionuclide	t 1/2 (hours)	E_{photon} (keV, %)	source
^{68}Ga	1.20	511 (178)	generator
^{64}Cu	12.8	511 (120)	reactor
^{82m}Rb	6.4	511	generator

1.3 TREATMENT OF CANCER

1.3.1 TYPES OF CANCER TREATMENT.

There are four main approaches used by physicians to destroy cancer cells selectively. The comparative usefulness of these may be helpfully illustrated by an analogy of weeds (cancer) and grass (normal cells). One weed in the middle of a plot of grass can be pulled out (surgery) or burned out (radiotherapy). If the weeds are widespread (disseminated cancer), then a solution of weedkiller (chemotherapy) can be sprayed on the lawn to destroy the weeds selectively, without destroying the grass. If there are only a few weeds throughout the grass, the addition of fertiliser (immunotherapy) to strengthen the growth of the grass may enable it to outgrow and choke the weeds.

The effectiveness of surgery is limited not by the size of the tumour but by its distribution. Chemotherapeutics on the other hand, have had some success against

metastatic disease, notably the drugs cisplatin (cis-($PtCl_2(NH_3)_2$)), carboplatin (C_3H_6-$C(CO_2)_2$-$PtCl_2(NH_3)_2$)) and 5-fluorouracil. Their use is limited not by the distribution but by the total mass of tumour since these drugs have unpleasant side effects; nausea, hair loss and an increased susceptibility to infection. Immunotherapy capitalises on the differences between cancer cells and normal cells and employs the body's own immune system in the treatment of the tumour (see section 1.5). Radiation therapy in the form of X-rays and γ-rays continues to be an important treatment modality for many forms of human cancer,[22] although normal tissue toxicity limits the total dose of radiation a patient can ultimately receive.

1.3.2 RADIOPHARMACEUTICALS IN TUMOUR THERAPY

Radionuclides used in therapy[23,24] must deliver a sterilising radiation dose to the tumour site sufficient to cause multiple double-strand cleavages of cellular DNA (600 - 4000 rads). Suitable isotopes for radioimmunotherapy are either β or possibly α emitters with very little or no γ content. Many of the principles outlined in 1.2.3.3 apply equally well to choice of radionuclides for therapy, but generally they have a longer half-life (1-10 days) allowing the dose to be delivered over a period of time.

FIGURE 1.8 *Therapeutic Radioisotopes for use in radioimmunotherapy.*[25]

Radionuclide	t $^1/_2$ (hours)	β_{max} (MeV, %)	mean range in tissue (mm)
^{90}Y	64	2.25 (100)	3.9
^{67}Cu	62	0.40 (45)	0.2
		0.48 (3)	
		0.58 (20)	
^{186}Re	90	1.07 (74)	1.1
		0.93 (21)	
^{188}Re	17	1.96 (18)	3.3
		2.12 (80)	
^{199}Au	75	0.25 (22)	0.1
		0.30 (72)	
^{111}Ag	179	1.04 (93)	1.1
		0.69 (6)	
^{161}Tb	166	0.45 (26)	0.3
		0.57 (64)	
		0.58 (10)	
^{131}I	193	0.61 (90)	0.4

1.3.3 SUMMARY OF ELEMENTS USED IN TUMOUR DIAGNOSIS AND THERAPY

A summary of the elements, both paramagnetic contrast agents and radioisotopes, used in diagnosis of disease and those used in tumour therapy is given below. Some elements have more than one useful isotope, iodine also has a gamma emitting isotope, copper and gallium also have positron emitting isotopes and dysprosium may also be used as a contrast agent in MRI.

FIGURE 1.9 *Periodic Table: summary of metals and radioisotopes used in diagnosis and therapy of tumours.*

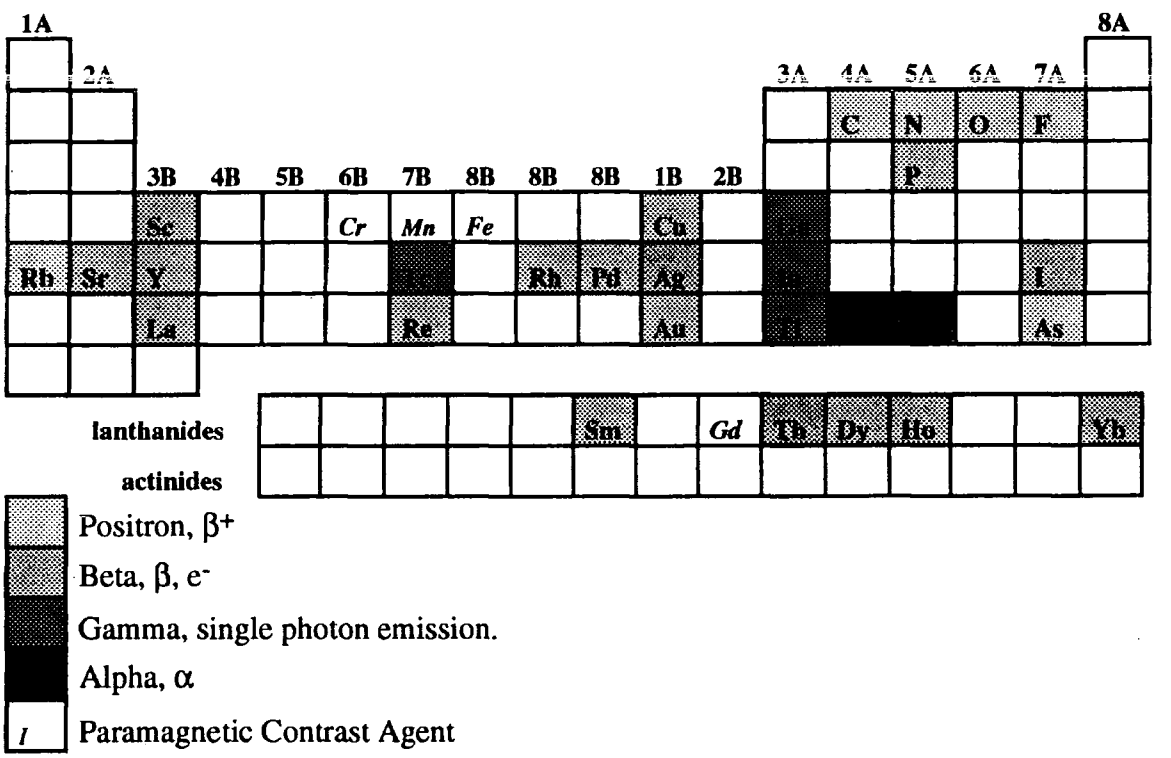

Some of these elements are more widely used in clinical practice or will be particularly highlighted in the following chapters, the properties that lead them to be considered in this way are summarised below.

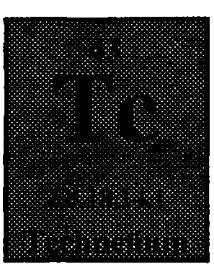

Technetium - 99m (m= metastable, excited nuclear state with unusually long lifetime)

FOR:

(1) Ideal gamma energy (used to 'tune' detection equipment.)

(2) Reasonable price - obtained from a generator.

(3) Obtained 'carrier free' via Al_2O_3/SiO_2 column chromatography.

(4) Very diverse chemistry - many complexes known.[26]

(5) Currently used in 90% of diagnostic scans in hospitals.[27]

AGAINST:

(1) Short half life - after 2 days most of activity is gone.

(2) No stable isotopes of Tc exist

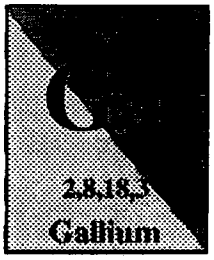

Gallium - 67 gamma emitter

(1) ^{67}Ga citrate concentrates in certain tumours and clears from the blood allowing imaging.[28]

Gallium - 68 positron emitter

(1) Reasonable price - available from a ^{68}Ge generator.[21]

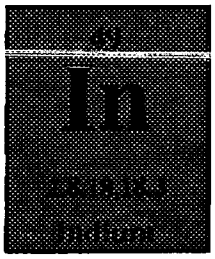

Indium - 111 gamma emitter

(1) Longer half-life than Tc, better for establishing high tumour : background relationships.

(2) In^{3+} released *in vivo* scavenged by iron sequestering agent.

(3) More expensive - obtained from a reactor.

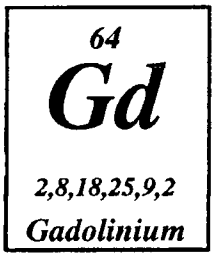

Gadolinium (III) Paramagnetic contrast agent.

(1) NOT a radioactive isotope used in diagnosis, but suitable for use as a paramagnetic contrast agent.

(2) ^{153}Gd is available (γ, $t^1/_2$ 241 days) for tracer work such as biodistribution studies.

1.4 COMPLEXING AGENTS

1.4.1 NECESSITY OF COMPLEXING AGENTS

Since the majority of the radioisotopes and contrast agents required for use in the above imaging and therapy techniques are toxic metals it is important that they are administered in a form which will not harm the patient. For safe use in the body the metal is administered as a coordination complex[26]; it is of utmost importance that this complex remains intact *in vivo* and many of the desirable properties of such complexes listed below relate to this.

(1) Good thermodynamic stability (log K_S) is important, this serves as a guide to overall stability, however for applications in living systems the kinetic stability is of greater importance.

(2) Conditions in blood are pH 7.4 at 37°C, but lower pH is encountered in bile/ stomach, there are also high local concentrations of certain metal ions. Metal

complexes must be kinetically stable with respect to acid catalysed or cation promoted dissociation pathways.

(3) Charge neutrality is preferred in order to resist attack by protons / cations and to aid diffusion through membranes.

(4) Coordinatively saturated complexes of an oxidation state which is stable *in vivo* are preferred to minimise electron transfer.

(5) The shape, size and lipophilicity of the complex must be tailored to aid transport *in vivo*.

(6) The complex should be cleared from the body intact after a suitable time.

(7) In the case of radiopharmaceuticals the complexation rate should be fast since the radioisotope is decaying during this time and a high radiolabelling yield is desired.[29] Also, in the case of therapeutic isotopes, the daughter product must form a stable complex with the same ligand.

1.4.2 ACYCLIC CHELATING AGENTS

It is well known that complexes formed between metals and chelating ligands are generally more thermodynamically stable than those involving monodentate donor groups - this is the so called 'chelate effect'.[30] Examples of conventional acyclic chelators are the polyaminocarboxylate ligands EDTA and DTPA. Both of these ligands demonstrate remarkable versatility in binding metal ions.

FIGURE 1.10 *Ethylenediaminetetraacetic acid (EDTA) and diethylene triaminepentaacetic acid (DTPA)*

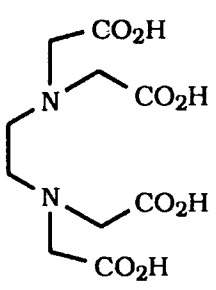

EDTA

EDTA	DTPA
donor set:	donor set:
N_2O_4	N_3O_5
hexadentate	octadentate

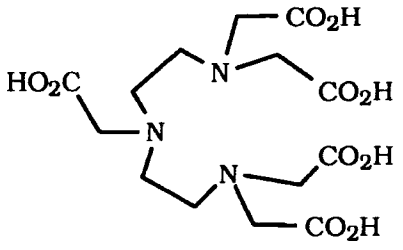

DTPA

Both of these ligands have been used in clinical practice, in the case of EDTA the ^{68}Ga complex has been employed to detect where brain tumours have caused disruption of the blood brain barrier.[31] Attempts have also been made to use the ^{62}Cu complex of EDTA but these have proved unsuccessful since this complex, and also that of ^{62}Cu-DTPA, is unstable *in vivo* and leads to Cu build-up in the liver. However the anionic

^{111}In-DTPA has been used with some success in evaluating cerebral spinal fluid pathways[32] and has a high stability ($\log K_{ML}$ = 29.0 at pH 7.4)[33] with DTPA chelating through all five O and three N donors available. The structure of ^{99m}Tc-DTPA by contrast is hexadentate although less well understood; it finds uses such as kidney and brain imaging.[26] Gd-DTPA is also well known, being used routinely as an MRI contrast agent (see section 2.3.1), and is marketed under the brand-name Magnevist.

FIGURE 1.11 *Acyclic complexing agents: further examples.*

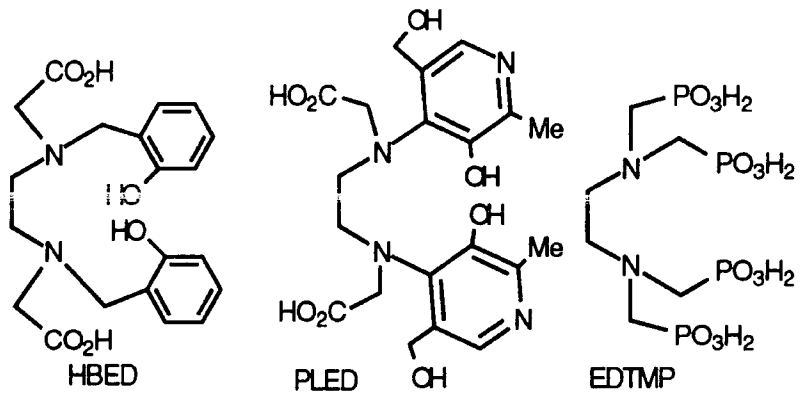

The ligands N,N'-bis(hydroxypyridyl)ethylenediamine-N,N'-diacetic acid (PLED) and N,N'-bis(2-hydroxybenzyl)ethylenediamine-N,N'-diacetic acid (HBED)[34] both form complexes with ^{68}Ga and are potential radiopharmaceuticals for PET, the former may be used for imaging the kidney since it clears from the body via the renal system, the latter is a liver imaging agent, being cleared by the biliary system. Finally a chelate undergoing trials as a therapeutic agent, ethylenediamine tetramethylenephosphonic acid (EDTMP) forms a complex with ^{153}Sm ($t^1/_2$ 46.27 hours, β^-), this is used for treatment of bone cancer pain,[35] although in this case the selective deposition of the radiolabel in the bone is the objective of the treatment.[36]

1.4.3 STABILITY OF ACYCLIC COMPLEXES

Although these complexes generally possess good thermodynamic stability their concentration in blood is very low and there is competition for the metal from transferrin, albumin and other metal binding proteins. In addition there is a high concentration of metals such as Zn^{2+} (10^{-5}M) and Ca^{2+} (10^{-3}M) in serum competing for the ligand and promoting metal ion loss.[37] Moreover these complexes are very susceptible to protonation and their stabilities are highly pH dependent.[38] Although acyclic ligands such as those described above are currently used in clinical practice, the

future success of imaging techniques depends on complexes which are less susceptible to dissociation *in vivo.*

1.4.4 IMPROVING STABILITY OF COMPLEXES

Each metal ion to be bound has distinctive coordination requirements. A chelating group may be designed to optimise the 'hardness', number of donor atoms and coordination geometry to provide a complex stable for *in vivo* use.

FIGURE 1.12 *'Hardness' according to the hard-soft acid-base principle of Pearson.*[39]

ACIDS	
HARD	**SOFT**
H^+, Li^+, Na^+, K^+, Be^{2+}, Mg^{2+}, Ca^{2+}, Sr^{2+}, Ba^{2+}, Al^{3+}, Sc^{3+}, Ga^{3+}, In^{3+}, La^{3+}, Gd^{3+}, Lu^{3+}, Cr^{3+}, Co^{3+}, Fe^{3+}, As^{3+}, Si^{4+}, Ti^{4+}, Zr^{4+}, Hf^{4+}, Th^{4+}, U^{4+}, Pu^{4+}, Ce^{4+}, Sn^{4+}	Cu^+, Ag^+, Au^+, Tl^+, Hg^+, Pd^{2+}, Cd^{2+}, Pt^{2+}, Hg^{2+}, Pt^{4+}, Te^{4+}, Br^+, I^+
BORDERLINE	
Fe^{2+}, Co^{2+}, Ni^{2+}, Cu^{2+}, Zn^{2+}, Pb^{2+}, Sn^{2+}, Sb^{3+}, Bi^{3+}, Rh^{3+}, Ir^{3+}	
BASES	
HARD	**SOFT**
H_2O, OH^-, F^-, $CH_3CO_2^-$, PO_4^{3-}, SO_4^{2-}, Cl^-, CO_3^{2-}, ClO_4^-, NO_3^-, ROH, RO^-, R_2O, NH_3, RNH_2, NH_2NH_2	R_2S, RSH, RS^-, I^-, SCN, $S_2O_3^{2-}$, R_3P, R_3As, $(RO)_3P$, CN^-, RNC, CO, C_2H_4, H^-, R^-
BORDERLINE	
$C_6H_5NH_2$, C_5H_5N, N_3^-, Br^-, NO_2^-, N_2, SO_3^{2-}	

When designing ligands it is also important to consider the size of the 'chelate ring'.[40, 41] It is commonly stated in textbooks that six membered chelate rings lead to less stable complexes than five membered chelate rings, but this conclusion is reached because stability is strongly related to the metal ion size and with the exception of Be (II) and B (III) most metals commonly studied are not small enough to form stable six membered chelate rings.

FIGURE 1.13 *The ideal geometry for (A) a five membered chelate ring, with ethylenediamine (EN) and (B) a six membered chelate ring with trimethylenediamine (TN). In each the organic part of chelate ring ideally requires the same geometry as the cyclohexane ring.*

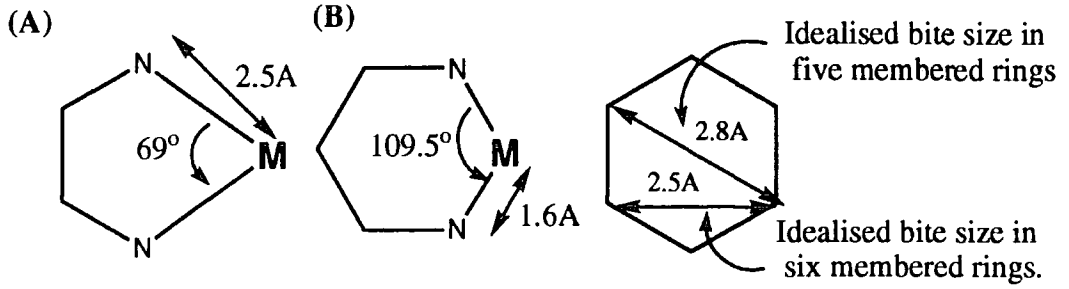

1.4.5 MACROCYCLES

Macrocyclic complexes, that is compounds containing at least nine atoms in a ring with at least three donor groups, are almost without exception more stable thermodynamically and kinetically than their corresponding open chain analogues. Termed the 'macrocyclic effect'[42] it is a more profound feature of macrocyclic complexes than simply an increased 'chelate effect' arising from the presence of an additional chelate ring.

Much calorimetric and spectroscopic work has been done to investigate the thermodynamic parameters involved in the macrocyclic effect. The outcome was that it is neither an enthalpic or entropic effect alone, but a combination which varies according to the cation and macrocycle involved. Another feature associated with the macrocyclic effect is the kinetic inertness of macrocyclic complexes towards metal ion dissociation. This is because the conformational restrictions of the macrocycle make the transition states in the stepwise dissociation energetically unfavourable. This contrasts with the acyclic complexes discussed previously which, being free to change conformations, are likely to be less kinetically inert.

Nature has long employed macrocyclic ligands in the transportation of metal ions. Some examples of these include haemoglobin, chlorophyll and vitamin B_{12}. The research into synthetic macrocycles was heralded by the discovery of crown ethers by Pedersen in the 1960's.[43] These cyclic polyethers were observed to form stable 1:1 complexes with alkali and alkaline-earth metal cations. The ring contained oxygen donor atoms and the metal was bound in the cavity through ion-dipole interactions to form 'host-guest' complexes. Since different sizes of crown ethers appeared to show preference for different sizes of metal ion the concept of 'size-match selectivity' was proposed.

FIGURE 1.14 *Examples of crown ethers , aza macrocycles and 9X3 macrocycles*

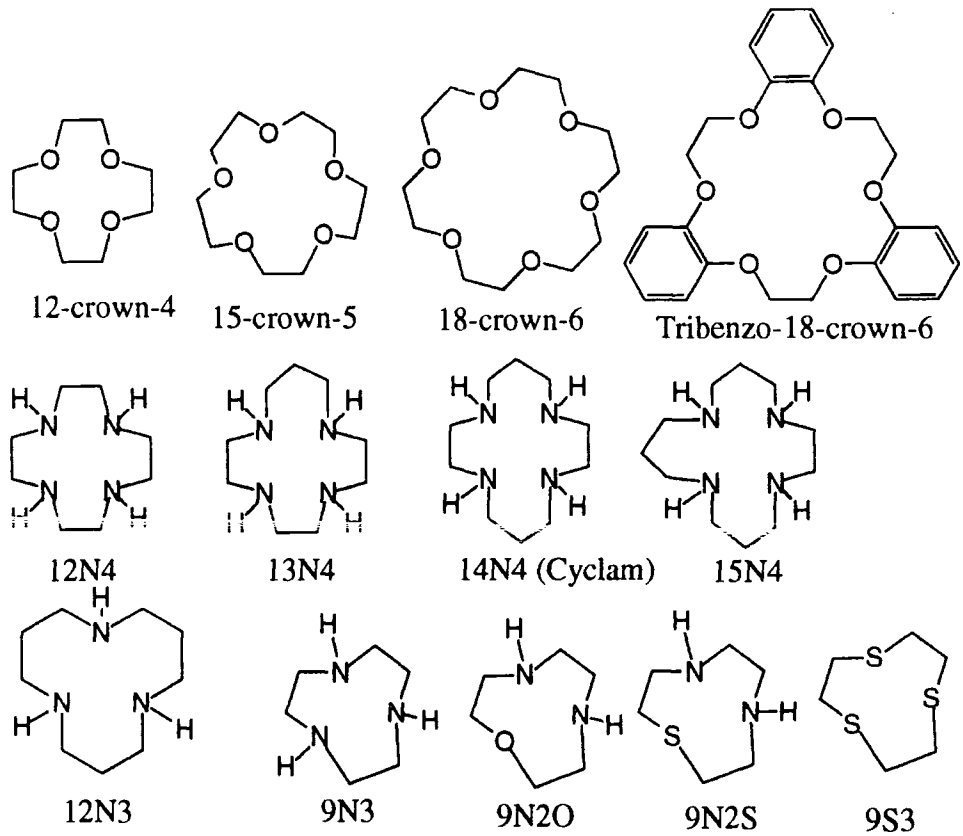

However this is not a general principle which extends to other groups of macrocycles. For example, among the tetraaza macrocycles, the 14N4 ligand (cyclam) shows a preference for Cu (II) yet for the much larger Pb (II) ion the complex stability decreases with increasing cavity size, 12N4 being the most stable. The observations in this and other cases may be explained not by 'size-match selectivity' but by chelate ring size considerations. In the case of the Pb complex, although the macrocyclic cavity is growing larger through the series, the five membered chelate rings are being changed to six membered and a large metal ion such as Pb (II) does not coordinate well in six membered chelate rings.[40]

Smaller macrocycles[44,45,46] such as 9N3 and to a lesser extent 12N3 have more rigid structures and do tend to show some size selectivity imposed by the stringent requirements as to the preferred size of metal ion for coordination to the three donor atoms.

Pendent donor groups have the ability to increase the stability of a macrocyclic complex still further. Among these are neutral oxygen donors, pyridyl, phenolate, 2-amino ethyl, phosphinate, carboxylate and amide groups. For use in aqueous solutions

the choice of ionisable group is very important, stability at low pH is increased by the ability of carboxylate or phosphinate to aid resistance to protonation on the heteroatoms of the ligand. Stability at high pH is enhanced by a phenolate or 2-hydroxypyridine. Of all these pendent donors the carboxylate and phosphinate groups demonstrate great steric efficiency, that is they coordinate to metal ions without bringing large numbers of atoms to lie close to the metal ion.

FIGURE 1.15 *Steric efficiency of carboxylate and phosphinate compared with the less efficient amine group.*[41]

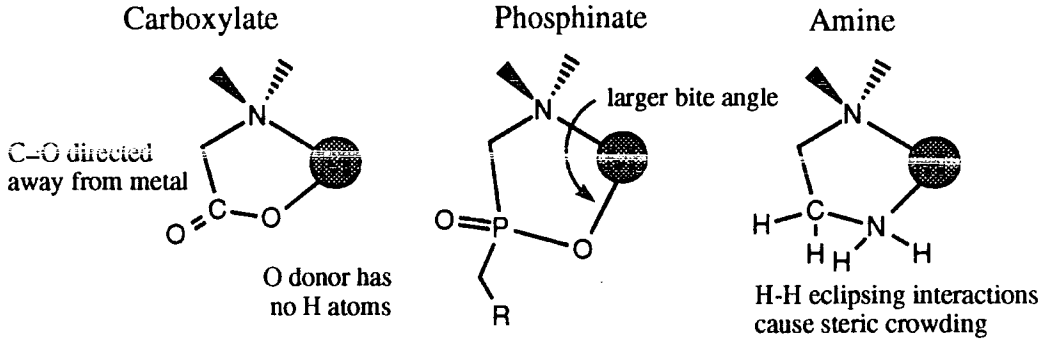

FIGURE 1.16 *Macrocycles with pendent donor groups.*

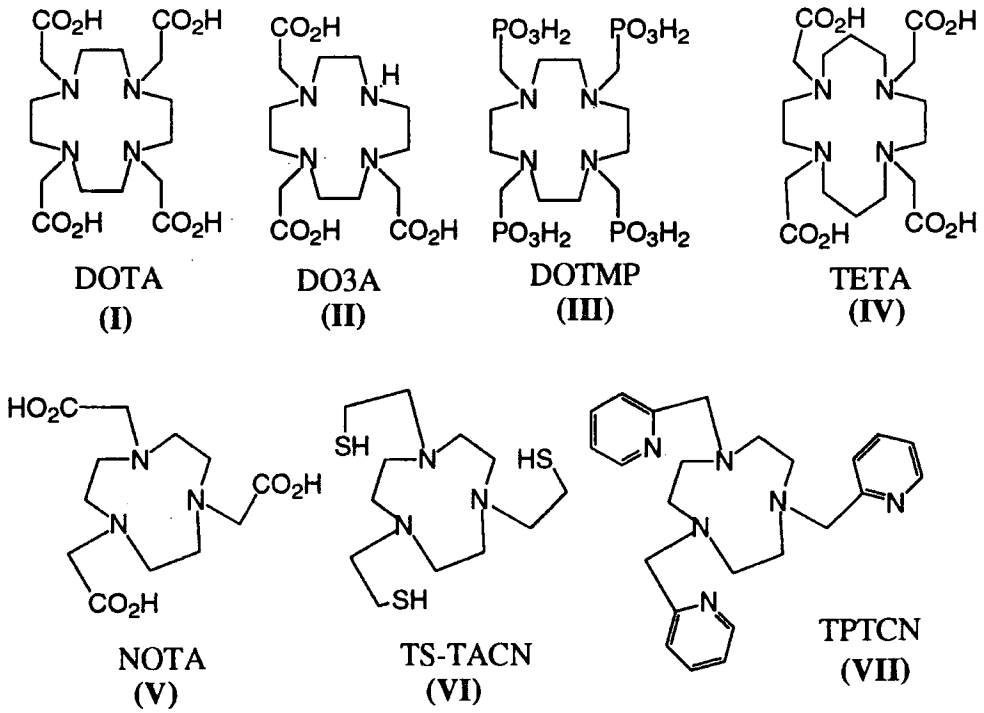

1.4.6 MACROCYCLE COMPLEXES IN TUMOUR IMAGING AND THERAPY

A number of 9N3 analogues have been studied with a view to forming stable Ga and In complexes. Of these, the ligand NOTA (**V**) has proved most successful, forming complexes of high thermodynamic and kinetic stability *in vivo*.[47,48] Indeed the ^{67}Ga-NOTA complex remained stable with respect to acid catalysed dissociation even in 6M nitric acid. The lipophilic indium complex of TX-TACN (**VIII**)[49] shows retention in liver and blood, making it a possible candidate for imaging the hepatobiliary pathway, but it is considerably less stable than NOTA. The TS-TACN (**VI**)[50,51] ligand has a much lower molecular weight whilst retaining some lipophilicity, its Ga and In complexes were studied to determine whether they were able to cross the blood brain barrier, but they proved less lipophilic than expected and were unable to do so.

FIGURE 1.17 *Macrocycles for use in imaging and therapy of cancer.*

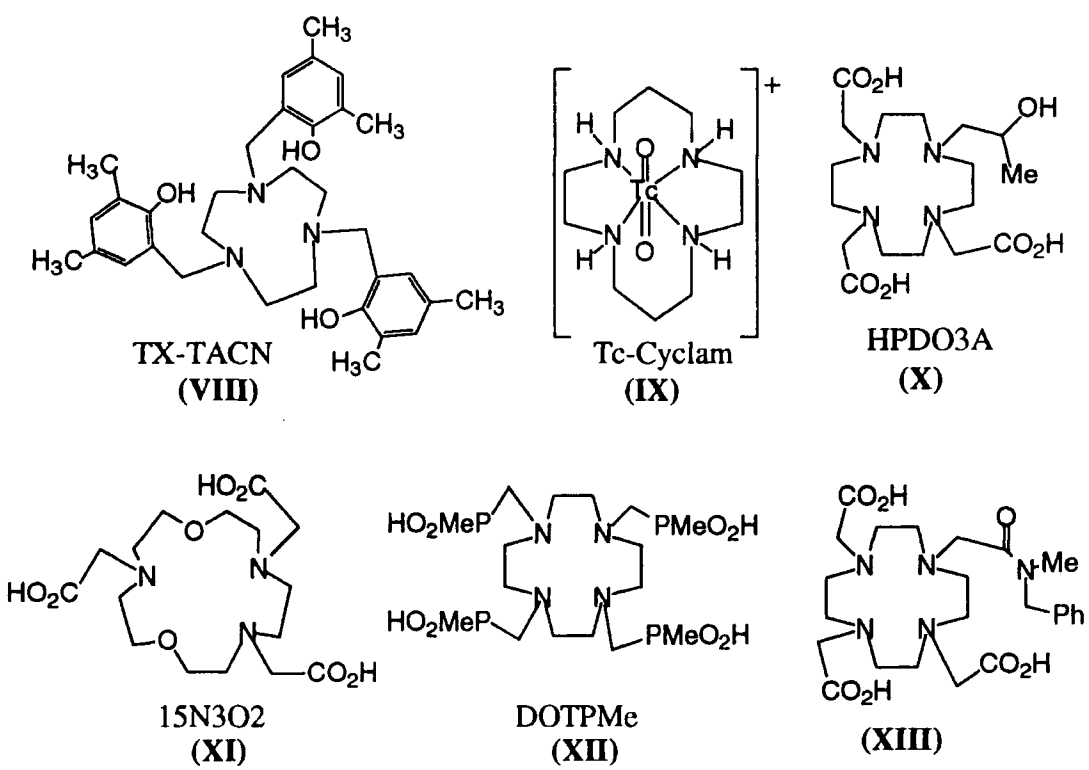

Tetraaza macrocycles have found a wide variety of uses.[16] Cyclam forms a dioxo complex with ^{99m}Tc (**IX**) for imaging although, being charged it does not cross the blood brain barrier. DOTA (**I**) and DO3A (**II**) both form seven coordinate complexes with ^{111}In which show greater stability in serum than the ^{111}In-DTPA complex discussed previously, demonstrating the suitability of the 12N4 based ligands for In labelling. DOTA (**I**) and HPDO3A (**X**) also form stable complexes with Gd[52] and are

used routinely as MRI contrast agents (see section 2.3.1). The larger macrocycles TETA (**IV**) and the 13N4 analogue TRITA both form Gd complexes which are more fluxional than DOTA, and the complexes are less kinetically stable with respect to dissociation which may be related to the presence of the six-membered chelate rings. These two ligands do however form stable ^{64}Cu complexes allowing the possibility of PET imaging. The therapeutic isotope ^{90}Y also forms stable complexes with 12N4 based ligands since the rare-earth Y^{3+} has a very similar coordination chemistry to the lanthanide Gd^{3+}. It is especially important that the yttrium-90 complexes remain intact in the body due to the lethal consequences of ^{90}Y building up in the bone. It is also important that these complexes form quickly giving a high radiolabelling yield for the forward complexation reaction. The 15N3O2 ligand (**XI**) binds Y too slowly to be useful since the radioactive isotope decays constantly during complexation. However, complexes of DOTPMe (**XII**) and 12N4 neutral amides such as (**XIII**) are suitable.

1.5 TUMOUR TARGETING

Nearly a century ago Ehrlich proposed that it may be possible to find a particular chemical which would eradicate a specific disease through the applications of drug action whilst leaving the host organism unharmed and so he coined the phrase 'magic bullet'. When applied to the diagnosis and therapy of cancer this approach seeks to capitalise on the differences between 'normal' and tumour cells. Since tumour cells are derived from normal cells such differences are limited. Differentiation between the cell types is evident in their rate of proliferation and hence vascularisation, different enzyme patterns albeit with the same enzymes, and tumour cells may possess different macromolecules on their surfaces such as antigens and macrophages.

The biodistribution of the majority of therapeutic and diagnostic agents discussed so far has been determined by blood-flow (perfusion). Where differences are observed they are due to factors such as the ability of the complex to cross the blood-brain barrier or its specificity for the hepatobiliary pathway. Such behaviour may be ascribed to factors such as complex shape, charge, redox properties and lipophilicity.

Alternatively the biodistribution may be determined by specific receptor binding, a given biochemical interaction or both. This gives scope for designing agents targeted to a particular tissue or organ as Ehrlich hypothesised. In this instance the uptake and retention of the pharmaceutical depends on the properties of the target molecule. Some such examples are:

(1) Antigen-antibody interactions.

(2) Enzymatic reduction within poorly vascularised hypoxic tumours of conjugates with electron poor heteroatomic compounds such as nitroimidazoles.

(3) Interaction of peptides with specific receptors such as those located on macrophages.

Such a targeting vehicle may be conjugated to a therapeutic agent like an α or β emitter or a cytotoxic drug like taxol or calicheamicin for therapy, or may be linked to a γ or positron emitter for diagnosis.

1.5.1 TARGETING USING ANTIBODIES

1.5.1.1 ANTIBODIES

Cancer therapy that relies on manipulation of the patients' immune system is defined as immunotherapy. There are a range of approaches under development;[53] one of the most extensive studies has been into the use of antibodies as targeting agents.

Antibodies are proteins (immunoglobulins or IgG) produced by animals in response to infection by foreign substances like bacteria, viruses or tumour cells. They are produced by white blood corpuscles called B-lymphocytes found in the lymph nodes and spleen. The basic antibody structure is shown in figure 1.18, it consists of two pairs of heavy and light polypeptide chains linked by disulphide bonds. One light chain folds over the first half of one heavy chain forming a F(ab) arm (Fragment antigen binding) which has a complex three dimensional structure as a binding site for a specific antigen.

Antigens are substances foreign to the body and antigens expressed by tumours are not usually produced by normal cells. The antibodies which bind to these antigens specifically can be generated in mice by means of 'hybridoma technology'[54] for use in targeting, making the 'magic bullet' seem an attainable goal.

Problems emerged because in some cases these 'murine' antibodies were rejected by the human immune system. This human anti-mouse antibody (HAMA) response may be reduced by transforming the murine monoclonal antibody into a 'chimaeric' antibody as shown in figure 1.19. Such an antibody combines a variable (V) or binding domain of mouse antibody with a human antibody constant (C) domain. Even more effective are the so called 'humanised' antibodies[55] which combine the minimum amount of murine antibody with a human framework. These are substantially less immunogenic in humans. Another problem that was encountered was that whole antibodies were

transported *in vivo* very slowly due to their large size and were excreted slowly causing tissue : blood ratios to remain low. This was largely overcome by the use of antibody fragments[56] which were excreted rapidly whilst retaining specificity thus producing much higher tissue : blood ratios.

FIGURE 1.18 *Antibody structure and structure of F(ab') and $(Fab')_2$ fragments.*

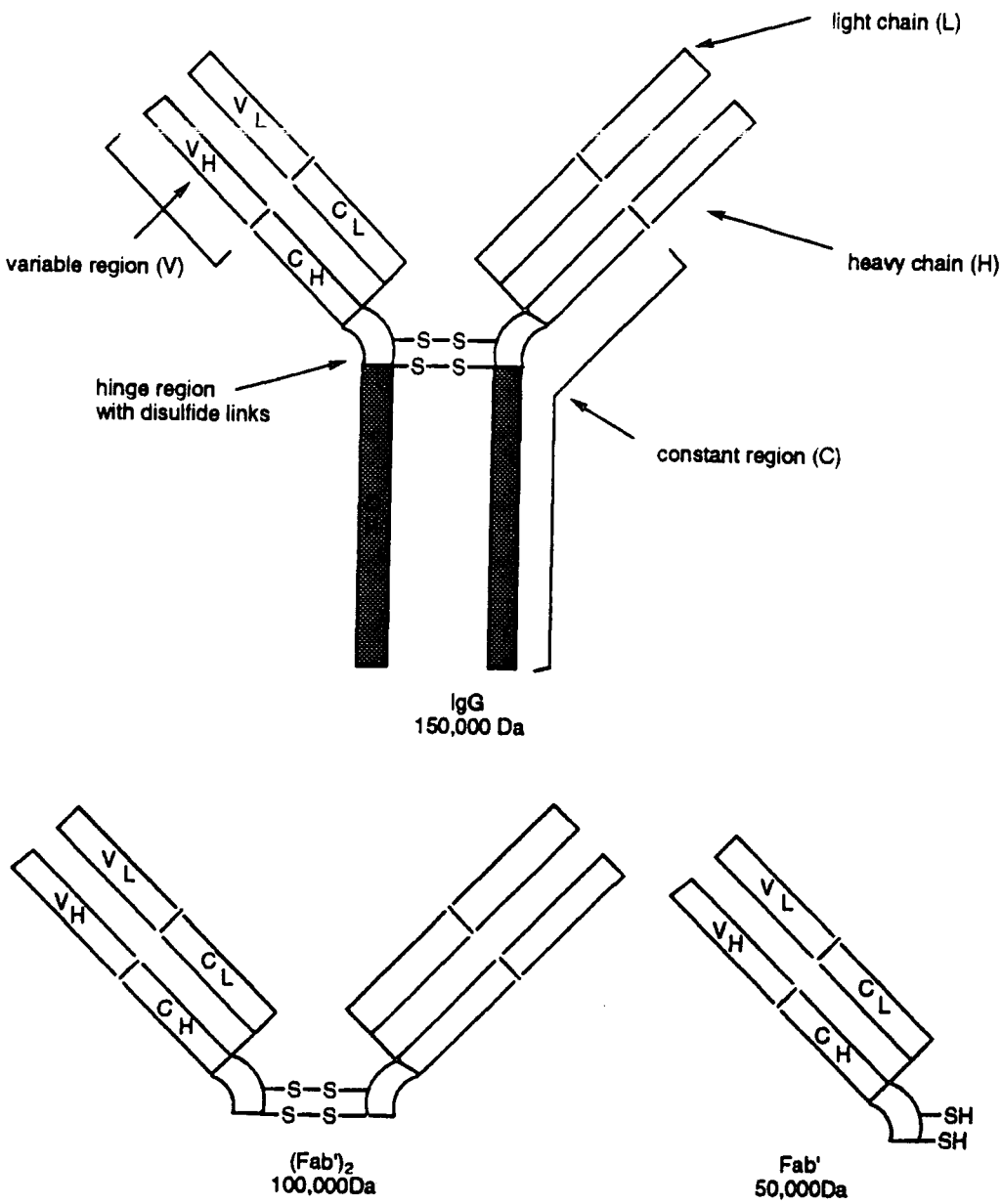

FIGURE 1.19 *A chimaeric antibody retains the entire V domain from the murine antibody, whereas a humanized antibody retains only the complementarity determining regions.*

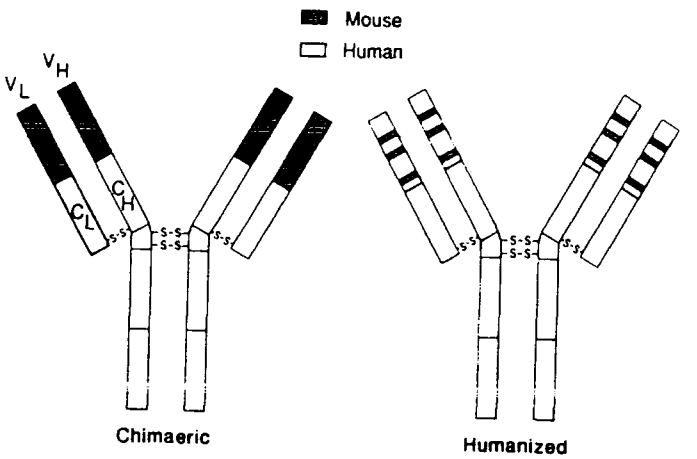

1.5.1.2 BIFUNCTIONAL COMPLEXING AGENTS

Much work has been carried out on direct, non-specific radiolabelling of antibodies and antibody fragments with ^{99m}Tc.[57] This is carried out by treating a F(ab) fragment with 2-iminothiolane to generate free sulfhydryl groups which, when incubated with TcO_4^- under reducing conditions bind to Tc quite avidly, but when formed these labelled antibodies have demonstrated relatively poor *in vivo* stability.

A more successful strategy for attaching radiometals to antibodies employs bifunctional complexing agents. These bind the metal strongly by means of a chelating agent such as a macrocycle and have another site through which the chelator can be linked to the antibody. Proteins such as antibodies are commonly coupled via the ε-amino groups of lysine residues of which there are about 90 in a typical monoclonal antibody. Suitable bifunctional complexing agents must therefore incorporate an acylating moiety such as an active ester. A range of suitable methods of linking bifunctional complexing agents to targeting vehicles is shown in figure 1.20.

It is important to consider each component carefully. The complexing agent should retain its denticity and the antibody retain its ability to bind specifically. In addition the linkage between them should be stable to hydrolysis *in vivo*.

FIGURE 1.20 *Methods of linking bifunctional complexing agents to antibodies.*

Entry	Precursor Ligand	Activated Ligand	Comment
1	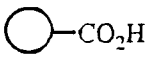	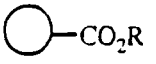	R = succinimidyl, p-nitrophenyl or tetrafluorophenyl
2	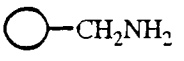	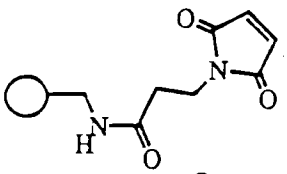	link to thiols rapidly in pH range 5 to 7
3	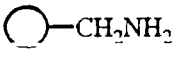	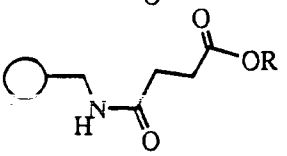	form with symmetrical bis-ester in excess
4	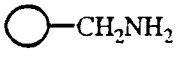	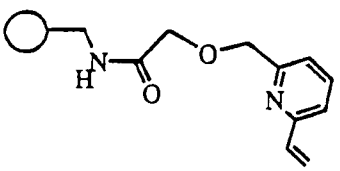	thiol selective in pH range 6-9 ; forms stable thioether
5	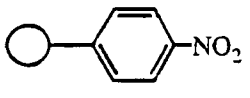	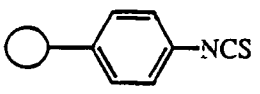	forms stable thiourea with amino groups; prepare with $CSCl_2$
6	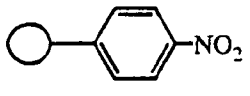	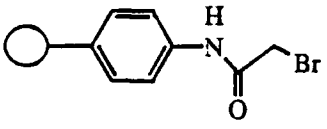	N-alkylation may compete in formation ; link to thiols

1.5.1.3 ANTIBODY CONJUGATES FOR USE *IN VIVO*.

The ^{111}In complex of DTPA-antimyosin is an example of an antibody conjugate in clinical use.[58] The DTPA is covalently linked with one carboxylate to a F(ab') fragment of the antimyosin antibody and the remaining four carboxylates coordinate to ^{111}In. Clearly when the ^{111}In-DTPA complex itself has limited *in vivo* stability (section 1.4.2), this conjugate in which only four carboxylates are binding the In, is susceptible to dissociation *in vivo*. A number of other ^{111}In, ^{99m}Tc and ^{186}Re antibody conjugates are undergoing clinical trials (figure 1.21), but all of these incorporate an acyclic chelating moiety and so do not benefit from the greater kinetic stability attainable by use of macrocyclic bifunctional chelating agents.

FIGURE 1.21 *Examples of antibody conjugates*

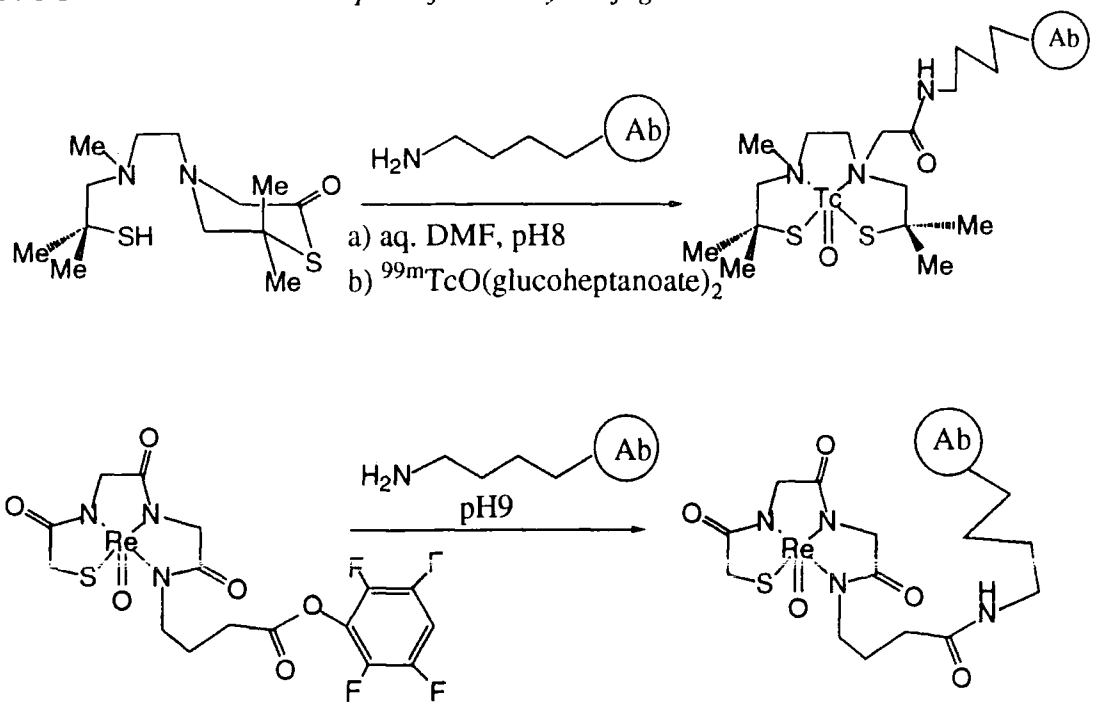

Examples of promising macrocyclic bifunctional complexing agents for antibody conjugation are shown in figure 1.22. Ligand p-NCS-Bz-NOTA (**XIV**) forms stable complexes with ^{67}Ga in which the aryl thiocyanate forms a stable thiourea linkage by reaction with the ε-amino group of an antibody lysine residue.[59] The DOTA-maleimide

FIGURE 1.22 *Macrocyclic bifunctional complexing agents for antibody conjugation.*

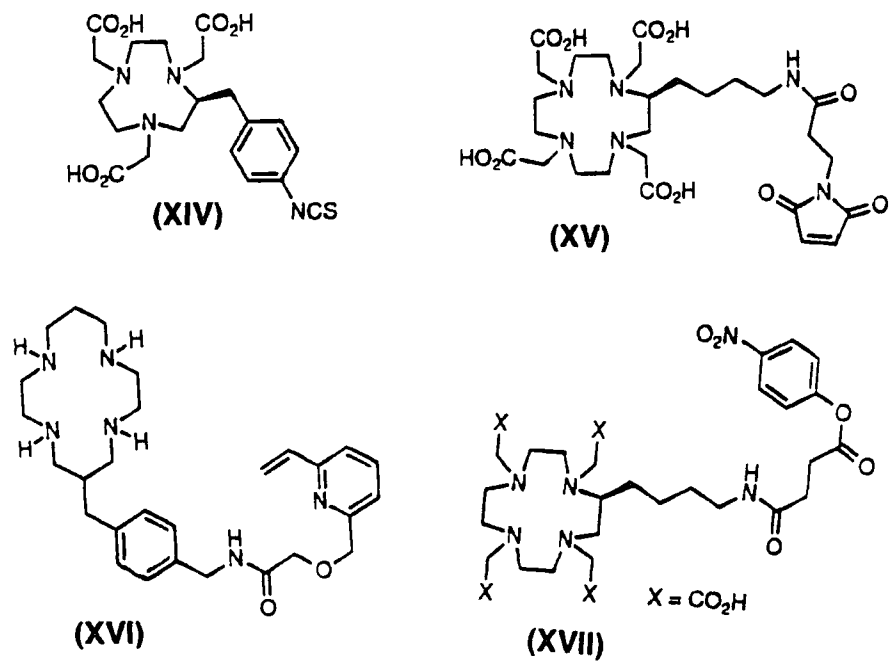

(XV) forms ^{111}In conjugates with antibodies, and can also be used in radioimmunotherapy with ^{90}Y.[60] The C-functionalised cyclam **(XVI)** was treated with a thiol specific vinyl pyridine linker molecule and subsequently conjugated to a thiol residue on an antibody. Biodistribution studies of the Cu (II) complex showed no observable build up of Cu in the kidneys or liver of mice, indicating that it is kinetically stable and potentially useful in tumour diagnosis.[61] The C-functionalised DOTA derivative **(XVII)**[62] was conjugated with B72.3, a tumour localising antibody which binds with a tumour-associated glycoprotein found in human breast and colorectal cancer. Biodistribution studies of the ^{90}Y complex in mice indicate that the highly toxic ^{90}Ydoes not dissociate *in vivo*.[63]

1.5.2 TARGETING USING PEPTIDES

Exciting work in the receptor binding area has shown that perhaps only the peptide sequence involved in receptor binding is necessary to achieve specific uptake in the given target tissue. For example, studies involving conjugates of radiolabelled bifunctional complexing agents with peptides have achieved tumour uptake. The use of peptides and other relatively low molecular weight species has many advantages over targeted macromolecules including comparatively higher metal and amino acid labelling efficiency, potentially rapid blood clearance and an increased ability to pass through capillary vessels into the interstitium.

1.5.2.1 OCTREOTIDE AND SOMATOSTATIN RECEPTOR BINDING

Conjugates of the peptide octreotide have been shown to be somatostatin receptor binding pharmaceuticals. Octreotide is an eight amino acid peptide containing the four amino acids (Phe-D-Trp-Lys-Thr) required for binding to the somatostatin receptor.[64] The structure of somatostatin itself is shown in figure 1.23; it is a 14 residue peptide normally found in hypothalamic extracts which inhibit secretion of growth hormone, insulin and glucagon.[65] Somatostatin receptor-positive tumours expressed on carcinoid tumours and malignant lymphomas may be imaged using radiolabelled octreotide. The ^{111}In labelled DTPA conjugate with octreotide **(XVIII)** exhibits strong binding to the somatostatin receptor with an IC_{50} value in the nanomolar range, and with non specific binding less than 10% of total binding.[66] Clinical studies in humans have shown very promising results[26] DTPA was covalently linked to D-Phe at one end of the octapeptide, although better tumour / tissue discrimination would be obtained if a C-linked DTPA or NOTA complexing agent had been used.

FIGURE 1.23 *Comparison of the structures of somatostatin and the DTPA-octreotide conjugate* **(XVIII)**.

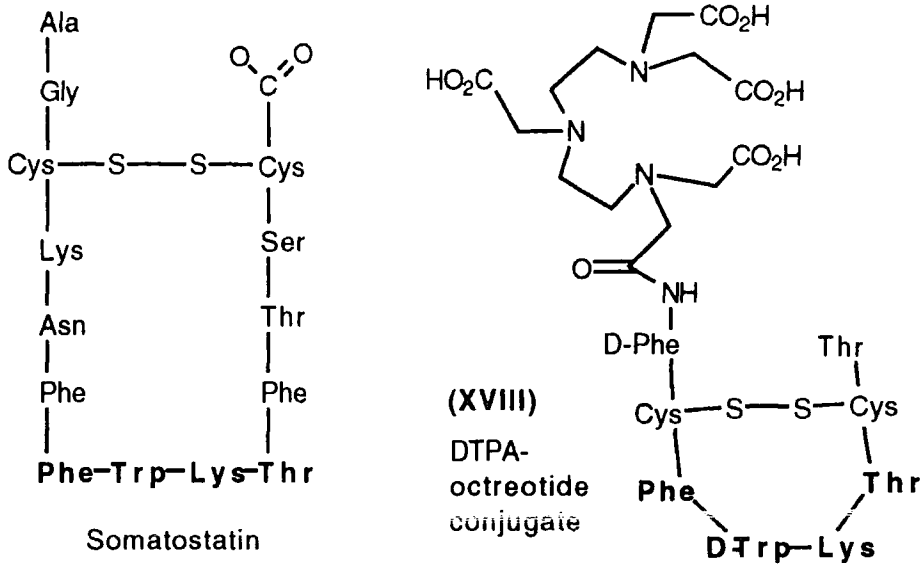

One of the major limitations of the use of peptides as pharmaceuticals is their susceptibility to proteolysis. In the case of octreotide, the four essential amino acids are stabilised to proteases in the body by disulphide cyclisation from the two cysteines incorporated in the molecule and by the placement of the D-amino acids.

1.5.2.2 TUFTSIN AND MACROPHAGE RECEPTORS

Tuftsin is a peptide which is targeted to normal host cells called macrophages associated with abnormal tissue in a tumour. Tuftsin is a naturally occurring linear tetrapeptide (L-Thr-L-Lys-L-Pro-L-Arg). It is generated in the body from a specific cytophilic fraction of the protein leukokinin through a two step enzymatic processing mechanism, employing tuftsin *endocarboxypeptidase* and then *leukokinase*. Tuftsin was isolated in the 1970's[67] and it was discovered that it possesses immunologically mediated anti-tumour potential;[68] being non toxic (LD_{50} mice 2.5g /kg) it became an ideal candidate for tumour targeting.

Macrophages are scavenger cells which form part of the immune system and demonstrate a range of immunological processes.[69] They recognise, engulf and dispose of damaged cells and foreign invaders by means of a process called phagocytosis, and participate in surveillance against microbial infections and cancer by antigen presentation, lymphocyte activation, tumoricidal and bactericidal activities.

Macrophages differ in morphology and possess receptors for many ligands. Those macrophages found in human tumours form a characterised sub-population of cells for

targeting. The macrophage content of tumours varies considerably and it has been shown that the macrophage densities are highest at the tumour periphery and in areas of necrosis. Targeting tumour-infiltrating macrophages may detect necrotic regions and delineate boundaries between normal and infiltrating neoplastic tissue, it may also assist in detection of small metastases since the macrophage densities are highest in smaller lesions.[70]

FIGURE 1.24 *Macrophage engulfing a foreign particle by phagocytosis.*

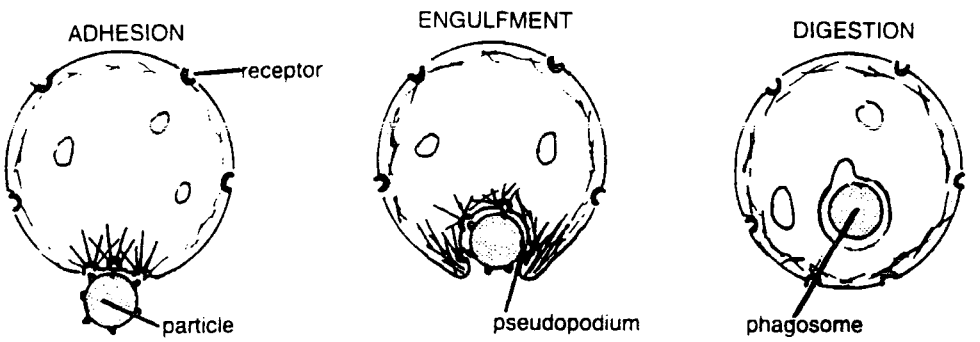

Macrophage phagocytic activity is stimulated by tuftsin. This takes place in stages:

(1) Association of peptide and macrophage cell is initially electrostatic in nature.

(2) Fast accommodation of tuftsin into specific receptor sites.

(3) Subsequent rapid internalisation of the peptide-receptor complex.

The nature of the binding site has been the subject of much research.[71,72,73] While still not well understood, it is clear that binding is specific, fast, saturable and reversible. Analysis has shown that there is only one type of site,[74] but that there may be 75,000 receptors per macrophage.[75]

Binding of tuftsin to macrophages depends on strict conservation of molecular structure,[76] in formation of conjugates the following actions often impair tuftsin activity:

(1) Amino acid substitution or deletion at the C-terminus, N-terminus or within the chain.

(2) Absence of free amino or carboxyl groups at peptide termini.

(3) Substitution or alteration of the guanidine side chain.

(4) Lengthening the chain by addition of amino acids at either terminus.

Tuftsin analogues which have been studied, and which retain biological activity are formed by extension of the C-terminus,[77] the ε-amino group of the Lys residue[78] or the N-terminus. The biologically active fluorescent tuftsin analogues shown in figure 1.25 were synthesised from the corresponding isothiocyanates to visualise the interaction of tuftsin with macrophages and similar cells. Tritium labelled tuftsin has also been utilised in these studies[74] but to date there have not been any reports of tuftsin used in tumour diagnosis.

FIGURE 1.25 *Biologically active fluorescent tuftsin conjugates.*

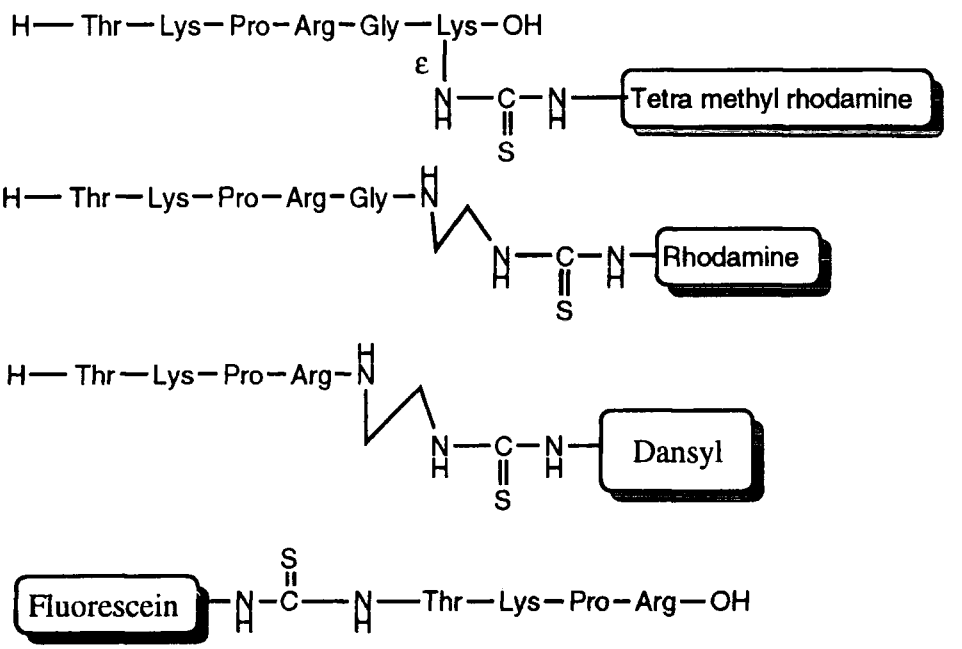

1.5.3 TARGETING USING NITROIMIDAZOLES

1.5.3.1 HYPOXIA AND RADIOTHERAPY

Many malignant tissues are low in oxygen due to poor vascularisation during their rapid growth. This oxygen deficiency is termed hypoxia.[79] Radiation causes biochemical changes that interfere with the cancer cells' ability to divide indefinitely. Ions and fast electrons produced when radiation energy is absorbed react with molecules to produce free radicals. These aqueous free radicals interact with DNA's purine and pyrimidine bases to form organic radicals or with the phosphate bond to disrupt the sugar phosphate chain. Organic radicals can in turn react with oxygen to produce organic peroxides that prevent restoration of the molecule. Unfortunately in hypoxic cancer cells the oxygen concentration is so low that these peroxides do not

form and the radiation dosage required to kill the cells may be as much as three times that required to destroy normal cells.[80]

1.5.3.2 RADIOSENSITISERS

Primary effort has focused on chemical agents able to enhance radiosensitivity of hypoxic cells in a manner analogous to oxygen, but which have no effect upon normoxic cells. These oxygen mimetics have the free radical properties of dioxygen. Some typical examples are the nitroxyl free radicals **(XIX)** and **(XX)**.

FIGURE 1.26 *Typical radiosensitisers.*

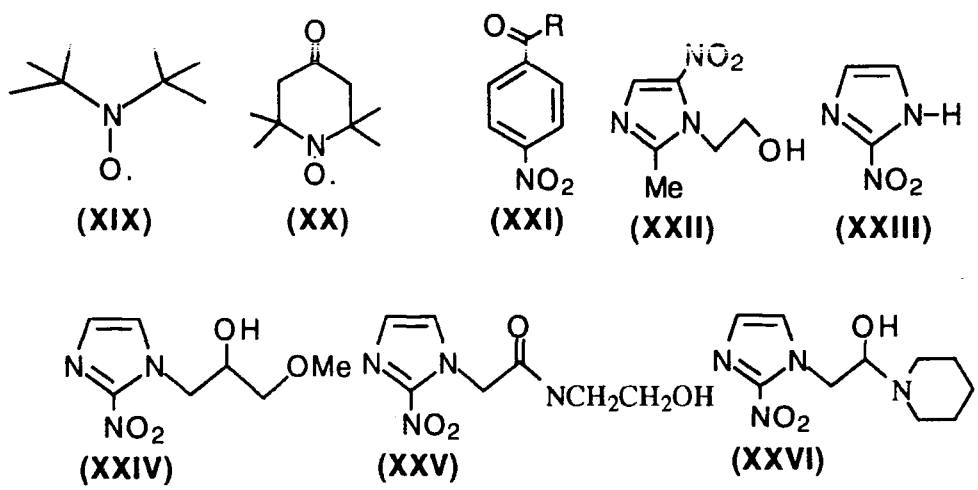

It was also observed that *in vitro* radiosensitising activity correlates with electron affinity, partition (logP) and pK_a. This prompted development of electron affinic agents which are (i) essentially non-toxic, (ii) able to diffuse into hypoxic cells and (iii) are not rapidly metabolised *in vivo*. The nitroarene **(XXI)**, many quinones including isoindole-4,7-diones and nitroheteroarenes such as **(XXII)** are just some examples. Most attention has focused on nitroimidazole derivatives[81,82] such as the natural antibiotic azomycin **(XXIII)** and its 2-propanol derivative misonidazole **(XXIV)** which both show *in vivo* radiosensitising properties. These properties substantially increase in the series of compounds including etanidazole **(XXV)** and pimonidazole **(XXVI)**.[22] It is assumed that the nitro group of the nitroimidazole is reduced enzymatically in the absence of oxygen and retained in hypoxic tissue with some selectivity.[83,84,85]

The one electron reduction of various nitroimidazoles has been reviewed.[81] In the absence of oxygen stable electron-adducts are observed which have been characterised as nitroimidazole radical anions. These react rapidly with oxygen or with other highly electron affinic compounds by one electron transfer reactions to regenerate the parent

nitroimidazole. Two and four electron reduction formally yield the corresponding nitroso (Ar-N=O) and hydroxylamine (Ar-NHOH) derivatives. These labile products are cytotoxic interacting with cellular components such as DNA and protein. They often undergo mutual condensation and further reduction to give azoxy and azo (Ar-N=N-Ar) derivatives respectively.

FIGURE 1.27 *The redox 'spectrum' showing electron affinity of nitroaromatic drugs compared to oxygen (most easily reduced). Nitro compounds with $E_{1/7}$ < -0.5 V are not reduced by biological systems ($E_{1/7}$ = one electron redox potential).*[86]

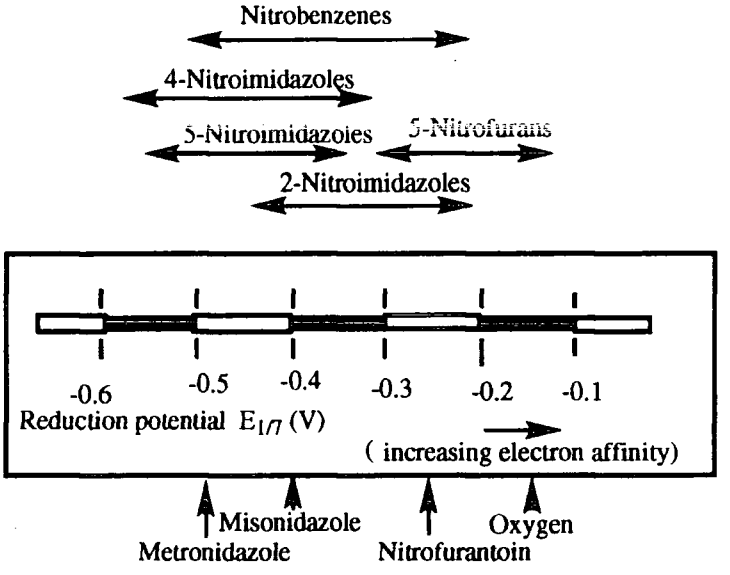

It was found that 2-nitroimidazole is a more efficient radiosensitiser than 5-nitroimidazole, which is in turn more efficient than the corresponding 4-isomer. This would be expected, due to the large difference in electron-affinity between the nitroimidazoles.[87] Attempts were made to further increase electron-affinity and so radiosensitisation by means of a series of 2-nitrofurans; these were more potent *in vitro*. However they were inactive *in vivo* due to poor distribution, metabolism and other biological interactions that removed the compounds before they could reach the tumours.

1.5.3.3 TARGETING OF HYPOXIC TUMOUR TISSUE

Identification of regions of hypoxia is of clinical interest, and since nitroimidazoles accumulate preferentially in hypoxic tissue there have been some studies carried out using radiolabelled nitroimidazoles in order to trace these tissues. Work conducted with ^{14}C and ^{3}H labelled misonidazole[88] showed accumulation in the human melanotic melanoma HX118,[89] a tumour known to be hypoxic. Good contrast between hypoxic

and normoxic regions of myocardial tissue was demonstrated using an ^{18}F-labelled derivative of misonidazole (**XXIV**).[90]

The 4-fluorobenzylamine conjugate of 2-nitroimidazole (**XXVII**) was proposed as a suitable PET hypoxia imaging agent and more recently tests have been carried out on the 3-iodo analogue for use in SPECT.[91] Another class of nitroimidazole conjugates (**XXVIII**) have been developed for use in boron neutron capture therapy of cancer,[92,93] but unfortunately their poor water solubilities have precluded biological evaluation to date.

FIGURE 1.28 *Potential nitroimidazole radiopharmaceuticals*

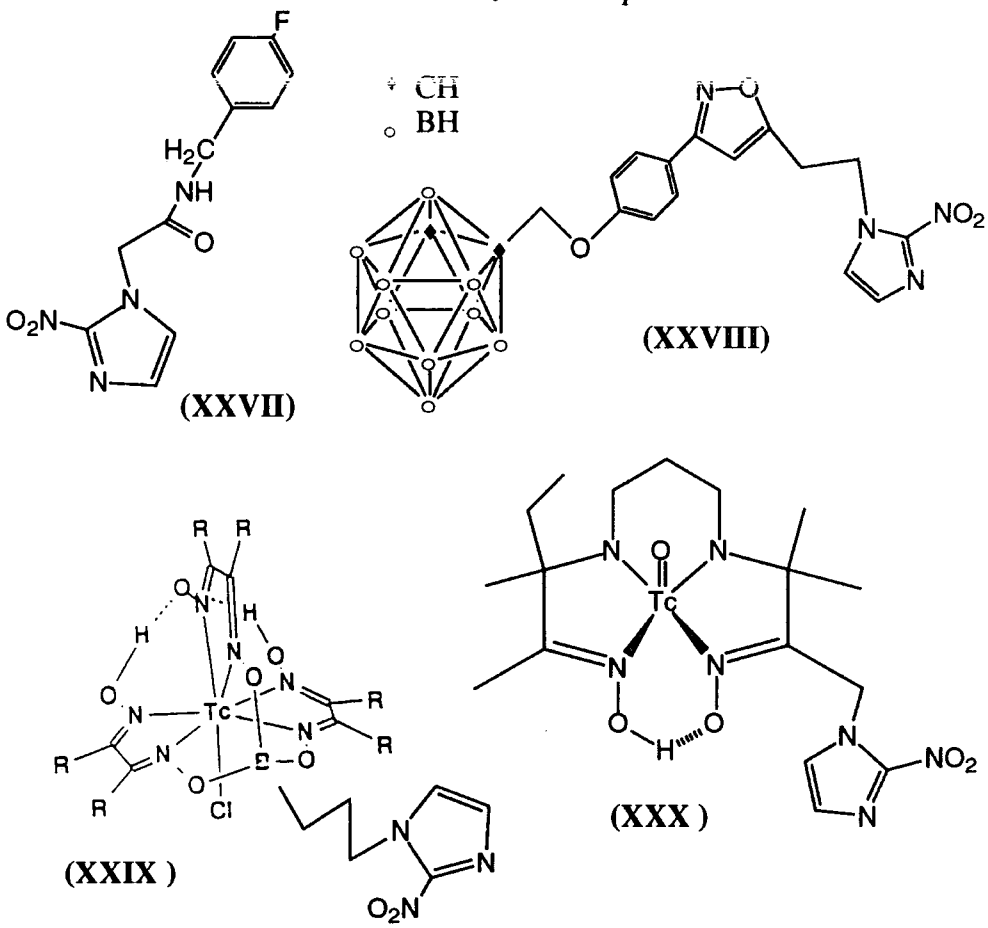

Boronic Acid Adducts of Technetium diOximes (BATOs) (**XXIX**) were originally developed as organ perfusion radiopharmaceuticals, but by incorporating a nitroimidazole group onto the boronic acid they can be targeted to hypoxic tissues. A number of these ^{99m}Tc compounds incorporating different linkage groups between the nitroimidazole and boronic acid group have been prepared and show promising initial biological results.[94] Another potential new radiopharmaceutical of great interest is TcO(PnAO)-1-(2-nitroimidazole) (**XXX**).[95,96] The complex is initially distributed by perfusion but is apparently retained selectively in regions of hypoxia within rabbit

hearts by metabolism. Results from electrochemical studies and enzyme studies at pH 7.4 with xanthine oxidase showed reduction of the 2-nitroimidazole group under hypoxic, but not oxic, conditions. The TcO(PnAO) moiety was unaffected under identical conditions. Thus a potential mechanism for preferential localisation of the radiopharmaceutical in hypoxic tissue was demonstrated.

1.5.4 TARGETING USING ACRIDINE INTERCALATORS.

1.5.4.1 DNA INTERCALATING AGENTS

Predating antibiotics and sulphonamides, aminoacridines such as 9-aminoacridine found uses as antibacterial agents and phenanthridines such as 'ethidium' as trypanocidal agents in cattle. Their mode of action was not well understood and there was little progress in studies of drug-DNA interactions until 1961 when it was proposed that proflavine intercalates into DNA, a process whereby the planar acridine ring comes to be inserted between the base pairs of the Watson-Crick helix.[97]

FIGURE 1.29 *Some examples of DNA intercalating agents.*

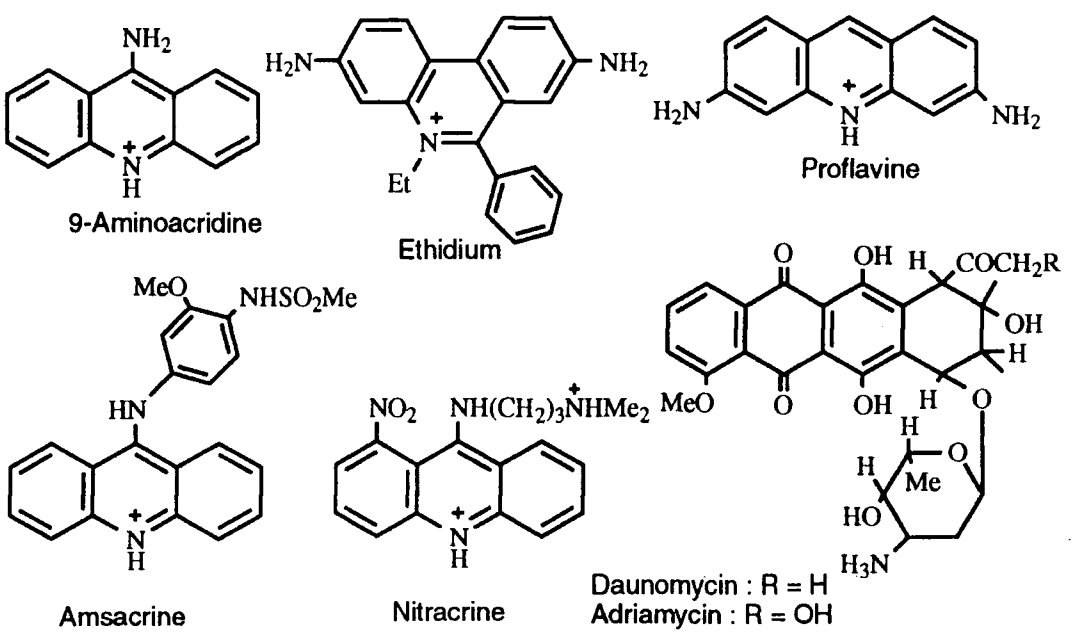

A rapid expansion in studies of physiochemical properties and the capacity of DNA intercalators to inhibit DNA function followed. In the 1970's attention became devoted largely to the development of intercalating antitumour agents; the anilinoacridine 'amsacrine', the 9-aminoacridine 'nitracrine' and the anthracycline antibiotic 'adriamycin' were all products of this era. Nowadays DNA intercalators with an established place in the clinic include 'actinomycin', 'daunomycin', 'adriamycin',

'amsacrine' and 'mitoxantone'. Many more intercalators are undergoing clinical trials as research in this field continues.

1.5.4.2 INTERCALATION

DNA is unusual as a drug receptor because its three-dimensional structure and dynamic properties are understood in great detail. In the simplified model shown in figure 1.30 (a) the sugar-phosphate backbone is represented as a smooth coil and the base pairs are shown in edgewise projection. DNA-intercalator complex formation is usually freely reversible, its driving force being a combination of electrostatic, entropic, hydrogen bonding, van der Waals and hydrophobic interactions. The planar intercalator molecule becomes inserted between the DNA base pairs as indicated in figure 1.30 (b). The major changes to the DNA upon intercalation are an increase in length and some unwinding of the helix around the intercalation site.

FIGURE 1.30 *The intercalation model: (a) double helical DNA (b) the same DNA containing intercalated drug molecules.*

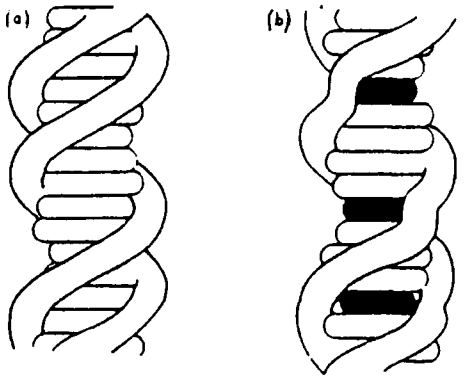

Intercalating agents are cytotoxic to dividing, but not quiescent cells, they generally prevent progression beyond the G2 + M phase of the cell cycle.[98] It is at the M stage of the cell cycle that the nuclear membrane is ruptured to allow division, and so drugs which are unable to be transported across this membrane may still access the chromosomes within the nucleus. Intercalating agents also induce chromosomal abnormalities, concentrate in the nucleus or nucleolus, condense chromatin and inhibit DNA and RNA synthesis.

FIGURE 1.31 *The cell cycle.*

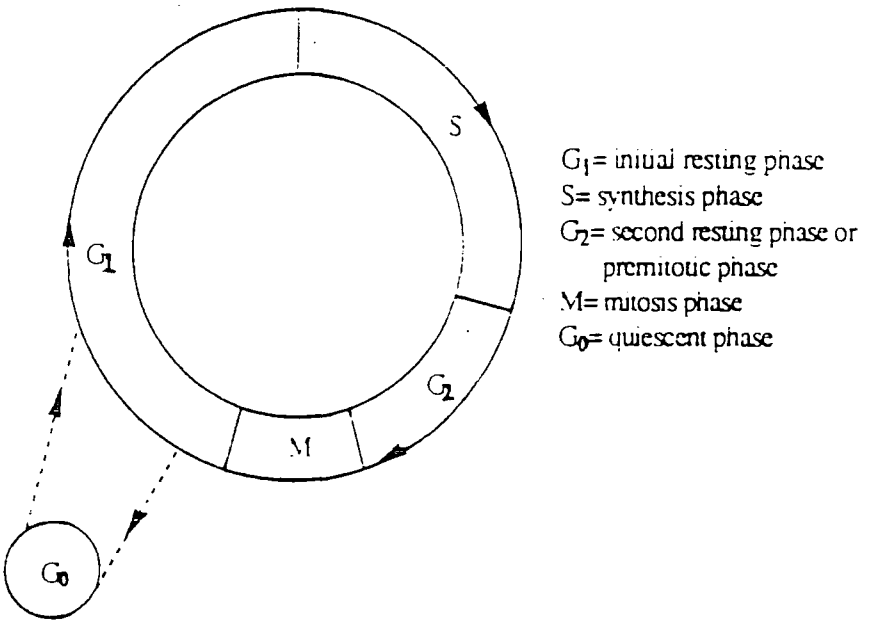

1.5.4.3 ACRIDINES

Acridines are often regarded as the archetypal DNA intercalating agents[99] since proflavine was first used to demonstrate this phenomenon. The driving forces for acridine intercalation are stacking and charge transfer interactions, with a lesser role being played by polar forces (H bonding and electrostatic forces). Acridines possess high association constants with DNA, even under high salt physiological conditions, where almost all intracellular acridine will be found bound to nucleic acids.

Nitracrine was developed in Poland, and still sees widespread use there for mammary and ovarian carcinomas. It owes at least some (if not all) of its activity to its aromatic nitro group, however this also leads to avid binding of DNA and prevents good transport *in vivo*. Amsacrine is widely used in the treatment of leukaemia and malignant lymphomas; it binds DNA selectively over RNA and also has the ability to inhibit certain enzymes.

A study was carried out to determine whether the charge-transfer and binding properties of 'amsacrine' could be improved by attaching a cationic side chain to the acridine.[100] One of the resulting acridines in particular, 9-aminoacridine-4-carboxamide **(XXXI)**[101] proved to have a high affinity for DNA. This compound is a dication at physiological pH (pK_a = 8.30) and in addition to intercalation of the acridine, the dimethylammonium side chain binds to the minor groove of DNA. It is active against leukaemia, but shows little activity against solid tumours. Removal of

the 9-amino group broadens the spectrum of activity to include solid tumours as observed with the acridine carboxamide (**XXXII**).[102] This compound is neutral at physiological pH (pK_a = 3.54), leading to a ten-fold decrease in DNA affinity, but it shows increased antitumour activity due to improved transport properties.

FIGURE 1.32 *Anti-tumour acridine carboxamides.*

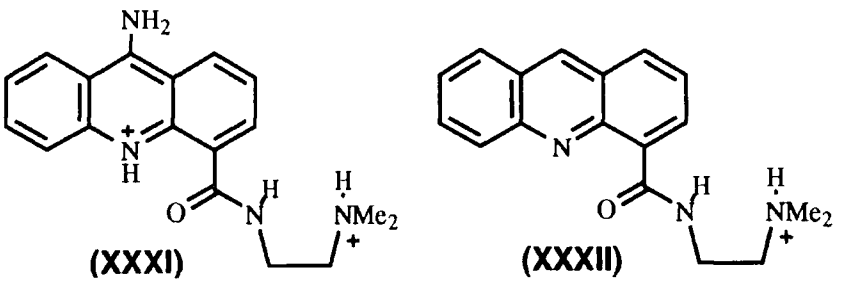

Acridines may be reversibly and predictably bound to cellular DNA, due to their classical planar, hydrophilic, weakly basic character. This favourable stability and accessibility of the acridine moiety has rendered the synthesis of a wide variety of modified structures possible.

1.5.4.4 TARGETING DNA WITH INTERCALATOR CONJUGATES

Attempts have been made to further enhance the selectivity of hypoxia selective nitroimidazoles by targeting them to the DNA of hypoxic cells with intercalating groups. For example the phenanthroline nitroimidazole conjugate (**XXXIII**)[103,104] was found to bind to DNA, show selectivity for hypoxic cells (8-fold) and produce radiosensitisation *in vitro*.

FIGURE 1.33 *Intercalator-nitroimidazole conjugates for targeting DNA.*

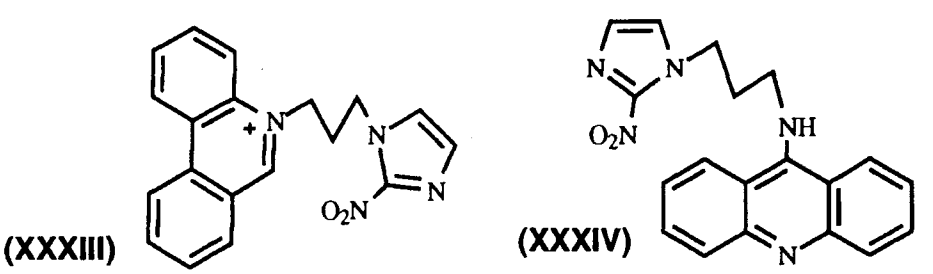

The analogous acridine compound (**XXXIV**)[105] has demonstrated a DNA binding affinity almost as high as 9-aminoacridine itself. It also has a similar pK_a value of 9.5, but lacks a permanent positive charge. The solubility and reduction potential were

similar to that of misonidazole, but its hypoxic selectivity was only 6-fold compared to 11-fold in the case of misonidazole. In addition this compound possesses a high cytotoxicity such that this group of compounds were unsuitable for use *in vivo*.

Many studies have been conducted on the interaction of metal complexes with DNA, the metal centre has found uses as a sensitive spectroscopic handle to examine the region of the nucleic acid to which it is bound. The iron (II) complex of methidium propyl-EDTA (MPE-Fe) **(XXXVIII)**[106] has gained rapid recognition as a DNA footprinting agent, useful in defining the location of small ligands that bind DNA. These synthetic nucleases, due to their small size and lack of specificity, have allowed a more accurate resolution of binding sites than other agents.

FIGURE 1.34 *Intercalator-metal complexes.*

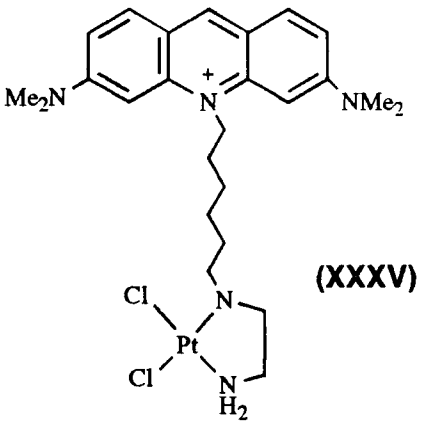

(XXXV)

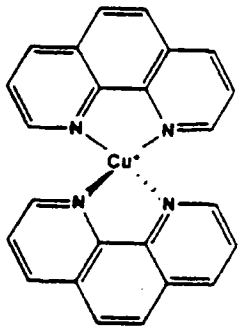

Cu(phen)$_2^+$

(XXXVI)

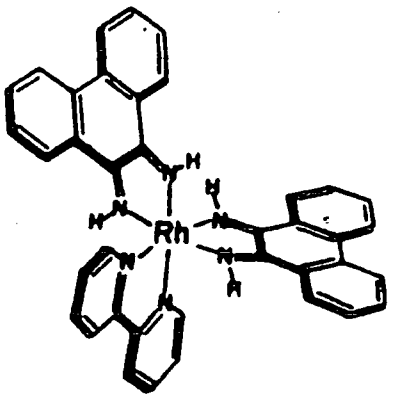

Rh(phi)2(bpy)$^{3+}$

(XXXVII)

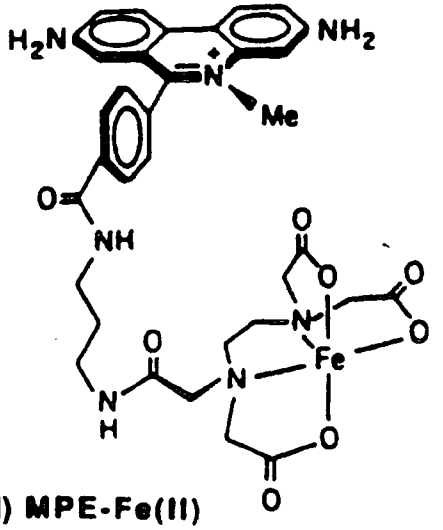

(XXXVIII) MPE-Fe(II)

Recently it was discovered that intercalation is not restricted to completely flat, square planar complexes, but partial intercalation of ligands coordinated to other metal centres

is feasible as well. Examples of this include the bis(phenanthroline) cuprous ion(**XXXVI**),[107] tris(phenanthroline)complexes of Co(II) and Rh(II) and the phenanthrenequinone diimine complexes of Rh(II) (**XXXVII**)[108] which may be used as spectroscopic tags or in redox cleavage of DNA.

There has also been interest in the DNA-binding properties of intercalators and platinum complexes in the presence of one another. The platinum (II) complex (**XXXV**)[109,110] has been prepared and studies conducted to examine the DNA-binding of the intercalator, and whether it enhanced the antitumour properties of the *cis*-diamminedichloro-platinum (II) moiety. It may clearly be seen how development of such ligands could lead to the production of radiolabelled intercalator conjugates for targeting DNA, and in particular the DNA of tumour cells.

1.6 SCOPE OF THIS WORK.

It has been suggested that the state of anticancer chemotherapy at present most probably equates to the state of antimicrobial chemotherapy at the turn of the century where compounds of mercury, antimony and arsenic were used. These of course were better than nothing, but hardly very effective and certainly accompanied by very serious side effects.

There exists much scope for improvement of cancer chemotherapy at present, in particular the design of new drugs which limit toxic effects by targeting the tumour cells and delivering their lethal dose specifically. This study contains work on ligands suitable for radioisotopes and paramagnetic complexing agents, for use in tumour diagnosis. It then goes on to address novel approaches to targeting using nitroimidazole, tuftsin and acridine conjugates of such ligands.

Radiopharmaceutical chemistry is very much an interdisciplinary effort, and requires the collaboration of scientists from various fields, including organic and inorganic chemistry, biochemistry, radiochemistry and nuclear medicine. This project involves collaboration with the MRC Radiobiology Unit in Chilton, the Royal Marsden Hospital and Celltech.

1.7 REFERENCES

1 All multicellular organisms except sharks, 20 years of studies at the Mote Institute, USA have failed to induce cancer in sharks; J. Mathews, *J. Nat. Cancer Institute*, 1992, **84**, 1237; J. Mathews, *J. Nat. Cancer Institute*, 1992, **84**, 1000.

2 Richard E. LaFond *Cancer the Outlaw Cell*, American Chemical Society, 1988.

3 *1993 World Health Statistics*, World Health Organisation, Geneva, 1994.

4 C. Muir, J. Waterhouse, T. Mack, J. Powell and S. Whelan, *Cancer Incidence in Five Continents*, Volume V, International Agency for Research on Cancer, Lyon, 1987.

5 *1993 Health in Scotland*, the Scottish Office, HMSO, Edinburgh, 1994.

6 E. Skinner, *Skin Cancer, the Sun and You, Your Questions Answered*, Cancer Research Campaign, London, 1991.

7 *Scottish Health Statistics 1993*, Information and Statistics Division, Directorate of Information Services, the National Health Service in Scotland, Edinburgh, 1993.

8 R.J. Black, L. Sharp and S.W. Kendrick, *Trends in Cancer Survival in Scotland, 1968-90.*, Information and Statistics Division, Edinburgh, 1993.

9 P.B. Farmer and J.M. Walker, *The Molecular Basis of Cancer*, Croom Helm, London, 1985.

10 R.D. Neirinckx, *Chem. Br.*, 1986, 335.

11 I.J. Fidler and I.R. Hart, *Science*, 1982, **217**, 998.

12 D.M. Kean and M.A. Smith, *Magnetic Resonance Imaging - Principles and Applications,* William Heinemann Medical Books, London, 1986.

13 R.B. Lauffer, *Chem. Rev.*, 1987, **87**, 901.

14 M.F. Tweedle in 'Lanthanide Probes in Life, Chemical and Earth Sciences', Eds. J-C.G. Bunzli and G.R. Choppin, Elsevier, Amsterdam, 1989, chapter 5, pp.127-173.

15 I. Bertini and C. Luchinat, 'NMR of Paramagnetic Molecules in Biological Systems', Benjamin Cummings, Boston, MA, 1986.

16 D. Parker, *Imaging and Targeting* in 'Comprehensive Supramolecular Chemistry', Volume 10, Chapter 17, Eds. D.N. Reinhoudt and J.M. Lehn, Pergamon, 1995.

17 G.P. Saha, 'Fundamentals of Nuclear Pharmacy' 2nd Ed., Springer-Verlag, New York, 1984, p. 84.

18 P.C. Jackson, 'Radionuclide Imaging in Medicine - Theory and Practice', Farrand Press, London, 1986.

19 M.E. Phelps, J.C. Mazziotta, 'Positron Emission Tomography: Human Brain Function and Biochemistry', *Science*, 1985, **228**, 799-809.

20 D. Parker, *Chem. Soc. Rev.*, 1990, **19**, 271-290

21 C.K. Bomford, I.H. Hunter and S.B. Sherriff, *Walter and Miller's Textbook of Radiotherapy: Radiation Physics, Therapy and Oncology*, 5 Ed., Longman, Singapore, 1993, p. 28.

22 M.J. Suto, 'Radiosensitizers', in *Annual Reports in Medicinal Chemistry*, Plattner Ed., Academic Press, 1991, pp 151-160.

23 H.A. O'Brien, in *Radioimmunoimaging and Radioimmunotherapy*, Eds. S.W. Burchiel and B.A. Rhodes, Elsevier Science Publishing Co., Amsterdam, 1983, p. 161.

24 S.C. Srivastava, 'Radiolabeled Monoclonal Antibodies for Imaging and Therapy', Plenum, New York, 1988.

25 D. Parker and K.J. Jankowski, in *Advances in Metals in Medicine*, eds. B.A. Murrer and M.J. Abrams, Jai Press, New York, 1993, Vol. 1, pp. 29-73.

26 S. Jurisson, D. Berning, Wei Jia and Dangshe Ma, *Chem. Rev.*, 1993, **93**, 1137.

27 H.M. Chilton and R.L. Witcofski, in *Pharmaceuticals in Medical Imaging*, Eds. D.P. Swanson, H.M. Chilton and J.H. Thrall, Macmillan Publishing Co., New York, 1990, p 285.

28 H.M. Chilton and R.L. Witcofski, in *Pharmaceuticals in Medical Imaging*, Eds. D.P. Swanson, H.M. Chilton and J.H. Thrall, Macmillan Publishing Co., New York, 1990, pp594-598.,

29 J.R. Morphy, D. Parker, R. Kataky, M.A.W. Eaton, A.T. Millican, R. Alexander, A. Harrison and C.A. Walker, *J. Chem. Soc., Perkin. Trans. 2*, 1990, 573.

30 J.J.R. Frausto da Silva, *J. Chem. Educ.*, 1983, **60**, 390.

31 K. Erkson, A. Lilja, M. Bergstrom, V.P. Collins, L. Erikson, E. Ehrin, H. Von Holst, H. Lunquist, B. Langstrom and M. Mosskin, *J. Comput. Assist. Tomogr.*, 1985, **9**, 683.

32 H.M. Chilton and R.L. Witcofski, in *Pharmaceuticals in Medical Imaging*, Eds. D.P. Swanson, H.M. Chilton and J.H. Thrall, Macmillan Publishing Co., New York, 1990, pp. 330-342.

33 C.H. Taliaferro, R.J. Motekaitis and A.E. Martell, *Inorg. Chem.*, 1984, **23**, 1188.

34 C.J. Mathias, Y. Sun, M.J. Welch, M.A. Green, J.A. Thomas, K. Wade and A.E. Martell, *Nucl. Med. Biol.*, 1988, **15**, 69.

35 W.A. Volkert, J. Simon, A.R. Ketring, R.A. Holmes, J. Simon and D. Wilson, *Drugs of Future*, 1987, **14**, 799.

36 W.A. Volkert and E.A. Deutsch, in *Advances in Metals in Medicine*, eds. B.A. Murrer and M.J. Abrams, Jai Press, New York, 1993, vol. 1, pp. 115-153.

37 T. Rhyl, *Acta Chem. Scand.*, 1972, **26**, 3955.

38 C.F. Meares, *Nucl. Med. Biol.*, 1986, **13** (4), 311.

39 G.R. Pearson, *J. Am. Chem. Soc.*, 1963, **85**, 3533.

40 R.D. Hancock, *J. Chem. Educ.*, 1992, **69**, 615.

41 R.D. Hancock and A.E. Martell, *Chem. Rev.*, 1989, **89**, 1875.

42 D.K. Cabbiness and D.W. Margerum, *J. Am. Chem. Soc.*, 1969, 6540.

43 C.J. Pedersen, *J. Am. Chem. Soc.*, 1967, **89**, 7017.

44 W.N. Setzer, C.A. Ogle, G.S. Wilson and R.S. Glass, *Inorg. Chem.*, 1983, **22**, 266.

45 R.D. Hancock and V.J. Thom, *J. Am. Chem. Soc.*, 1982, **104**, 291.

46 S.M. Hart, J.C.A. Boeyens, J.P. Michael and R.D. Hancock, *J. Chem. Soc., Dalton Trans.*, 1983, 1602.

47 E.T. Clarke and A.E. Martell, *Inorg. Chim. Acta*, 1991, **181**, 273-280.

48 A.S. Craig, D. Parker, H. Adams and N.R. Bailey, *J. Chem. Soc., Chem. Commun.*, 1989, 1792.

49 D.A. Moore, P.E. Fanwick and M.J. Welch, *Inorg. Chem.*, 1989, **28**, 1504.

50 D.A. Moore, P.E. Fanwick and M.J. Welch, *Inorg. Chem.*, 1990, **29**, 672.

51 Rong Ma, M.J. Welch, J. Reibenspies and A.E. Martell, *Inorg. Chim. Acta*, 1995, submitted.

52 J.P. Dubost, M. Leger, M.H. Langlois, D. Meyer and M.C. Schaefer, *C.R. Acad. Sci., Paris Ser. 2*, 1991, **312**, 349.

53 Richard E. LaFond, *Cancer the Outlaw Cell*, American Chemical Society, 1988, p 240.

54 G. Kohler and C. Milstein, *Nature*, 1974, **256**, 495.

55 M.S. Co and C. Queen, *Nature*, 1991, **351**, 501.

56 L. Yuanfang and W. Chuanchu, *Pure Appl. Chem.*, 1991, **63**, 427.

57 E.B. Hawkins, K.D. Pant and B.A. Rhodes, *Antibody, Immunoconj. and Radiopharm.*, 1990, **3**, 17.

58 H.M. Chilton, R.J. Callahan and J.H. Thrall, in *Pharmaceuticals in Medical Imaging*, Eds. D.P. Swanson, H.M. Chilton and J.H. Thrall, Macmillan Publishing Co. New York, 1990, pp 419-461.

59 M.W. Brechbiel, T.J. McMurray and O.A. Gansow, *Tetrahedron Lett.*, 1993, **34**, 3691.

60 A. Harrison, C.A. Walker, D. Parker, K.J. Jankowski, J.P.L. Cox, A.S. Craig, J.M. Sansom, N.R.A. Beeley, R.A. Boyce, L. Chaplin, M.A.W. Eaton, A.P.H. Farnsworth, K. Millar, A.T. Millican, A.M. Randall, S.K. Rhind, D.S. Secher and A. Turner, *Nucl. Med. Biol.*, 1991, **18**, 469.

61 J.R. Morphy, D. Parker, R. Kataky, M.A.W. Eaton, A.T. Millican, R. Alexander, A. Harrison and C. Walker, *J. Chem. Soc., Perkin Trans. 2*, 1990, 573.

62 K.P. Pulukkody, T.J. Norman, D. Parker, L. Royle and (in part) C.J. Broan, *J. Chem. Soc., Perkin Trans. 2*, 1993, 605.

63 C.A.K. Bonebaeck and J.W. Larrick, *Therapeutic Monoclonal Antibodies*, Stockton Press, 1990, New York.

64 W.H. Bakker, R. Albert, C. Bruns, W.A.P. Breeman, L.J. Hofland, P. Marbach, J. Pless, D. Pralet, B. Stolz, J.W. Koper, S.W. LambertsT.J. Visser and E.P. Krennings, *Life Sci.*, 1991, **49**, 1593.

65 L. Stryer, 'Biochemistry', 2 ed., W.H. Freeman, San Francisco, 1981.

66 W.H. Bakker, E.P. Krenning, J.C. Reubi, C. Bruns, W.A.P. Breeman, B. Setyono-Han, M. de Jong, P.P.M. Kooij, C. Bruns, P.M. van Hagen, P. Marbach, T.J. Visser, J. Pless and S.W.J. Lamberts, *Life Sci*, 1991, **49**, 1583.

67 V.A. Najjar and K. Nishioka, *Nature*, 1970, **228**, 672.

68 K. Nishioka, *Br. J. Cancer*, 1979, **39**, 342.

69 P. Gottlieb, E. Tzehoval, M. Feldman, S. Segal and M. Fridkin, *Ann. NY. Acad. Sci.*, 1983, **419**, 107.

70 A.A. Amoscato, P.J.A. Davies, G.F. Babcock and K. Nishioka, *Ann. NY. Acad. Sci.*, 1983, **419**, 114.

71 R.M.G. Nair, B. Ponce and H.H. Fudenberg, *Immunochem.*, 1978, **15**, 901.

72 Z. Spier, V. Zakuth, N. Bogar and M. Fridkin, *Eur. J. Immunol.*, 1977, **7**, 69.

73 A.A. Amoscato, P.J.A. Davies, G.F. Babcock and K. Nishioka, *RES*, 1983, **34**, 53.

74 Y. Stabinsky, P. Gottlieb, V. Zakuth, Z. Spirer and M. Fridkin, *Biochem. Biophys. Res. Comm.*, 1978, **83**, 599.

75 P. Gottlieb, Y. Stabinsky, Y. Hiller, A. Beretz, E. Hazum, E. Tzehoval, M. Feldman, S. Segal, V. Zakuth, Z. Spirer and M. Fridkin, *Ann. NY. Acad. Sci.*, 1983, **419**, 93.

76 Y. Stabinsky, P. Gottlieb and M. Fridkin, *Mol. Cell. Biochem.*, 1980, **30**, 165.

77 P. Gottlieb, E. Hazum, E. Tzehoval, M. Feldman, S. Segal and M. Fridkin, *Biochem. Biophys. Res. Comm.*, 1984, **119**, 203.

78 P. Gottlieb, A. Beretz and M. Fridkin, *Eur. J. Biochem*, 1982, **125**, 631.

79 T.C. Jenkins, 'Hypoxia-Selective Agents: Radiosensitisers and Cytotoxins', in 'Chemistry of Antitumour Agents', D.E.V. Wilman Ed., Chapman and Hall, New York, 1990.

80 J. Parrick, M. Porssa and T.C. Jenkins, *J. Chem. Soc., Perkin Trans. 1*, 1993, 2681.

81 C.E. Smithen and C.R. Hardy, *The Chemistry of Nitroimidazole Hypoxic Cell Radiosensitizers*, in 'Advanced Topics on Radiosensitizers of Hypoxic Cells', Breccia, Rimondi, Adams, Eds. Plenum, New York, 1982.

82 C.E. Smithen, E.D. Clarke, J.A.Dale, R.S. Jacobs, P. Wardman, M.E. Watts and M. Woodcock, 'Novel (nitro-1-imidazolyl)-alkanolamines as potential radiosensitizers

with improved therapeutic properties', in 'Radiation Sensitisers: Their Use in the Clinical Management of Cancer', Ed. L.W. Brady, New York, 1980, pp 22-32.

83 R.J. Maxwell, P. Workman and J.R. Griffiths, *Int. J. Radiat. Oncol. Biol. Phys.*, 1989, **16**, 925.

84 A.J. Franko, J.A. Raleigh, R.G. Sutherland and K.J. Soderlind, *Biochem. Pharmacol.*, 1989, **38**, 665.

85 M.B. Parliament, J.D. Chapman, R.C. Urtasun, A.J. McEwan, L. Goldberg, J.R. Mercer, R.H. Mannan and L.I. Wiebe, *Br. J. Cancer*, 1992, **65**, 90.

86 D.I. Edwards, 'DNA Binding and Nicking Agents' in *Comprehensive Med. Chem.*, Volume 2, 738.

87 I. Ahmed, I.J. Stratford and T.C. Jenkins, *Drug Res.*, 1985, **35**, 1763.

88 L.M. Cobb, J. Nolan and S. Butler, *Int. J. Radiat. Oncology Biol. Phys.*, 1990, **18**, 347.

89 J.M. Walling, J. Deacon, S. Holliday and I.J. Stratford, *Cancer Chemother. Pharmacol.*, 1989, **24**, 28.

90 P.E. Valk, C.A. Mathis, M.D. Prados, W.J. Jagust and T.F. Budinger, *J. Nucl. Med.*, 1991, **32**, 955.

91 A. Najafi, A. Sosa, M.M. Alauddin and M.E. Siegel, *Abs. Papers Am. Chem. Soc.*, 1991, **202**, 76.

92 M. Scobie and M.D. Threadgill, *J. Chem. Soc., Chem. Commun.*, 1992, 939.

93 M. Scobie, M.F. Mahon and M.D. Threadgill, *J. Chem. Soc., Perkin Trans. 1*, 1994, 203.

94 N. Raju, K. Ramalingam and D.P. Nowotnik, *Tetrahedron*, 1992, **48**, 10233.

95 R.J. Di Rocco, A. Bauer, B.L. Kuczynski, J.P. Pirro, K.E. Linder, R.K. Narra and A.D. Nunn, *J. Nucl. Med.*, 1992, **33**, 865.

96 K.E. Linder, J. Cyr, Y.W. Chan, N. Raju, K. Ramalingam and D.P. Nowotnik, A.D. Nunn, *J. Nucl. Med.*, 1992, **33**, 919.

97 L.P.G. Wakelin and M.J. Waring, 'DNA Intercalating Agents' in *Comprehensive Med. Chem.*, Volume 2.

98 C. Norbury and P. Nurse, *Ann. Rev. Biochem.*, 1992, **61**, 441.

99 W.A. Denny in *Chemistry of Antitumour Agents,* D.E.V. Wilman Ed., Chapman and Hall, New York, 1990.

100 W.A. Denny, B.F. Cain, G.J. Atwell, C. Hansch, A. Panthananickal and A. Leo, *J. Med. Chem.*, 1982, **25**, 276.

101 G.J. Atwell, B.F. Cain, B.C. Baguley, G.F. Finlay and W.A. Denny, *J. Med. Chem.*, 1984, **27**, 1481.

102 G.J. Atwell, G.W. Rewcastle, B.C. Baguley and W.A. Denny, *J. Med. Chem.*, 1987, **30**, 664.

103 R. Panicucci, R. Heal, K. Laderoute, D. Cowan, R.A. McClelland and A.M. Rauth, *Int. J. Radiation Oncol. Biol. Phys.*, 1989, **16**, 1039.

104 D.S.M. Cowan, V.M. Kanagasabapathy, R.A. McClelland and A.M. Rauth, *Int. J. Radiation Oncol. Biol. Phys.*, 1992, **22**, 541.

105 W.A. Denny, P.B. Roberts, R.F. Anderson, J.M. Brown and W.R. Wilson, *Int. J. Radiation Oncol. Biol. Phys.*, 1992, **22**, 553.

106 J. Stubbe and J.W. Kozarich, *Chem. Rev.*, 1987, **87**, 1107.

107 D.S. Sigman, *Acc. Chem. Res.*, 1986, **19**, 180.

108 A. Silani, E.C. Long, A.M. Pyle and J.K. Barton, *J. Am. Chem. Soc.*, 1992, **114**, 2303.

109 B.E. Bowler, L.S. Hollis and S.J. Lippard, *J. Am. Chem. Soc.*, 1984, **106**, 6102.

110 B.E. Bowler, K.J. Ahmed, W.I. Sundquist, L.S. Hollis, E.E. Whang and S.J. Lippard, *J. Am. Chem. Soc.*, 1989, **111**, 1299.

Chapter Two

Synthesis, Structure and Biodistribution of Simple Complexes of Ga, In, Gd and Y

2.1 TRIAZACYCLONONANE COMPLEXES

2.1.1 PREVIOUS WORK

Recent work[1] has shown that gallium complexes of hexadentate macrocycles such as those shown in Figure 2.1 are kinetically stable *in vivo* and are excreted intact. The Ga complex of (**1**) also tends to be retained in a malignant melanoma (a xenograft of a skin cancer in a mouse: HX118). Each of these ligands gives a radiolabelled yield of >98% at pH 5.5 (5μM, 37°C) and the radiolabelled complex following injection in a mouse is excreted quite rapidly (>99.8% after 72 hours) usually via the kidney, figure 2.2

FIGURE 2.1

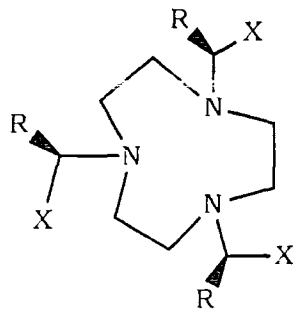

(**1**) X = CO_2H	R = H (NOTA)	(**4**) X = PCH_2PhO_2H	R=H
(**2**) X = $PMeO_2H$	R = H	(**5**) X = CO_2H	R= Me
(**3**) X = $PPhO_2H$	R = H	(**6**) X = CO_2H	R= Ph

FIGURE 2.2 *Biodistribution of ^{67}Ga-NOTA in tumour and tissues.*

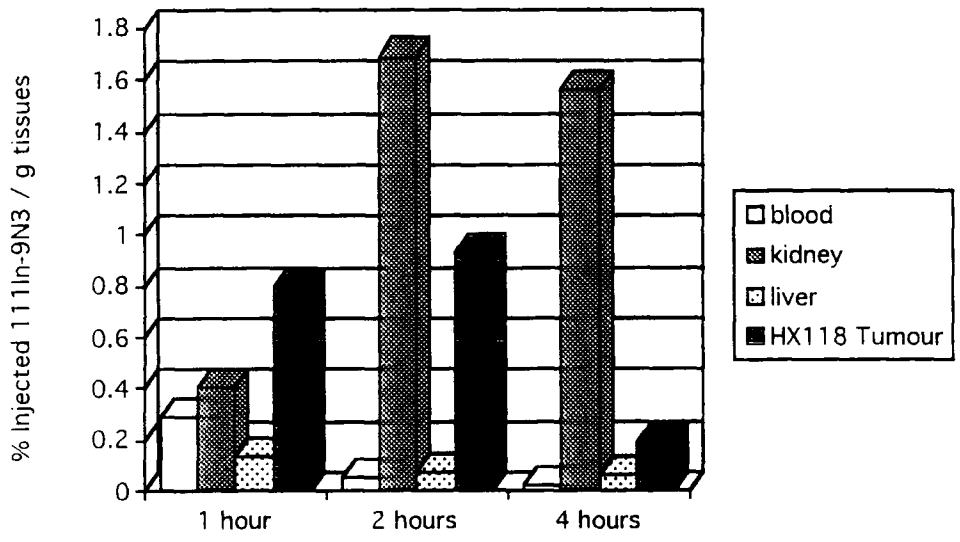

2.1.2 Ga COMPLEXES OF NOTA

1,4,7-Triazacyclononanetriacetate (NOTA)[2] (**1**) was prepared starting from 1,4,7-triazacyclononane (9N3) (**7**) in two steps. Initial treatment of 9N3 with ethylbromoacetate in dry ethanol in the presence of caesium carbonate afforded the triacetate (**8**) in 64% yield after gravitational alumina column chromatography. Subsequent hydrolysis produced (**1**) quantitatively.

The gallium complex of NOTA (**9**) was formed by adding a solution of gallium nitrate in 0.004M nitric acid to a solution of the ligand in nitric acid and maintaining the mixture at room temperature for 24 hours. Recrystallisation from water produced the desired complex as white crystals in 68% yield.

SCHEME 2.1

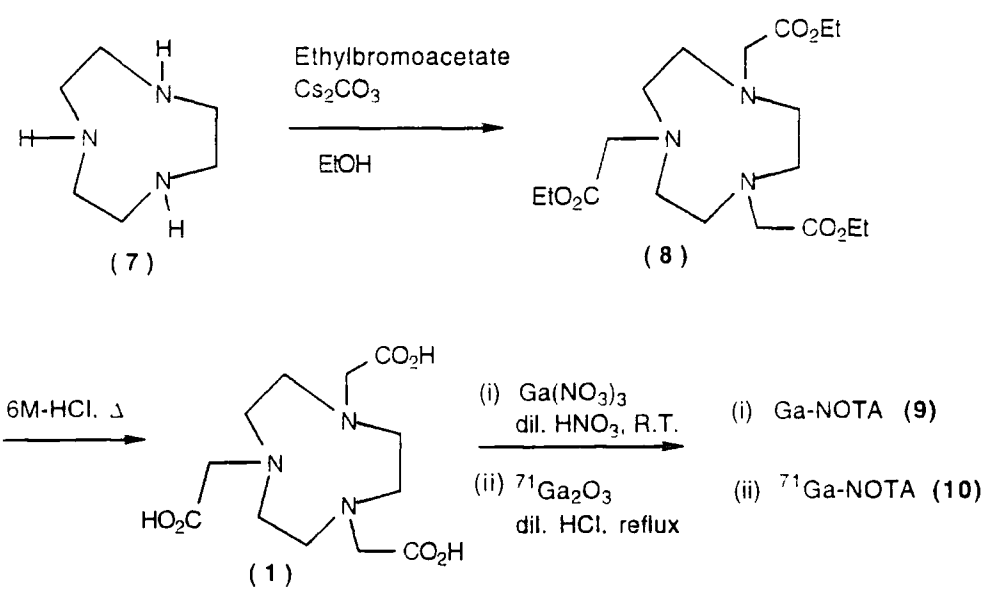

2.1.3 GALLIUM NMR

2.1.3.1 BACKGROUND TO Ga NMR

Gallium has two naturally occurring isotopes, ^{69}Ga and ^{71}Ga which are 60.4% and 39.6% abundant respectively. Both possess a nuclear spin (I = 3/2) but the latter has the higher receptivity and narrower line width[3] as shown in figure 2.3 making it more favourable for NMR despite the less favourable natural abundance.

The observed linewidth of the gallium resonance ($\omega_{1/2}$) may be related to the local symmetry at gallium and to the stability of the complex with respect to exchange

processes. In general a ^{71}Ga linewidth is much greater than would be expected by comparison with say, ^{27}Al.[6] One reason for this is that Ga^{3+} may undergo an exchange process such as self hydrolysis in aqueous solution[7] to produce the $[Ga(OH)(H_2O)_5]^{2+}$ ion. Hydrolysis is suppressed at low pH, so the linewidth is greatly reduced if spectra are obtained in acidic solution.

FIGURE 2.3 *Comparison between the two natural isotopes of gallium.*

	^{69}Ga [4]	^{71}Ga [5]
% Abundance	60%	39.6%
I	$^3/_2$	$^3/_2$
Relative receptivity*	237	319
δ_{Ga}ppm$[Ga(H_2O)_6]^{3+}$in H_2O (Linewidth $\omega_{1/2}$ Hz)	0 (1300)	0 (200-300)
δ_{Ga}ppm$[GaCl_4]^-$ in H_2O (Linewidth $\omega_{1/2}$ Hz)	+243 (870)	+257 (100)

* Relative to ^{13}C

The linewidth of the gallium resonance is also proportional to the interaction of the electric field gradient at the nucleus with the nuclear quadrupole moment. In highly symmetric complexes such as $Ga(OH)_4^-$ and $Ga(H_2O)_6^{3+}$ the electric field gradient at the nucleus is small, and relatively sharp lines may be obtained. The sharp singlet observed in the ^{71}Ga NMR spectrum of [Ga-NOTA] indicates that the C_3 symmetry observed in the solid state (figure 2.4) is maintained in solution. Comparison with other Ga complexes made in figure 2.5 indeed supports the conclusion that the C_3 symmetry leads to the observation of an uncharacteristically narrow ^{71}Ga resonance.

FIGURE 2.4 *X-ray crystal structure of Ga-NOTA showing C_3 symmetry.* [2]

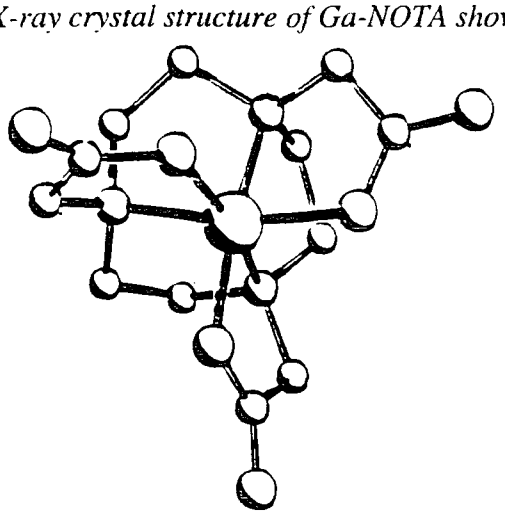

FIGURE 2.5 *Comparison of ^{71}Ga NMR linewidth for a number of complexes.*

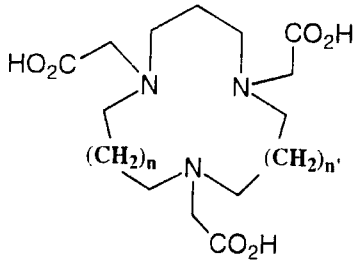

Macrocycle		ligand
9N3		**(1)**
10N3	n=n'=1	**(11)**
11N3	n=1, n'=2	**(12)**
12N3	n=n'=2	**(13)**

ligand	complex	linewidth (Hz)
(1)	Ga.NOTA **(9)**	210
(13)	Ga.**(13)**^{2}	3400
(11)	Ga.**(11)**^{2}	2000
(12)	Ga.**(12)**^{2}	unobservable

2.1.3.2 SYNTHESIS OF ^{71}Ga NOTA COMPLEX

An alternative route to the Ga-NOTA complex was also developed using enriched $^{71}Ga_2O_3$ obtained from Oakridge USA (99% ^{71}Ga). NOTA was stirred in dilute HCl and a solution of $^{71}Ga_2O_3$ in conc. HCl was added and refluxed overnight. White crystals of **(10)** formed directly upon cooling and were used as such in ^{71}Ga NMR experiments.

FIGURE 2.6 *Comparison of ^{71}Ga NMR spectra for complex* **(9)** *and* **(10).**

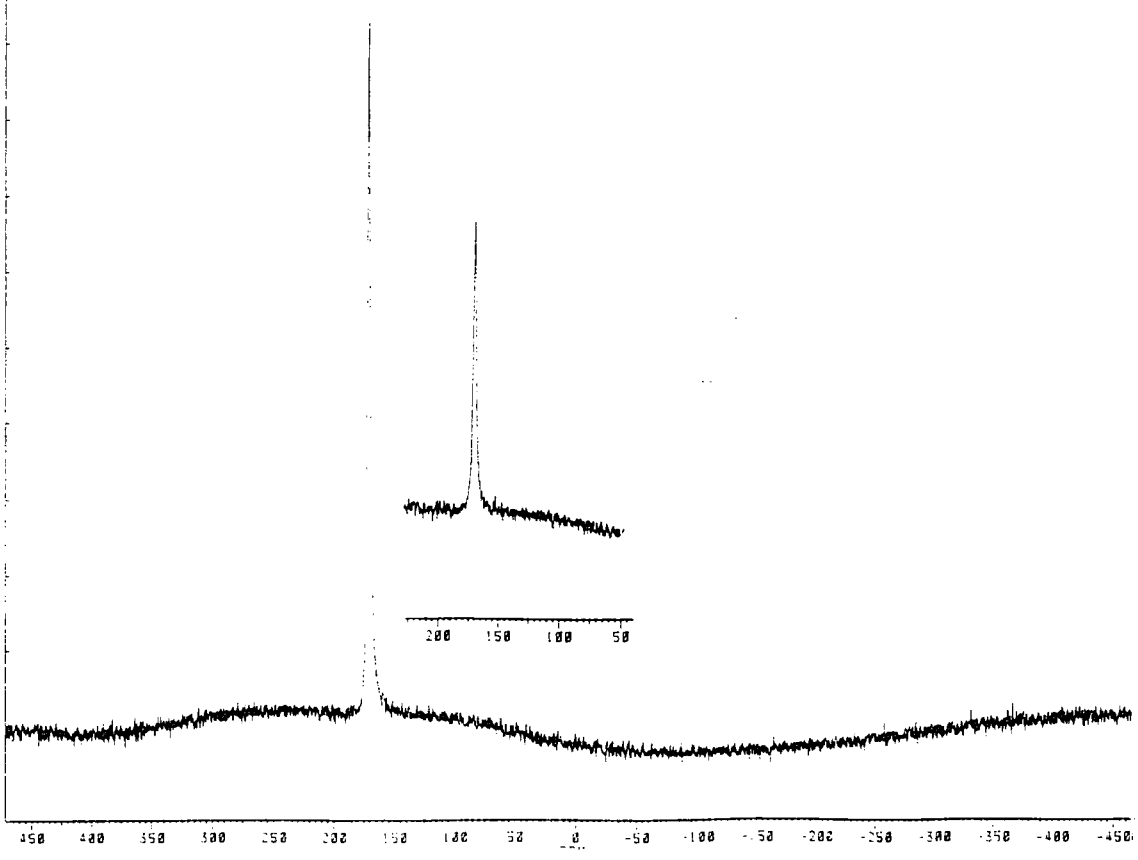

2.1.3.3 *IN VITRO* ^{71}Ga NMR

A comparison of the ^{71}Ga NMR spectra obtained under identical conditions from solutions of equal concentration of Ga-NOTA (**9**) and enriched ^{71}Ga-NOTA (**10**) clearly shows that the former has an integral 40% of the size of the latter (See figure 2.6) reflecting the natural abundance of ^{71}Ga compared to the ^{71}Ga supplied by Oakridge.

2.1.3.4 *IN VIVO* ^{71}Ga NMR

The Ga complex of NOTA had previously been observed by ^{71}Ga NMR spectrometry[2] in the liver of an anaesthetised mouse. 20 minutes after an intravenous injection of an aqueous sample (64µg of complex per gm of tissue) (figure 2.7). The spectrum was acquired with the aid of a Varian external 3cm surface coil probe tuned to ^{71}Ga at 61.0 MHz which was placed over the "sample" to be analysed. The spectrum was callibrated using an authentic sample of Ga.NOTA complex giving δ_{Ga} +171ppm.

FIGURE 2.7 *In vivo ^{71}Ga NMR (a) in the liver of an anaesthetised mouse and (b) in aqueous solution.*[2]

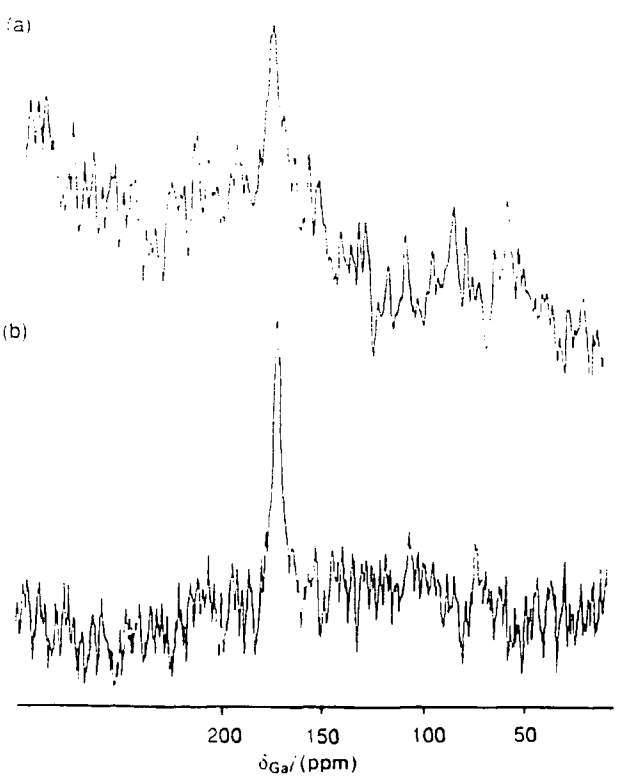

Now using enriched ^{71}Ga compex it was possible to make further studies using the same method to acquire spectra of the complex in the bladder and in a tumour

(HX118). Figure 2.8 clearly shows that 2 hours following injection of a 1.1mg sample the complex was still intact in the bladder of the mouse. However no conclusion could be drawn from the spectrum acquired from the tumour 2 hours following injection. The problems encountered here could be due to the difficulty of directing the probe at specific organs or a tumour in such a small animal. But the δ_{Ga} shift does show that the complex is kinetically robust and suitable for *in vivo* use.

FIGURE 2.8 *In vivo ^{71}Ga NMR in bladder and tumour of mouse.*

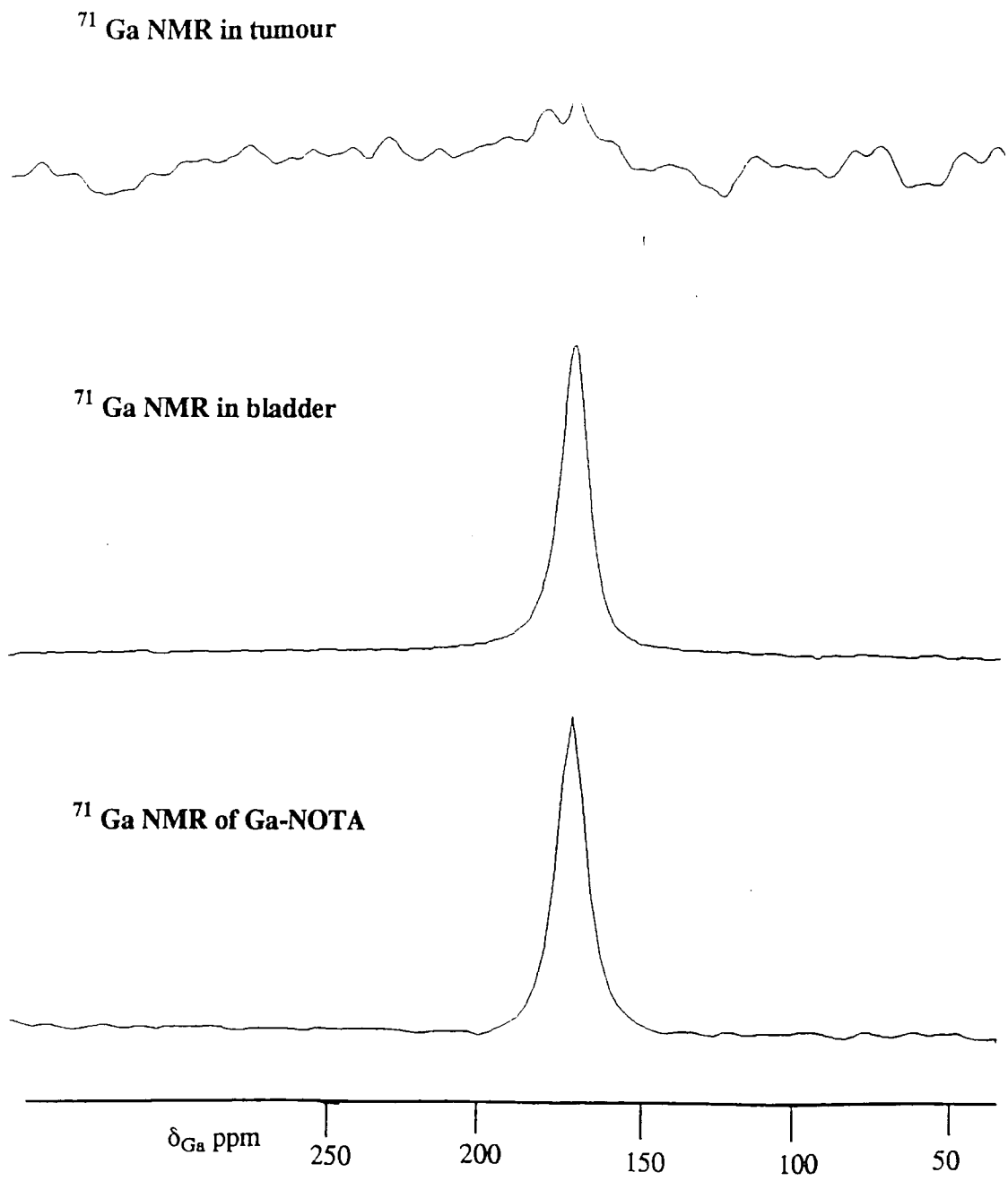

2.1.4 INDIUM COMPLEX OF NOTA

Despite differences in ionic radius, Ga and In share an almost identical aqueous coordination chemistry[8]. The indium complex of NOTA was formed in a similar way to (**9**) and used for biodistribution studies in tumour bearing mice. Figure 2.9 shows the distribution of ^{111}In-NOTA in tumour and tissues. It is interesting to note the high ratios of tumour:blood = 16.6:1 and tumour:liver = 13.3:1 (after 2 hours) especially compared to those for ^{67}Ga-NOTA (13.1:1 and 0.425:1 respectively). Clearly if the complex is taken up by the tumour in amounts adequate for imaging it is advantageous if it also clears from the blood sufficiently fast to provide a low background at early times after administration.

FIGURE 2.9 *^{111}In NOTA biodistribution in tumour and tissues*

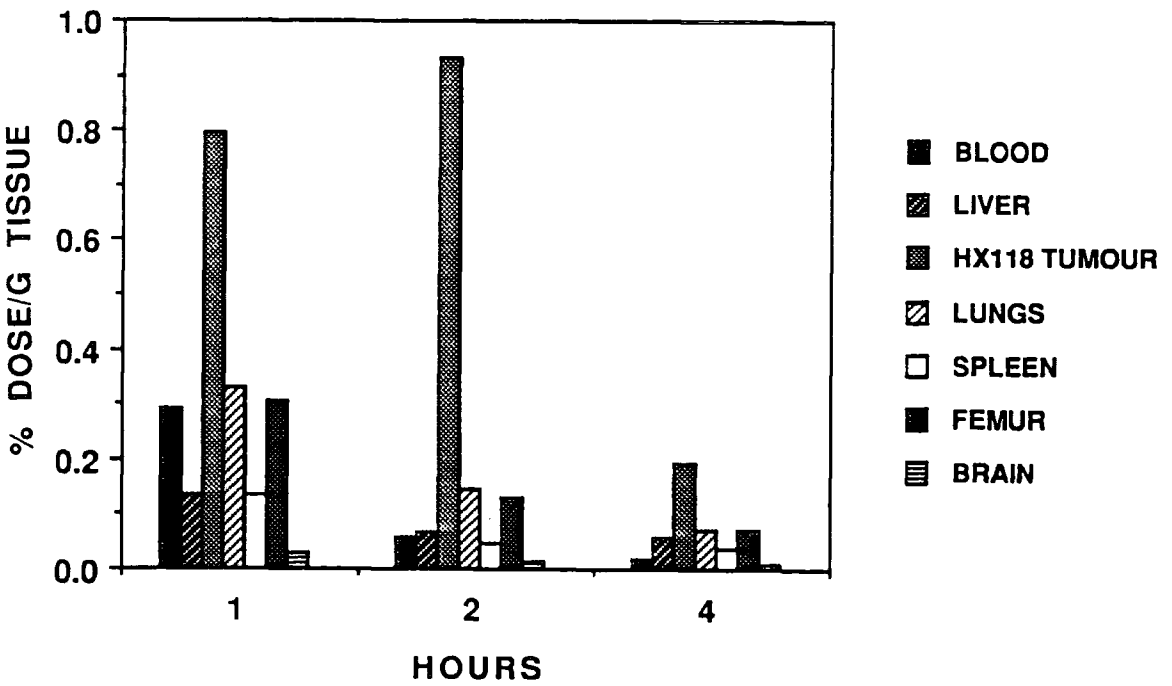

Similar levels of ^{111}In are also found in xenografts of human colorectal tumour (HT 29)[9]. The reason for the differences observed in the biodistributions of the Ga and In complexes are not well understood, they could stem from a number of factors.[10] For example the In complex having a slightly larger mass, or the difference in shape between the octahedral Ga complex and the trigonally distorted In complex could both contribute to the observed difference in uptake into the liver.

2.2 AZAPHOSPHINIC ACID LIGANDS

2.2.1 BACKGROUND

It has been previously found that the complexes of indium and gallium with azaphosphinic acid ligands based on a triazacyclononane ring are well suited to radioisotope labelling.[11-14] One of their main differences from the α-aminocarboxylate ligands described previously is that the phosphinate moiety is more difficult to protonate on oxygen than the corresponding carboxylate. This lower pK_a is observed in both free ligand and metal complex and leads to greater kinetic stability with respect to acid catalysed metal dissociation, this in turn should enhance the *in vivo* stability of the complex. An additional difference is that the pentavalency of the phosphorus allows functionalisation of the ligand in order to influence the mass, solubility and lipophilicity by variation of the alkyl or aryl substituent at phosphorus. The structures of some of these ligands are given below. Each ligand gave a radiolabelling yield of >98% at pH5.5 (5μM, 37°C) and the radiolabelled complex following injection in a mouse is excreted quite rapidly (>99.8% after 72hours).

FIGURE 2.10 *Some azaphosphinic complexes which have been studied in vivo.*

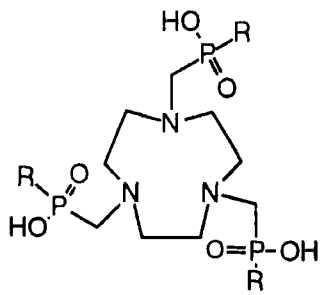

ligand		R substituent	molecular weight of In complex	excretion of In complex
NOTPMe[15]	**(2)**	Me	517	renal
NOTPPh[15,16]	**(3)**	Ph	703	biliary
NOTPBz[15]	**(4)**	Bz	745	biliary

It appears that the mode of excretion of these neutral complexes can vary from predominantly renal to biliary. Comparing these data with another class of related compounds (figure 2.11) a pattern was seen to emerge. The complexes with the larger aromatic groups appeared to excrete via the endogenous faecal route.

FIGURE 2.11 *Triazacyclononane complexes studied in vivo.*

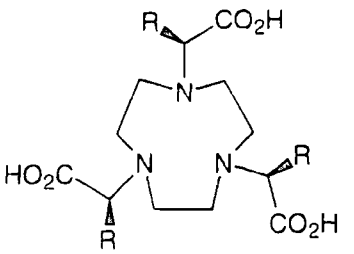

ligand		R substituent	molecular weight of In complex	excretion of In complex
NOTA	(1)	H	418	renal
NOTAMe[17]	(5)	Me	460	renal
NOTAPh[18]	(6)	Ph	646	biliary

2.2.2 BLOOD BRAIN BARRIER

A stable azaphosphinic complex for use in SPECT/PET in the brain[19] was identified as an important target. Such a complex should be of relatively low molecular weight (< 500 - 600) allowing it to cross the blood brain barrier, but of relatively high lipophilicity[20]. NOTPPri (**16**) was chosen as a suitable target molecule having a molecular weight of 550 in its Ga complex and a relatively high lipophilicity.

2.2.3 SYNTHESIS OF NOTPPri

Isopropyldiethoxyphosphine (**14**) was synthesised by slow addition of diethylchlorophosphite to isopropylmagnesiumchloride in anhydrous tetrahydrofuran at 0°C (scheme 2.2).

SCHEME 2.2

Distillation gave a sample of the phosphine which was used immediately in a co-condensation reaction with 1,4,7-triazacyclononane and paraformaldehyde in tetrahydrofuran under anhydrous conditions to yield the triester (**15**). The triester was readily purified by chromatography on neutral alumina,[21] before being hydrolysed using 6M HCl to yield the phosphinic acid (**16**) shown in scheme 2.3.

SCHEME 2.3

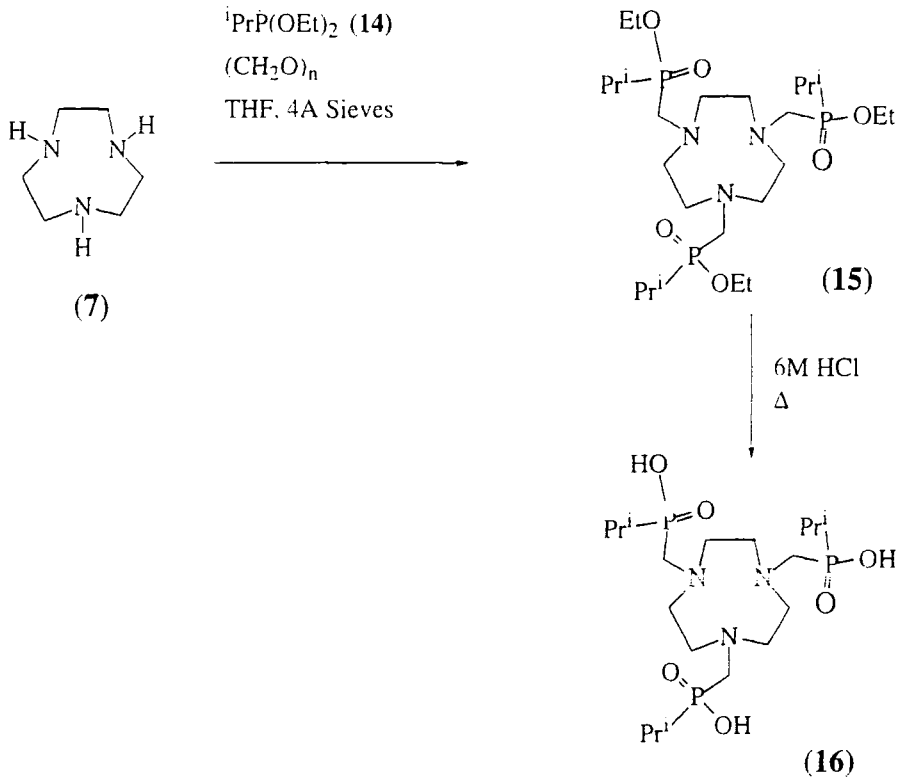

Admixture of stoichiometric quantities of the ligand (**16**) with metal nitrate salts in aqueous solution led to rapid formation of the metal complexes. In this case neutral Ga complex (**17**) and In complex (**18**) were formed.

2.2.4 BIODISTRIBUTION STUDIES

Biodistribution studies were carried out on the gallium-67 complex of (**16**) at one and 24 hours after administration as shown in figure 2.12. The percentage of the injected dose of ^{67}Ga per gram of tissue was measured in different tissue types: the amount of ^{67}Ga in the kidney after one hour was very large by comparison with other tissues and is shown here at one tenth of the actual quantity. The uptake in the brain was examined but no significant amount was found to build up there during the time of observation indicating that this complex was unable to cross the blood brain barrier as hoped.

The biodistribution of the Indium-111 complex of (**16**) was also studied and compared with other neutral phosphinic acid ligands. It could be seen from the one hour data shown in figure 2.13 that NOTPPri cleared mainly by the endogenous faecal route, as did the other more lipophilic benzyl analogue. These complexes cleared rapidly; after 24 hours most of the activity had cleared from the animal. These properties could allow selective imaging of the gall bladder and small intestine using such complexes.

FIGURE 2.12 *Biodistribution of ^{67}Ga complex of* **(16)** *at 1 and 24 hours.*

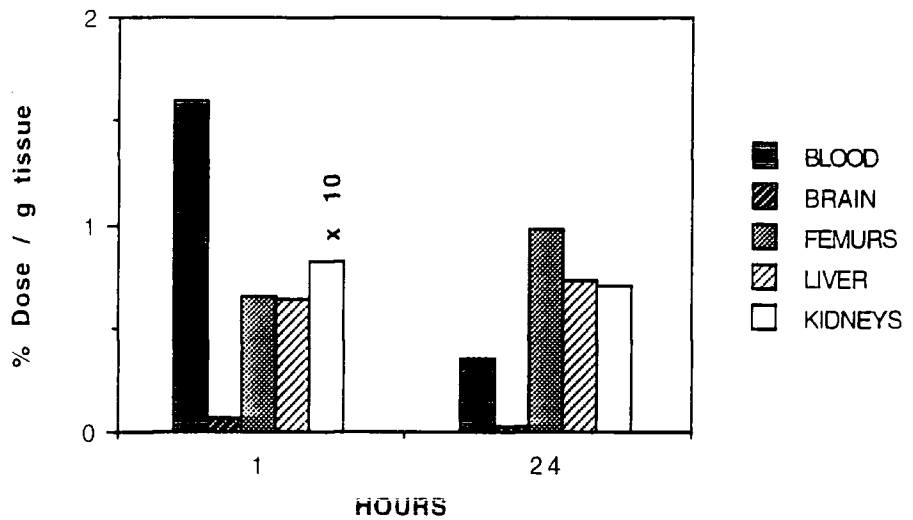

FIGURE 2.13 *One hour ^{111}In biodistribution data for neutral phosphinic acid ligands.*

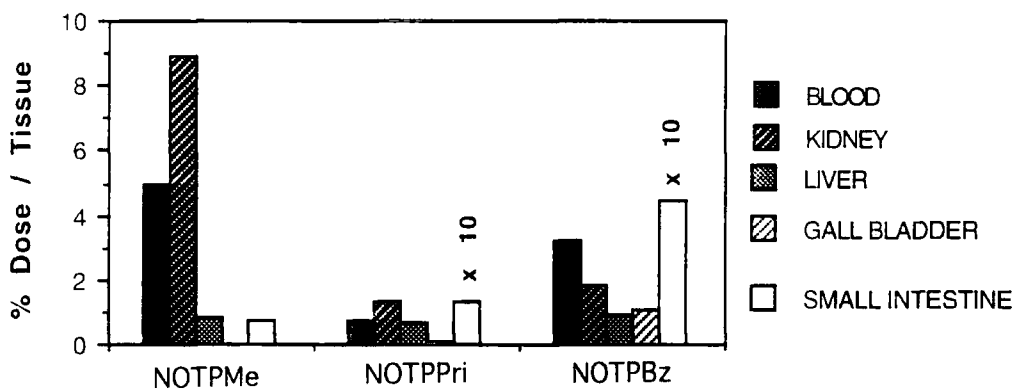

2.2.5 RELATIVE LIPOPHILICITY STUDIES

The partition coefficient P is a measure of the amount of a compound dissolved in one solvent phase relative to another solvent phase under equilibrium conditions. Here the partition coefficients between octanol and water, octanol and phosphate buffered saline (PBS), butanol and water, and butanol and PBS are considered as a means of comparing lipophilicities of different complexes. PBS was chosen because, being buffered at pH 7.4, it provides a better comparison with physiological conditions.

The relative lipophilicity of the indium-111 complex of **(16)** was compared with that of other 9N3 complexes at the MRC Radiobiology Unit[22] as shown in figure 2.14. A reasonably good correlation between the log P values and the route of elimination from

a mouse that had been injected with the corresponding radiolabelled complex was observed. A high (more positive) log P value relates to increased lipophilicity. Table 2.14 confirms that lipophilic compounds are more likely to be eliminated from the body by the hepato-biliary route than the renal route.

FIGURE 2.14 *Correlation of excretion pathway with partition coefficient (log P) for ^{111}In labelled 9N3 complexes*

Log P					
Octanol-water	Octanol-PBS	Butanol-water	Butanol-PBS	In.9N3 complex	
-4.51	-4.92	-2.54	-2.98	NOTA	**(1)**
-3.68	-3.80	-1.88	-2.06	NOTPMe	**(2)**
-3.62	-3.38	-1.79	-2.22	NOTAMe	**(5)**
-1.89	-1.92	-0.98	-0.99	NOTPPri	**(16)**
-	-1.34	-	-	NOTAPh	**(6)**
+0.10	+0.13	+0.54	+0.34	NOTPBz	**(4)**
+0.24	+0.33	+0.63	+0.49	NOTPPh	**(3)**

2.3 ACYCLIC LIGANDS

2.3.1 LIGANDS FOR GADOLINIUM

Contrast agents for Magnetic Resonance Imaging (MRI) are paramagnetic substances that enhance water proton longitudinal (T_1) and tranverse (T_2) relaxation rates.[23] Many studies have been carried out using Gd (III) since it is a nine coordinate, spin $^7/_2$ paramagnetic ion which combines a high magnetic moment with a long electronic relaxation time ($\tau_S = 10^{-9}s$), two features that ensure effective nuclear spin relaxation.[24] Several Gd (III) complexes are now routinely used in clinical practice.

Macrocyclic and acyclic complexing agents for gadolinium are mainly based on diethylenetriamine pentaacetic acid (DTPA) or 1,4,7,10-tetraazacyclododecane tetraacetic acid (DOTA) and their analogues. Current examples of commercially available compounds are DTPA itself which is marketed by Schering as "Magnevist" and DTPA bis methyl amide marketed by Nycomed as "Omniscan". These are less stable *in vivo* compared to the DOTA complexes Gd-DOTA marketed as "Dotarem" and Gd-HPDO3A marketed as "Prohance" also shown. However they are cheaper and

easier to produce, and since they are cleared from the body relatively quickly they are well tolerated and their toxicity is surprisingly low.

FIGURE 2.15 *Commercially available complexing agents for Gd.*

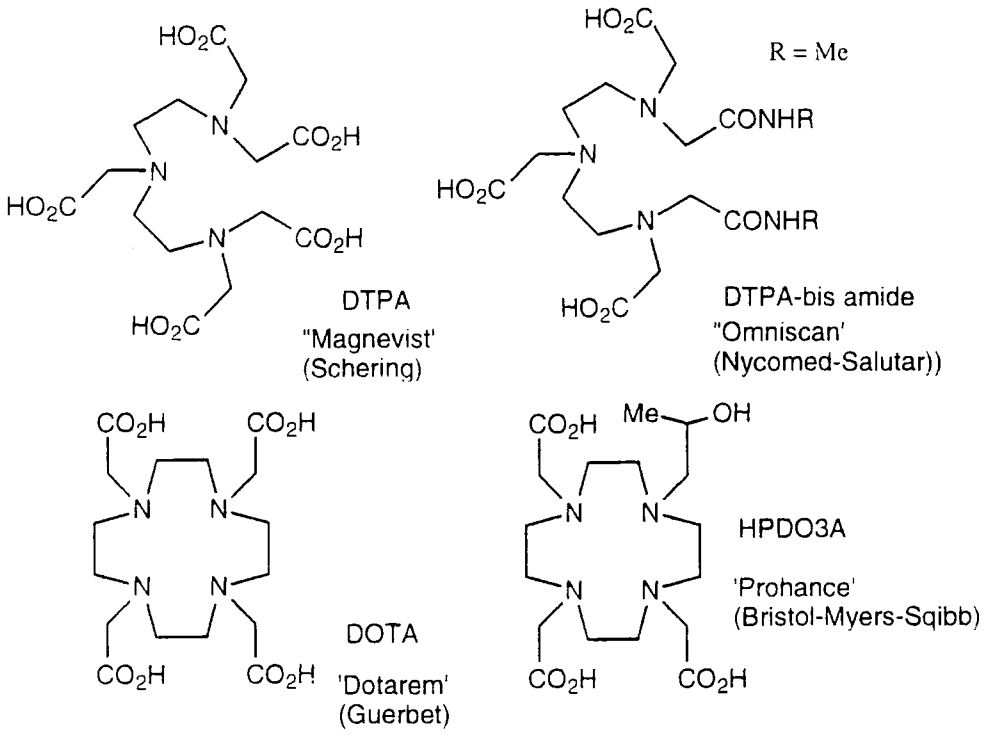

Other compounds based on the acyclic DTPA backbone are being developed; these include BOPTA produced by the Italian company Bracco of Milan[25] and EOBDTPA produced by Schering[26], both of which have been approved for clinical use.

FIGURE 2.16 *Lipophilic anionic complexing agents approved for clinical use.*

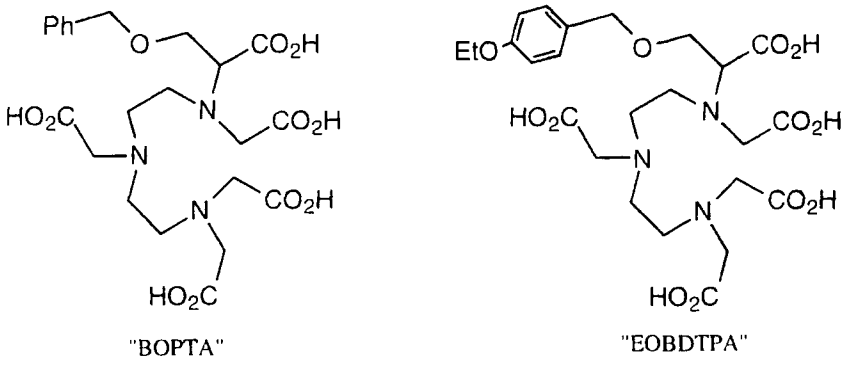

However both of these are lipophilic anionic compounds which causes some advantages and disadvantages. The advantage of the lipophilicity is that they clear with some selectivity via the biliary system by being taken up into the liver by the "organic

ion transporter'' [27] but they still have the disadvantage as dianionic complexes of the hyperosmolality of their aqueous solutions.[28]

It seemed desirable therefore to target the lipophilic neutral complex DTPA-bis benzyl amide (**19**) as a potential contrast agent for the biliary system without the problems associated with ionic complexes.

2.3.2 SYNTHESIS OF DTPA-BIS AMIDE

When diethylenetriamine pentaacetic dianhydride in pyridine was treated with benzylamine in the presence of DMAP it gave the bis-amide (**47**) as a white solid from a solution at pH 3.5 in high yield.

SCHEME 2.4

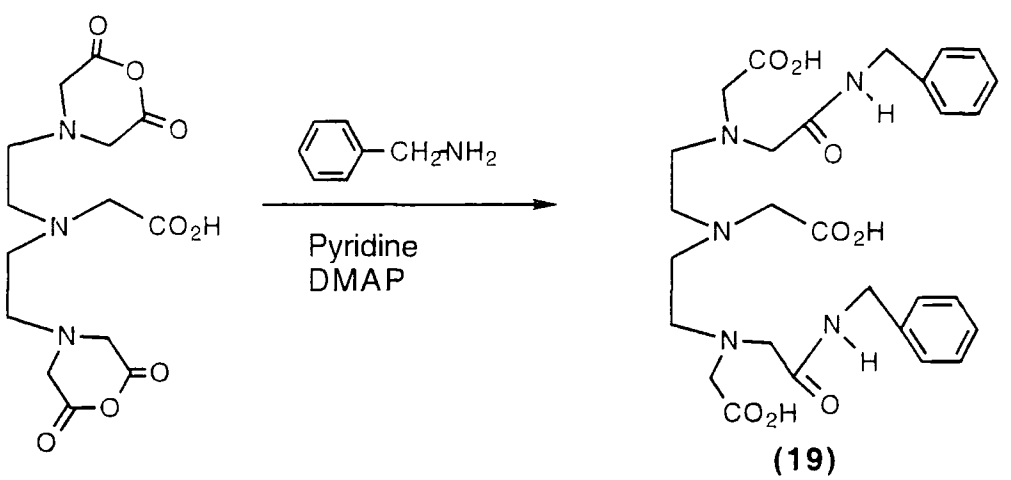

(19)

2.3.3 YTTRIUM COMPLEX OF DTPA-BIS AMIDE

It had previously been demonstrated that yttrium and gadolinium showed very similar complexation properties when comparing the crystal structures of Gd.DOTA[29] and Y.DOTA[30]. In each case DOTA acts as an octadentate ligand with a ninth site occupied by water. In the case of the gadolinium complex of DTPA-bis(ethylamide) observed by Raymond[31] the gadolinium ion is in a nine coordinate ligand environment comprising the three amine nitrogens, three carboxylic acid oxygens, two amide oxygens, and one water molecule. It was anticipated that the DTPA-bis(benzylamide) ligand could also form a complex in a somewhat similar way with yttrium, with the advantage that NMR measurements could also be undertaken.

The yttrium complex (**20**) of (**19**) was formed by heating the ligand in dilute HCl with yttrium nitrate. In the yttrium complex there was a marked coordination shift in the stretching frequency of the amide carbonyl band (37 cm^{-1} coordination shift) consistent with amide oxygen ligation.

2.3.4 NMR EXPERIMENTS CARRIED OUT ON YTTRIUM COMPLEX

The yttrium complex of DTPA bis-benzylamide (**20**) was characterised by ^{89}Y NMR, this clearly showed a peak at +80.0 ppm due to the desired complex. If the ligand was heated for too long during complexation partial hydrolysis of the amide took place and a second peak was observed in the ^{89}Y NMR spectrum at 81.6 ppm due to the Y complex of DTPA. This ^{89}Y NMR data was compared with ^{89}Y data for a number of other Y compexes as shown in figure 2.17. The absence of a pattern in the chemical shifts showed that ^{89}Y NMR was not a useful diagnostic tool, although it was observed that the Y shift was the same in H_2O as D_2O for each complex.

FIGURE 2.17 *^{89}Y NMR data for a range of Y complexes in D_2O.*[39]

Complex	δ_Y (ppm)	comment
Y-EDTA$^-$	+123.5	Same in H_2O
Y-DTPA^{2-}	+81.6	same in H_2O
Y-DTPA-bis(benzylamide) (**20**)	+80.0	neutral complex
Y-DOTA$^-$	+111.8	quintet
Y-DOTPMe$^-$	+156.8	quintet
Y-DOTPBz$^-$	+152.8	same in H_2O
Y-$N_4P_3CONBu_2$	+168.3	neutral complex

The ^1H NMR spectrum for the complex (**20**) was found to be quite complicated and broad. A series of spectra were obtained in D_2O at various temperatures, 5°C, 10°C, 20°C, 30°C, 40°C and 50°C in an attempt to achieve some resolution. Some further broadening of peaks was observed in the spectrum obtained at 5°C, but over this temperature range no coalescence was evident indicating that exchange was either very fast or very slow in the NMR time scale. An example of one of the spectra recorded at 50°C is shown in figure 2.18.

FIGURE 2.18 *400MHz ^1H NMR spectrum of* **(20)** *in D_2O obtained at 50°C during VT experiment.*

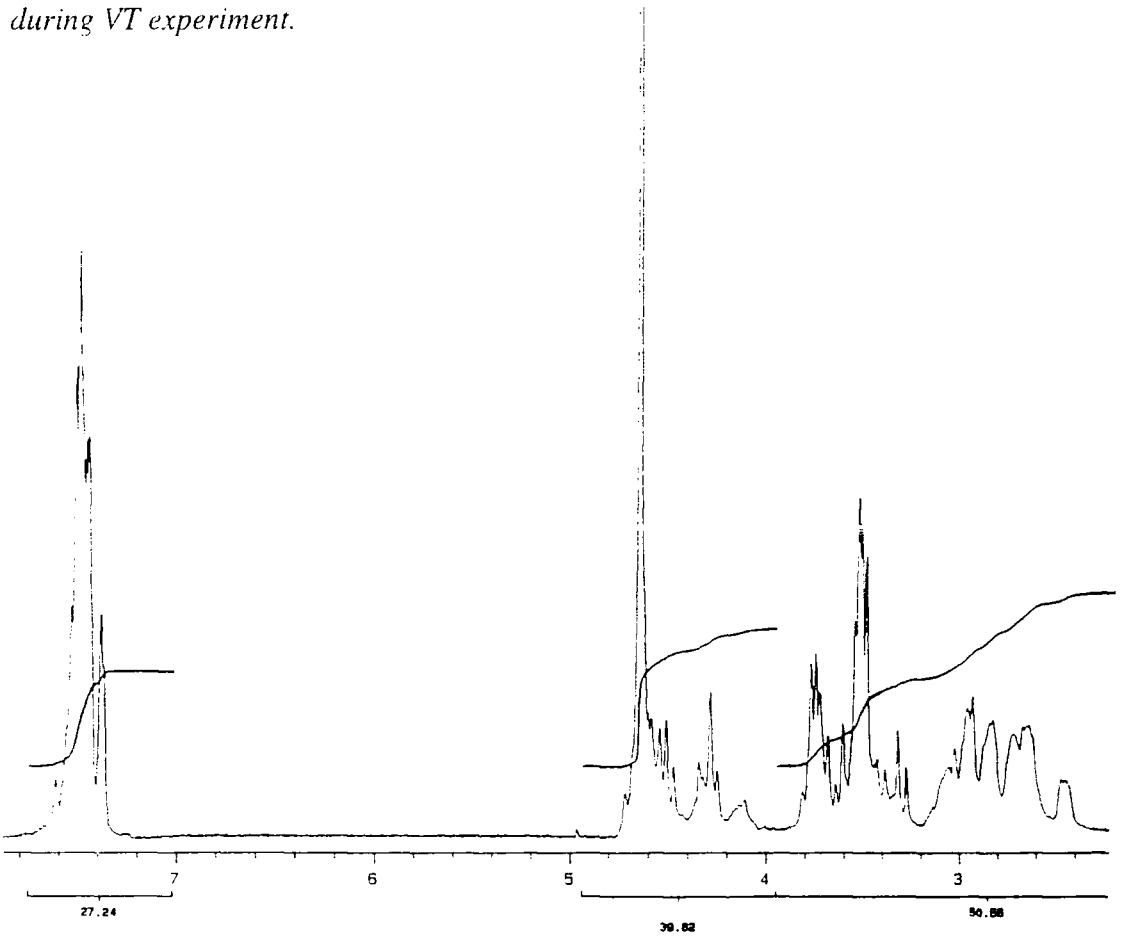

2.3.5 CRYSTAL STRUCTURE OF YTTRIUM COMPLEX

Crystals of the yttrium bis benzylamide complex formed overnight from the aqueous solution and the molecular structure was established by an X-ray single crystal diffraction study, and is shown in figure 2.19 and 2.20.

Analysis of the bond lengths reveals short M-O bonds with a mean value of 2.33Å in **(20)** compared to 2.36Å and 2.41Å in Gd-DTPA-bis ethylamide and Gd-DTPA. The bonding of the negatively charged carboxylate and formally neutral amide groups with yttrium has essentially the same character as shown by the similar average M-O distances. The mean M-O (amide O) distance was 2.35 Å, and 2.33 Å for the M-O (carboxylate) bond length. The M-N bonds were longer by about 0.3Å at 2.64Å in **(20)** compared to 2.70 and 2.64 in Gd DTPA-bis ethylamide and Gd-DTPA. This demonstrates the comparative weakness and lability of the less polar M-N bonds in these strongly ionic complexes. Amides, and also sulphoxides have large dipole moments compared to alcohols, ethers and water for example. Among neutral donors, amides and sulphoxides are intrinsically good σ-donors for charge dense cations.

FIGURE 2.19 *Molecular structure of* [Y **(19)** (H_2O)].$3H_2O$ *with hydrogens omitted except for the amide group.*

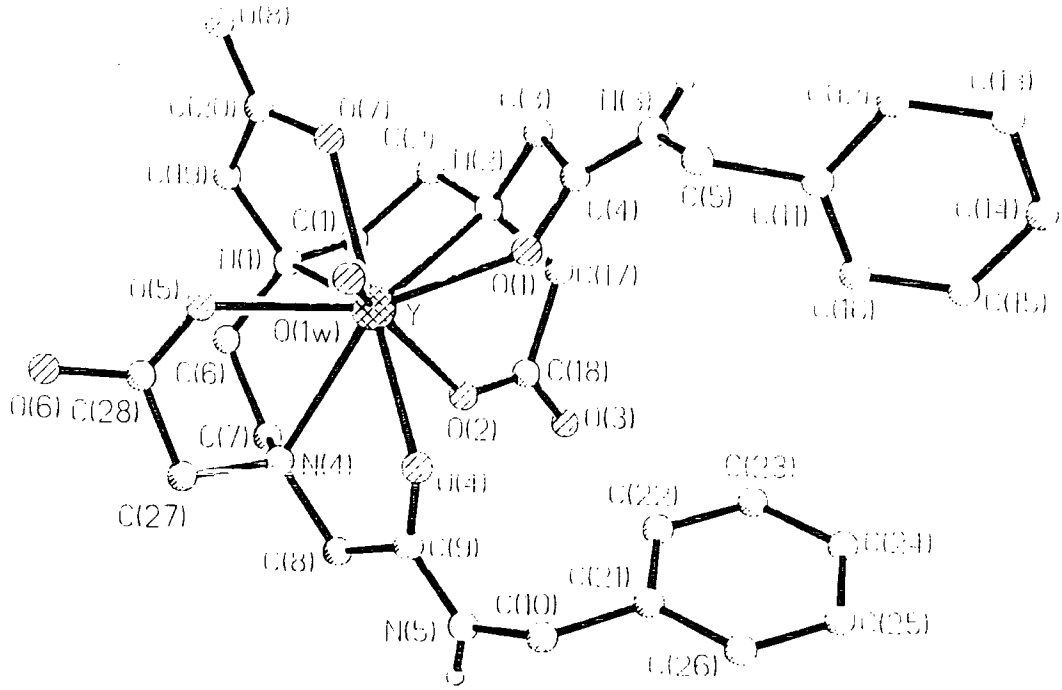

FIGURE 2.20 *Hydrogen-bonding network in the structure of* [Y **(19)** (H_2O)].$3H_2O$]; *projection of the (01 1) plane*

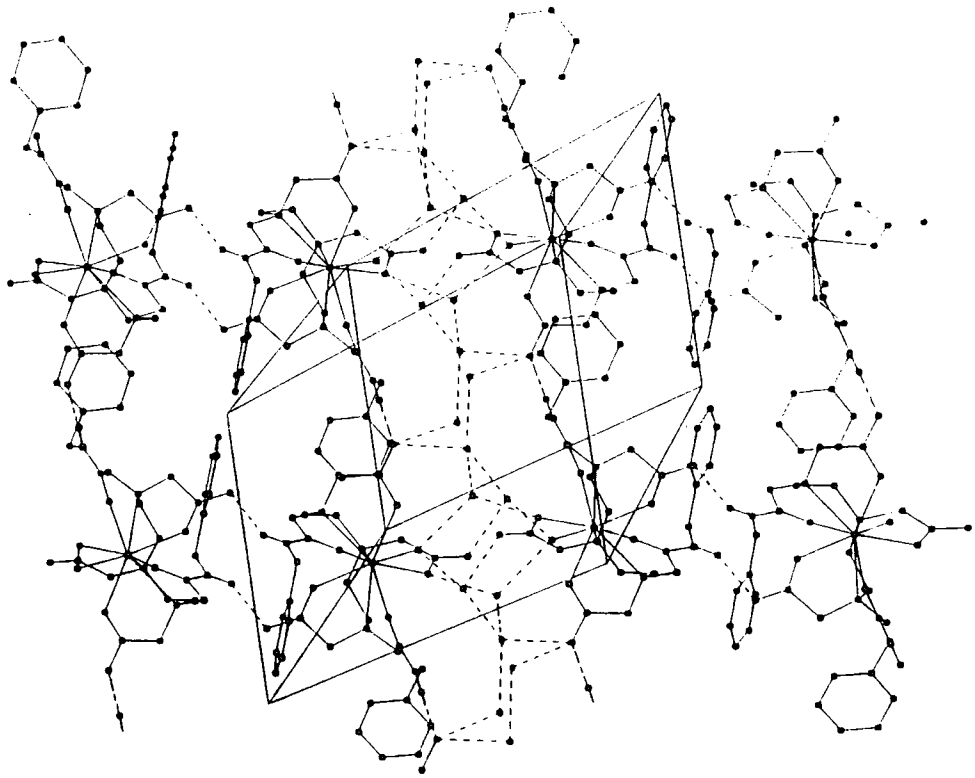

The favoured geometry, at the metal, of such 9-coordinate complexes can be a tricapped trigonal prism, as in the case of Gd-BOPTA or a monocapped square antiprism as in the case of **(20).** The chelating octadentate ligand coordinates the Y atom in a square-antiprismatic mode. The three amine nitrogen atoms and one carboxyl group oxygen comprise one square base of the antiprism, while oxygen atoms of the two remaining carboxylate groups and two amide groups form another base. The latter is capped by an aqua-ligand. Further details of this structural analysis are reported in appendix 1 and are discussed elsewhere.[32]

FIGURE 2.21 *Tricapped trigonal prismatic Gd-BOPTA and monocapped square antiprism* **(20)**

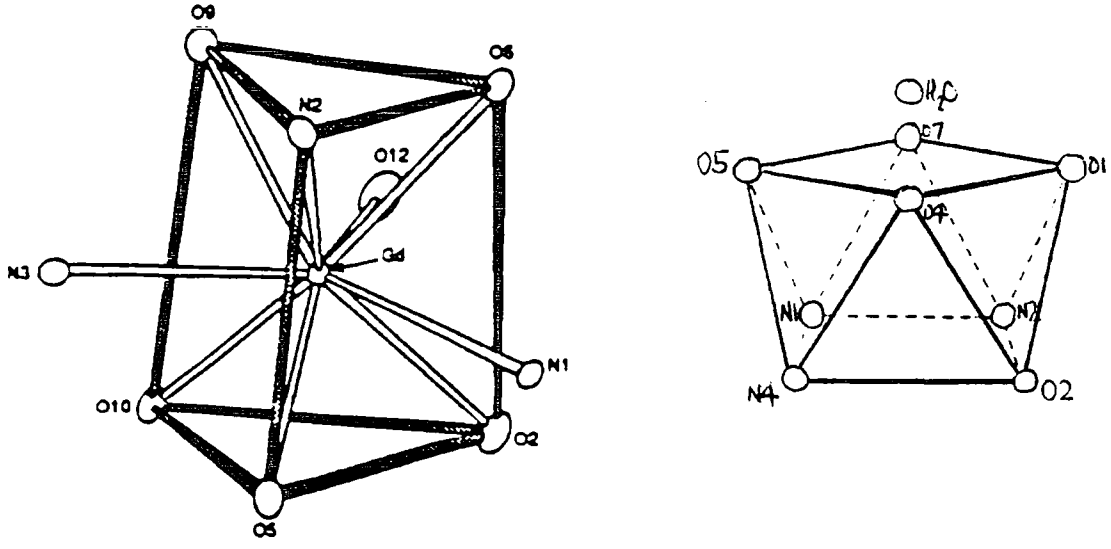

2.3.6 BIODISTRIBUTION OF DTPA-BIS BENZYLAMIDE

Until recently[27] there has been a lack of published data regarding the pharmacokinetic and pharmacological properties of potential MRI contrast agents based on Gd complexes of DOTA and DTPA. Two notable exceptions are Gd-BOPTA[25] and Gd-EOBDTPA.[26] These are both DTPA derivatives and show clearance by the hepato-biliary pathway. Although the biodistribution pattern and excretion pathway of a compound cannot be predicted accurately from the charge or structure it was anticipated that the lipophilic neutral DTPA-bis benzylamide might behave in a similar way.

Complexes were prepared using a mixture of stable and radioactive ^{153}Gd at the MRC Radiobiology Unit. About 0.1μM of complex per kg body weight was injected into nude athymic mice. Biodistribution studies were carried out after 5 minutes in order to

determine the excretion pathway, and again at 24 hours as a means of determining how much Gd had dissociated and accumulated in the liver and bones.

Figure 2.22 shows the 5 minute and 24 hour biodistribution of ^{153}Gd-DTPA-bis benzylamide (**21**) showing the percentage of the injected dose in each tissue type. This clearly shows that this complex exhibits mildly hepato-philic properties, the liver, gall bladder and small intestine accounting for 10% of the injected dose. Figure 2.23 shows how this compares with Gd-DTPA and Gd-BOPTA in which the percentage of the injected dose in these tissues is 4 and 33% respectively.

Figure 2.22 also shows the liver and skeletal content of ^{153}Gd at 24 hours; at 2% of the injected dose this was more than twice the measured amount for either BOPTA or DTPA. This indicates some dissociation of the complex *in vivo*, although much less than the 74% observed for Gd-citrate.

In this instance the lipophilic benzyl group was used with some success to target the hepato-biliary system. Because of the high dosage of contrast agent required in MRI the level of *in vivo* dissociation observed may render this complex less favourable than DOTA based macrocycles for development. However, possessing similar stability to the analogous methyl and ethyl amides in clinical use, it may be well tolerated because of its rapid excretion. This method of targeting using DTPA-bis amides is further developed in chapter 3.

FIGURE 2.22 *^{153}Gd Biodistribution of bis benzylamide* (**21**) *at 5 mins and 24 hours*

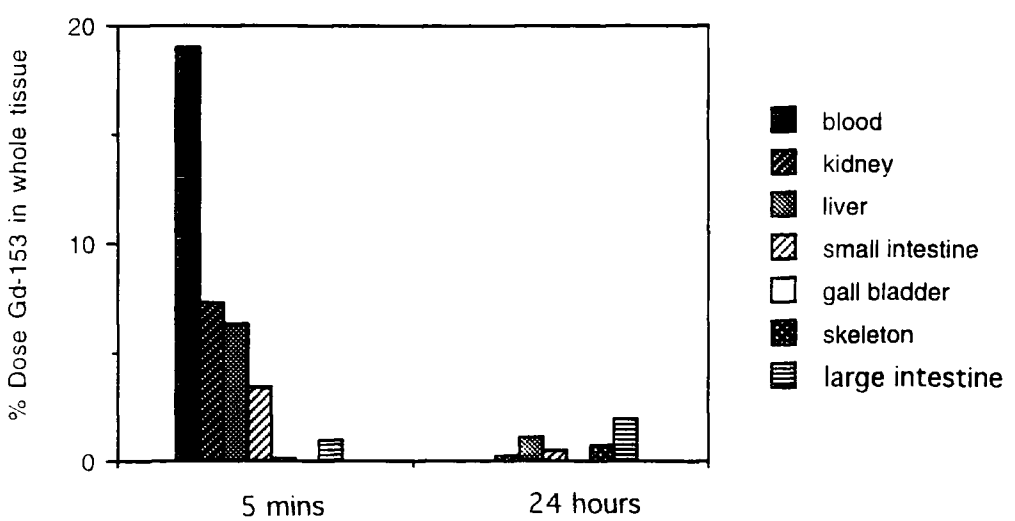

FIGURE 2.23 *5 minute ^{153}Gd biodistributions of DTPA, DTPA-bis benzylamide and BOPTA*

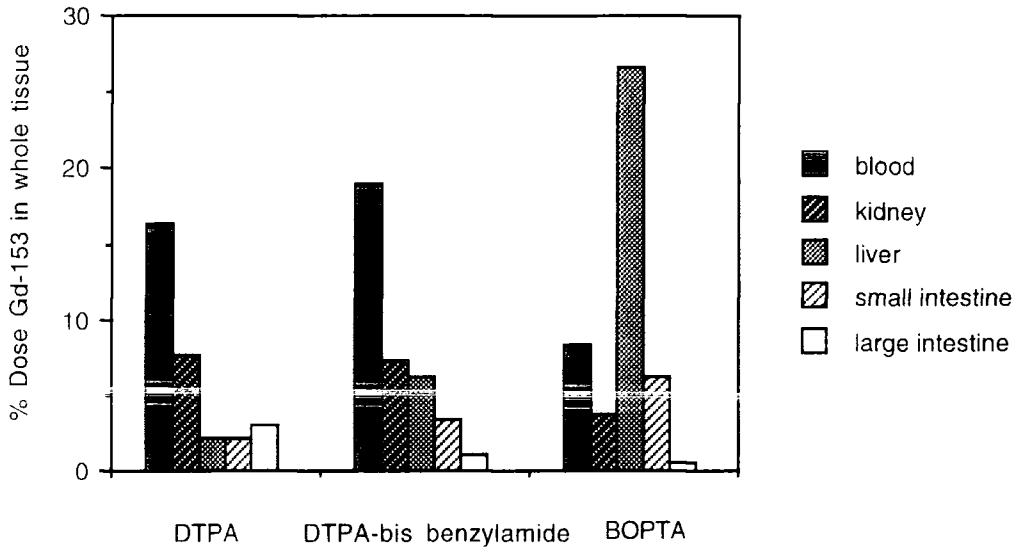

2.4 9N3 AND 12N3 BASED LIGANDS FOR GADOLINIUM

2.4.1 BACKGROUND

Current interest in lanthanide complexes as aqueous NMR shift reagents and MRI contrast agents has led to the synthesis of many new macrocycles derived from cyclic polyaza and cyclic polyaza polyoxa ligands with a wide variety of ionizable functional groups. The thermodynamic stability constants of these depend upon internal cavity size rigidity and the nature of donating atoms. Variation of stability constant with ionic radius of the lanthanides for four common ligands is shown in figure 2.24.

Clearly Ln(NOTA) complexes are much less stable than DOTA and DTPA complexes. This is partly due to the fact that it is a hexadentate chelate, and partly due to the restricted size of the triazacyclononane ring.

The work described in the following section examines a group of novel ligands based on the triazacyclononane ring, but incorporating a further three nitrogen donor atoms and a potentially larger cavity size for lanthanide complexation.

FIGURE 2.24 *Literature values for EDTA and DTPA [33] (open circles) and literature values for DOTA, DTPA and NOTA [34] (closed circles) of stability constant variation with ionic radius of lanthanides.*

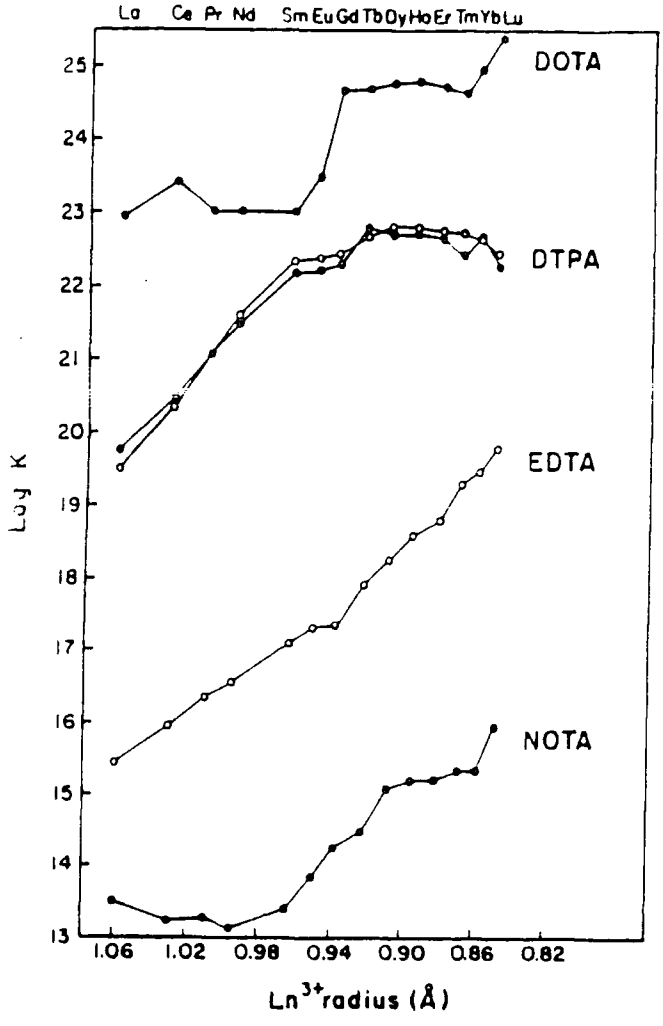

2.4.2 SYNTHESIS OF NOVEL 9N3 BASED LIGANDS

1,4,7-Triazacyclononane (**7**) was heated to reflux in acetonitrile with potassium carbonate and 2-bromo-N-methylethanamide for 24 hours. This afforded the white tris-amide (**22**), recrystallised from toluene in 69% yield. Initial attempts to reduce the tris-amide to the desired tris-amine using sodium borohydride resulted only in a small quantity of an intractable pale yellow oil. However heating to reflux with lithium aluminium hydride in diethyl ether, followed by careful quenching and filtration provided tris-amine (**24**) in 25% yield. Yields were not optimised but it was believed that this relatively low yield was due to the amine being more soluble in water than the organic solvents into which it was extracted. It was observed that this compound was

somewhat unstable to prolonged storage in air. After a short period the oil became discoloured and the accurate mass was unable to be measured.

The benzyl derivative (**23**) was synthesised using 2-chloro-N-benzylethanamide in the method of (**22**) and purified by column chromatography in 29% yield. Reduction using $LiAlH_4$ afforded tris-amine (**25**) in 73% yield.

The introduction of carboxymethyl groups was effected by reaction of amine (**24**) with ethyl bromoacetate (K_2CO_3, MeCN, 40°C, 3 hours) to afford the triester (**26**). In the same way amine (**25**) was converted to the triester (**27**) in 77% yield following purification by alumina column chromatography. Acid hydrolysis of the latter (6M HCl, 24 hours) gave the acid (**28**) quantitatively.

Complexation was carried out by reaction of 1.2 equivalents of gadolinium oxide with ligand (**28**) (pH 2, 80°C) until a clear solution was obtained. The pH was adjusted and heating continued (pH6, 80°C, 3 hours) to give the desired complex (**29**) in a 15% yield after preparative tlc.

SCHEME 2.5

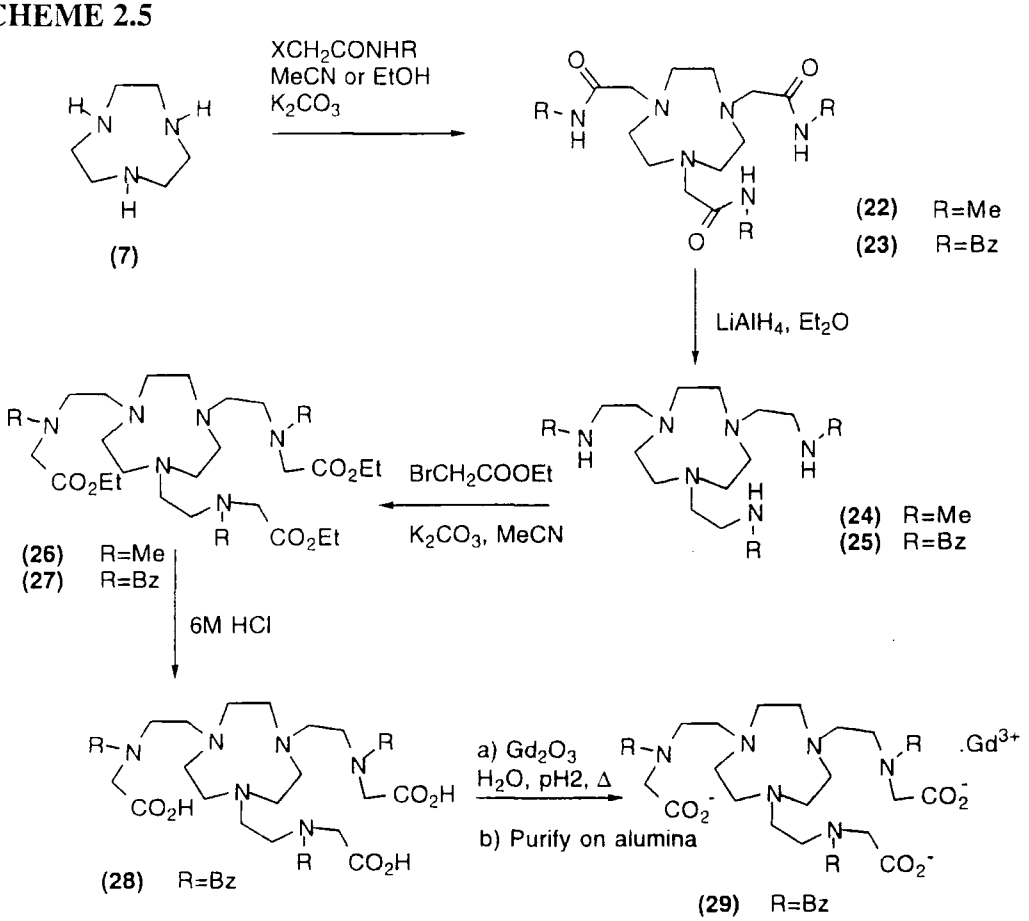

2.4.3 BIODISTIBUTION STUDIES OF Gd-9N3N3 COMPLEX

The biodistribution of the ^{153}Gd complex of (**28**) in mice was studied at 5 minutes and 24 hours after administration of a 0.1 μmol/kg dose of complex. The percentage dose in the whole tissue for several types of tissue was studied, the five minute results showed little or no preference between clearance by the hepato-biliary route (14% of dose) and renal clearance (13% of dose). The biodistribution after 24 hours showed that much of the complex had cleared from the animal, however the high percentage in the liver and the skeleton indicated that the complex may be somewhat labile and free gadolinium was being retained in these tissues.

FIGURE 2.25 *5 minute and 24 hour biodistribution of ^{153}Gd in mice after administration of 0.1 μmol/kg dose.*

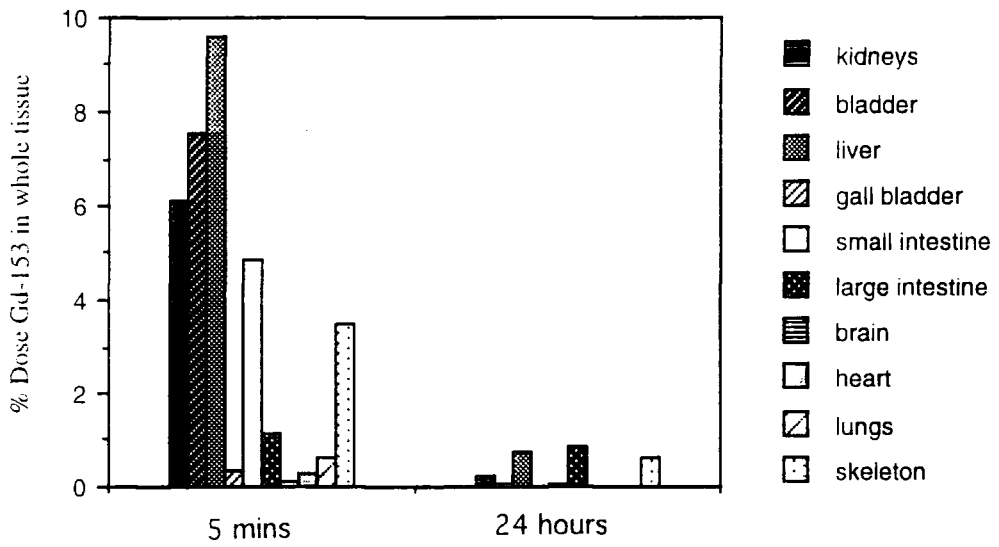

The 0.1 μmol/kg dose of complex administered was relatively low so a further biodistribution study was carried out using a sample of radiolabelled complex combined with cold gadolinium complex allowing the larger dose of 50 μmol/kg to be administered. The study was also extended to a third time point at seven days. Data for the high dose support the findings at the low dose, i.e. retention of gadolinium in the skeleton, as shown in figure 2.26. The percentage dose per gram in the femur at seven days actually exceeded that at 24 hours while the amount in the liver decreased, this was probably due to gradual clearance of Gd from the liver into the blood stream followed by re-location in the bone in a similar manner to that observed in the case of Gd-DTPA. The relative instability of this complex *in vivo* may make such a ligand undesirable for use as a contrast agent.

FIGURE 2.26 *5 minute, 24 hour and 7 days biodistribution of ^{153}Gd in mice after administration of 50μmol/kg dose.*

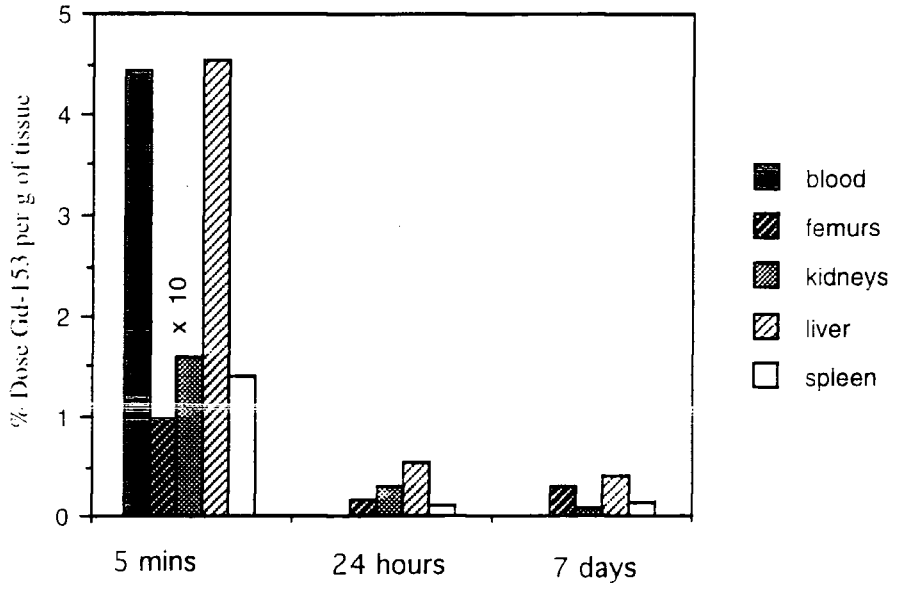

2.4.4 SYNTHESIS OF 12N3 ANALOGUE

It was proposed that the 1,5,9-triazacyclododecane ring with its larger cavity size may provide a better foundation upon which to build a ligand for complexation of gadolinium. A synthetic route somewhat similar to that used for the triazacyclononane analogue was employed.

1,5,9-Triazacyclododecane was heated to reflux in dry ethanol with potassium carbonate and 2-chloro-N-methylethanamide for 24 hours. After alumina column chromatography this gave a 50% yield of the amide (**30**). Reduction using $LiAlH_4$ in diethyl ether afforded amine (**32**) in 63% yield. The benzyl derivatives were prepared in an analogous way, using 2-chloro-N-benzylethanamide to provide a 74% yield of amide (**31**), and amine (**33**) in 61% yield.

Trialkylation of the secondary amine sites of (**32**) with ethyl bromoacetate in acetonitrile in the presence of potassium carbonate gave the triester (**34**) in 93% yield. However the remainder of the synthesis was carried out on the benzyl derivative only since it became apparent that the chromophore would be necessary for HPLC purification in later stages.

Treatment of the amine (**33**) with ethylbromoacetate (ethanol, K_2CO_3, 50°C, 3 hours) to yield the triester (**35**) (74% after alumina column chromatography), or with t-

butylbromoacetate (ethanol, K_2CO_3, 40°C, 18 hours) to yield the triester (**36**) (81% after flash silica column chromatography) appeared to be successful (from NMR and IR spectra) although some difficulty was experienced in attempts to obtain accurate mass spectra on these molecules having masses of 828 and 914 respectively. These difficulties may be due to the problems associated with obtaining a high degree of accuracy at such high masses, or due to the structure of the molecules themselves, each containing labile ester groups. Each of the esters (**35**) and (**36**) underwent acid hydrolysis (6M HCl, 110°C, 48 hours) quantitatively to give the same acid (**37**) which was purified by semi preparative HPLC. Unfortunately, due to the use of such a weak chromophore, recovery of the material was poor owing to the difficulty of detection and collection.

SCHEME 2.6

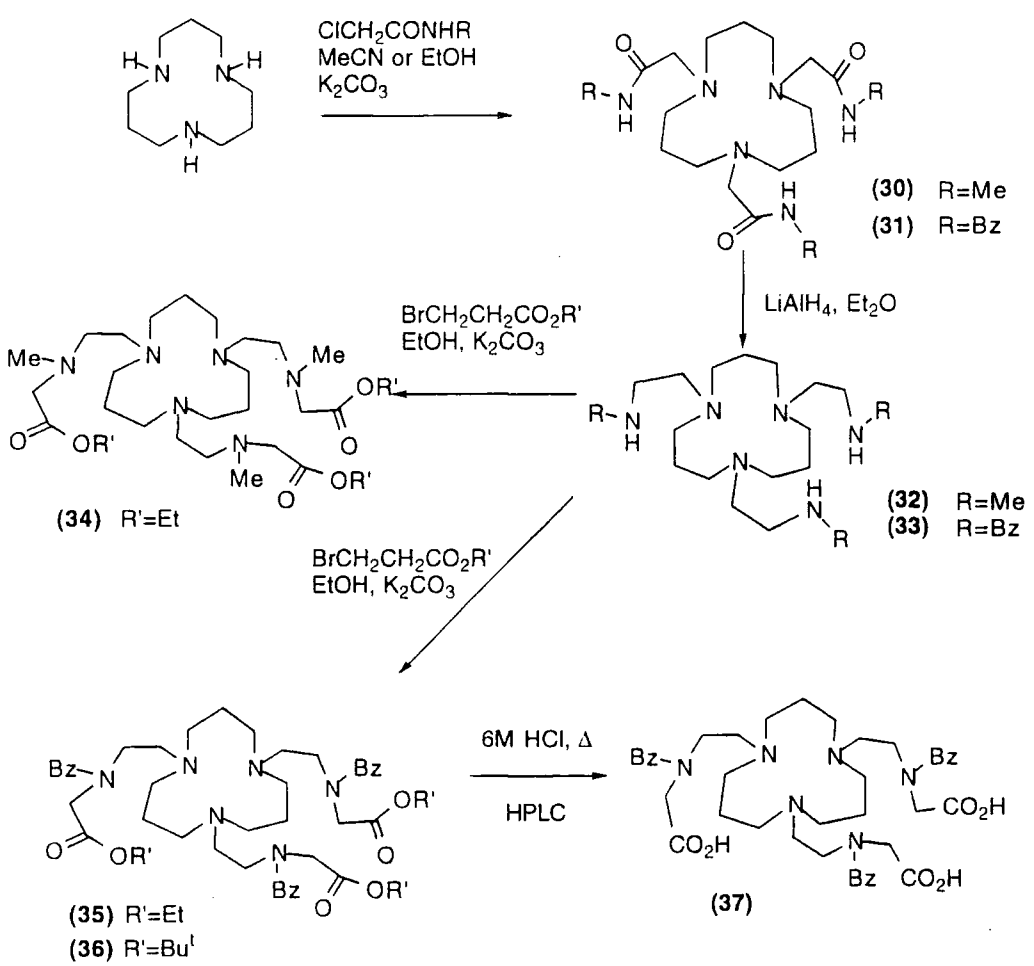

The samples obtained were used in attempts to form a gadolinium complex in the method of (**28**) and in the labelling method employed by the MRC radiobiology unit for forming ^{153}Gd complexes. However after the standard time period for complexation, and also after heating to reflux for a further week, no Gd complex was observed. It was

proposed that the complex failed to form because of the high energy barrier to removal of the tightly bound H^+ in the plane of the ring nitrogens and replacement with Gd^{3+}. It had previously been observed[35] in the case of triazacyclododecane itself and its derivatives that this bifurcated H bond was very strong and a pK_a as high as 13 has been determined.

2.4.5 SYNTHESIS OF PHOSPHINIC ACID ANALOGUES

The ability of azaphosphinic acid ligands to form stable complexes has already been discussed in section 2.2. An intrinsic advantage of the $-NCH_2PRO_2H$ moiety over CH_2CO_2H is that structural variation is readily achieved at the P-R group. This allows for example, groups with chromophores to be incorporated in a ligand to facilitate HPLC purification or to influence the solubility of a ligand. The synthesis of ligands based on two ring systems triazacyclononane and triazacyclododecane, and using two different dialkoxyphosphines are described below.

SCHEME 2.7

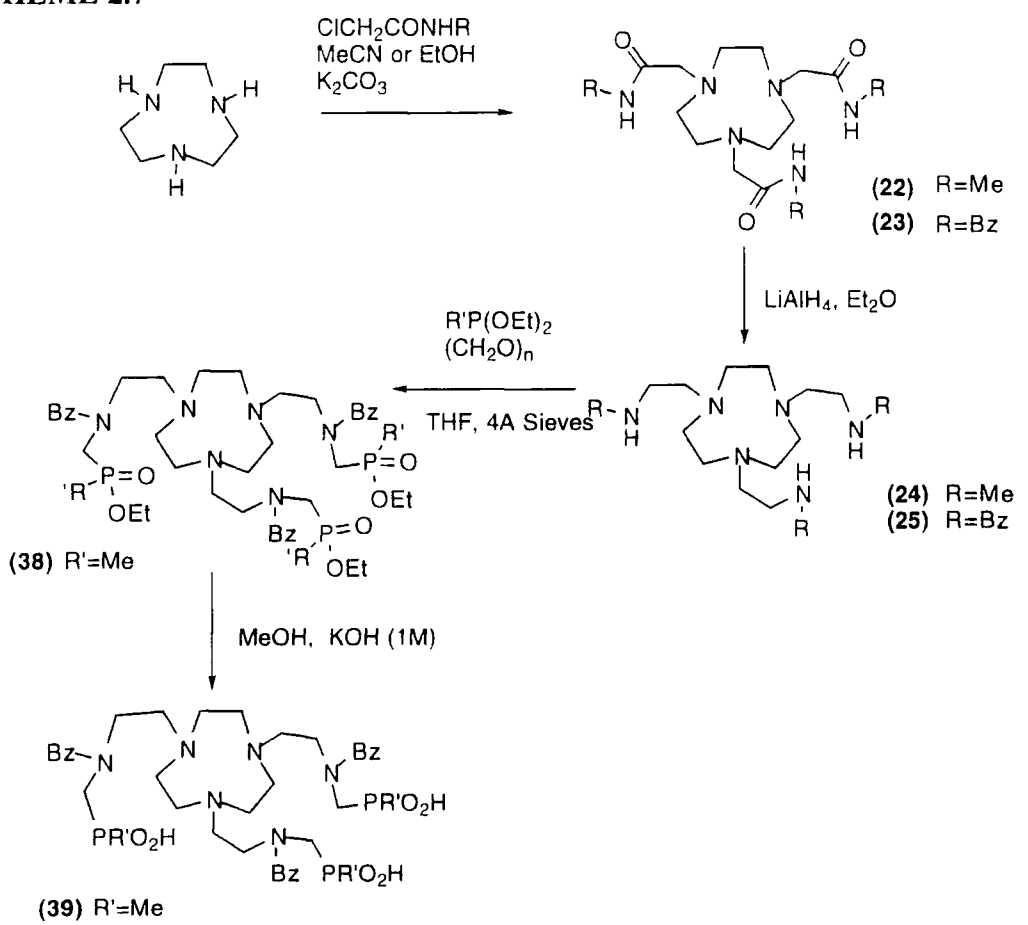

Scheme 2.7 shows that having started with 1,4,7-triazacyclononane the amine (**25**) was synthesised as described in section 2.4.2. Condensation of paraformaldehyde and (**25**)

in dry tetrahydrofuran followed by addition of methyldiethoxyphosphine, synthesised using the standard procedure from diethylchlorophosphite and methylmagnesium bromide, gave the triphosphinate ester (**38**) in a yield of 69% following alumina column chromatography. Base hydrolysis (MeOH, 1M KOH, reflux, 16 hours) was followed by HPLC purification to yield the aminophosphinic acid (**39**).

Similarly in scheme 2.8 the route beginning with triazacyclododecane is described. In this case condensation of paraformaldehyde and amine (**33**) in tetrahydrofuran is followed by addition of benzyldiethoxyphosphine providing the triphosphinate ester (**40**) in a low yield following column chromatography. Acid hydrolysis was employed (6M HCl, reflux, 20 hours) to yield the aminophosphinic acid (**41**) quantitatively as the dihydrochloride salt.

SCHEME 2.8

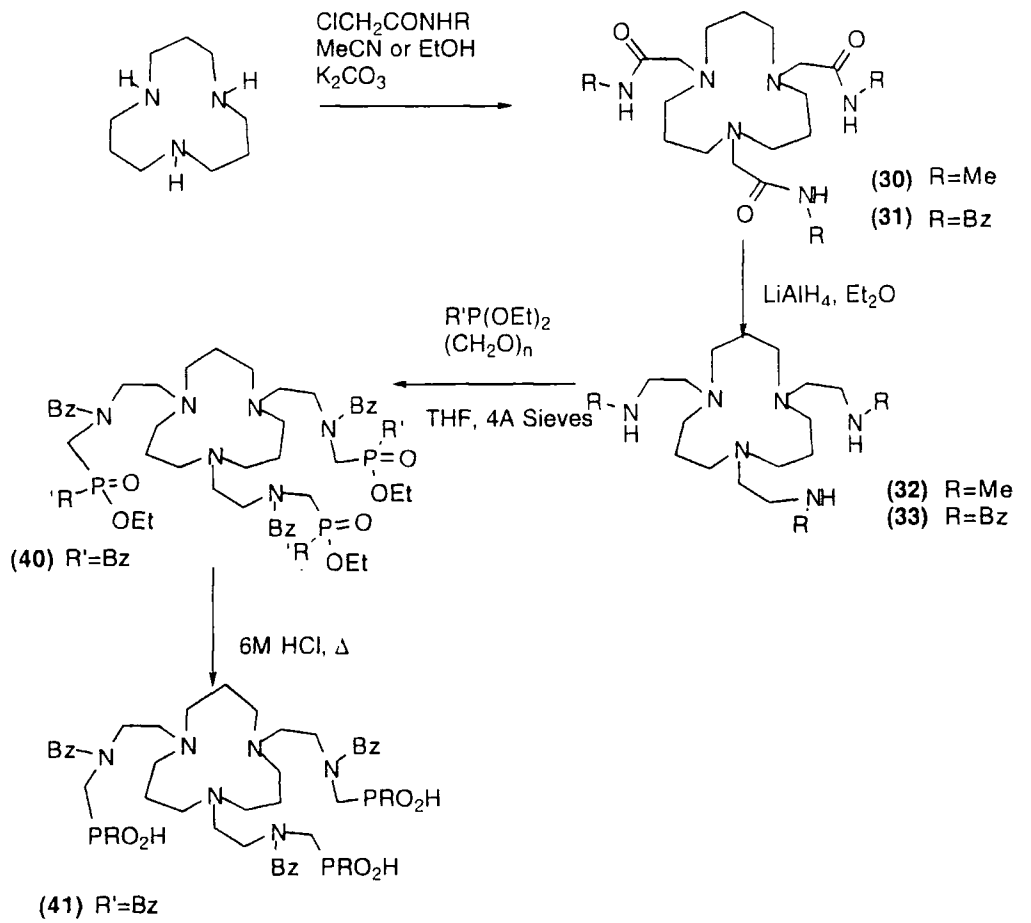

2.4.6 YTTRIUM COMPLEXATION

Since yttrium (III) often exhibits similar complexation chemistry to gadolinium (III) (as explained in section 2.3.3) it was decided to examine the yttrium complex formation of the aminophosphinic acids (**39**) and (**41**). It was hoped that ^{31}P NMR would provide a

useful tool to follow complex formation and that shifts observed in ^{1}H NMR spectra may provide additional information.

The exploitation of anhydrous lanthanide triflate salts in organic synthesis was reported by Forsberg.[36] Yttrium triflate (**42**) was also found to behave in a similar fashion. These triflate salts were prepared by treating the oxide with concentrated trifluoromethanesulfonic acid and the resulting hydrate dried by heating under vacuum. These salts were soluble in organic solvents such as methanol and acetonitrile, indeed anhydrous conditions were required to prevent formation of insoluble lanthanide hydroxides.

The use of lanthanide triflates in organic solvents to produce macrocyclic lanthanide complexes has also been reported.[37] Here work towards forming yttrium complexes in a similar way is described. Initially the well known ligand DOTA was heated in methanol with yttrium triflate and the complex produced (**43**)[38] was characterised and compared with an authentic sample of Y-DOTA to verify that this was a viable route to such yttrium complexes.

The triazacyclononane based phosphinic acid ligand (**39**) was heated with an equimolar quantity of yttrium triflate in methanol. The resulting white complex (**44**) was separated by centrifuge. The triazacyclododecane analogue (**45**) was prepared using the above method from ligand (**41**). These complexes were examined by ^{31}P NMR and ^{1}H NMR and IR specrometry. In each case a shift was observed from the ligand spectrum, however owing to the difficulty encountered in obtaining FAB mass spectra these structures could not be unequivocally assigned.

2.4.7 CONCLUDING COMMENTS

While this series of novel ligands for Gd and Y initially showed some interesting properties in the instance of (**27**), problems encountered in purification, with solubility and also in complex formation indicate that ligands of this form would not be useful for tumour imaging techniques. However there is still scope for modification of this basic structure to provide a more suitable ligand.

2.5 REFERENCES

1. A. Harrison, C.A. Walker, K.A Pereira, D. Parker, L. Royle, R.C. Matthews and A.S. Craig, *Nucl. Med. Commun.*, **13**, 1992, 667.

2. C.J. Broan, J.P.L. Cox, A.S. Craig, R. Kataky, D. Parker, A. Harrison, A. M. Randall and G. Ferguson, *J. Chem. Soc., Perkin Trans. 2*, 1991, 87.

3. S.M. Bradley, R.A. Kydd and R. Yamdagni, *J. Chem. Soc., Dalton Trans.*, 1990, 413.

4. A. Fratiello, R.E. Lee and R.E. Schuster, *Inorg Chem.*, 1970, **9**, 82.

5. J.W. Akitt, N.N. Greenwood and A. Storr, *J. Chem. Soc.*, 1965, 4410.

6. J.W. Akitt, in *Multinuclear NMR*, edited by J. Mason, Plenum Press, New York, London, 1987.

7. J.W. Akitt and D. Kettle, *Magnetic Resonance in Chemistry*, Vol 27, Wiley 377-379, 1989.

8. D.J. Clevette, D.M. Lyster, W.O Nelson, T Rihela, G.A.Webb and C. Orvig, *Inorg. Chem.*, 1990, **29**, 667-672.

9. A. Harrison, C.A. Walker, K.A. Pereira, C. Counsell, D. Parker, L. Royle, R.C. Matthews, A.S. Craig and F.C. Smith, *Nucl. Med. Commun.*, 1995. in preparation.

10. E.T. Clarke and A.E. Martell, *Inorg. Chim. Acta*, 1991, **181**, 273-280.

11. C.J. Broan, K.J. Jankowski, R. Kataky and D. Parker, *J. Chem. Soc., Chem. Commun.*, 1990, 1738.

12. C.J. Broan, K.J. Jankowski, R. Kataky, A.M. Randall and A. Harrison, *J. Chem. Soc., Chem. Commun.*, 1990, 1739; *ibid*, 1991, 204.

13. D. Parker, *Chem. Soc. Rev.*, 1990, **19**, 271.

14. D. Parker and K.J. Jankowski, in *Advances in Metals in Medicine*, eds. B.A. Murrer and M.J. Abrams, Jai Press, London, 1993, vol 1, pp. 29-73.

15. E. Cole, PhD. Thesis, University of Durham, 1994.

16. E. Cole, D. Parker, G. Ferguson, J.F. Gallagher and B. Kaitner, *J. Chem. Soc., Chem. Commun.*, 1991, 1473.

17. R.C. Matthews, D. Parker, G. Ferguson, B. Kaitner, A. Harrison and L. Royle, *Polyhedron*, 1991, **10**, 1951-1953.

18. Unpublished results, MRC Radiobiology Unit.

19. S. Jurisson and E.O. Schlemper, *Inorg. Chem.*, 1986, **25**, 543.

20. T.R. Carroll, 'Technetium Heart and Brain Perfusion Imaging Agents' in *Advances in Metals in Medicine*, Eds M.J. Abrams and B.A. Murrer, vol 1, Jai Press, London, 1993, p 14-21.

21. E. Cole, C.J. Broan, K.J. Jankowski, D. Parker, K. Pulukkody, B.A. Boyce, N.R.A. Beeley, K. Millar and A.T. Millican, *Synthesis*, 1992, 63.

22. E. Cole, R.C.B. Copley, J.A.K. Howard, D. Parker, G. Ferguson, J.F. Gallagher, B. Kaitner, A. Harrison and L. Royle, *J. Chem. Soc., Dalton Trans.*, 1994, 1619.

23. R.B. Lauffer, *Chem. Rev.*, 1987, **87**, 901.

24. I. Bertini and C. Luchinat, *NMR of Paramagnetic molecules in Biological Systems*, Benjamin Cummings, Boston MA, 1986.

25. P. Pavone, G. Parrizio, C. Buoni, E. Tettamanti, R. Pasariello, C. Musu, P. Tirone and E. Felder, *Radiology*, 1990, **176**, 61.

26. H-J. Weinmmann, G. Schuhmann-Giampieri, H. Schitt-Willich, H. Vogler, T. Frenzel and H. Gries, *Magn. Reson. Med.*, 1991, **22**, 233.

27. G. Elizondo, C.J. Fretz and D.D. Stark, *Radiology*, 1991, **178**, 73; P. Pavone, G. Patrizio and C. Buoni, *Radiology*, 1990, **176**, 61; G. Schuhmann-Giampiere, H. Schmitt-Willich and U. Speck, *Radiology*, 1992, **183**, 53.

28. M.F. Tweedle, in *Lanthanide Probes in Life, Chemical and Earth Sciences*, eds. J-C.G. Bunzli and G.R. Choppin, Elsevier, Amsterdam, 1989, chapter 5, pp127-173.

29. J.P. Dubost, M. Leger, M.H. Langlois, D. Meyer and M.C. Schaefer, *C.R. Acad. Sci., Paris Ser. 2*, 1991, **312**, 349.

30. J.P.L. Cox, K.J. Jankowski, R. Kataky, N.R.A. Beeley, B.A. Boyce, M.A.W. Eaton, K. Millar, A.T. Millican, A. Harrison and C.A. Walker, *J. Chem. Soc., Chem. Commun.*, 1989, 797.

31. M.S. Konings, W.C. Dow, D.B. Love, K.N. Raymond, S.C. Quay and S.M. Rocklage, *Inorg. Chem.*, 1990, **29**, 1488.

32. D. Parker, K. Pulukkody, F.C. Smith, A. Batsanov and J.A.K. Howard, *J. Chem. Soc., Dalton Trans.*, 1994, 689.

33. A.E. Martell and R.M. Smith, *Critical Stability Constants*, Plenum, New York, 1974, Vol 1.

34. W.P. Cacheris, S.K. Nickle and A.D. Sherry, *Inorg. Chem.*, 1987, **26**, 958.

35. R. Kataky, K.E. Matthes, P.E. Nicholson, D. Parker and H-J. Buschmann, *J. Chem. Soc., Perkin Trans. 2*, 1990, 1425.

36. J.H. Forsberg, V.T. Spaziano, T.M. Balasubramanian, G.K. Liu, S.A. Kinsley, C.A. Duckworth, J.J. Poteruca, P.S. Brown and J.L. Miller, *J. Org. Chem.*, 1987, **52**, 1017-1021.

37. P.H. Smith and K.N. Raymond, *Inorg. Chem.*, 1985, **24**, 3469-3477.

38. J.R. Morrow, S. Amin, C.H. Lake and M.R. Churchill, *Inorg. Chem.*, 1993, **32**, 4566-4572.

39. K.P. Pulukkody, T.J. Norman, D. Parker, L. Royle and (in part) C.J. Broan, *J. Chem. Soc., Perkin Trans. 2*, 1993, 605.

Chapter Three

Nitroimidazole Conjugates

3.1 NITROIMIDAZOLES AS TARGETING AGENTS

It has been established that nitroimidazoles tend to localise in poorly oxygenated cells of normal and malignant tissues. This binding is related to the presence in the cells of reductase enzymes; the effect of these enzymes is enhanced in areas of low oxygen tension.

Misonidazole (**45**) has been shown to be retained preferentially in oxygen deficient (hypoxic) regions of tumours. This work was conducted using both ^{14}C and ^{3}H labelled misonidazole.[1] A number of fluorine derivatives of misonidazole have recently been synthesised and studied as potential imaging agents using ^{18}F in PET imaging or ^{19}F for possible MRI.[2,3,4]

FIGURE 3.1 *Misonidazole* (**45**) *and three fluorinated derivatives.*

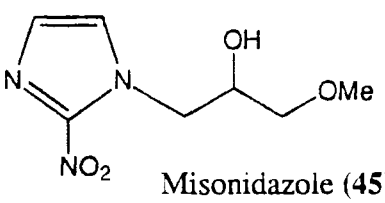

Misonidazole (**45**)

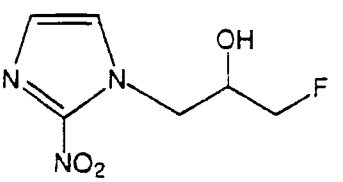

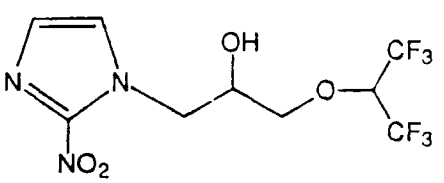

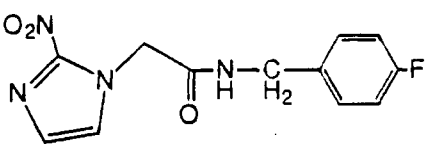

The possibility of targeting hypoxic tumour tissue by conjugating a suitable complexing agent to a nitroimidazole has already been surveyed briefly in section 1.5.3.3 with some promising outcomes. In this section, conjugates of a 2-nitroimidazole with bifunctional complexing agents known to form kinetically stable complexes with ^{111}In, ^{67}Ga or Gd are discussed. Biological studies were also carried out at the MRC Unit to determine whether attachment of the complexing agent affected the tumour localising properties of the 2-nitroimidazole.

3.1.2 HYPOXIC CELLS FOR BIOLOGICAL STUDIES

In vitro studies comparing hypoxic and normoxic conditions have been carried out. Chinese hamster lung fibroblasts (V-79 cells) were incubated with the radiolabelled complex to be tested under either hypoxic (N_2 / CO_2) or normoxic (air / CO_2) conditions.

The uptake and retention of the complex in the cells was measured by comparing the ratio of activity in cells with that in to the incubation medium. For example in the case of tritium labelled misonidazole[5] the ratio of activity in the cells to that in the medium was 5.6 : 1. Later studies revealed that ^{3}H misonidazole also binds under normoxic conditions, showing that further investigations were necessary into suitable *in vitro* experiments.

In vivo studies required a tumour type with a high degree of hypoxic tissue. A number of studies have been carried out using KHT sarcomas[6] which typically possess about 10% hypoxic cells, although other research has suggested that 15-20% hypoxia is common. This figure varies, however, depending on the stage of the cell cycle (the majority of hypoxia being found in the G_1 stage). It may also be altered by addition of hydralazine which induces 100% hypoxia within 1 hour of administration.[7]

3.1.3 PREVIOUS NITROIMIDAZOLE - MACROCYLE CONJUGATES

Some pilot studies[8,9] have been carried out on conjugates (**46**) and (**47**). Since the molecular weights of radiometal complexes are three or four times greater than nitroimidazoles, such as misonidazole, it was necessary to demonstrate whether the attachment of a radiometal complex reduced the binding efficiency or tumour localisation of 2-nitroimidazole *in vitro* or *in vivo*. The results were compared with radiolabelled misonidazole and with the simple complexes of NOTA and DOTA.

FIGURE 3.2 *Previous nitroimidazole - macrocycle conjugates.*

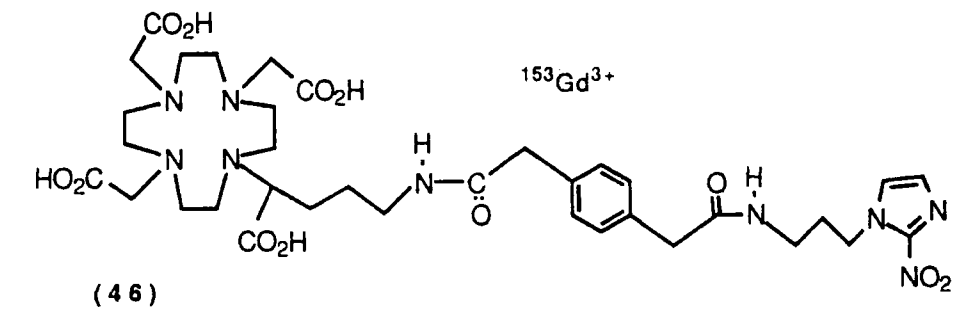

(46)

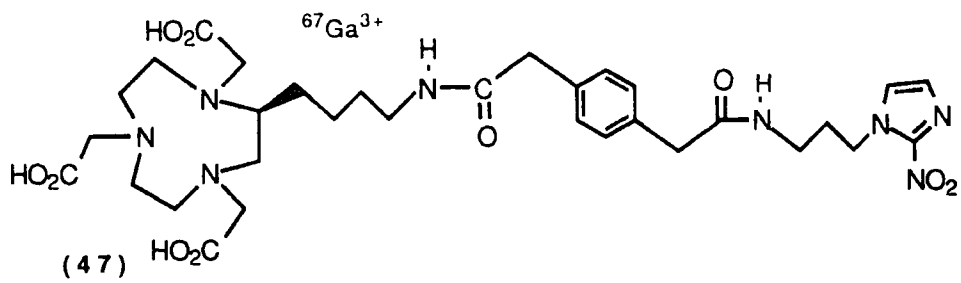

(47)

It was shown that ^{153}Gd-(**46**) and ^{67}Ga-(**47**) were cleared via the intestinal tract (duodenum to large intestine) six to eight times more than ^{153}Gd-DOTA and ^{67}Ga-NOTA were cleared by the same route. The reason for this difference is unclear, however it is the first indication that the metabolism of the 2-nitroimidazole complexes is at variance with the complexes alone and bears some resemblance to the metabolism of misonidazole (**45**). Excretion via the intestinal tract is one characteristic of misonidazole although urinary excretion predominates.

Compound (**46**) forms an anionic complex with ^{153}Gd. This consequently was not readily taken up by cells and was excreted rapidly. NOTA and the 9N3 conjugate (**47**) on the other hand are charge neutral complexes and are able to diffuse passively into cells. In mice bearing the human melanotic melanoma, HX-118, some modest tumour localisation was noted for ^{67}Ga-(**47**); indeed the tumour to blood ratio was higher than for tritium labelled misonidazole. A satisfactory explanation for the greater uptake by the tumour and tumour / blood ratios of ^{67}Ga-(**47**) and ^{67}Ga-NOTA[10] recorded in figure 3.3 has not yet emerged. The possible application of 9N3 trivalent metal complexes for imaging melanoma cannot be dismissed, however it was clear that more extensive studies had to be carried out.

FIGURE 3.3 *Biodistribution in tumour bearing mice of ^{67}Ga-(47) compared to ^{67}Ga-NOTA and ^{3}H-(45)*

	^{67}Ga -NOTA			^{67}Ga -(47)			^{3}H-(45)
Time (Hours)	4	8	24	4	8	24	24
Blood (% dose/g)	0.006	0.008	0.0022	0.008	0.005	0.0016	0.0018
HX118 tumour (% dose/g)	0.127	0.097	0.042	0.085	0.075	0.022	0.014
tumour / blood ratio	21.6	14.8	19	14	15.8	14.0	7.70

Following these results it was decided to target the following molecules (**48**)-(**51**) as primary synthetic goals. It was expected that they would form neutral complexes with either In, Ga or Gd making them suitable for tumour diagnosis using SPECT or MRI.

FIGURE 3.4 *Target molecules* **(48) - (51).**

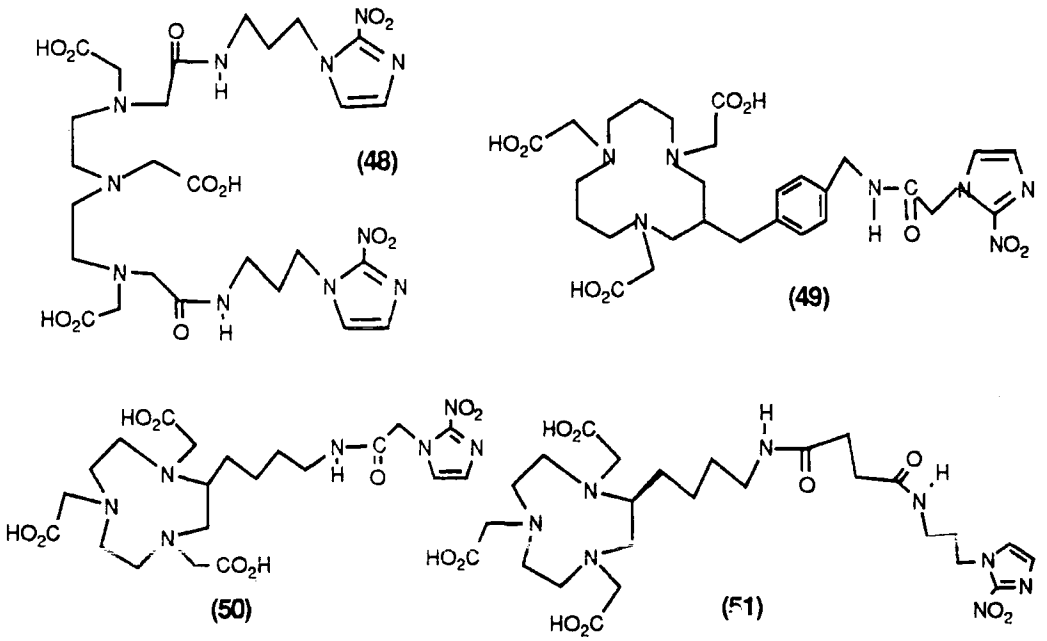

3.2 ACYCLIC DTPA - NITROIMIDAZOLE CONJUGATES

3.2.1 SYNTHESIS OF DTPA - BIS NITROIMIDAZOLE AMIDE

The nitroimidazole amine (**53**) was prepared by treating 2-nitroimidazole (azomycin) with potassium t-butoxide in DMF to generate the anion and addition of N-(3-bromopropyl)phthalimide provided the white solid intermediate (**52**). Deprotection by hydrazinolysis gave the desired 1-(3-aminopropyl)-2-nitroimidazole (**53**) in good yield.[11,12]

SCHEME 3.1

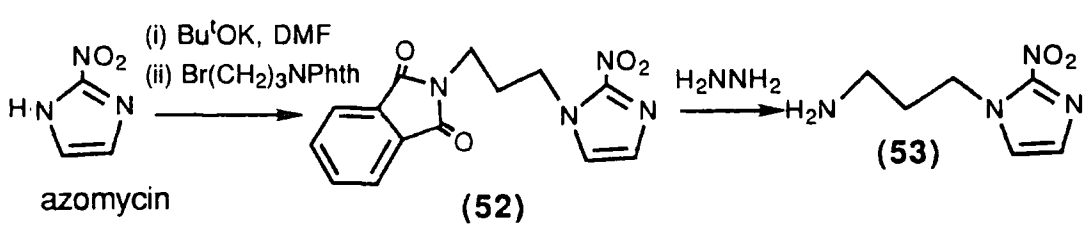

Following the successful synthesis of the DTPA-bis benzylamide (**19**) the analogous reaction with 1-(3-aminopropyl)-2-nitroimidazole was attempted. Diethylenetriamine pentaacetic dianhydride in pyridine was treated with the nitroimidazole amine (**53**) in the presence of DMAP. Upon work up some white solid did precipitate from methanol in the presence of sulphuric acid. This was not the methyl ester as hoped, and was suspected

to be the sulphate salt. The desired DTPA bis amide (**48**) was separated using semi-preparative reverse phase HPLC, and was isolated as a pale yellow oil in 64% yield.

SCHEME 3.2

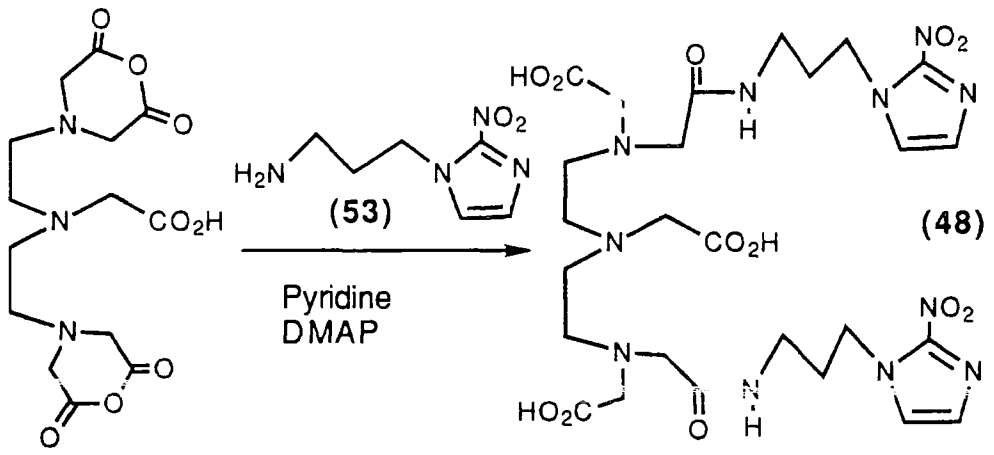

3.2.2 COMPLEXATION

The Gd complex of the DTPA-bis amide was prepared by heating the bis-amide (**48**) to reflux in dilute HCl (pH 2) with gadolinium oxide for 2 hours. After adjusting the pH to 6 the solution was allowed to cool. As no precipitate formed the product was purified using semi-preparative reverse phase HPLC (under the standard conditions, but in the absence of TFA) to give the white solid complex (**54**). The corresponding terbium complex was prepared by heating the DTPA-bis amide (**48**) to reflux in water with terbium acetate for 2 hours. The pH was adjusted to 6, the solution cooled and purified by HPLC, the terbium complex (**55**) was isolated as a white solid.

3.2.3 LUMINESCENCE STUDIES ON TERBIUM COMPLEX

3.2.3.1 LANTHANIDE LUMINESCENCE AND ITS USES

The luminescence properties of the lanthanide series have been thoroughly investigated.[13,14] The central five members of the series in particular, Sm^{3+}, Eu^{3+}, Gd^{3+}, Tb^{3+} and Dy^{3+}; all show long-lived luminescence, although the remainder of the series rarely luminesce. Some of the characteristics of these luminescent lanthanides are:

1) Large Stokes shifts, of the order 250-350nm.
2) Long-lived luminescence (of the order of milliseconds), allowing monitoring after short-lived background fluorescence has decayed.
3) Narrow lines in the emission spectrum.

4) They are very poor light absorbers, (ε typically < 1 $dm^3mol^{-1}cm^{-1}$), so they are difficult to excite by direct irradiation unless laser sources are used.

Luminescent lanthanides have found uses as probes in biological systems such as in fluoroimmunoassays, replacing conventional fluorescent organic molecules such as fluorescein as lumophores. The fine structure of the spectra and the measured lifetimes also provide information about local site symmetry and coordination number.

3.2.3.2 TERBIUM COMPLEX CONTAINING NITROIMIDAZOLE ANTENNA

The luminescence properties of the lanthanides described above make them highly suitable as lumophores with the singular disadvantage that they are very poor light absorbers. To make use of their emitting properties it is necessary to indirectly populate the excited states. One way of achieving this involves complexation with a ligand which incorporates a suitable chromophore, or antenna. A suitable chromophore must absorb strongly at a given wavelength such that efficient energy transfer may take place from the triplet excited state of the chromophore to the emissive state of the metal ($^5D_4$ in the case of Tb).

FIGURE 3.5 *Ultra-violet spectrum of Tb complex of DTPA bis nitroimidazole amide (55)*

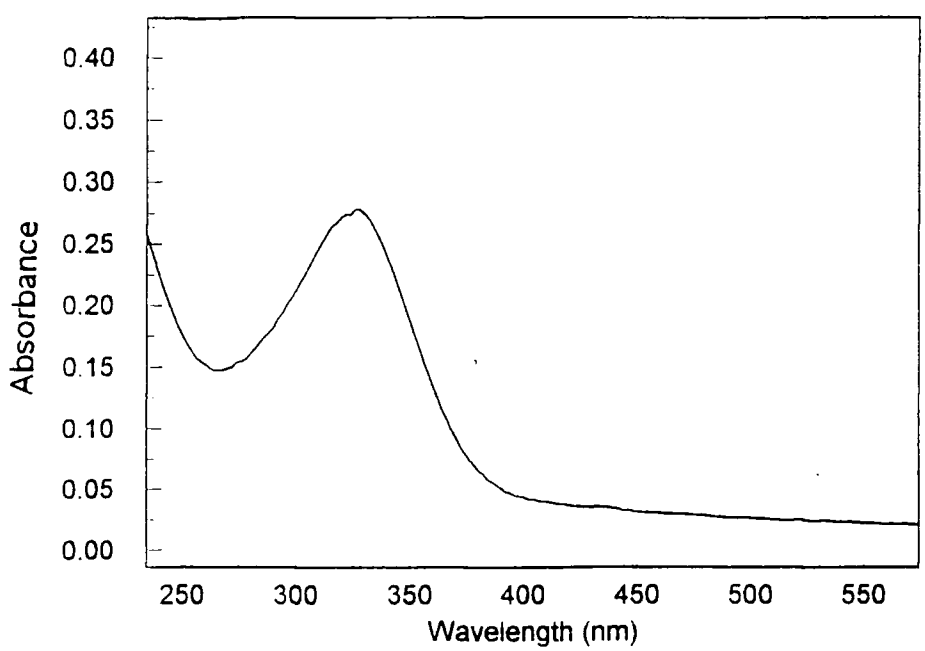

In an attempt to determine whether the 2-nitroimidazole chromophore might behave in this way, studies were carried out on the Tb^{3+} complex (**55**). The ultra-violet spectrum shows a strong absorbance at 320nm characteristic of 2-nitroimidazole. However the luminescence quantum yield (ϕ_{D2O}^{298K}) proved to be low.

3.2.3.3 DETERMINING THE NUMBER OF COORDINATED WATER MOLECULES

It has been observed that the luminescence lifetimes and intensities of Eu and Tb complexes are often much greater when measured in D_2O than H_2O. This occurs because there exists a radiationless deexcitation pathway from the lanthanide emissive level via energy transfer to the high energy O-H vibrations of coordinated water. The O-H oscillator then rapidly loses energy to the surroundings. This process takes place to a much lesser extent in the case of O-D owing to poorer Franck-Condon overlap of vibrational wavefunctions.[15]

Horrocks[16,17] has exploited this difference in excited state lifetimes as a means of calculating the number of water molecules directly coordinated to the lanthanide ion. A brief summary of the method follows:

The rate of depopulation of the emissive state, k_{depop}, is the reciprocal of the observed excited state lifetime, τ_{obs}, and is the sum of several terms including k_{OH}. The term k_{OH} is the rate constant for energy transfer to O-H oscillators and when the lifetime is measured in D_2O the k_{OH} term vanishes. The value of k_{OH} may be calculated by measuring the lifetimes in both H_2O and D_2O and using the equations:

$$k_{OH} = \Delta\tau^{-1} = \tau_{obs}(H_2O)^{-1} - \tau_{obs}(D_2O)^{-1} \quad \ldots\ldots\ldots\ldots \quad (1)$$

The number of water molecules, or number of O-H oscillators, in the first coordination sphere, q, is proportional to k_{OH}. In the case of Tb^{3+}, the empirical proportionality constant is 4.2 and in the case of Eu^{3+} it is 1.05:

$$q_{Tb} = 4.2\, k_{OH} = 4.2\, [\tau(H_2O)^{-1} - \tau(D_2O)^{-1}] \quad \ldots\ldots\ldots\ldots \quad (2)$$

$$q_{Eu} = 1.05\, k_{OH} = 1.05\, [\tau(H_2O)^{-1} - \tau(D_2O)^{-1}] \quad \ldots\ldots \quad (3)$$

This method was employed to determine the number of water molecules directly bound to the Tb^{3+} ion in the DTPA bis nitroimidazole amide complex. The luminescence properties of the complex were studied using a Perkin-Elmer LS50B. Lifetime

measurements were carried out by monitoring the luminescence intensity after a range of delay times. The minimum possible gate times were used, whilst still allowing reasonable emission intensities, thereby reducing the uncertainty in the luminescence intensity. The emission spectrum (figure 3.6) shows the expected bands typical of Tb complexes involving transitions from the emissive state ($^5D_4$) to the ground state (^7F_J, J = 0,1,2,3,4). The excitation spectrum (figure 3.7) does not match the absorption spectrum of the nitroimidazole, clearly indicating that energy transfer does not occur from the nitroimidazole moiety. It is probable that energy transfer occurs from a charge transfer state, (LMCT).

FIGURE 3.6 *Corrected emission spectrum of (55) in H_2O (excitation wavelength 320nm, delay time 0.1ms, gate time 10ms, 293K)*

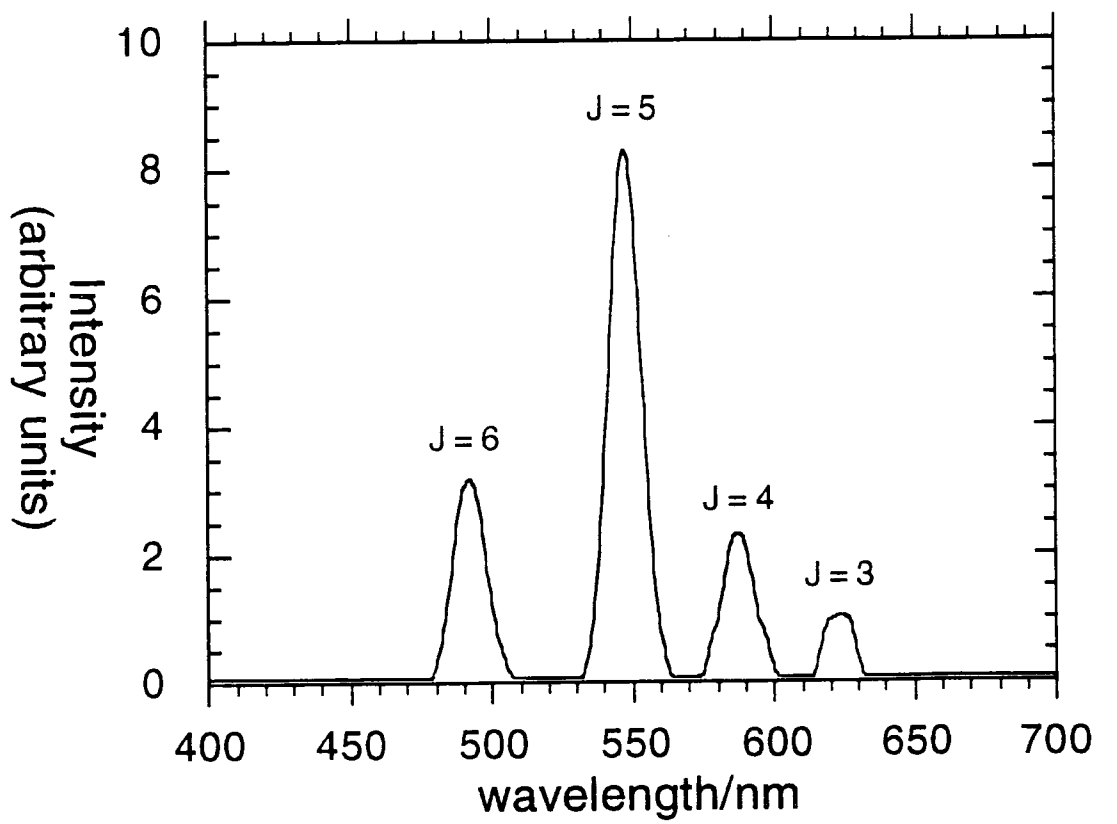

The luminescence intensity (I_t) (at 545 nm) in water at a range of times (t in ms) was recorded following pulsed excitation at 320nm: it showed exponential decay, consistent with first order kinetics of deactivation. These relate to the lifetime (τ) by the equation (4):

$$I_t = I_0 e^{-t/\tau}$$

$$\ln I_t = \ln I_0 - t/\tau \qquad \text{.....} \qquad (4)$$

FIGURE 3.7 *Phosphorescence excitation spectrum of (55) (emission wavelength 545nm, delay time 0.1ms, gate time 10ms, 293K)*

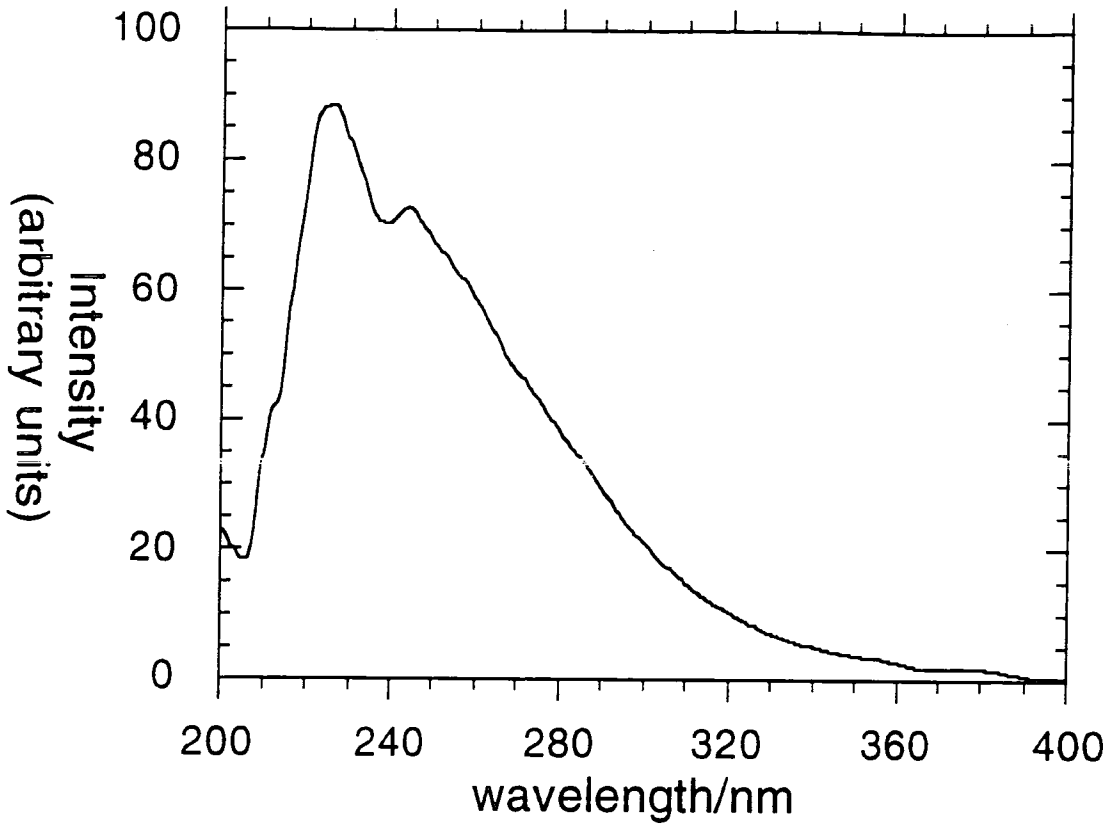

FIGURE 3.8 *Comparison of corrected emission spectra for (55) measured (a) in H_2O (lower peaks) and (b) in D_2O (upper peaks), excitation wavelength 320nm, delay time 0.1ms, gate time 10ms, 293K.*

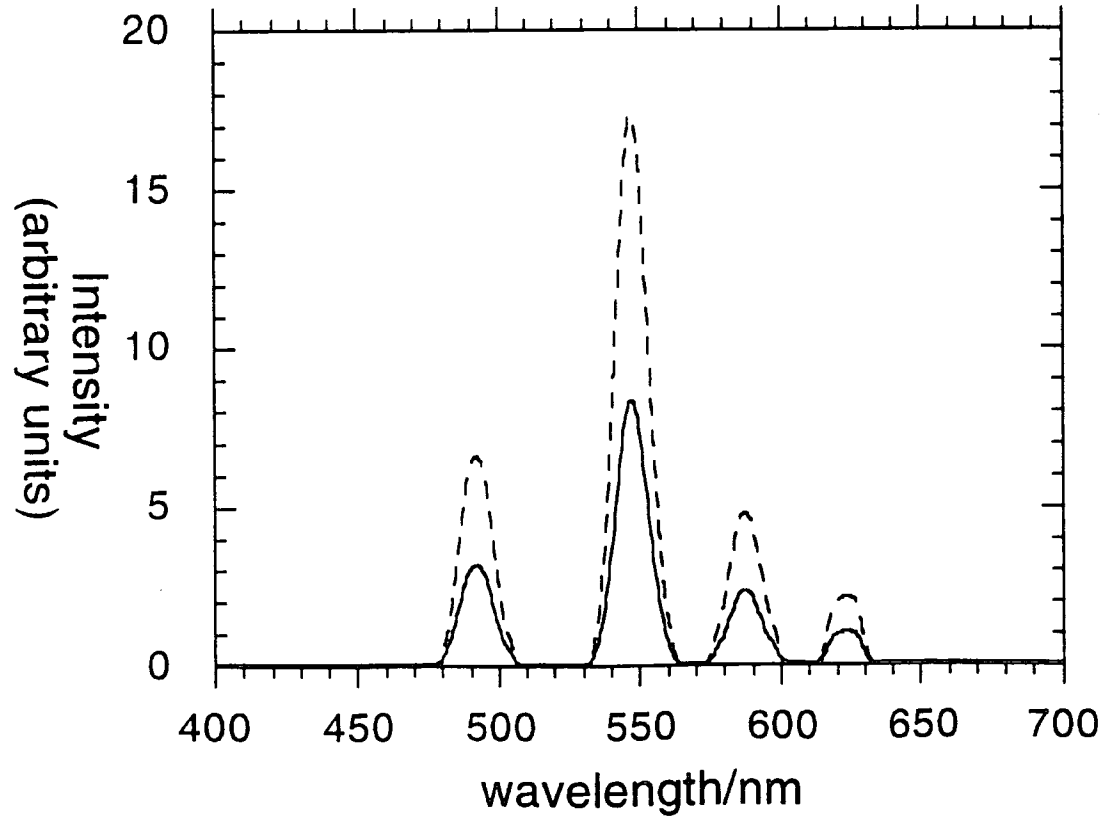

Plotting ln I_t against t for a range of different excitation wavelengths allowed an average value for τ to be calculated from the gradient. The procedure was repeated for a solution with an equal absorbance at the excitation wavelength in D_2O; the upper trace in figure 3.8 clearly shows the greater intensity observed in D_2O as a solvent, compared to the lower trace observed in H_2O.

The values calculated were τ (H_2O) = 1.49 ms and τ (D_2O) = 2.22 ms. Using equation (2) the number of water molecules (q) was calculated as 0.9. Given the experimental uncertainty in these measurements, this result is a clear indication that the complex possesses one bound water molecule.

For many ligands the Gd complex and Tb complex are isostructural.[18] This allows deductions about the Gd complex to be made based on independently determined properties of the Tb complex. In simple Gd complexes, the value of the relaxivity at high field is mostly a function of q and the rotational correlation time, with complexes having bound water molecules generally displaying higher relaxivities. Since the Tb complex (**55**) possesses one bound water molecule it may be anticipated that the Gd complex (**54**) will also have one coordinated water making it an attractive candidate as an 'inner sphere' contrast agent.

3.2.4 BIODISTRIBUTION STUDIES ON GADOLINIUM COMPLEX

The biodistribution of the ^{153}Gd complex of DTPA-bis nitroimidazole amide was examined in mice. Immunocompetent mice bearing a xenograft of a KHT sarcoma, a tumour type in which the proportion of hypoxic cells is particularly high, were used in these studies.

Because the dose of nitroimidazole conjugate to be administered was relatively low, it was administered along with a larger dose of misonidazole (100μmol kg^{-1}) in order to avoid the premature bioreduction of the nitroimidazole within the conjugate in the bloodstream. A control experiment was also carried out using ^{153}Gd-DTPA, co-administered with the same proportion of misonidazole.

The neutral ^{153}Gd-(**48**) conjugate was slower to clear from the blood than the control [^{153}Gd-DTPA]$^{2-}$ as might be expected. Figure 3.9 shows the percentage dose per gram of tissue at 4 and 24 hours for ^{153}Gd-(**48**) and ^{153}Gd-DTPA. The principal differences lie in the lower concentration of ^{153}Gd in the blood, femur and tumour of the control mice. The greater retention of ^{153}Gd in the skeleton of the mice given the nitroimidazole conjugate at 4 and 24 hours is consistent with release of ^{153}Gd from the complex.

The ratio of the percentage dose per gram of tissue for the experimental versus control is shown in figure 3.10. This shows that the tumour uptake of ^{153}Gd in the experimental group was marginally greater than in the control, but taking into account the greater blood level in the experimental mice, the comparison reveals that it is unlikely that there is significant tumour localisation due to the nitroimidazole groups.

FIGURE 3.9 *Biodistribution of (a) ^{153}Gd-DTPA-nitroimidazole amide and (b) ^{153}Gd-DTPA in mice bearing the murine KHT sarcoma.*

(a)

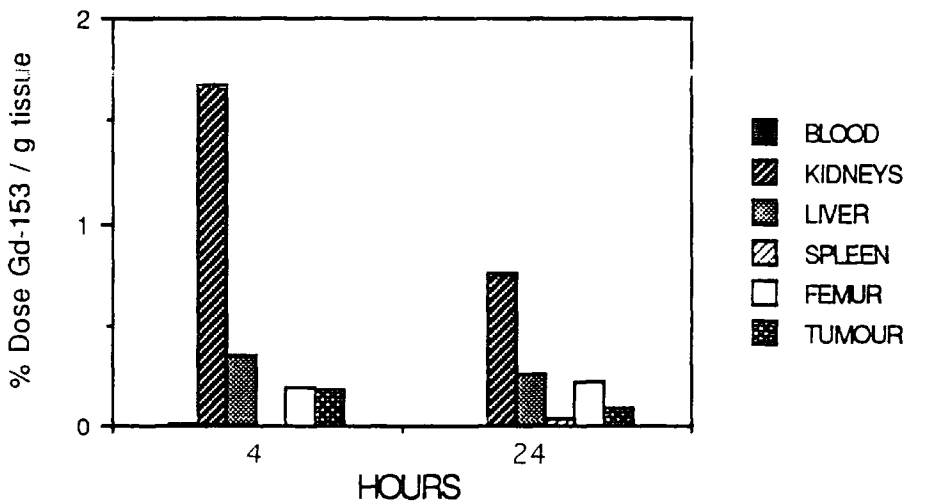

(b)

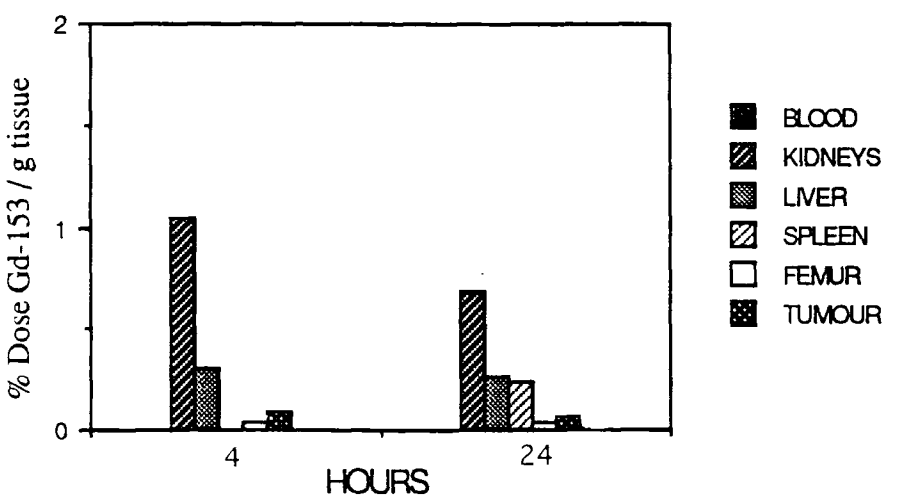

FIGURE 3.10 *Biodistribution of [^{153}Gd(**48**)] compared to [^{153}Gd-DTPA]$^{2-}$ in mice bearing a KHT tumour (ratio of experimental to control, % injected dose per g tissue)*

Tissue	4 hours	24 hours
Blood	7.1	20
Kidneys	1.6	1.1
Liver	1.1	1.0
Spleen	-	0.18
Femur	4.7	5.6
Tumour	1.9	1.5

The inferior *in vivo* stability of DTPA-bis amide complexes compared to DTPA complexes themselves has been noted previously[19,20] and is manifested by deposition of the radiolabel in the bone. This disadvantage may reduce the clinical usefulness of this complex in the long term. On the other hand the release of a small amount of ^{153}Gd does not compromise tumour uptake. Since this complex is relatively cheap and accessible, and is cleared from the body relatively quickly it may still find uses in future exploratory studies to determine the usefulness of 2-nitroimidazole as a tumour targeting vehicle.

3.3 12N3 - NITROIMIDAZOLE CONJUGATES

3.3.1 SYNTHESIS OF C-FUNCTIONALISED DERIVATIVES OF 12N3

Hexadentate macrocycles are also known based on N- and C- substituted 12N3 ligands.[21] The 12N3 triacetate derivative ^{111}In complex has already been shown to be kinetically stable *in vivo*.[22] In order to direct the ^{111}In gamma emitter towards hypoxic tissue the synthesis of the novel target ligand (**49**) was attempted.

The starting diamide (**56**) had already been synthesised by reaction of the p-cyanobenzyl derivative of diethyl malonate with triazanonane.[23] Tosylation of (**56**) using toluene-p-sulphonyl chloride and triethylamine in dichloromethane gave (**57**) quantitatively. This sequence of reactions, avoiding direct borane reduction of (**56**), avoids the possibility of formation of a robust boron complex during borane reduction and led to the formation of the N-tosylamide (**58**) in 79% yield. Detosylation with hydrogen bromide in the presence of phenol yielded the tetra-amine (**59**) (62%).

SCHEME 3.3

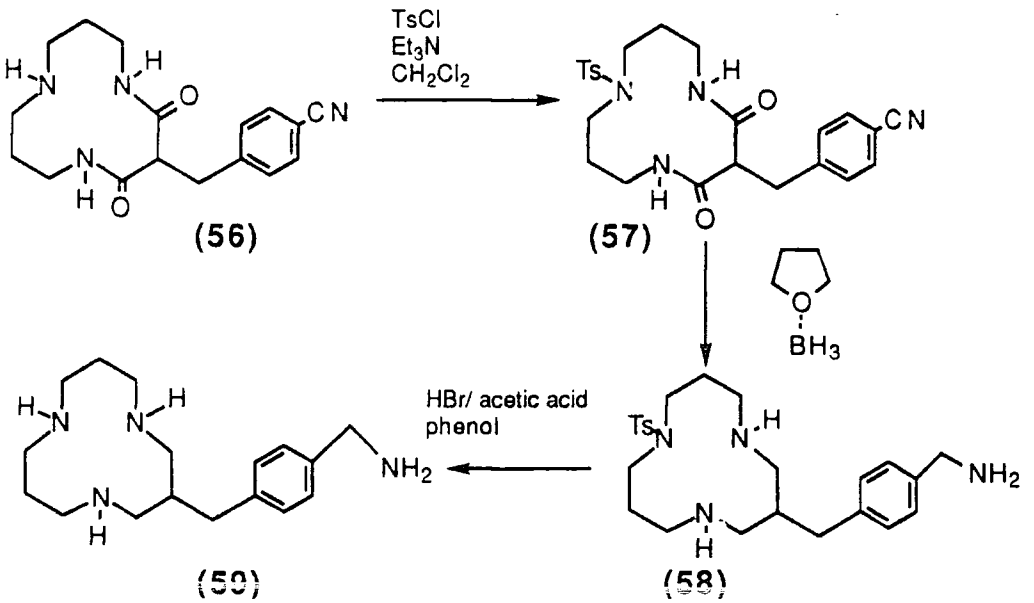

The route to the target 12N3 - nitroimidazole conjugate required coupling of the tetra-amine (**59**) with an imidazole acid. The acid chosen was 2-nitroimidazole-1-acetic acid (**60**) which was synthesised from 2-nitroimidazole by the route shown in scheme 3.4.[24] The coupling techniques initially employed involved coupling in the presence of DCC or reaction with the p-nitrophenol active ester of the nitroimidazole acid.

SCHEME 3.4

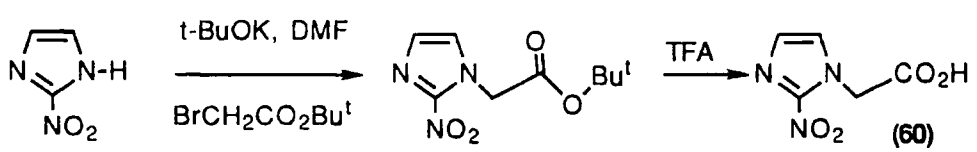

Initial attempts at reaching target (**49**) involved protection of the tetra-amine (**59**) with molybdenum hexacarbonyl in n-butyl ether leaving only the remote amine group to undergo amide coupling with 2-nitroimidazole-1-acetic acid under standard DCC conditions. However attempts by this method failed to produce a significant amount of the desired compound (**62**). It was thought that this was due to the air-sensitivity of the molybdenum complex (**61**), and the difficulty in monitoring the reaction's progress.

SCHEME 3.5

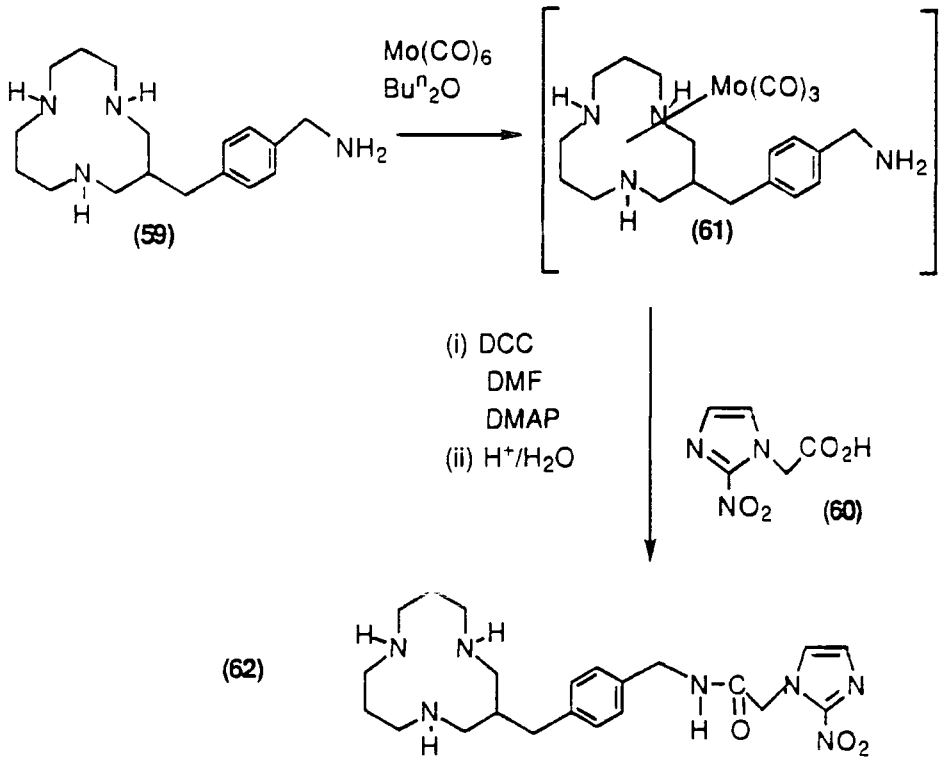

SCHEME 3.6

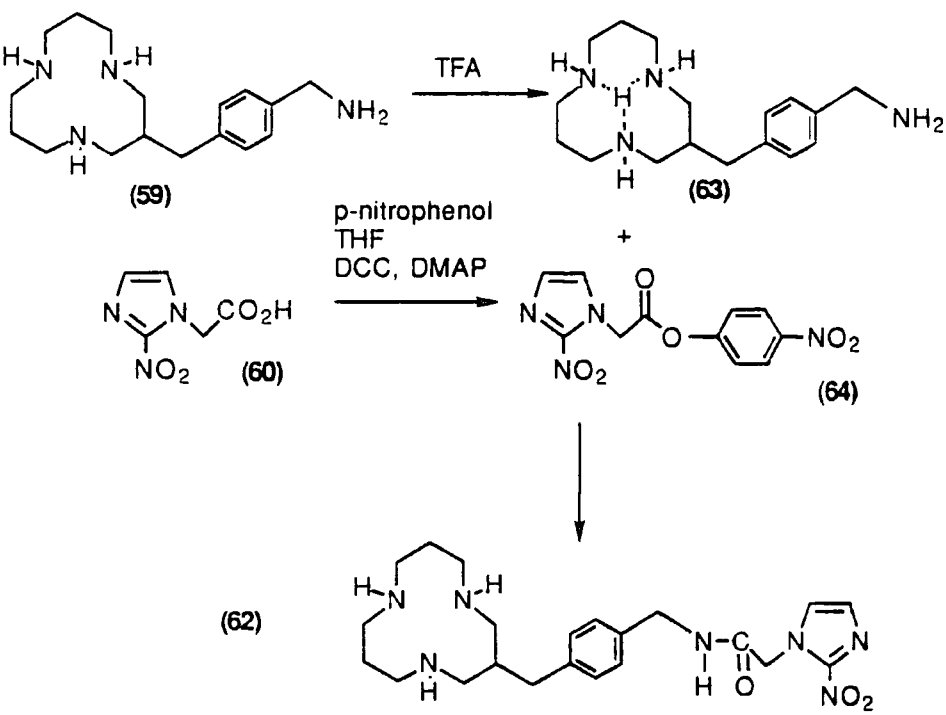

An alternative method which did not require molybdenum protection but which involved protection of the ring nitrogens from electrophilic attack by protonation with TFA (pK_a=13.2 and 7.4 for the parent amine) was employed. The nitroimidazole-p-nitrophenol activated ester **(64)** was formed *in situ* by DCC coupling, filtered to remove

DCU and added directly to the protonated macrocycle (**63**), and the resulting solution stirred at room temperature with tlc monitoring for 24 hours. Although IR analysis of the resultant material appeared to show the presence of an amide, ^{1}H NMR and mass spectrometry indicated that an intractable complex mixture had been produced. Consequently no definitive statement as to the viability of this sequence could be made.

3.3.2 ALTERNATIVE AMIDE COUPLING REAGENTS - DPPA, PBOP

Subsequently it was decided to use a different reagent for amide coupling, namely diphenylphosphoryl azide (DPPA) which has been used extensively in peptide coupling.[25,26,27] Initially a model reaction was attempted to establish the suitability of DPPA as a coupling agent where nitroimidazole acid was involved. 2-nitroimidazole-1-acetic acid (**60**) was stirred in DMF with sodium bicarbonate and isobutylamine; DPPA was added to the mixture last and stirring continued for 24 hours. Work up and purification by alumina PLC gave the desired amide (**65**).

SCHEME 3.7

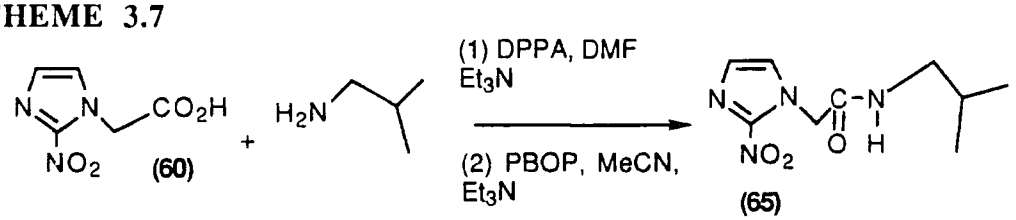

Another phosphorus based reagent used in amide coupling is benzotriazol-1-yloxy-tripyrrolidinophosphonium hexafluoro phosphate (PBOP).[28] An analogous model reaction was carried out on the imidazole acid using this reagent. 2-Nitroimidazole-1-acetic acid (**60**) was stirred in acetonitrile with triethylamine and isobutylamine, PBOP was added and stirring continued for a further 18 hours. Work up and alumina PLC also gave the desired amide (**65**) as previously.

SCHEME 3.8

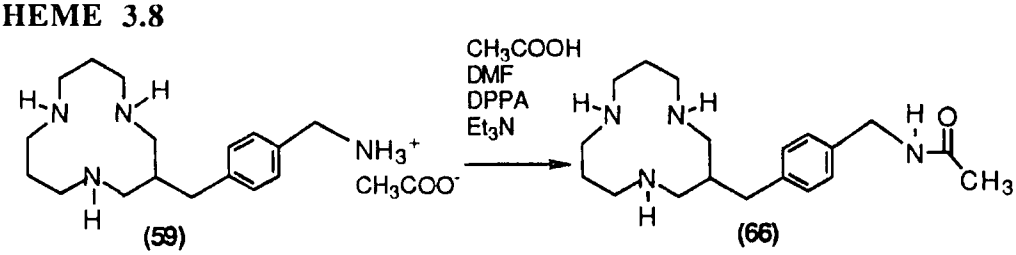

Next it was decided to test the suitability of DPPA for coupling a macrocyclic ligand and acid by using it to prepare the known acetamide (**66**). Tetra-amine (**59**) was treated with glacial acetic acid to protect the ring nitrogens from electrophilic attack, then this salt

was dissolved in DMF and was treated with triethylamine, acetic acid and DPPA for 2 weeks affording the desired acetamide (**66**).

3.3.3 SYNTHESIS OF 12N3 - NITROIMIDAZOLE CONJUGATE

In light of this success, the tetraamine (**59**) was treated with TFA to protect the ring nitrogens. The resultant salt was dissolved in DMF and reaction with triethylamine, 2-nitroimidazole-1-acetic acid and DPPA (0°C, 4 days, monitored by cation exchange HPLC) afforded the desired nitroimidazole conjugate (**62**) in low yield. Trialkylation of the secondary amine sites with ethylbromoacetate in ethanol in the presence of potassium carbonate appeared by tlc to give the triester (**67**) but on such a small scale that purification proved difficult. Before this procedure was repeated on a more manageable scale it was decided to pursue the syntheses of 9N3 - nitroimidazole conjugates being carried out in parallel in order to determine whether the nitroimidazole moiety would indeed enhance tumour localisation.

SCHEME 3.9

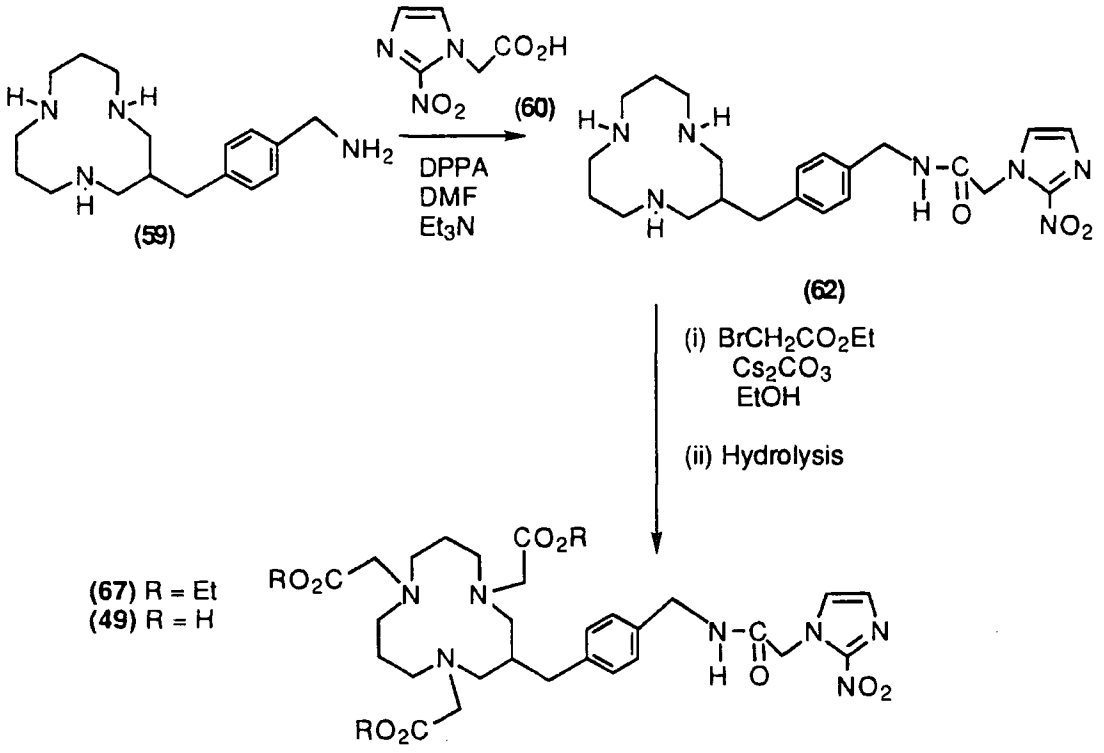

3.4 9N3 - NITROIMIDAZOLE CONJUGATES

3.4.1 SYNTHESIS OF C-FUNCTIONALISED DERIVATIVES OF 9N3

The amino acid (2S)-lysine was used as the starting material for the synthesis of the C-functionalised derivatives of 1,4,7-triazacyclononane-1,4,7-triyltriacetic acid (NOTA), target compounds **(50)** and **(51)**, and the following well established synthesis was employed.[29] Reaction of the methyl ester of lysine **(68)** (as the dihydrochloride) with warm ethylenediamine (in excess) afforded the monoamide **(69)**. Under these conditions the competitive formation of the 7-ring lactam by intra molecular cyclisation was suppressed, although when methanol was present it did occur.

SCHEME 3.10

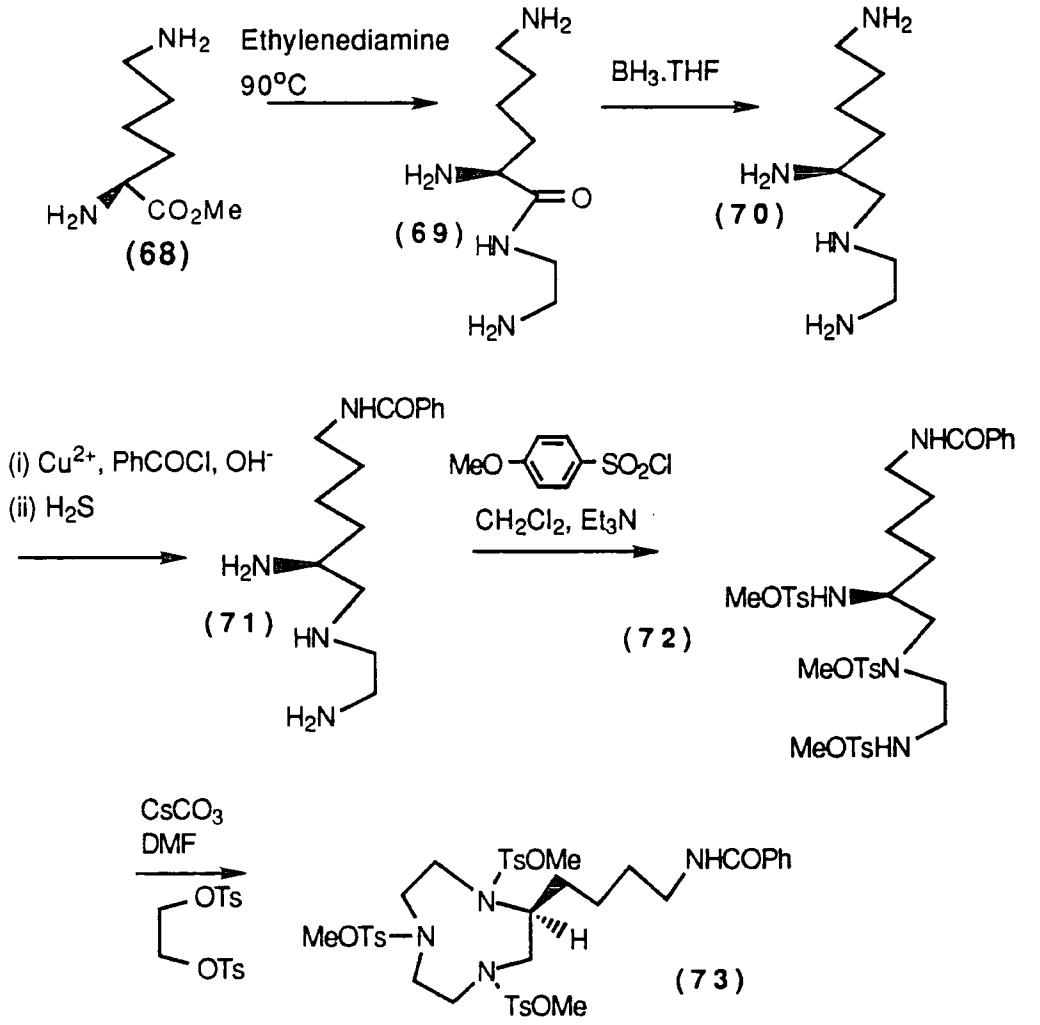

The amide was reduced with borane -tetrahydrofuran to yield the tetra-amine **(70)** and reaction with copper (II) ions (as basic copper carbonate) in aqueous solution generated the blue diethylenetriamine-copper (II) complex which effectively protected the three

nitrogens from electrophilic acylation. Reaction with benzoyl chloride in the presence of base permitted acylation on the remote amino group and treatment of the copper complex with hydrogen sulphide permitted isolation of the free benzamide (**71**) (53%). Protection with p-methoxybenzenesulphonyl chloride afforded (**72**) which was co-condensed with ethylene glycol ditosylate under standard conditions (Cs_2CO_3, DMF, 65°C, 18 hours) to afford the nine membered ring compound (**73**) in 72% yield.

SCHEME 3.11

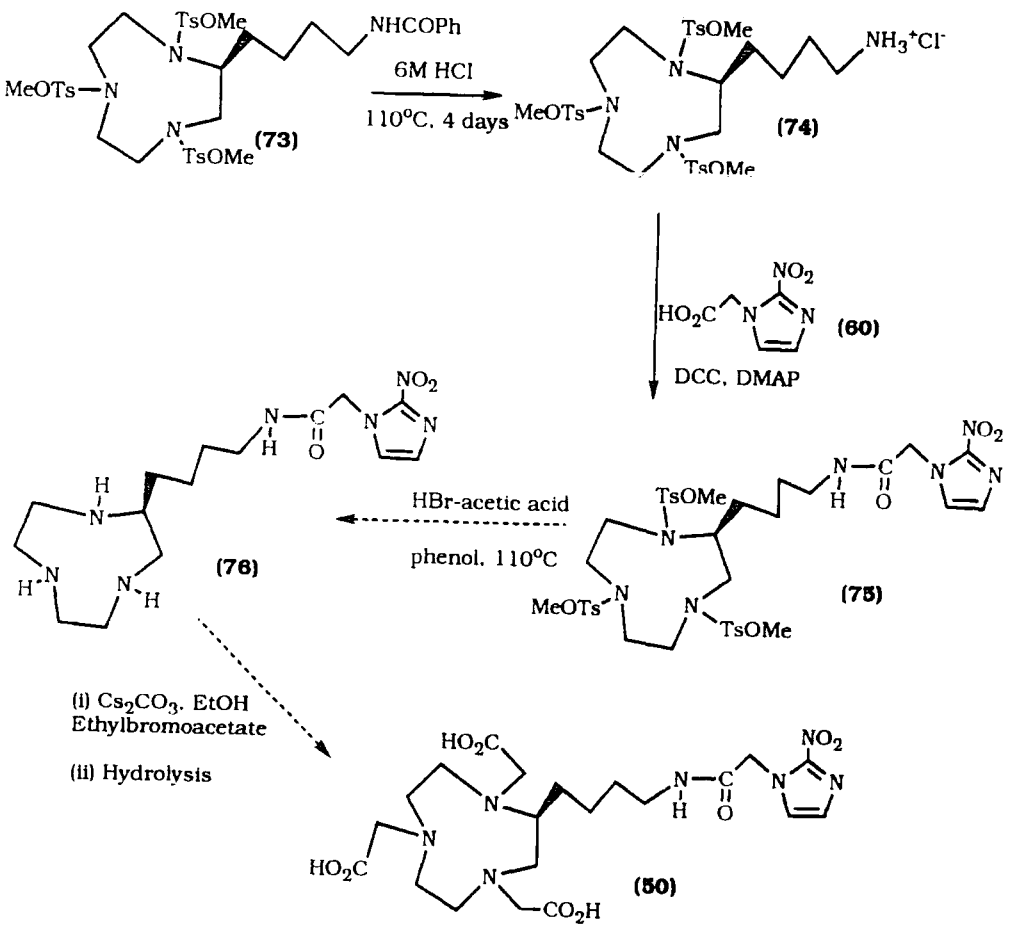

Initial attempts to prepare ligand (**50**) involved coupling a 2-nitroimidazole directly to the amide. The intermediate (**73**) was prepared and while the triamine was still protected debenzylation of the remote amino group was effected using standard conditions (6M HCl, 110°C, 48 hours). The relative insolubility of this compound (**73**) caused this reaction to proceed in poor yield (27%) and very efficient stirring and careful monitoring by TLC were essential. The amine hydrochloride (**74**) was converted to the free amine before coupling with 2-nitroimidazole-1-acetic acid (**60**) was attempted using DCC, DMAP in dichloromethane at 0°C for 24 hours. Again, with this reaction solubility problems were encountered. THF was used as a co-solvent, but the conditions for this step were not optimised. When accomplished, deprotection using HBr-acetic acid and

phenol followed by addition of carboxymethyl groups provides a well precedented route to the desired ligand (**50**).

3.4.2 ALTERNATIVE 9N3 NITROIMIDAZOLE COUPLING REACTIONS

Another possible route to (**50**) was explored starting from the protected triamine (**73**). Deprotection was achieved using 98% sulphuric acid to give the triamine (**75**) which was hydrolysed (6M HCl, 110°C, 4 days) affording the tetra-amine (**77**) quantitatively. The ring nitrogens were protected with molybdenum hexacarbonyl in n-butyl ether, leaving only the primary amine free to undergo coupling with 2-nitroimidazole-1-acetic acid (**60**) (DCC, DMF, DMAP, 25°C). However when the product was deprotected with 10% HCl none of the desired product (**76**) was found. Attempts to effect this coupling using the reagent DPPA as described in section 3.3.3 and using the p-nitrophenyl active ester of the nitroimidazole (**64**) as in section 3.3.1 also failed to produce the desired product.

SCHEME 3.12

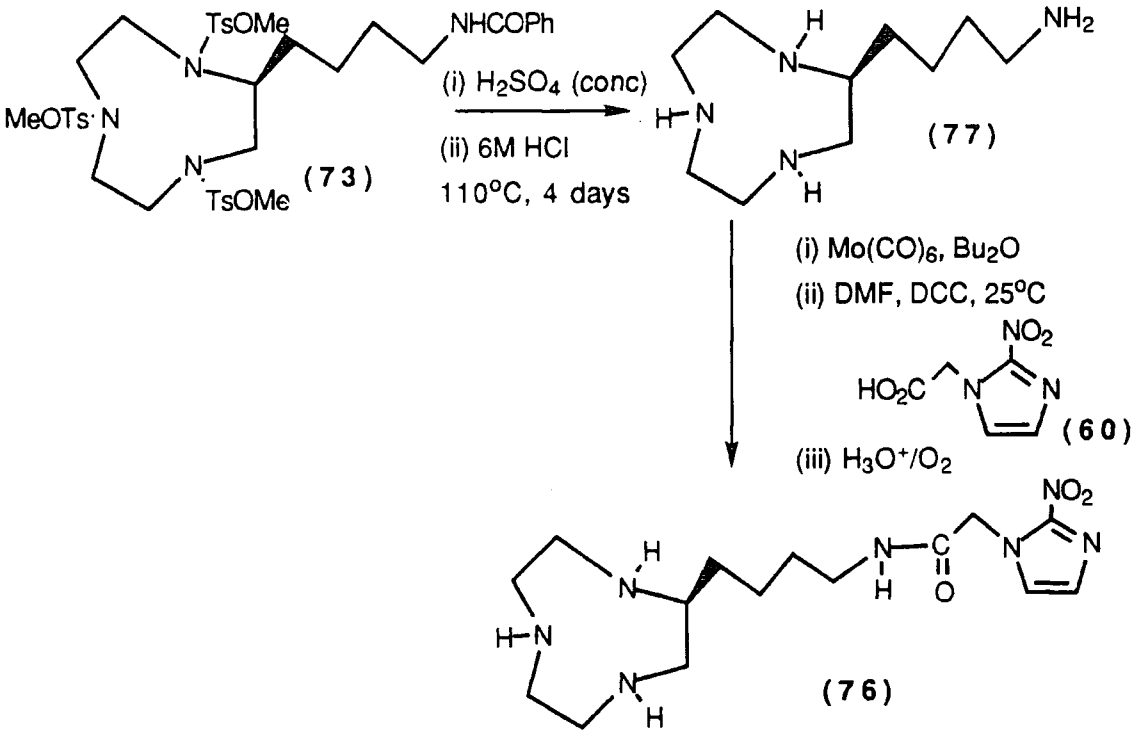

Deprotection of (**73**) was carried out using the alternative method of hydrogen bromide in acetic acid in the presence of phenol (110°C, 48 hours, 70%) and this material (**75**) was used in the synthetic route to target compound (**51**). The required carboxymethyl groups were introduced prior to coupling with nitroimidazole by reaction of (**75**) with ethylbromoacetate (K_2CO_3, EtOH) to give the triester (**78**) (63%) which could be

purified by gravitational alumina chromatography and then hydrolysed to amino acid (**79**) (6M HCl, 48 hours) quantitatively.

SCHEME 3.13

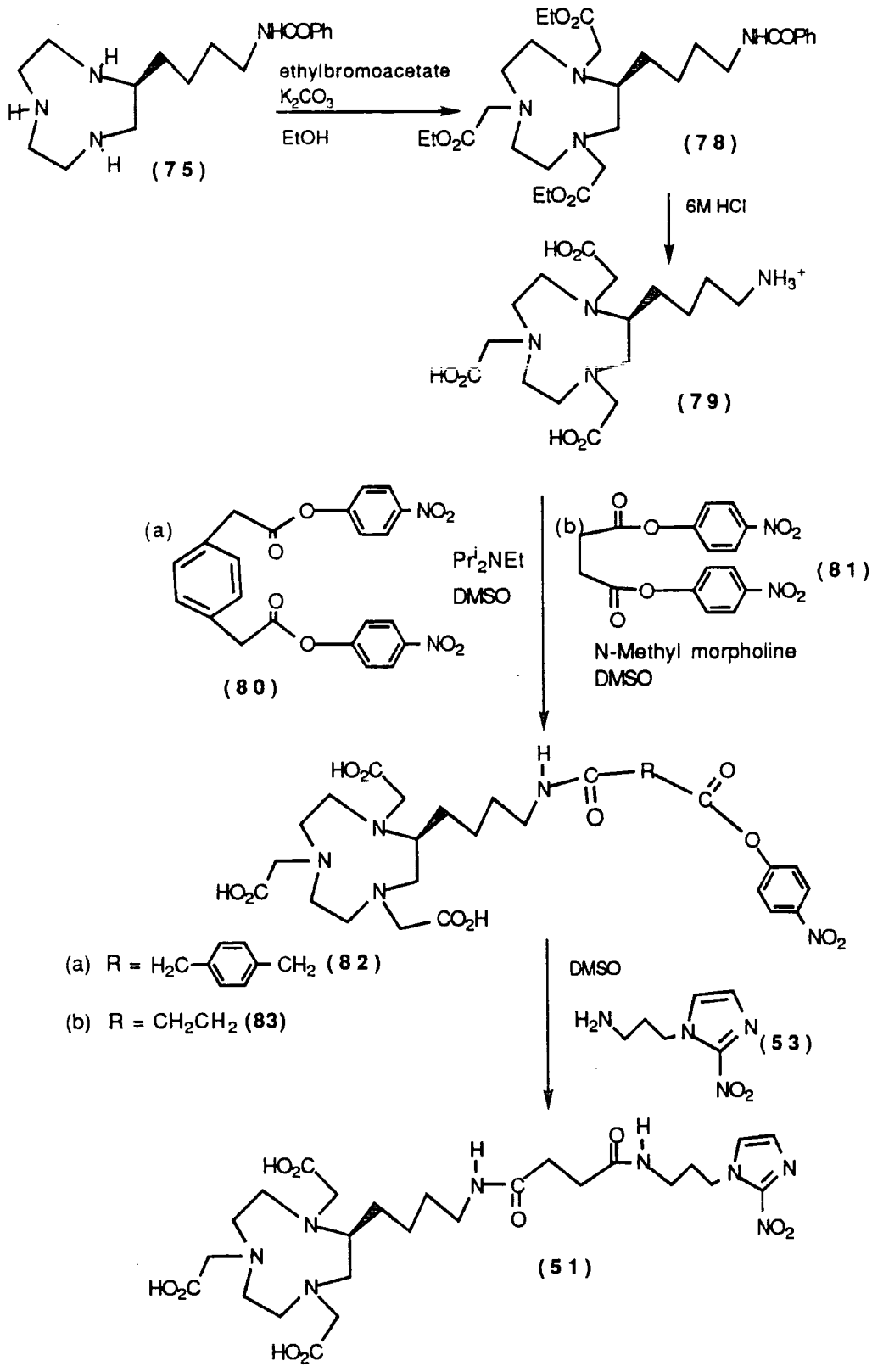

The next step involved reacting amino acid (**79**) with bis-[p-nitrophenyl-1,4,phenylenediacetate] (**80**) in the presence of base in DMSO and monitoring by HPLC (reverse phase). However despite there being evidence for the formation of the desired amide (**82**) within 20 minutes of the start of the reaction R_t=16 minutes, analytical HPLC showed that it had begun to decompose again before it could be purified by preparative HPLC.

Since it was desirable to minimise the molecular weight of the conjugate in order to enhance its transport properties *in vivo*, and also to bring the nitroimidazole moiety into closer proximity to the metal complex, the smaller succinate bis ester (**81**) was employed. The above procedure was repeated, then amino acid (**79**) was treated with bis-p-nitrophenyl succinate (**81**) in DMSO in the presence of N-methyl morpholine and mixed vigorously at 50°C for 1 hour. At this point HPLC monitoring indicated formation of the active ester had taken place and that it was beginning to decompose. The reaction was 'stopped' by storing the mixture at -78°C, while it was separated by preparative HPLC in batches. The active ester (**82**) was checked for analytical purity by HPLC and ^{1}H NMR and then used directly in the next step. Treatment with the nitroimidazole amine (**53**) in DMSO afforded the desired nitroimidazole conjugate (**51**) in low yield after HPLC purification.

3.4.5 BIODISTRIBUTION OF 9N3 - NITROIMIDAZOLE

The ^{111}In complex of the 9N3-nitroimidazole conjugate (**51**) was formed with a radiolabelling efficiency of 87%. The biodistribution was studied in normal mice, and 0.1 μmol kg^{-1} of complex was administered together with 500μmol kg^{-1} of misonidazole to minimise the destruction in the bloodstream of nitroimidazole linked to the macrocycle. The recommended interval for optimal uptake of 2-nitroimidazoles in tissues is 24 hours: the tissue biodistribution of ^{111}In was measured at this time. It has been observed that labelled 2-nitroimidazoles accumulate by bioreduction in certain normal tissues such as the oesophagus, eye lids and liver in addition to hypoxic tumour tissue. In this experiment a range of tissues were examined to determine whether the radiolabelled ^{111}In 9N3 nitroimidazole conjugate (**51**) showed any behaviour characteristic of the 2-nitroimidazole moiety.

It can be seen from figure 3.11 that the biodistribution of ^{111}In-(**51**) differs from the ^{111}In NOTA control in so far as the percentage dose per gram remaining in the tissues at 24 hours is statistically greater for ^{111}In-(**51**). Comparison of the ^{111}In-NOTA control with previous ^{111}In-NOTA results show that the misonidazole added had no effect on distribution. However there is little or no evidence for preferential uptake in hypoxic

tissues. Successful imaging of tissues requires, not a high tissue uptake, but a high tissue to background ratio. Figure 3.12 shows a comparison of tissue to blood ratios for both groups, this demonstrates that in fact the simple ^{111}In-NOTA shows greater tissue differentiation.

FIGURE 3.11 *^{111}In Biodistribution in mice of* **(51)** *compared with NOTA in a range of tissues.*

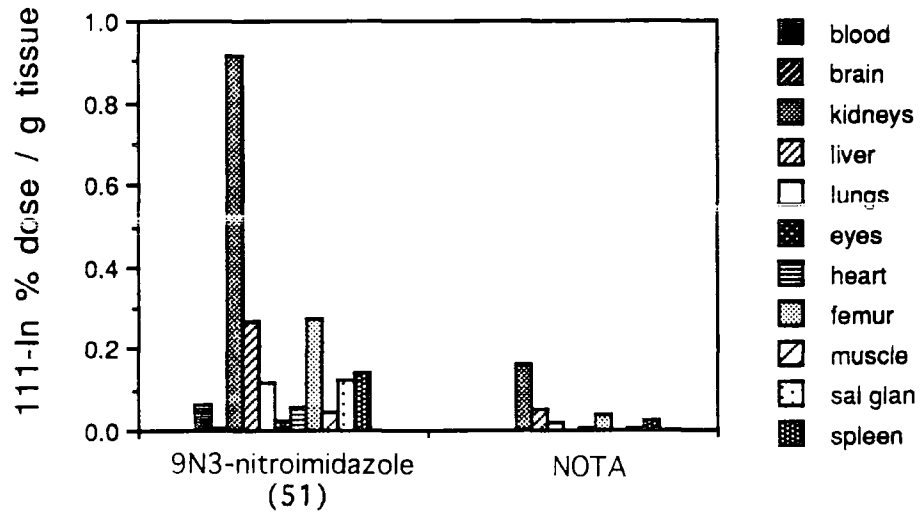

FIGURE 3.12 *1hour ^{111}In biodistribution of* **(51)** *compared to NOTA (Ratio of tissue : blood)*

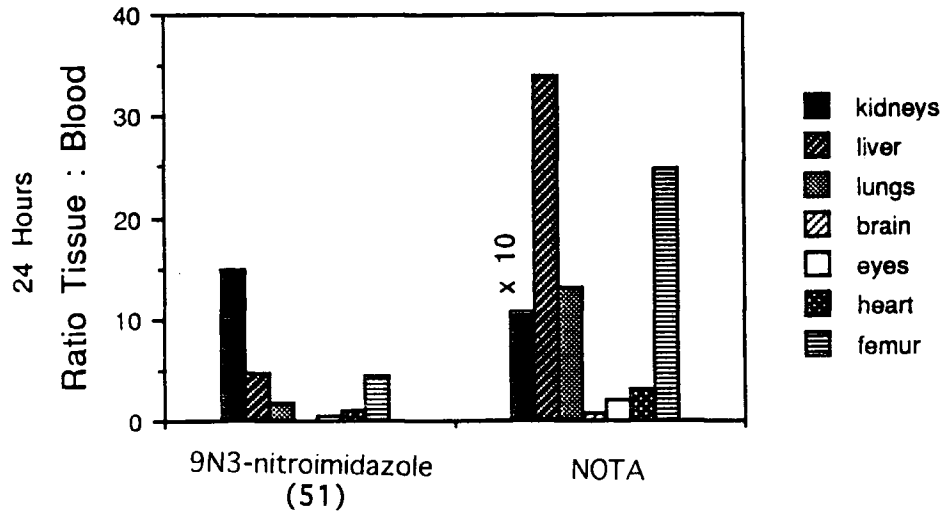

3.5 CONCLUDING COMMENTS

The Gd complex of DTPA bis nitroimidazole amide (**48**) did show some evidence for slight accumulation in hypoxic tissues. Despite its apparent low kinetic stability *in vivo* it may find uses in the future in further investigations into the tumour targeting potential of nitroimidazoles. The selective targeting of hypoxic tissues by the 9N3 based macrocyclic radiolabelled complex ^{111}In-(**51**) was not unequivocally established in the animal model employed. Further studies in hypoxic tumour bearing mice using the 9N3 or 12N3 based conjugates may provide additional useful information. However their relatively poor ability to localise in regions of hypoxia may be related to their relatively high molecular weight which may preclude cellular uptake. Alternatively it may be due to the fact that during this *in vivo* work these complexes were given at a relatively low dose, even though misonidazole was co-administered.

3.6 REFERENCES

1 L.M. Cobb, J. Nolan and S. Butler, *Int. J. Radiat. Oncol. Biol. Phys.*, 1990, **18**, 347.

2 A. Najafi, A. Sosa, M.M. Alauddin and M.E. Siegel, *Abs. Papers Am. Chem. Soc.*, 1991, **202**, 76.

3 P.E. Vaulk, C.A. Mathis, M.D. Prados, W.J. Jagust and T.F. Budlinger, *J. Nucl. Med.*, 1991, **32**, 955.

4 R.J. Maxwell, P. Workman and J.R. Griffiths, *Int. J. Radiat. Oncol. Biol. Phys.*, 1989, **16**, 925.

5 D.J. Chapman, J. Lee and B.E. Meeker, *Int. J. Radiat. Oncol. Biol. Phys.*, 1989, **16**, 911.

6 D.W. Siemann and P.C. Keng, *Br. J. Cancer*, 1987, **55**, 33.

7 Alice Harrison, personal communication.

8 C. Walker, L. Royle, A. Harrison, K. Pereira, I.J. Stratford, M. Stephens, M. Fielden, M. Naylor and D. Parker, 'Intracellular Binding, Biodistribution and Tumour Uptake of 2-Nitroimidazole Linked-Radiometal Complexes and Radiometal Complexes Alone', MRC Report, 1992.

9 Louise Royle, PhD. Thesis, University of Durham, (1995).

10 A. Harrison, C.A. Walker, K.A. Pereira, C. Counsell, D. Parker, L. Royle, R.C. Matthews, A.S. Craig, *Nucl. Med. Commun.*, 1992, **13**, 667.

11 I. Ahmed, I.J. Stratford and T.C. Jenkins, *Drug Res.*, 1985, **35(II)**, 1763

12 M.E. Perlman, J.A. Dunn, T.A. Piscitelli, J. Earle, W.C. Rose, G.L. Wampler, J.E. MacDiaarmid and T.J. Bardos, *J. Med. Chem.*, 1991, **34**, 1400.

13 J. -C.G. Bunzli in 'Lanthanide Probes in Life, Chemical and Earth Sciences', eds J.-C.G. Bunzli and G.R. Choppin, Elsevier, 1989.

14 Gareth Williams, PhD. Thesis, University of Durham, (1995).

15 P.W. Atkins, 'Physical Chemistry', 3rd ed., Oxford University Press, Oxford, 1989.

16 W. DeW. Horrocks, G.F. Schmidt, D.R. Sudnick, C. Kittrell and R.A. Bernheim, *J. Am. Chem. Soc.*, 1977, **99**, 2378.

17 W. DeW. Horrocks and D.R. Sudnick, *J. Am. Chem. Soc.*, 1979, **101**, 334.

18 D. Parker, 'Imaging and Targeting' in *Comprehensive Supramolecular Chemistry*, Volume 10, Chapter 17, Eds. D.N. Reinhoudt and J.M. Lehn, Pergamon, 1995.

19 M.S. Konings, W.C. Dow, D.B. Love, K.N. Raymond, S.C. Quay and S.M Rocklage, *Inorg. Chem.*, 1990, **29**, 1488.

20 D. Parker, P.K. Pulukkody, F.C. Smith, A. Batsanov and J.A.K. Howard, *J. Chem. Soc., Dalton. Trans.* 1994, 689.

21 A.E. Martin, T. M. Ford, J.E. Bulkowski, *J. Org. Chem.*, 1982, **47**, 412.

22 A.S. Craig, I.M. Helps, K.J. Jankowski, D. Parker, N.R.A. Beeley, B.A. Boyce, M.A.W. Eaton, K. Millar, A. Phipps, A. Harrison and C. Walker, *J. Chem. Soc., Chem. Commun.*, 1989, 794.

23 I.M. Helps, D. Parker, K.J. Jankowski, J. Chapman and P.E. Nicholson, *J. Chem. Soc. Perkin Trans. 1*, 1989, 2079.

24 A.G. Beaman, W. Tautz and R. Duschinsky, *Antimicrobial Agents and Chemotherapy*, 1967, 520.

25 T. Shioiri, K. Ninomiya and S. Yamada, *J. Am. Chem. Soc.*, 1972, **94**, 6203.

26 S.F. Brady, S.L. Varga, R.M. Freidinger, D.A. Schwenk, M. Medlowski, F.W. Holly and D.F. Veber, *J. Org. Chem.*, 1979, **44**(18), 3101.

27 S.F. Brady, R.M. Freidinger, W.J. Paleveda, C.D. Colton, C.F. Homnick, W.L. Whitter, P. Curley, R.F. Nutt and D.F. Veber, *J. Org. Chem.*, 1987, **52**, 764-769.

28 B. Castrino, J.R. Dormoy, G. Evin and C. Selve, *Tetrahedron Lett.*, 1975, **14**, 1219.

29 J.P.L. Cox, A.S. Craig, I.M. Helps, K.J.Jankowski, D. Parker, M.A.W. Eaton, A.T. Millican, K. Millar, N.R.A. Beeley and B.A. Boyce, *J. Chem. Soc., Perkin Trans. 1*, 1990, 2567.

Chapter Four

Tuftsin Conjugates

4.1 TARGETING TUMOUR MACROPHAGES USING TUFTSIN

Tuftsin is a naturally occurring linear tetrapeptide (L-Thr-L-Lys-L-Pro-L-Arg) which was first isolated in the 1970's.[1] It is a non-toxic fragment of the heavy chain of all human IgG isotypes.[2] Current interest in this peptide has increased since it was discovered that it possesses immunologically mediated anti-tumour potential.[3] The accessibility and low toxicity of tuftsin make it an attractive candidate for tumour targeting.

The method by which tuftsin may target tumours is via macrophages present on the boundary of the tumour or in necrotic regions of tissue. Macrophages possess receptors for many ligands including different IgG isotypes and complement components, this receptor ligand complex is then rapidly internalised by means of phagocytosis.[4] Whilst the macrophage content of tumours varies considerably, it has been shown that the macrophage densities are highest at the tumour periphery and in areas of necrosis. Targeting tumour-infiltrating macrophages may detect necrotic regions and delineate boundaries between normal and infiltrating neoplastic tissue. It may also assist in the detection of small metastases since the macrophage densities are highest in smaller lesions.[5]

4.1.1 FLUORESCENT TUFTSIN CONJUGATES

FIGURE 4.1 *Fluorescent labelling of tuftsin using fluorescein isothiocyanate.*

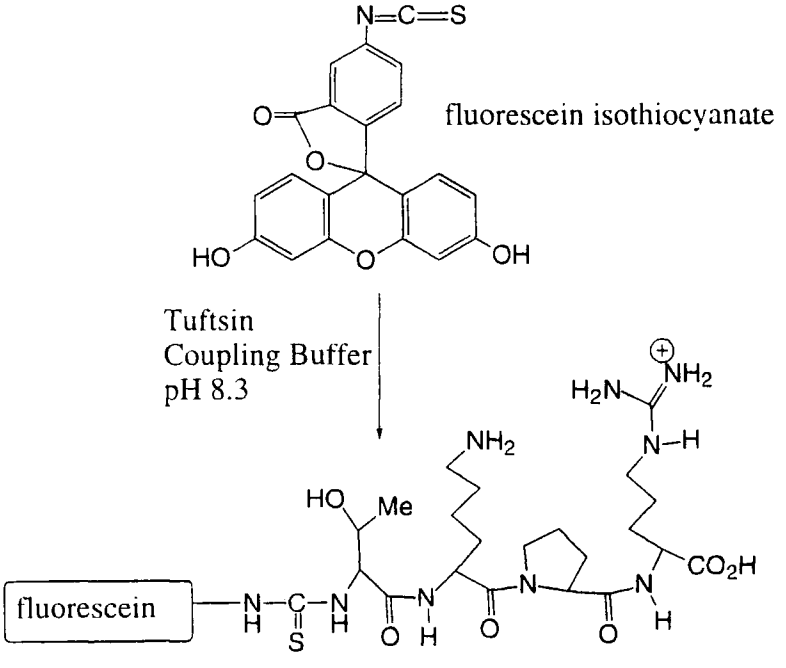

The mechanism of action of tuftsin following binding to its receptor and the fate of the tuftsin molecule itself were not known. In order to visualise these interactions via video intensification microscopy (VIM), biologically active fluorescent derivatives of tuftsin were prepared.

FIGURE 4.2*Fluorescent labelling of tuftsin using tetramethylrhodamine isothiocyanate*

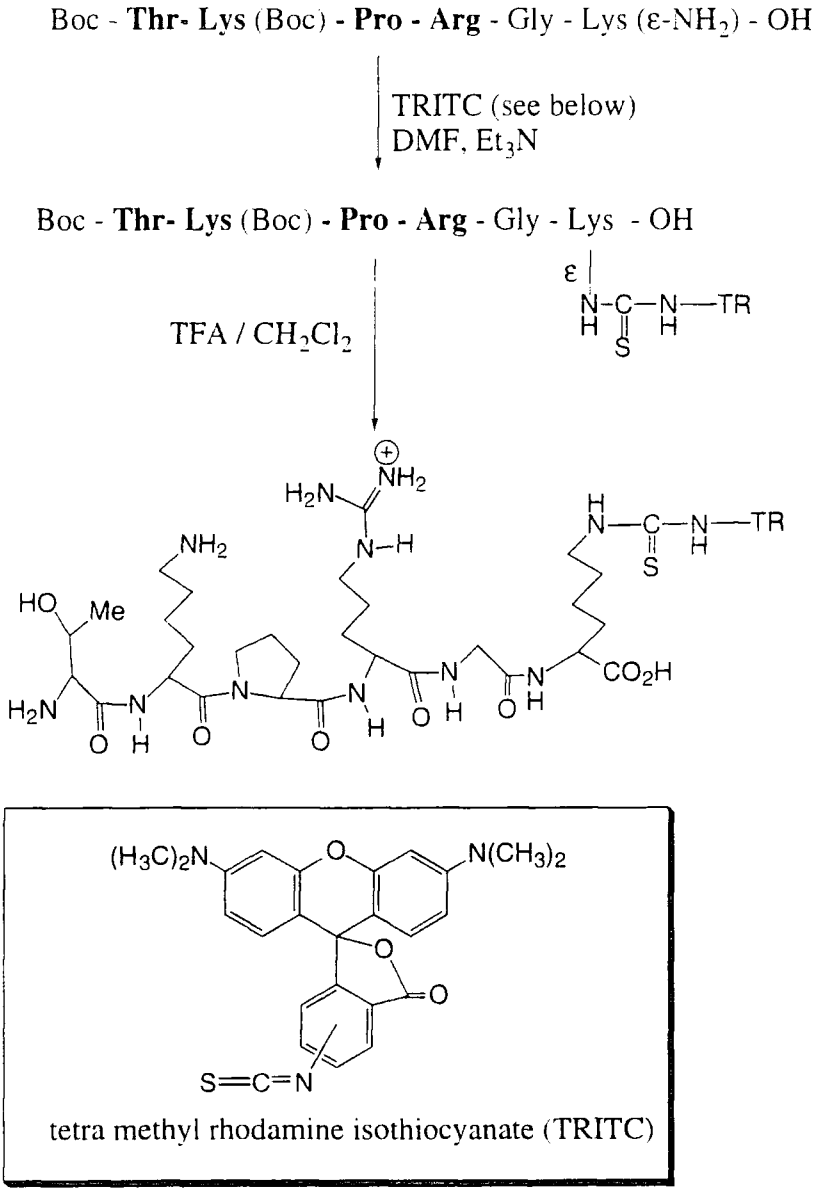

Tuftsin was simply coupled with fluorescein isothiocyanate as shown in figure 4.1.[6,4] The labelled tuftsin was separated from excess tuftsin using a Sephadex column. Characterisation of the coupling site confirmed that the NH_2-terminus had been modified and that the ε-amino group of lysine remained free. This might be expected since fluorescein isothiocyanate reacts with unprotonated amino groups; the only

unprotonated amino group at the chosen coupling pH of 8.3 exists at the α-amino terminus, as can be concluded from the respective pK_a values of the tuftsin functional groups. The pK_a of the α-NH_2 terminus is 7.1 and the pK_a of the lysine ε-NH_2 is 10.0.[7] Comparison of the biological activity of tuftsin with the fluorescein derivative revealed that the analogue retained both the phagocytic and bactericidal-stimulating activity of natural tuftsin.

Tuftsin was coupled with another highly fluorescent molecule, tetramethyl rhodamine as shown in figure 4.2.[8,9,10] This procedure involved the use of tuftsin which had been elongated at the C-terminus by addition of two amino acids, glycine and lysine. Coupling was carried out in DMF in the presence of triethylamine, following removal of Boc protecting groups the product was purified on a Sephadex column. In this instance, where the coupling site was the ε-NH_2 of the lysine, the conjugate was found to compete specifically for tuftsin binding sites and stimulate phagocytosis.

4.1.2 STRUCTURES OF BIOLOGICALLY ACTIVE TUFTSIN ANALOGUES

Binding of tuftsin to macrophages depends on strict conservation of molecular structure:[11] the formation of conjugates often impairs tuftsin activity. Early reports[12] claimed that the structural requirements for tuftsin activity were so strict as to preclude any amino acid substitution or deletion anywhere in the peptide, any absence of free amino or carboxyl groups at the peptide termini, any substitution or alteration of the guanidine side chain on arginine, or any lengthening of the chain by addition of amino acids at either terminus.

Later however, some analogues in which the N-terminus had been cyclised were reported to possess considerable biological activity.[5] The tuftsin fluorescein analogue described in section 4.1.1 is a further example of N-terminal substitution in which biological activity is retained. Other recent work[10] has demonstrated that C-terminal additions to tuftsin's backbone often lead to analogues possessing tuftsin-like biological activity. It has become clear that the restrictions upon formation of biologically active tuftsin analogues are not as rigid as once supposed. Although conservation of the molecular structure is clearly of great importance, the most effective ways of forming analogues have not been unequivocally established. In this study synthetic tuftsin was used in the formation of conjugates through one of the N-termini.

4.1.3 CONFORMATION OF TUFTSIN

Detailed 2D NMR and NOE spectrographic studies have allowed a conformational analysis of tuftsin to be carried out both in aqueous solution and DMSO.[13] Since most proton resonances were split, it was concluded that there were two families of conformations due to cis-trans isomerisation around the Lys-Pro bond. The ^1H data in $(CD_3)_2SO$ showed that the Arg NH was internally H bonded to the Pro N and was inaccessible to solvent. The rigid folded trans isomer, shown in figure 4.3(A), was found to be the preferred conformation in DMSO solution. This is not necessarily the bioactive form however, since such a small molecule still retains considerable flexibility to adapt to the receptor.

FIGURE 4.3 *Molecular models of (A) the only conformer, among the energy minima, that shows a nearly complete solvent inaccessibility of Arg NH and of (B) the best conformer among the energy minima.*[13]

One of the major limitations of the use of peptides as pharmaceuticals is their susceptibility to proteolysis. In the case of octreotide the four essential amino acids were stabilised to proteases in the body by disulphide cyclisation from the two cysteines incorporated in the molecule and by the placement of the D-amino acids. In the case of tuftsin, work has been carried out using high temperature quenched molecular dynamics (QMD)[14] to simulate cyclic analogues of tuftsin which retain very similar backbone structures and side chain conformations. The two derivatives, cyclo[Thr-Lys-Pro-Arg-Gly] and cyclo[Thr-Lys-Pro-Arg-Asp], were suggested as a result of this work and the former of these has been synthesised and shown to be more active than tuftsin. In the future, conjugates of such analogues may become desirable targets for synthesis.

4.2 12N4 - TUFTSIN CONJUGATE

Ligands based on the tetraazacyclododecane (12N4) skeleton such as DOTA are well known as complexing agents for lanthanides like gadolinium, and these complexes find uses as paramagnetic contrast agents in MRI. As can be seen from figure 4.4 a number of other metal (III) ions have very similar ionic radii and so are able to form stable complexes with these ligands also. Of particular interest in this study is the Tb^{3+} ion which has excellent long lived luminescence properties, emitting visible photons long after other background fluorescence from organic molecules has disappeared. Such luminescent lanthanide complexes have found uses as probes in biological systems replacing conventional fluorescent organic molecules such as fluorescein. One of the objectives of this study was to prepare a tuftsin conjugate of a terbium complex for uses such as those of the fluorescent tuftsin conjugates described in section 4.1.1.

FIGURE 4.4 *Effective ionic radii vs coordination number.*

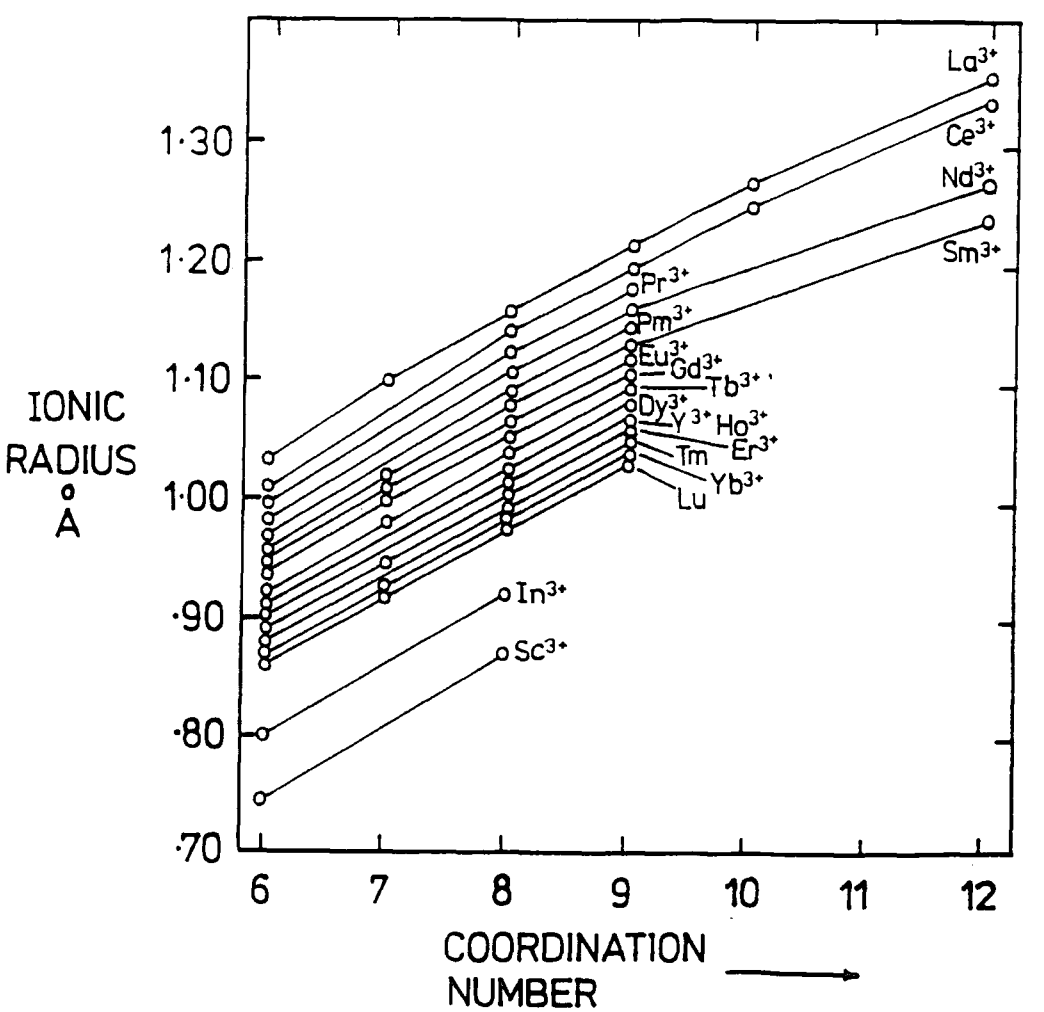

4.2.1 SYNTHESIS OF 12N4 COMPLEXING AGENT

Charge neutral complexes were desirable because of their improved transport properties and so a tri-acidic ligand was sought, with alkylation of the fourth ring amine allowing variation of the side chain enabling conjugation with targeting vehicles.

SCHEME 4.1

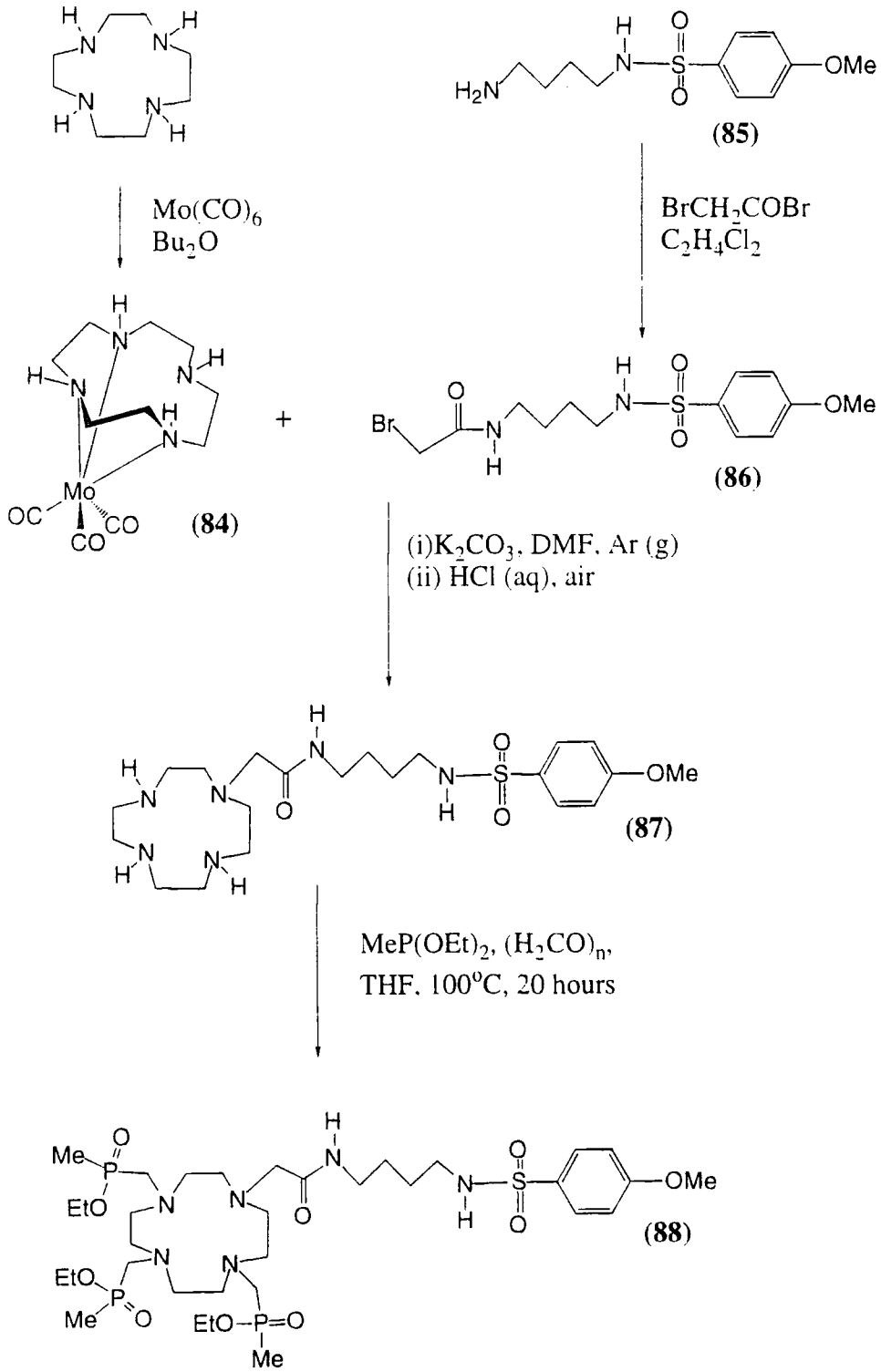

In practice three of the 12N4 ring nitrogens were protected while alkylation of the fourth was accomplished. This type of protection has been reported using either the octahedral chromium[15] or molybdenum[16] tricarbonyl complex of tetraazacyclododecane. In this case tetraazacyclododecane was treated with molybdenum hexacarbonyl in dibutyl ether giving the bright yellow molybdenum tricarbonyl complex (**84**). The α-bromoamide (**86**) had previously been prepared by reaction of bromoacetyl bromide with the mono protected butane-1,4-diamine (**85**). Because of the relative instability of the molybdenum complex it was immediately suspended in DMF and treated with the α-bromoamide (**86**). Decomplexation of molybdenum was achieved by stirring the reaction mixture in dilute HCl and the monoalkylated amine (**87**) was subsequently extracted in 62% yield.

The alkylphosphinate residues were introduced using the standard procedure. The monosubstituted 12N4 derivative was condensed with paraformaldehyde in dry tetrahydrofuran to form the imine which was trapped in this case by methyldiethoxyphosphine. Arbuzov rearrangement led to the desired triphosphinate ester (**88**). HBr in acetic acid was used in the presence of phenol to selectively hydrolyse the amide-triester leaving the amide intact while simultaneously deprotecting the terminal amine. The trihydrobromide salt (**89**) was precipitated from diethyl ether. Such a bifunctional complexing agent has great versatility possessing a pendant amine suitable for conversion to an active ester or maleimide and subsequent conjugation with a suitable targeting vehicle, in this case tuftsin.

4.2.2 CONJUGATION WITH TUFTSIN

Tuftsin was obtained commercially and samples were examined by ^{1}H NMR using D_2O and $(CD_3)_2SO$ as solvents. These spectra were compared with previous NMR data[7] and were found to be consistent.

In order to examine the reactivity of the terminal amines with p-nitrophenolate active esters a pilot acylation reaction was studied on a small scale by mixing dry p-nitrophenyl acetate with a solution of tuftsin in deuterated DMSO. The progress of this reaction followed by ^{1}H NMR. The appearance of the distinctive p-nitrophenol aromatic ^{1}H doublets at δ 8.05 and 6.8 and the disappearance of the starting p-nitrophenyl acetate confirmed that reaction had taken place. In addition to the distinctive acetate peak at δ 1.88 there were also changes in the lysine NH which became a triplet at δ 7.93 and the lysine ε-CH_2 shifted to δ 2.98 ppm. Following purification on a Sephadex column, mass spectrometry confirmed that tuftsin acetate

(**90**) had been formed. However it also indicated that a minor amount of the diacetamide was present, suggesting that reaction was not entirely selective on the lysine amine.

SCHEME 4.2

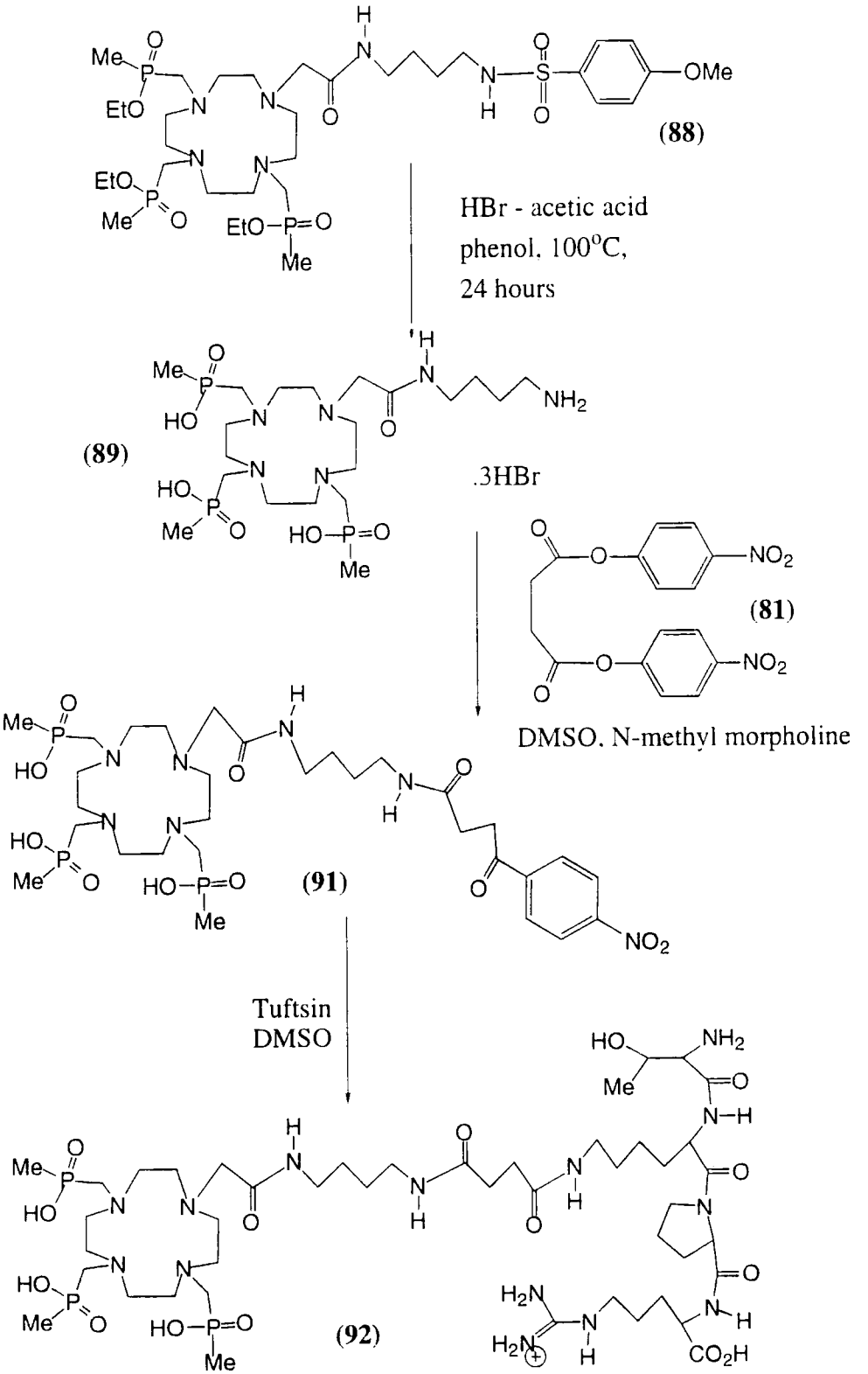

Since successful reaction of tuftsin with a p-nitrophenolate active ester had taken place, it was decided to employ an analagous method in forming the 12N4 - tuftsin conjugate. The trihydrobromide salt (**89**) was stirred in DMSO in the presence of base; p-nitrophenyl bis ester (**81**) was added and the reaction was monitored by HPLC. Purification by reverse phase HPLC provided the desired active ester (**91**).

Subsequent treatment with tuftsin in deuterated DMSO again allowed monitoring of the reaction via ^{1}H NMR. An attempt to direct conjugation towards linkage of one tuftsin with one molecule of (**91**) was made by using excess tuftsin. The increased size of the p-nitrophenyl ester in this case was anticipated to direct conjugation towards the less hindered site on lysine. The product (**92**) formed as a fine brown precipitate and so much of the excess tuftsin and p-nitrophenol were removed by filtration prior to purification on a Sephadex column. Electrospray mass spectrometry was attempted but unfortunately proved unsuccessful. ^{1}H NMR analysis showed that one tuftsin was conjugated with the bifunctional complexing agent, although due to the complexity of the spectrum the site of conjugation could not be unequivocally assigned. However, given the solution conformation of tuftsin, and the results of the model acylation reaction, it was assumed that conjugation would occur at the Lys ε-amino group.

4.2.3 COMPLEXATION AND BIOLOGICAL STUDIES

An alternative route to (**92**) was attempted in which the terbium complex was formed at an earlier stage in the reaction sequence in order to allow monitoring via luminescence techniques and purification by HPLC despite the lack of chromophore. Formation of the terbium complex of (**89**) was accomplished by treatment of the trihydobromide salt with aqueous terbium (III) acetate at reflux followed by adjustment of the pH to 6. Purification by HPLC provided the desired complex (**93**) but the terbium complex proved not to be as effective a chromophore for this purpose as expected. In addition there was evidence to suggest that the complex was somewhat unstable under the acidic conditions employed in this reverse phase HPLC purification. Terbium is known to be a poor light absorber, its efficiency can be improved by incorporating an antenna in the ligand. In future experiments, such an antenna could be incorporated as a substituent on phosphorus and transfer absorbed light to the metal ion.

It was decided that it was preferable to carry out complexation reactions in the final stage of this synthesis, the previous study serving to demonstrate the ease of terbium complex formation. The sample of 12N4 - tuftsin conjugate (**92**) obtained was sent to the Royal Marsden Hospital where complexation will be carried out immediately prior to some initial biological tests.

4.3 9N3 - TUFTSIN CONJUGATE

Investigations were also carried out into linking tuftsin to the triazacyclononane moiety in a similar fashion to the 9N3 - nitroimidazole conjugate discussed in chapter 3. The synthesis of the C-functionalised derivative of NOTA, shown in section 3.4.1, was somewhat lengthy and so a shorter route to an N-functionalised dervivative was employed.[17]

4.3.1. SYNTHESIS OF 9N3 COMPLEXING AGENT

Synthesis of the N-functionalised NOTA derivative was accomplished using the parent polyazamacrocycle triazacyclononane as a starting material. Alkylation of this allowed one or more suitable aminoalkyl side chains to be attatched.

2-Bromo-N-benzoyl-5-aminopentyl ethanoate (**96**) was prepared in two steps from N-benzoyl-δ-amino valeric acid (**94**) available from SIGMA. Bromination of (**94**) was effected with red phosphorus and bromine according to the literature method.[18] The resulting racemic α-bromoacid (**95**) was converted to the α-bromoester (**96**) by heating to reflux in ethanol and 5% acetyl chloride, followed by 'flash' silica column chromatography.

SCHEME 4.3

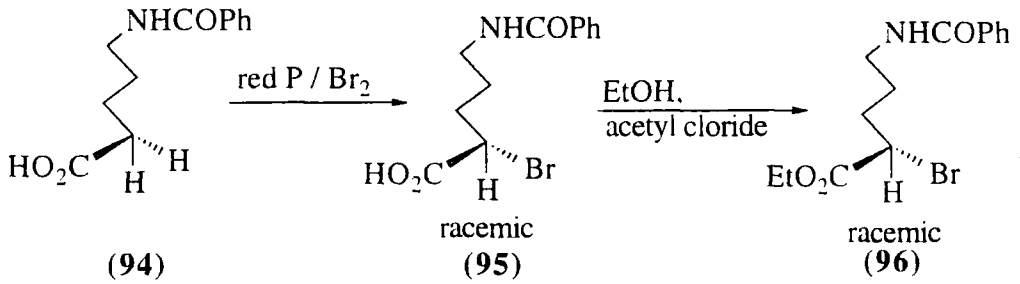

(94) **(95)** **(96)**

The α-bromoester reacted with the triazacyclononane in a manner analagous to ethylbromoacetate. Two equivalents of triazacyclononane were heated in DMF in the presence of potassium carbonate. A solution of the α-bromoester (**96**) was added dropwise over several hours in order to direct the reaction towards production of the mono substituted product (**97**). Analytical HPLC showed that the two products (**97**) and (**98**) were produced in the ratio 3:1. Samples of each product were obtained by purification using semi-preparative reverse phase HPLC under standard conditions.

SCHEME 4.4

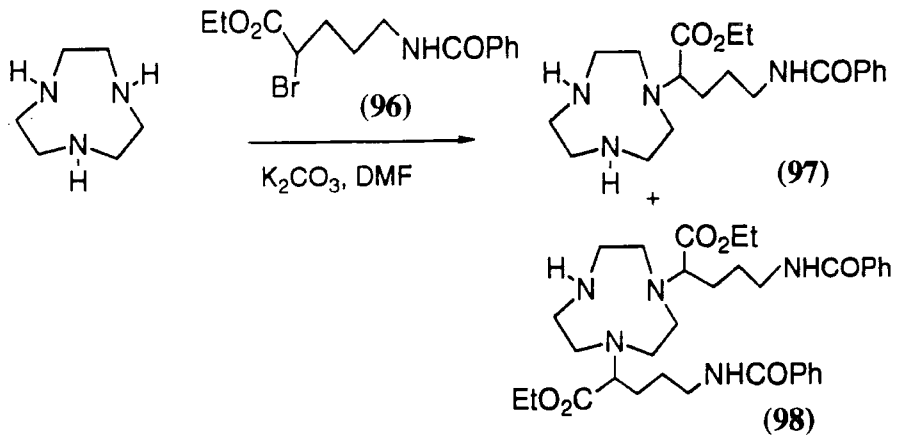

SCHEME 4.5

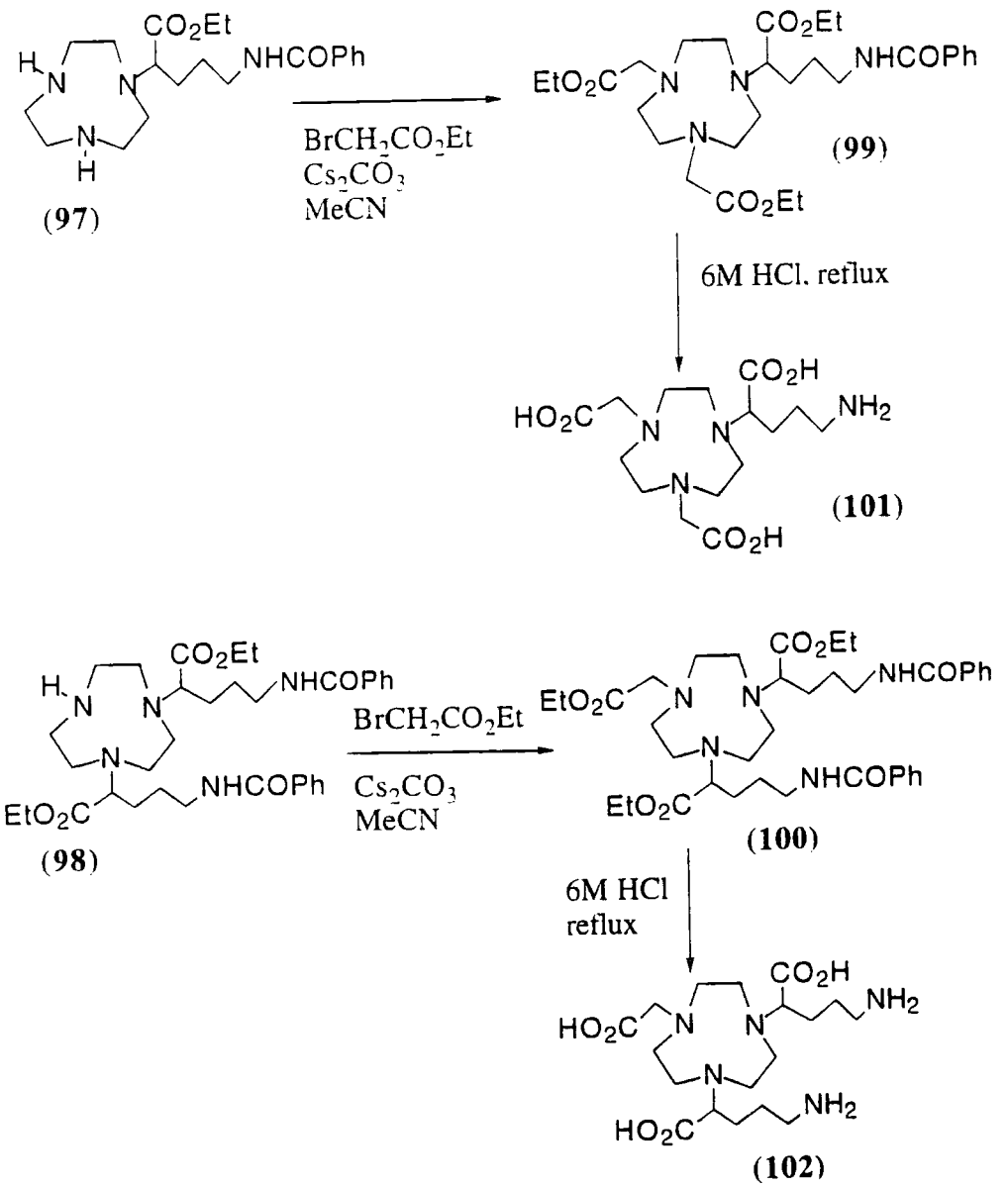

The monoalkylated compound and dialkylated compound were reacted separately with ethyl bromoacetate in acetonitrile in the presence of caesium carbonate to produce the triesters (**99**) and (**100**) respectively. Subsequent acid hydrolysis gave the triacids (**101**) and (**102**) quantitatively. When a mixture of the monoalkylated (**97**) and dialkylated (**98**) compounds was treated with ethylbromoacetate in the same fashion, a mixture of the two triesters was obtained as expected. A very careful attempt was made to separate these by gravitational alumina column chromatography but only very limited separation was achieved due to the very similar R_f values of both compounds under these conditions.

Following the successful formation of tuftsin conjugates from p-nitrophenolate active esters discussed in section 4.2.1.2, a similar method was employed in the case of the 9N3 conjugate. The triacid (**102**) was treated with the bis p-nitrophenyl ester (**81**) in the presence of N-methyl morpholine, and purification by HPLC provided the bis active ester (**103**) in 28% yield. Triacid (**101**) was treated in the same way to give the mono active ester (**104**) in 90% yield.

Previous studies[19] on 'mono' and 'di'- N-functionalised macrocycles in which maleimide conjugates were formed had demonstrated that purification could be carried out in the final stage of the synthesis. In a similar way a quick and convenient route to the two active esters was followed in which a mixture of the 'mono' and 'di-' functionalised material was treated with (**81**) in the method shown in scheme 4.6. HPLC separation was readily carried out since the p-nitrophenyl chromophore allowed easy detection and the retention times under standard conditions were 13.8 mins and 17 mins for (**104**) and (**103**) respectively.

Having obtained the active esters, the mono ester (**104**) was employed in the formation of the tuftsin conjugate. It was dissolved in $(CD_3)_2SO$ and solid tuftsin added to the solution. The progress of the reaction could be monitored by ^1H NMR spectrometry as before. When complete, the solid product (**105**) was simply obtained by filtering and washing; having a lower molecular weight than (**92**) the electrospray mass spectrum was successfully obtained.

SCHEME 4.6

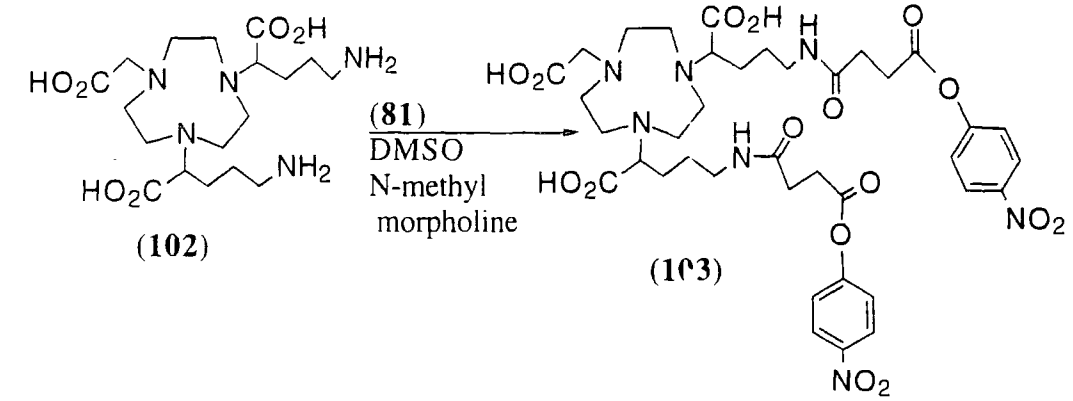

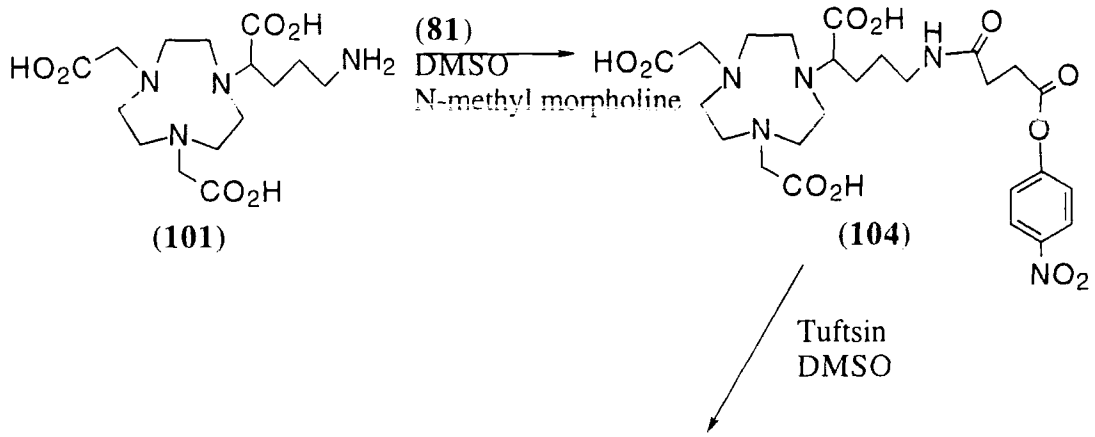

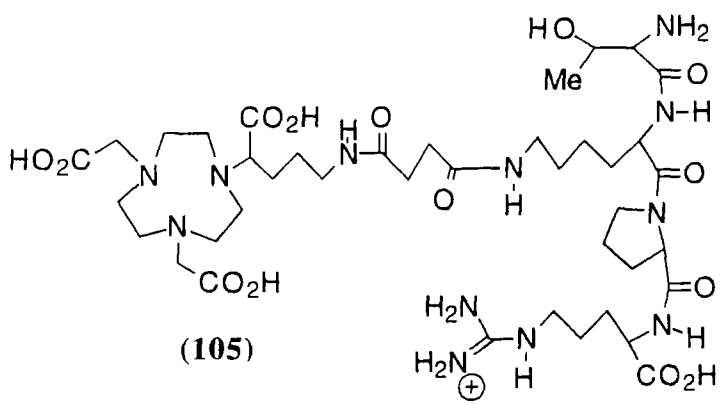

4.3.2 COMPLEXATION AND BIOLOGICAL STUDIES

The complexation chemistry of NOTA and its derivatives is well understood. Detailed studies have also been carried out on the ligand (*R*)-1,4,7-tris(2'-methylcarboxymethyl)-triazacyclononane (**5**) which has been described as a good model for N-functionalised ligands such as those discussed here.[20] This novel 9N3 - tuftsin conjugate has potential as an imaging agent using either the ^{67}Ga, ^{68}Ga or ^{111}In complex. Initial biological studies will be carried out on the indium complex of (**105**) at the Royal Marsden Hospital in order to determine its biodistribution and tumour targeting ability.

4.4 CONCLUDING COMMENTS

Once initial biodistribution results have been obtained it will be possible to determine whether the conjugated tuftsin has retained its selectivity for the receptors on the macrophages. In addition, some indication of the transport properties of these molecules may be available. Based on this information, further studies of these conjugates may be initiated on a larger scale, or on possible means of modification of these synthetic routes to conjugates with increased receptor selectivity or improved transport properties.

4.5 REFERENCES

1 V.A. Najjar and K. Nishioka, *Nature*, 1970, **228**, 672.

2 P. Gottlieb, A. Beretz and M. Fridkin, *Eur. J. Biochem*, 1982, **125**, 631.

3 K. Nishioka, *Br. J. Cancer*, 1979, **39**, 342.

4 P. Gottlieb, E. Tzehoval, M. Feldman, S. Segal and M. Fridkin, *Ann. NY. Acad. Sci.*, 1983, **419**, 107.

5 A.A. Amoscato, P.J.A. Davies, G.F. Babcock and K. Nishioka, *Ann. NY. Acad. Sci.*, 1983, **419**, 114.

6 A.A. Amoscato, P.J.A. Davies, G.F. Babcock and K. Nishioka, *RES*, 1983, **34**, 53.

7 M. Blumenstein, P.P. Layne and V.A. Najjar, *Biochemistry*, 1979, **18**, 5247.

8 P. Gottlieb, E. Hazum, E. Tzehoval, M. Feldman, S. Segal and M. Fridkin, *Biochem. Biophys. Res. Comm.*, 1984, **119**, 203.

9 P. Gottlieb, Y. Stabinsky, Y. Hiller, A. Beretz, E. Hazum, E. Tzehoval, M. Feldman, S. Segal, V. Zakuth, Z. Spirer and M. Fridkin, *Ann. NY. Acad. Sci.*, 1983, **419**, 93.

10 P. Gottlieb, A. Beretz and M. Fridkin, *Eur. J. Biochem*, 1982, **125**, 631.

11 Y. Stabinsky, P. Gottlieb and M. Fridkin, *Mol. Cell. Biochem.*, 1980, **30**, 165.

12 Y. Stabinsky, P. Gottlieb, V. Zakuth, Z. Spirer and M. Fridkin, *Biochem. Biophys. Res. Comm.*, 1978, **83**, 599.

13 A. D'Ursi, M. Pegna, P. Amodeo, H. Molinari, A. Verdini, L. Zetta and P.A. Temussi, *Biochemistry*, 1992, **31**, 9581.

14 S.D. O'Connor, P.E. Smith, F. Al-Obeidi and B. Montgomery Pettitt, *J. Med. Chem.*, 1992, **35**, 2870.

15 J.-J. Yaouanc, N. Le Bris, G. Le Gall, J.-C. Clement, H. Handel and H. des Abbayes, *J. Chem. Soc., Chem. Commun.*, 1991, 206.

16 K.P. Pulukkody, T.J. Norman, D. Parker, L. Royle and (in part) C.J. Broan, *J. Chem. Soc., Perkin Trans. 2*, 1993, 605.

17 J.P.L. Cox, A.S. Craig, I.M. Helps, K.J. Jankowski, D. Parker, M.A.W. Eaton, A.T. Millican, K. Millar, N.R.A. Beeley and B.A. Boyce, *J. Chem. Soc., Perkin Trans. 1*, 1990, 2567.

18 J.C. Eck and C.S. Marvel, *Org. Synth. Coll. Vol. 2*, 1943, 74.

19 A.S. Craig, PhD. Thesis, University of Durham, 1989.

20 R.C. Matthews, D. Parker, G. Ferguson, B. Kaitner, A. Harrison and L. Royle, *Polyhedron*, 1991, **10**, 1951.

Chapter Five

Acridine Conjugates

5.1 ACRIDINE INTERCALATOR CONJUGATES

5.1.1 DNA INTERCALATING AGENTS

The targeting vehicles discussed in previous chapters have been of the type which are directed towards a specific tissue type or type of cell. Intercalating agents differ in that they bind to DNA, which is present in all cell types. This property of intercalators would allow a tumour imaging or therapeutic agent to bind to the DNA of a tumour cell after being transported there by means of an antibody fragment or other targeting agent.

Intercalating agents are cytotoxic to dividing, but not resting cells, and so are particularly toxic to rapidly dividing tumour cells. They generally prevent progression beyond the G2+M phase of the cell cycle (see figure 1.31).[1] At the M stage of the cell cycle the nuclear membrane is ruptured to allow division. It is at this time that an intercalator conjugate could access the DNA of the tumour cells.

The process of intercalation takes place when a planar intercalator molecule is inserted between the base pairs in DNA.[2] The binding is freely reversible, being driven by stacking, charge transfer, hydrogen bonding, Van der Waals and hydrophobic interactions. The DNA binding activity of Fe (II) methidium propyl-EDTA[3] and acridine orange linked to $[Pt(en)Cl_2]$[4,5] demonstrated that the formation of conjugates with metal complexing agents did not reduce intercalation.

5.1.2 AUGER EMITTING RADIOISOTOPES

Once the macrocycle-metal complex is bound to the cellular DNA, new possibilities are opened up in the field of tumour therapy. The use of short range isotopes in the macrocycle complex would become possible. One of their main advantages is that their destructive action would concentrate on the DNA of the tumour cells, resulting in less damage to healthy tissue.

FIGURE 5.1 *Auger emitting metal isotopes for use in tumour therapy*

Auger emitter	Energy Range (keV)	Range in Tissue	Relative Abundance
^{111}In	200 - 0.5	480μm - 20nm	
^{67}Ga	7.5 - 0.05	1.3μm - 2nm	
^{64}Cu	6.4 - 0.8	1.7μm - 38nm	less than ^{111}In or ^{67}Ga
^{67}Cu	7.4 - 0.9	1.3μm - 45nm	less than ^{64}Cu

The Auger effect is the emission of a second electron after high energy radiation has expelled another. The first electron to depart leaves a hole in a low-lying orbital, and an upper electron falls into it. The energy released may result in the ejection of the secondary electron of the Auger effect. These are characteristic of the element and have a short range. A number of Auger emitting metals suitable for therapy have been investigated, although ^{123}I is currently the favoured element. Their properties are summarised in the table in figure 5.1.[6,7]

Indium -111 would be the most effective of these since its energy deposition is about 19 eV per nm;[7] it is also readily available commercially. Indeed the ^{111}In in indium oxine has been shown to induce cell death. ^{67}Ga citrate has also been shown to enhance cell death. However it is estimated that 2366 atoms of ^{67}Ga must be incorporated into the nuclear DNA to sterilise the cell. This indicates that to kill a cell with Augers exclusively may require a large quantity of drug to be administered. An alternative approach may be to use the two copper isotopes, combining longer range β radiation with short range Augers.

The efficacy of each of these isotopes may be examined by forming their complexes with a NOTA-based macrocycle conjugate.

5.1.3 TARGET INTERCALATOR - MACROCYCLE CONJUGATES

Acridine is a readily available, stable intercalator with well-understood properties.[8] It was therefore the intercalator of choice when some initial macrocycle-intercalator conjugates were identified as target molecules. Target molecules **(107)** and **(108)** also bear a maleimide moiety, suitable for attatching an antibody fragment. It was proposed that such an antibody fragment would target the tumour tissue specifically and the intercalator would bind the molecule to the DNA of the cells in that tissue.

5.2 SYNTHESIS OF ACRIDINE COMPOUNDS

Some exploratory studies were undertaken to define the synthetic accessibility of N-linked acridine derivatives and their ease of conjugation to complexing agents and / or proteins. First 9-chloroacridine was prepared by the standard literature procedure.[9,10] N-Phenylanthrolinic acid was heated with phosphorus oxychloride and concentrated sulphuric acid in an acid catalysed reaction. Prior to reaction of 9-chloroacridine with a C-functionalised NOTA derivative such as **(79)** to provide target **(106)**, a model reaction was attempted using isobutylamine. The acridine was taken up in phenol and heated with isobutylamine.[11] Recrystallisation from methanol provided the desired

compound (**109**) in 78% yield. An alternative route using more common solvents in which the NOTA derivative (**79**) was soluble was also employed. First sodium methoxide was used to convert the 9-chloroacridine to the methoxide and then this was treated with isobutylamine hydrochloride in water/methanol to provide the same compound (**109**). However when the analagous reaction with the NOTA derivative was carried out, none of the target compound (**106**) was obtained.

FIGURE 5.2 *Target acridine-macrocycle conjugates* (**106**) - (**108**).

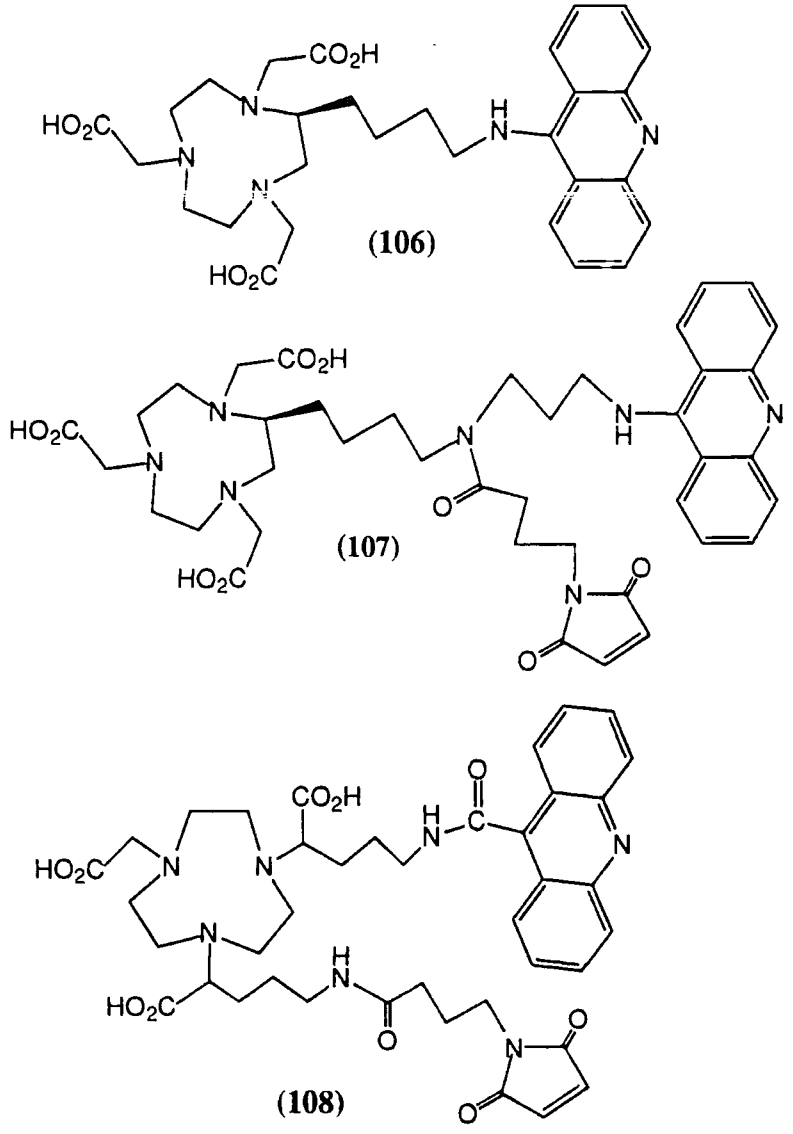

As an alternative to reaction of the 9-chloroacridine with a NOTA derivative, a reactive acridine compound was sought for direct combination with the terminal amino group of the NOTA derivative. The strategy was to use the acridine (**110**) to alkylate on the terminal amine of a NOTA derivative, providing a secondary amine for further elaboration, for example with an active ester of a maleimide. The bromo compound (**110**) was synthesised from phenoxy acridine by addition of 3-bromopropylamine

hydrobromide in phenol. Tosylation of this compound however proved unsuccessful. This protection step was necessary in the proposed route to target (**107**) in order to prevent the subsequent reaction with the maleimide taking place at both sites.

SCHEME 5.1

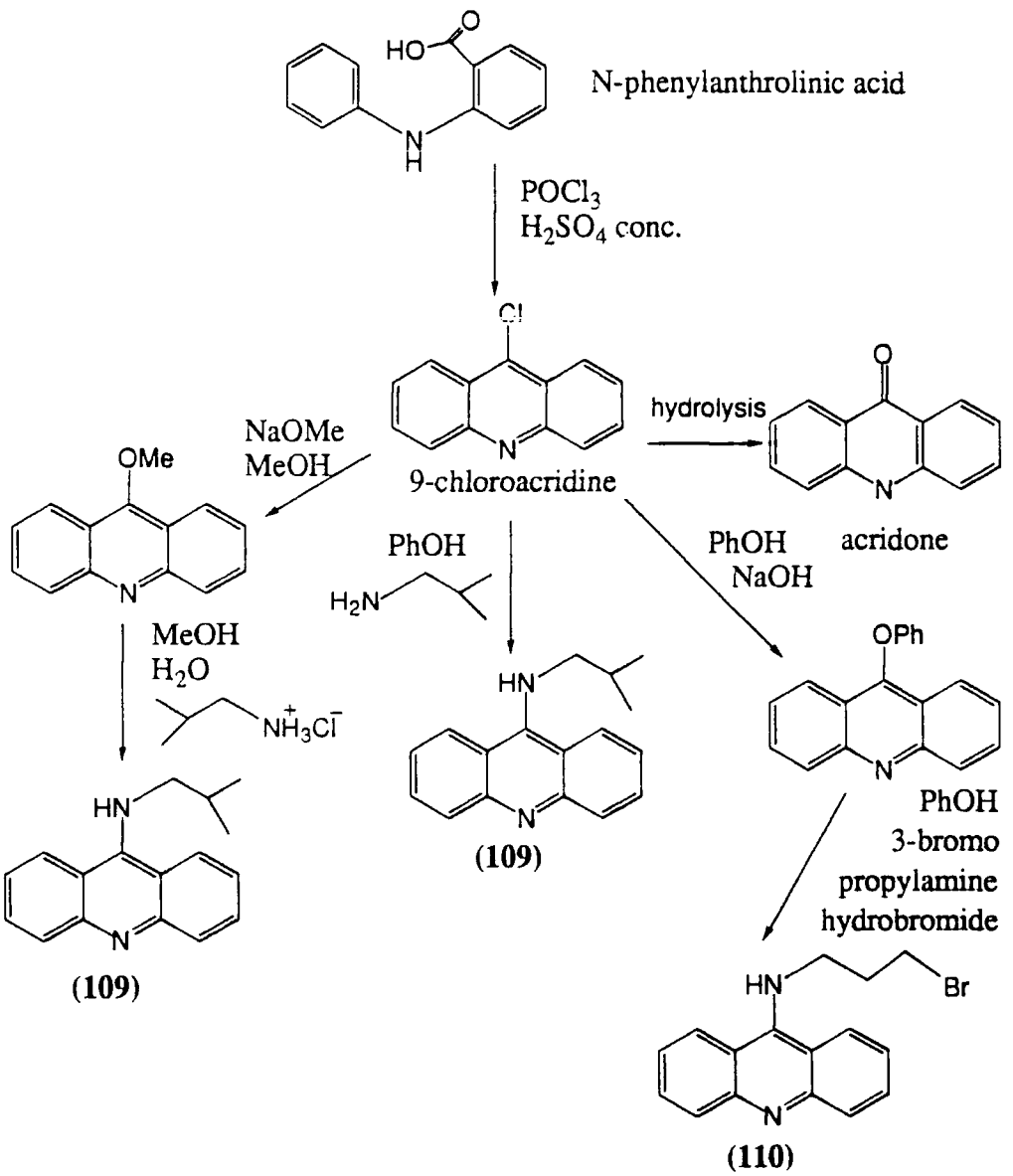

The strategy using the triacid (**102**) appeared more straightforward since one of the side chains could be used for conjugation with acridine and the other with a maleimide suitable for antibody binding. Commercially available 9-acridine carboxylic acid was used in an alternative method of forming the macrocycle-acridine linkage. It was readily converted into the acid chloride and then treated with the NOTA derivative (**102**) in DMF in the presence of triethylamine. However none of the desired acridine-

macrocycle conjugate could be identified in the resulting mixture of compounds and so target (**108**) was not achieved.

The difficulties encountered here in forming an acridine-macrocycle linkage appeared to indicate that the simple 9-chloroacridine and 9-acridine carboxylic acids were not suitable for direct reaction with the terminal amino group of the NOTA derivatives. Studies on previous antitumour acridines had suggested that attachment of a cationic side chain to the acridine would improve the binding properties, as in the case of the acridine carboxamides discussed in section 1.5.4.3.[12] Therefore it was proposed that an acridine 9-carboxylic acid derivative with a cationic side chain be synthesised. This could be designed with scope for incorporating a macrocyclic complexing agent and tumour targeting antibody fragment. The following recently reported work on multifunctional acridine and fluorophore DNA probe was used as a starting point for developing this strategy.

5.3 ACRIDINE AND FLUOROPHORE DNA PROBE

Research has recently been conducted to investigate methods of probing the reversible association of oligonucleotides with complementary nucleic acid sequences. Currently these association phenomena are detected using the UV photometric method.[13] However this is a time consuming technique which is not suitable for more complicated nucleotide molecules.

Recently Shinozuka[14] has developed a novel multifunctional fluorescent labelling agent (**111**). As shown in figure 5.3 it is based on a tris amine conjugated with acridine, fluorescein and the oligomer to be studied. It was observed that (**111**) bound the complementary DNA strand more effectively than the unlabelled DNA oligomer. The (**111**) duplex was also more stable at higher temperatures than the unlabelled duplex, being stabilised by the intercalative action of the acridine moiety.

The fluorescein based fluorescence intensity of (**111**) was detected following irradiation at the wavelength of the acridine excitation maximum and subsequent intramolecular energy transfer. Examination of the fluorescence intensity showed that the intensity was strongly affected by the formation of a double DNA strand. In this way reversible association of oligonucleotides could be monitored using this novel multifunctional DNA probe.

This work clearly demonstrated the way in which the acridine intercalator greatly enhanced the DNA binding of the conjugate. The use of the central tris-amine allowed

development of a multifunctional agent. It was decided to employ a similar strategy to construct a novel multifuctionally labelled antibody bearing a macrocycle and intercalator.

FIGURE 5.3 *Multifunctionally labelled DNA probe* **(111)** *compared with proposed multifunctionally labelled macrocycle-acridine-antibody conjugate* **(112).**

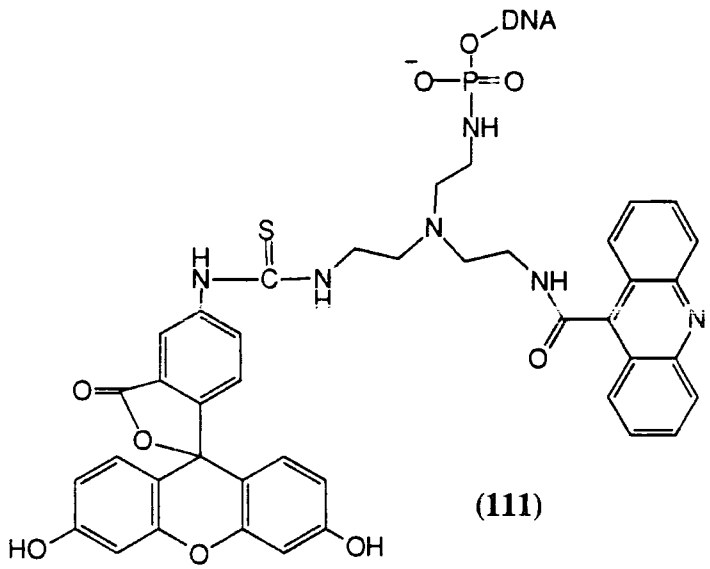

(111)

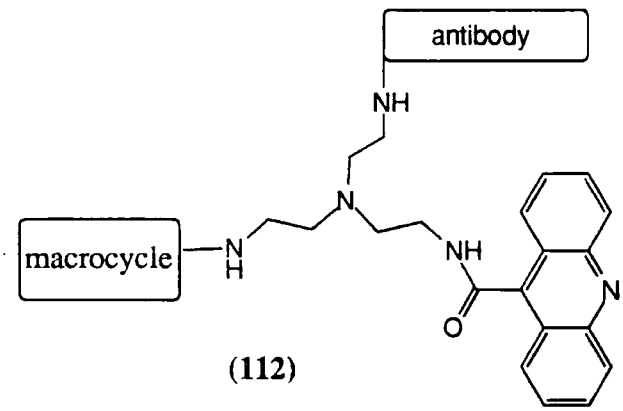

(112)

5.4 SYNTHESIS OF MULTIFUNCTIONAL ACRIDINE COMPOUNDS

9-Acridine carboxylic acid was treated with thionyl chloride to provide the bright yellow acid chloride. This was dissolved in anhydrous dichloromethane and added dropwise to an excess of stirred and cooled tris(2-aminoethyl) amine. Analytical HPLC revealed the presence of three products as shown in figure 5.4. Upon separation by semi-preparative HPLC it was determined that the major product was the desired mono-acridine conjugate **(113)**. The second peak corresponded to the 'di' substituted compound **(114)**, and it was expected that the third peak corresponded to the 'tri'

substituted compound (**115**) although only 1mg of the material was isolated and a full characterisation was not possible.

SCHEME 5.2

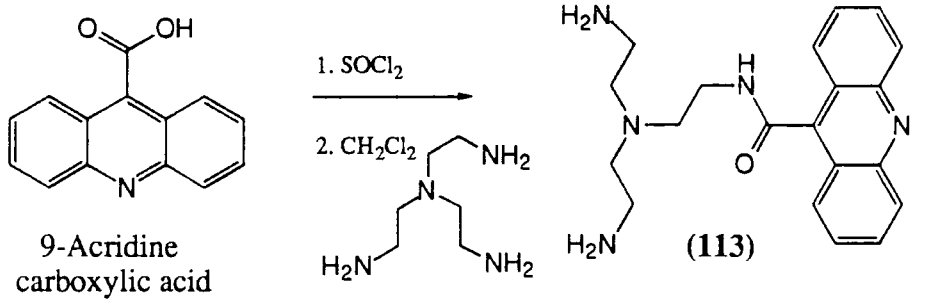

Ratio Mono : Bis : Tris
= 150 : 70 : 1

Purified By HPLC

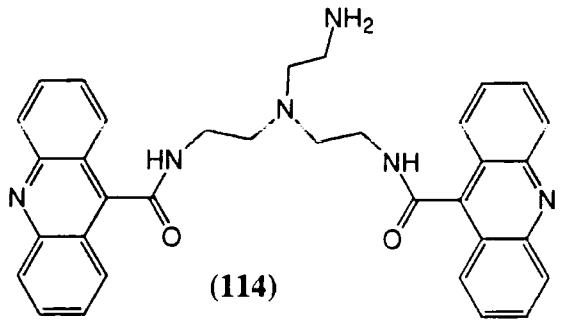

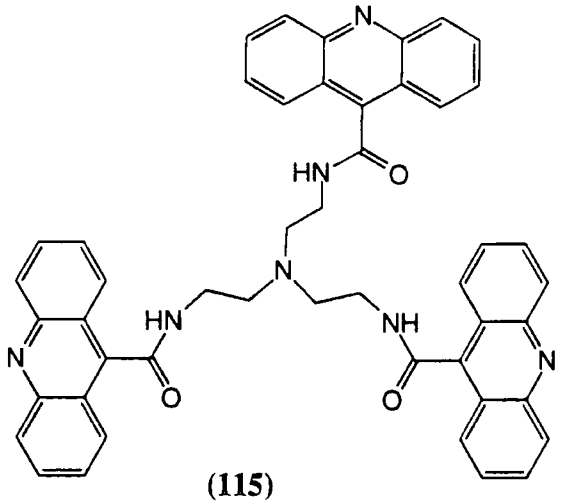

The mono acridine conjugate (**113**) was used in attempts to prepare the macrocycle acridine conjugate (**116**). Conditions for this reaction were not optimised, but in principle, the remaining free amino group is available for reaction with a maleimide which can easily be linked to an antibody fragment to provide a compound of the desired type (**112**).

FIGURE 5.4 *HPLC chromatogram showing mixture of mono* **(113)**, *bis* **(114)**, *and tris* **(115)** *acridine compounds.*

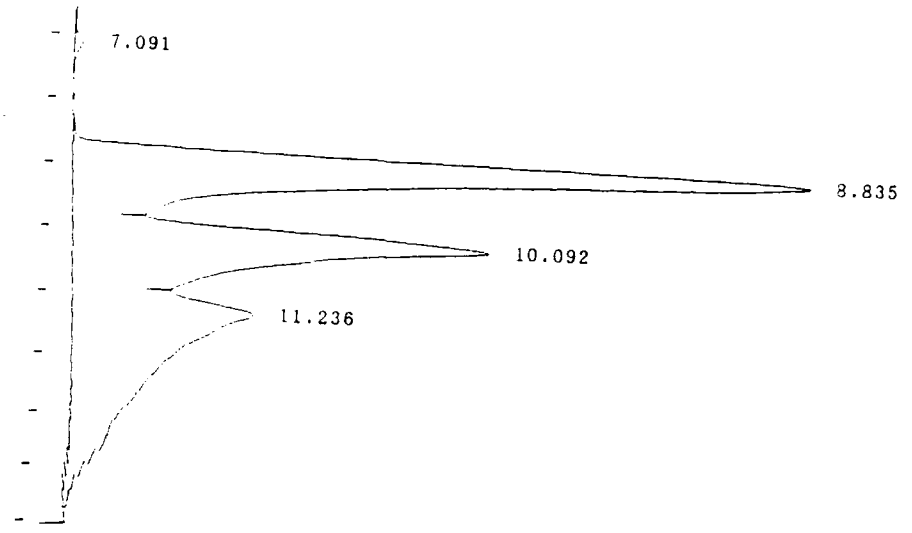

SCHEME 5.3

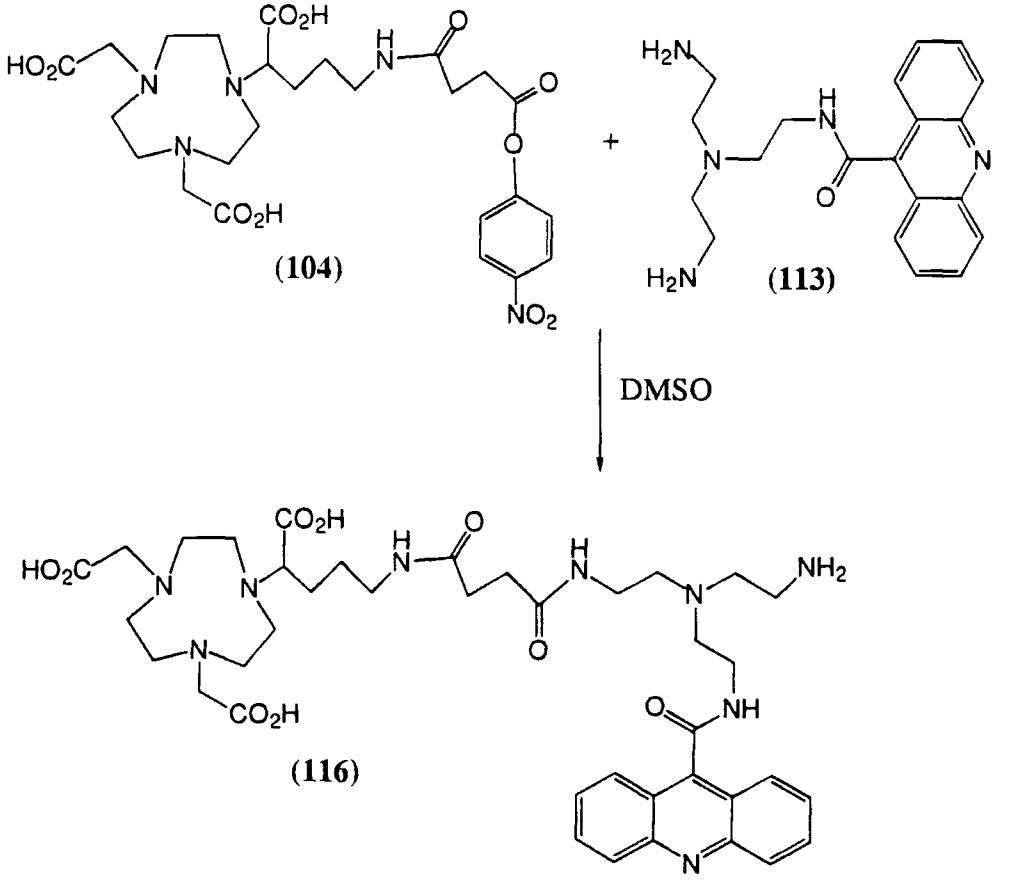

A similar procedure was carried out using N^2-methyldiethylenetriamine in place of tris(2-aminoethyl) amine. 9-Acridine carboxylic acid was converted to the acid chloride using thionyl chloride as before. This was added slowly to a five-fold excess of N^2-methyldiethylenetriamine with stirring at 0°C. Upon completion of the reaction the excess triamine was removed by distillation. Analytical HPLC showed that there were

two acridine products, the major product with retention time 6.1 minutes and the minor product at 9.3 minutes. Separation by semi-preparative HPLC provided the mono acridine conjugate (**117**) in 63% yield, and the bis acridine conjugate (**118**) in 10% yield.

SCHEME 5.4

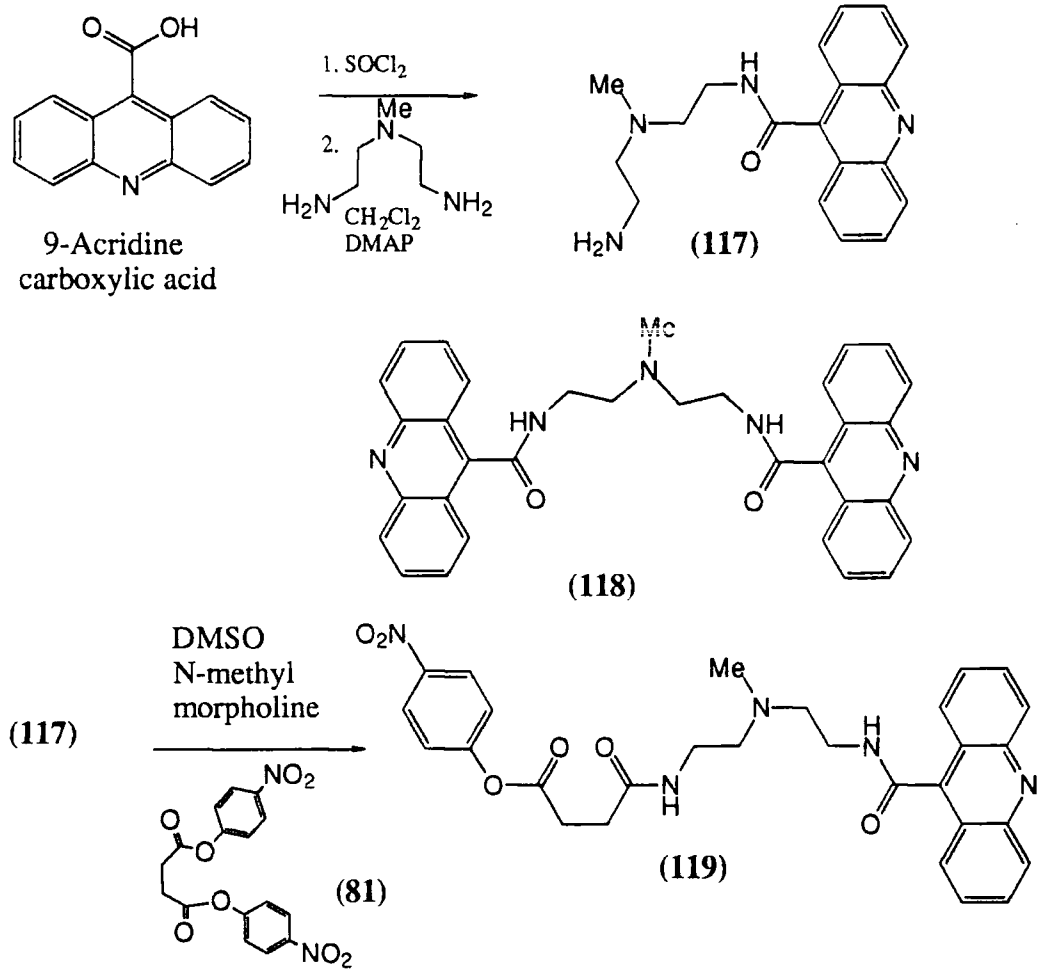

The mono acridine conjugate (**117**) was treated with p-nitrophenyl succinate (**81**) under standard conditions to give the p-nitrophenolate active ester (**119**) in 96% yield after HPLC purification.

The p-nitrophenolate acridine active ester (**119**) was not only readily synthesised in the method described previously. It was obtainable in high yield, 61% over two steps. Optimisation of the conditions for the formation of the mono-acridine compound over the bis-acridine would further increase the yield. In addition (**119**) was readily purified by semi-preparative HPLC, bearing two very strong chromophores. Figure 5.5 shows the spectral overlay plot of the ultra-violet spectra for the mixture of excess starting materials and products of this reaction. The acridine substrate (**117**) and product (**119**)

are clearly distinguishable from the p-nitrophenyl compounds. The HPLC chromatogram shown in figure 5.6 shows the excellent separation obtainable for these materials. This combined with the strong yellow colour of the solution of (**119**) visible to the naked eye simplified the practical aspects of preparative HPLC purification.

FIGURE 5.5 *Spectral overlay plot of Ultra-Violet spectra.*

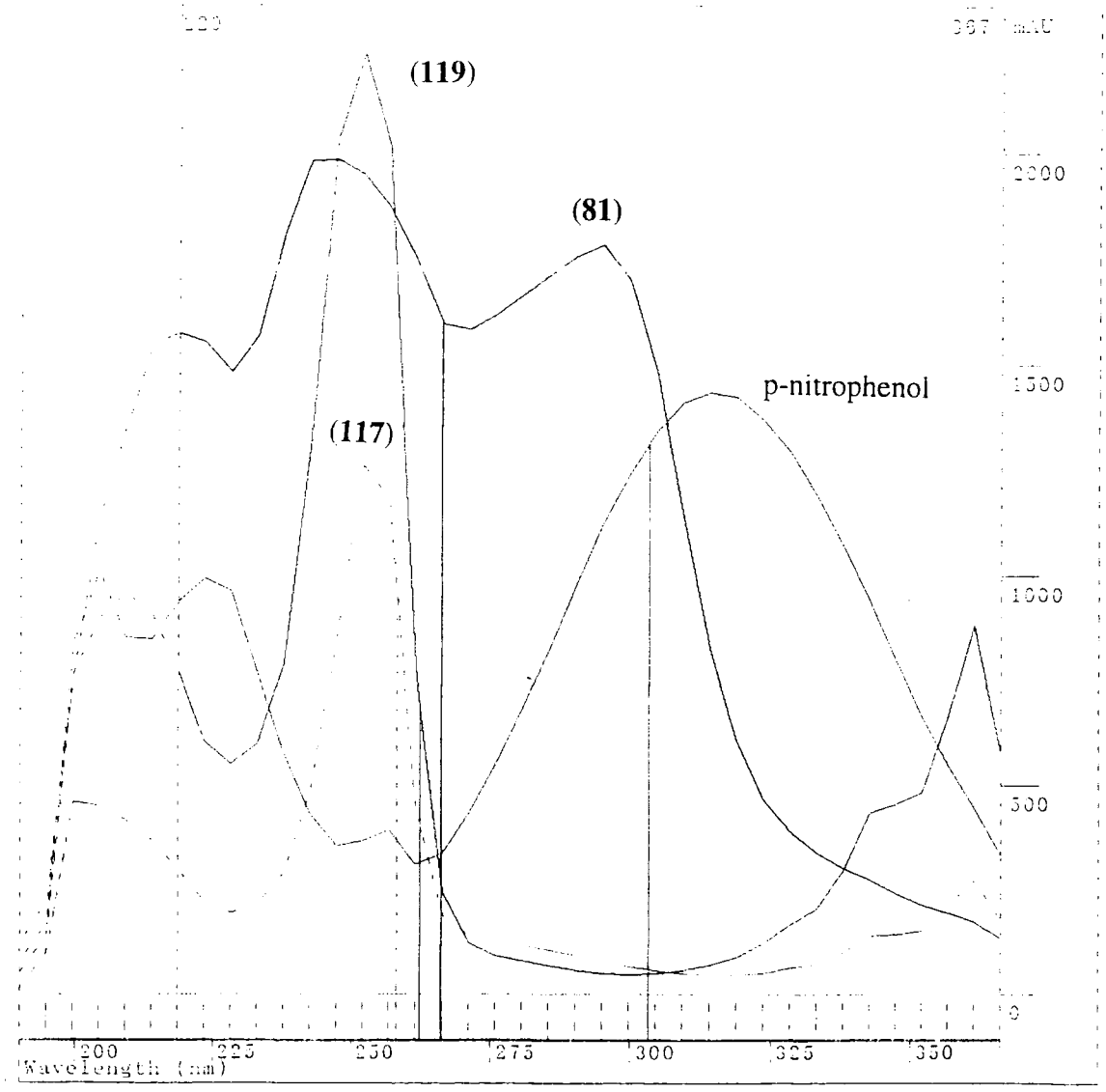

5.5 LABELLING WITH ACRIDINES

The acridine active ester (**119**) has potential as a versatile agent for acridine labelling of a variety of compounds. In the first instance it will be tested by collaborators at Celltech in non-specific acridine labelling of antibody fragments (**120**) to determine whether the presence of the acridine intercalator enhances the binding of the antibody. It will also be used to bind to the antibody fragment of a 9N3-antibody conjugate to form a compound such as (**121**) to be used in ^{111}In labelling experiments.

Since the distance between the radioisotope and acridine in compound (**121**) may be relatively large and not well defined, the short range isotopes may be held at too great a distance from the cellular DNA to have maximum effect. Compounds of the type (**122**) may then be developed in which the acridine and radioisotope are in greater proximity; the by-product of the synthesis of (**122**) would be the bis intercalator (**123**) which may itself be of interest.

A wide range of other possibilities for future development of this work exist. The versatility of (**119**) is such that it may also be used in the formation of conjugates with many other macrocycles and in conjunction with many other targeting vehicles.

FIGURE 5.6 *HPLC chromatogram of reaction mixture in synthesis of* (**119**)

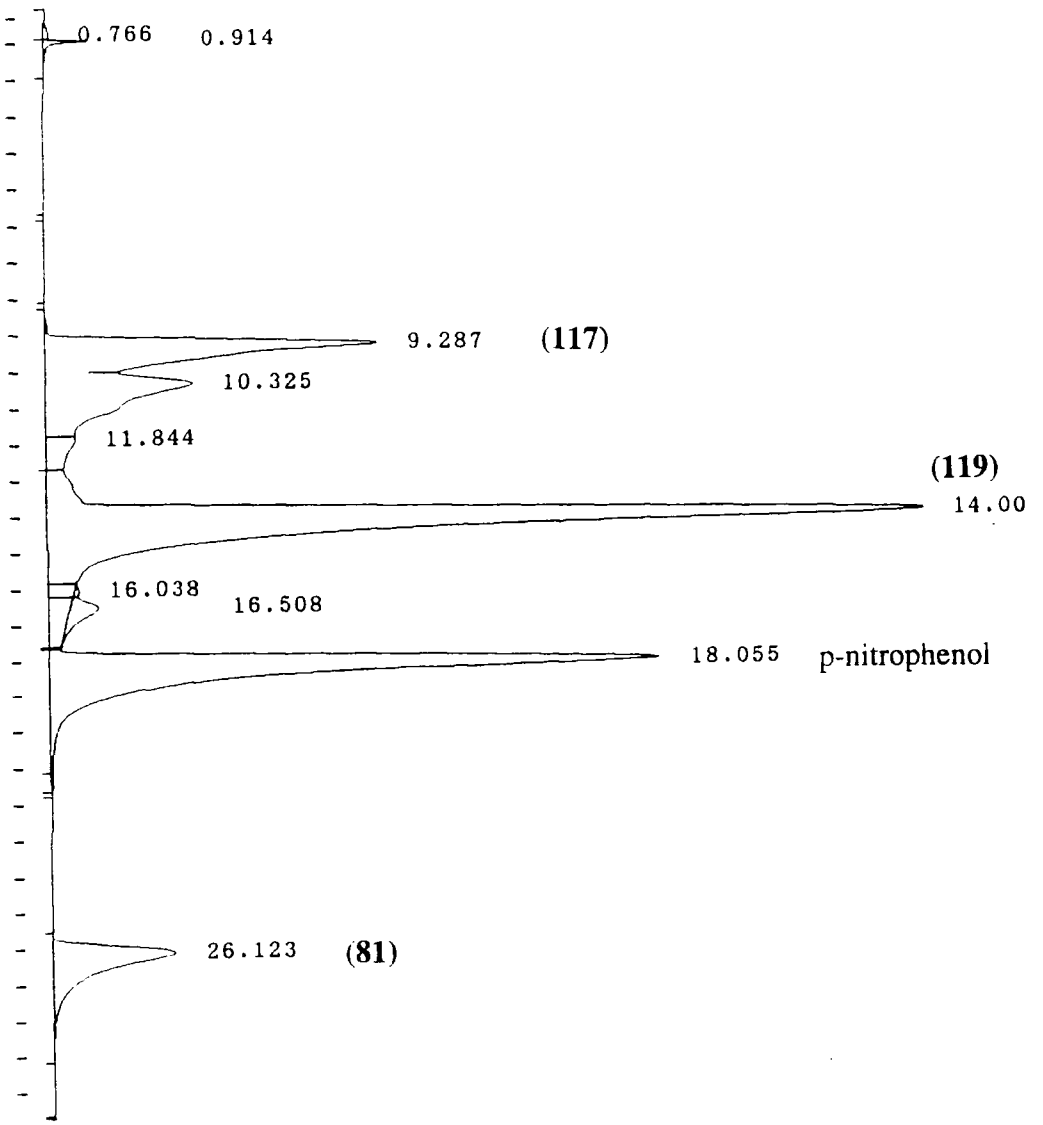

FIGURE 5.7 *Proposed structure of acridine-antibody conjugates.*

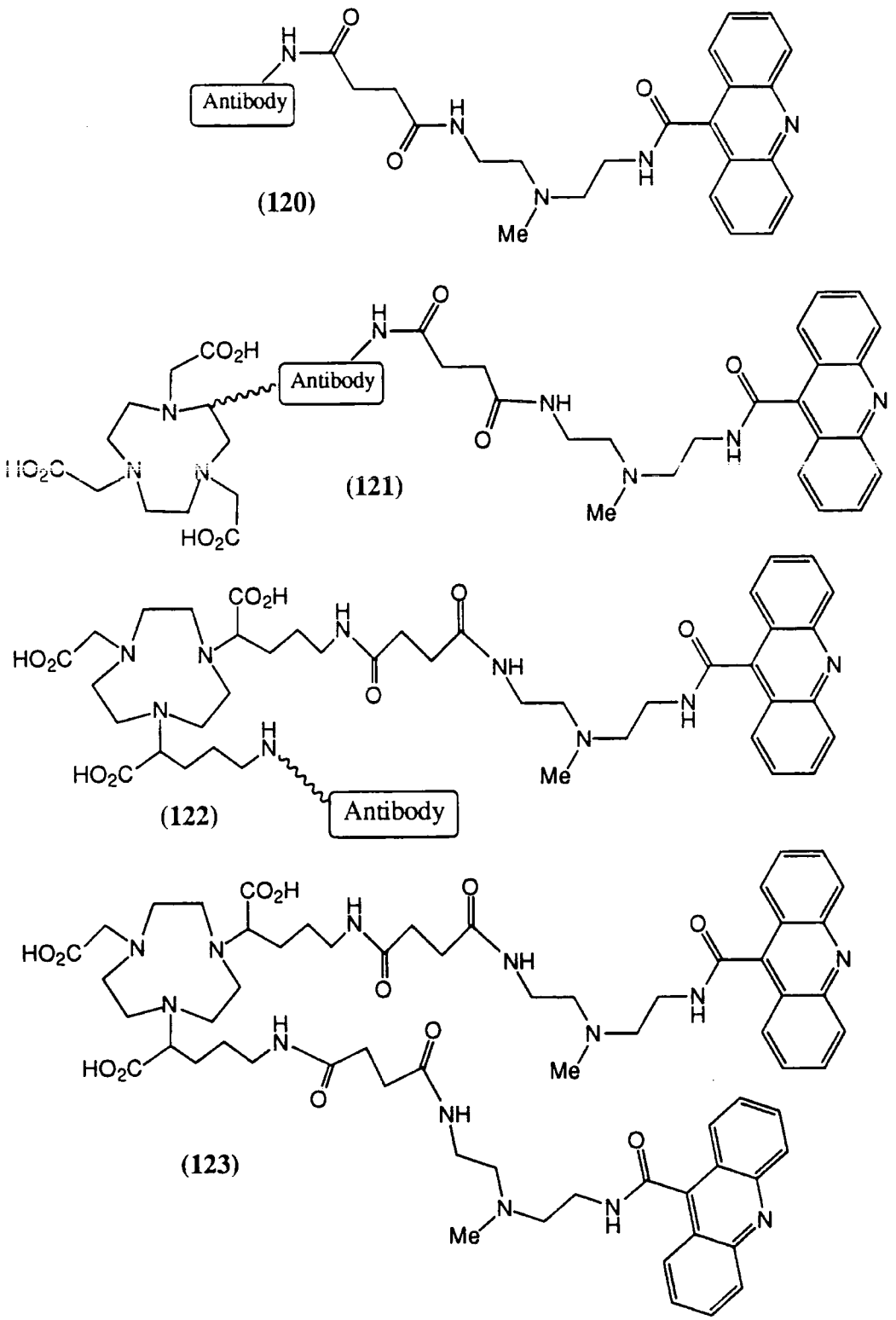

5.6 REFERENCES

1 C. Norbury and P. Nurse, *Ann. Rev. Biochem.*, 1992, **61**, 441.

2 L.P.G. Wakelin and M.J. Waring, 'DNA Intercalating Agents' in *Comprehensive Med. Chem.*, Volume 2.

3 J. Stubbe and J.W. Kozarich, *Chem. Rev.*, 1987, **87**, 1107.

4 B.E. Bowler, L.S. Hollis and S.J. Lippard, *J. Am. Chem. Soc.*, 1984, **106**, 6102.

5 B.E. Bowler, K.J. Ahmed, W.I. Sundquist, L.S. Hollis, E.E. Whang and S.J. Lippard, *J. Am. Chem. Soc.*, 1989, **111**, 1299.

6 ICRP Publication 38, *Radionuclide Transformations*, Pergammon Press, 1983; A. Birchall, *Health Physics*, 1986, **50**, 389-397.

7 D.A. Lea, 'Action of Radiations on Living Cells', Cambridge University Press, 1956.

8 W.A. Denny in *Chemistry of Antitumour Agents*, D.E.V. Wilman Ed., Chapman and Hall, New York, 1990.

9 A. Albert and B. Ritchie, *Org. Synth. Coll. Vol. 3*, 1955, 53.

10 R.M. Acheson Ed., *Heterocyclic Compounds: Acridines*, Vol 9, 2nd Ed., Interscience.

11 D.J. Dupre and F.A. Robinson, *J. Chem. Soc.*, 1945, 549.

12 W.A. Denny, B.F. Cain, G.J. Atwell, C. Hansch, A. Panthananickal and A. Leo, *J. Med. Chem.*, 1982, **25**, 276.

12 G.J. Atwell, B.F. Cain, B.C. Baguley, G.F. Finlay and W.A. Denny, *J. Med. Chem.*, 1984, **27**, 1481.

12 G.J. Atwell, G.W. Rewcastle, B.C. Baguley and W.A. Denny, *J. Med. Chem.*, 1987, **30**, 664.

13 W.Saenger, *Principles of Nucleic Acid Structure*, Ed. C.R. Cantor, Springer-Verlag, New York, 1984, pp. 143-149.

14 K. Shinozuka, Y. Seto and H. Sawi, *J. Chem. Soc., Chem. Commun.*, 1994, 1377.

Chapter Six

Experimental

6.1 EXPERIMENTAL METHODS

For all the reactions performed, temperatures are quoted in degrees celsius. All reactions were carried out in apparatus which had been oven dried and cooled under nitrogen.

Alumina refers to Merck Alumina activity II - III that was soaked in ethyl acetate for 24 hours prior to use. Silica refers to Merck silica gel F^{60} (230-400 mesh).

^{1}H and ^{13}C NMR spectra were obtained with a Bruker AC 250 operating at 250.13 and 62.90 MHz respectively, Varian Gemini 200 operating at 200 and 50 respectively or a Varian VXR 400S operating at 400MHz. All chemical shifts are given in ppm (referenced to Me_4Si (TMS) at 0 ppm). ^{31}P NMR spectra were obtained with a Bruker AC250 operating at 101MHz, chemical shifts are given to a higher frequency of H_3PO_4/H_2O (external reference). ^{89}Y NMR spectra were obtained on a Bruker AM-500 operating at 24.5 MHz, chemical shifts are given to higher frequency of YCl_3 (1 mol dm^{-3}, δ = 0 ppm). ^{71}Ga NMR spectra *in vitro* were obtained using a Bruker AC250 operating at 76.3MHz. Chemical shifts are given to a higher frequency of $Ga(NO_3)_3$ in 1moldm^{-3} HNO_3.

Mass spectra were recorded on a VG 7070E mass spectrometer, operating on DCI or FAB ionisation modes from CH_2Cl_2 or MeOH solutions with ammonia as the impingent gas, or using H_2O as a matrix. Thermospray mass spectra were obtained using a VG TRIO1000 spectrometer. Electrospray mass spectra were obtained using a VG AutoSpec or were performed by the SERC Mass Spectrometry Service at Swansea.

Infra-red spectra were recorded on a Perkin-Elmer 577 or Perkin Elmer 1600 FT-IR spectrometer as a thin film, KBr disc or Nujol Mull as stated.

Melting points were determined on a Kofler block and are uncorrected.

All solvents used were dried from an appropriare drying agent and water was purified by the PURITE system

Preparative TLC was carried out using MERCK 5726 Alumina PLC 150 F_{254} (type T) pre-coated 1.5mm plates.

Analytical and semi-preparative HPLC was perfomed with a Varian Vista 5500 or Star 5065 instruments fitted with reverse phase columns ("Dynamax" or "Spherisorb" 5 ODS 2). λ=254nm unless otherwise stated. Flow rates of 1.4 cm^3min^{-1} and 10.0 cm^3 min^{-1}

were used for analytical and semi-preparative columns respectively. Column and gradient elution conditions were as follows: for semi preparative reverse phase "Dynamax", t=0 min, 90% H_2O (0.1% trifluoroacetic acid), 10% MeCN (0.1 % trifluoroacetic acid); t=20 min, 25% H_2O, 75% MeCN; t=30 mins end time. For analytical reverse phase "Spherisorb" ODS t=0 min, 95% H_2O (0.1% trifluoroacetic acid), 5% MeCN (0.1% trifluoroacetic acid); t=20 min, 5% H_2O, 95% MeCN; t=30 mins end time.

6.2 CHAPTER TWO EXPERIMENTAL

6.2.1 SYNTHESIS OF Ga NOTA

Triethyl-1,4,7-triazacyclononanetriyltriacetate **(8)**[1]

1,4,7 Triazacyclononane (0.25g, 1.94 mmol) was stirred in EtOH (7 cm^3) with Cs_2CO_3 (1.96g, 6.02 mmol). Ethylbromoacetate was added (0.66 cm^3, 0.99g, 5.92 mmol) and the mixture heated to 60°C for 6 hours while monitoring by TLC. When reaction was complete the mixture was cooled, filtered and evaporated under reduced pressure and the residue taken up in dichloromethane. The insoluble solid material was washed out with water (3 x 10cm^3) and the organic layer dried (K_2CO_3) and evaporated. The product was purified by gravitational alumina chromatography [gradient 0-5% MeOH in CH_2Cl_2] to provide a pale yellow oil, (0.48g, 64%); δ_H ($CDCl_3$) 4.14 (6H, q, CH_2O), 3.25 (6H, s, CH_2), 2.68 (12H, s, ring) and 1.22 (9H, t, CH_3).

1,4,7-Triazacyclononane-1,4,7-triacetic acid **(1)**[1]

Triester **(8)** (0.136g, 0.395 mmol) was hydrolysed in 6M HCl (15 cm^3) by heating the solution under reflux overnight. The product was cooled and evaporated under reduced pressure to yield a white crystalline solid (0.159g, quantitative); δ_H (D_2O) 3.89 (6H, s, CH_2CO_2H) and 3.37 (12H, s, ring).

Gallium III complex of 1,4,7-triazacyclononane N,N', N'' triacetate **(9)**[1]

A solution of gallium nitrate (0.17 mmol, 0.04g) in dilute nitric acid (0.75 cm^3) was added to a solution of the ligand **(1)** (0.05g, 0.17 mmol) in dilute nitric acid (0.75 cm^3) and allowed to stand at R.T. for 24 hours. Acetone (2 cm^3) was added to the aqueous solution until a slight turbidity remained. A white solid precipitated, this was washed and dried under reduced pressure (0.013g, 0.034 mmol, 20%); δ_H (D_2O) 3.69 (6H, s, CH_2CO), 3.31 (6H, m, CH_2N) and 3.06 (6H, m, CH_2N); δ_{Ga} 170.2, external reference $Ga(NO_3)_3$ in HNO_3 (aq).

71-Gallium III complex of 1,4,7-triazacyclononane N, N', N'' triacetate **(10)**

A solution of $^{71}Ga_2O_3$ (0.033g, 0.176 mmol) in HCl (conc.) (1 cm^3) was added to a solution of the ligand **(1)** (0.107g, 0.353 mmol) in dilute HCl. The mixture was heated under reflux overnight until all the solids dissolved. As the solution cooled crystals appeared, these were washed in cold water and dried under reduced pressure. (0.018g, 0.05 mmol, 14%); δ_H (D_2O) 3.69 (6H, s, CH_2CO), 3.31 (6H, m, CH_2N) and 3.06 (6H, m, CH_2N); δ_{Ga} 170.2.

6.2.2 SYNTHESIS OF NOTPPri

Isopropyldiethoxyphosphine **(14)**

Isopropylmagnesiumchloride (2M in ether, 0.03 mol, 0.015 l) was stirred in a further 15 cm^3 of ether and cooled in ice/salt/ethanol bath to -10°C. Diethylchlorophosphite (0.03 mol, 4.77g, 4.77 cm^3) was added dropwise maintaining a temperature < 0°C. The mixture was allowed to warm to room temperature under Argon then the white solid was filtered under Argon giving a clear liquid which was purified by distillation (R.T., 0.01 mm Hg) and collected in a liquid air cooled trap. (2.339g, 48%). δ_P ($CDCl_3$) 166.6. The product was used immediately without further purification.

Triethyl 1,4,7-triazacyclononane N,N',N'' tris[methylene(isopropylphosphinate)] **(15)**

1,4,7-Triazacyclononane (0.258g, 2 mmol) was heated to reflux in dry THF over activated 4Å molecular sieves. Paraformaldehyde (0.237 g, 8.8 mmol) and finally freshly prepared isopropyldiethoxyphosphine **(14)** (1.44g, 8.8 mmol) were added. The mixture was heated under reflux for 16 hours and monitored by TLC. Upon completion the mixture was filtered and solvent removed under reduced pressure. The resulting pale yellow oil was purified by gravitational alumina column chromatography (gradient elution 0-2% MeOH in CH_2Cl_2) to yield a clear oil (0.54g, 47%). R_f 0.5 (alumina, CH_2Cl_2: MeOH, 98:2); Found (M^++1) 574.330 $C_{24}H_{54}N_3O_6P_3$ requires 574.330; *m/z* (DCI) 574 (M^++1), 454, 438 and 137; δ_H ($CDCl_3$) 3.94 (6H, m, OCH_2), 2.6 (18H, m, CH_2N, NCH_2P), 1.95 (3H, m, CH), 1.15 (9H, t, J = 7 Hz, $CH_2C\underline{H}_3$) and 1.03 (18H, dd, $^3J_{PH}$ = 16Hz, ^3J = 7 Hz, $CHC\underline{H}_3$); δ_C ($CDCl_3$) 60.8 (d, J=5Hz, POC), 57.5 (m, $N\underline{C}H_2CH_2$), 55.8 (d, J=105Hz, NCH_2P), 26.7 (d, J=88Hz, CH), 17.1 (d, J=15Hz $CH\underline{C}H_3$) and 15.8 (d, J=20Hz, $CH_2\underline{C}H_3$); δ_P ($CDCl_3$) 57.0; ν_{max}(film) 3400, 1659, 1024 cm^{-1}.

1,4,7-Triazacyclononane N,N',N'' tris[methylene(isopropylphosphinic)] acid **(16)**

Triethyl 1,4,7-triazacyclononane N,N',N'' tris[methylene(isopropylphosphinate)] **(15)** (0.187 g, 0.326 mmol) was heated to reflux in 6M-HCl (70 cm^3) for 48 hours. The solvent was removed under reduced pressure to leave a brown glass (0.33 mmol, quant.) δ_H (D_2O, pD=0.5) 3.5-3.0 (18H, m, NCH_2), 1.9-1.4 (3H, m, CH), 0.95 (9H, d,

J=7Hz, CH_3) and 0.87 (9H, d, J=7Hz, CH_3); δ_P (D_2O, pD=0.5) 50.8 , 49.7 (major peak); δ_C (D_2O, pD=0.5) 17.0 (CH_3), 30.6 (d, J_{PC} = 90Hz, P<u>C</u>H), 54.4 (N<u>C</u>H_2 ring), 54.5 (d, J_{PC} = 80Hz, N<u>C</u>H_2P); ν_{max} (film) 2955vs, 1655, 1471, 1176 and 959cm^{-1}; *m/z* (Thermospray) 490 (M^++1), 449, 436, 418.

Gallium complex of 1,4,7-triazacyclononane N,N',N'' tris[methylene (isopropylphosphinic)] acid **(17)**

1,4,7-Triazacyclononane N,N',N'' tris[methylene(isopropylphosphinic)] acid **(16)** (0.05 g, 0.01 mmol) was heated with $Ga(NO_3)_3.H_2O$ (0.01 mmol, 0.026 g) in 0.04M HNO_3 (3.5 cm^3) for 2 hours. The pH was then adjusted to 4 and the solution allowed to cool to R.T. The solvent was evaporated under reduced pressure to yield a hydroscopic yellow oil (0.01 mmol, quant.). δ_H (D_2O) 3.5-2.7 (18H, br.m, NCH_2), 2.0-1.7 (3H, m, CH) and 1.15-0.85 (18H, br. m, CH_3). δ_P (D_2O) 46.5. δ_{Ga} (D_2O) 132.1. *m/z* (FAB) 556 (M^+), 436, 131 and 56. ν_{max} (KBr) 3416, 2969, 1650, 1644, 1633, 1556, 1469, 1392, 1368, 1289, 1143vs, 1021vs, 800, 751, 685 and 587cm^{-1}.

Indium complex of 1,4,7-triazacyclononane N,N',N'' tris[methylene (isopropylphosphinic)] acid **(18)**

1,4,7-Triazacyclononane N,N',N'' tris[methylene(isopropylphosphinic)] acid **(16)** (0.05g, 0.01 mmol) was heated with $InCl_3$ (0.1 mmol, 0.022 g) in 0.04M HCl (2 cm^3) for 2 hours, the pH was then adjusted to 4.5-5.0 and the solution allowed to cool to R.T. The solvent was removed under reduced pressure to yield a hydroscopic pale brown solid (0.1 mmol, quant.). δ_H (D_2O) 3.4-2.8 (18H, br. m, CH_2N), 2.0-1.7 (3H, m, CH) and 1.1-0.85 (18H, br.m, CH_3). δ_P (D_2O) 44.3. *m/z* (FAB) 602 (M^+), 556, 185, 115, 93. ν_{max} (KBr) 3446, 2965, 1684, 1654, 1636, 1559, 1458, 1385, 1144vs, 1020vs, 886 and 792cm^{-1}.

6.2.3 SYNTHESIS OF DTPA-BIS AMIDE

N,N''-Bis(benzylcarbamoylmethyl)diethylenetriamine-N,N',N''-triacetic acid **(19)**

To the dianhydride of diethylenetriamine-N,N,N',N'',N''-pentaacetic acid (0.357g, 1 mmol) in pyridine (3 cm^3) was added benzylamine (0.321g, 3 mmol) and DMAP (5mg). An immediate white precipitate was observed which dissolved after 30 min. The solution became clear and yellow, the mixture was heated at 50°C for 14 hours, solvent removed under reduced pressure and H_2O added (1cm^3) to give a solution at pH 4.5. Dilute HCl (0.1 mol dm^{-3}) was added dropwise until the pH was 3.5 when a white solid formed which was filtered, washed with dilute HCl (pH 3.5, 3 x 2 cm^3) and dried under reduced pressure to yield a white free flowing solid (0.41g, 0.72 mmol, 72%); m.p 112-113°C (Found: C, 55.34; H, 6.74; N, 11.28%. $C_{28}H_{37}N_5O_8.2H_2O$ requires C, 55.4; H,

6.75; N, 11.53%); R_f 0.4 [silica gel, CH_2Cl_2-MeOH (95:5)]; Mass spectrum for the trimethyl ester: *m/z* (DCI) 614 (M^++1), 237, 150 and 108; *m/z* (FAB) 572 (M^+), 514, 425, 350, 336, 277 and 249; δ_H [$(CD_3)_2SO$] 8.60 (2H, t, NHCO), 7.28 (10H, m, aromatic H), 4.28 (4H, d, J=15Hz, $C\underline{H}_2Ar$), 3.39 (6H, s, $C\underline{H}_2CO_2H$), 3.32 (4H, s, CH_2CO), 2.95 (4H, m, CH_2N) and 2.83 (4H, m, CH_2N); δ_C [$(CD_3)_2SO$] 172.6 (CONH), 170.4 (CO_2H), 169.7 (CO_2H), 139.5 (q, aromatic C), 128.3, 127.2, 126.7 (aromatic CH), 57.4, 55.1, 52.1, 50.8 and 41.9 (CH_2N); ν_{max} (KBr) 3736m, 3315s, 3034m, 2550br, 1653, 1630vs (CO_2^-), 1559s, 1375, 1222, 1101 (CO), 738 and 695 cm^{-1}

Yttrium complex of N,N''-Bis(benzylcarbamoylmethyl)diethylenetriamine-N,N',N''-triacetic acid **(20)**

To a solution of the dibenzylamide **(19)** (0.1g, 0.175 mmol) in water (0.5 cm^3) was added a solution of yttrium nitrate (0.064g, 0.175 mmol) in HCl (pH2, 1 cm^3) and the mixture was heated under reflux until the solution was completely clear. After cooling to room temperature, the pH was adjusted to 4. Crystals formed on standing which were filtered, washed with cold water (3 x 1cm^3) and dried under vacuum (0.095 g, 74%). *m/z* (FAB) 658 (M^++1), 600, 367, 277 and 241; (Found: C, 46.36; H, 5.42; N, 9.52. $C_{28}H_{34}N_5O_8Y.4H_2O$ requires C, 46.03; H, 5.79; N, 9.59%); ν_{max} (KBr) 3407br (OH), 3250s, 3089m, 1616vs, br, 1497m, 1384vs, 1255m, 1097, 1029, 995, 931, 825, 705 and 619cm^{-1}; δ_H (D_2O) 7.37 (10H, m, aromatic H), 4.45 (4H, br. m., CH_2Ph), 4.12 (2H, br. m, CH_2CO), 3.61-3.38 (10H, br. m, CH_2N) and 2.9-2.3 (8H, br. m, CH_2N); δ_Y (D_2O) +80.0.

6.2.4 9N3 BASED LIGANDS FOR Gd

1,4,7-Tris(methylcarbamoylmethyl)-1,4,7-triazacyclononane **(22)**

1,4,7-Triazacyclononane (0.5g, 3.9 mmol) was stirred in dry MeCN, K_2CO_3 (12 mmol, 1.66g) and 2-bromo-N-methylethanamide (12 mmol, 1.8g) were added and the mixture heated to reflux for 24 hours. Upon cooling the inorganic solids were filtered and the solvent removed under reduced pressure, the resulting brown oil was taken up in 1M HCl and washed with CH_2Cl_2 (10cm^3). The pH was adjusted to 14 and the product extracted with CH_2Cl_2 (4 x 20cm^3), dried over K_2CO_3, filtered and evaporated to give a yellow oil. This was recrystallised from toluene to give a white solid (0.91g, 2.7 mmol, 69%); ν_{max} (oil) 1650 cm^{-1}; δ_H ($CDCl_3$) 7.45 (3H, q, *J* = 4.7Hz, NH), 3.17 (6H, s, NCH_2CO), 2.74 (9H, d, *J* = 3.6Hz, CH_3) and 2.67 (12H, s, CH_2N); δ_C ($CDCl_3$) 172.5 (CO), 62.0 (CH_2O), 55.4 (CH_2N) and 26.4 (CH_3); *m/z* (DCI) 343 (M^++1), 286, 272; (Found: M^+, 342.2367 $C_{15}H_{30}N_6O_3$ requires 342.2379).

1,4,7-Tris(benzylcarbamoylmethyl)-1,4,7-triazacyclononane(**23**)

1,4,7-Triazacyclononane (0.4814g, 3.7 mmol) was heated to reflux in MeCN (10cm^3) with 2-chloro-N-benzylethanamide (11.6 mmol, 2.12g) and K_2CO_3 (11.6 mmol, 1.6g) for 24 hours. It was then cooled, filtered and evaporated to give an orange/brown oil. This was purified by gravitational alumina column chromatography (gradient eluant 0-2% MeOH/ CH_2Cl_2) to yield a pale yellow oil (0.613g, 1.05 mmol, 29%). R_f = 0.2 (streaked); Found 570.3696 $C_{33}H_{42}N_6O_3$ calculated 570.3318; *m/z* (DCI) 571 (M^++1), 255; ν_{max} (oil) 3295 (NH), 3029 (ArCH), 2924, 1665 (amide) and 1529cm^{-1}; δ_H ($CDCl_3$) 7.36-7.15 (18H, m, NH and Ar), 4.37 (6H, d, *J* =5.8Hz, $NHC\underline{H}_2$), 3.04 (6H, s, CH_2CO) and 2.61 (12H, s, CHN); δ_C ($CDCl_3$) 171.4 (CO), 138.8 (Ar quat), 129.2, 128.4, 128.1(Ar), 62.3 (NCH_2CO), 56.8 (CH_2N) and 43.7 (CH_2Ar).

1,4,7-Tris(N-methyl-2-aminoethyl))-1,4,7 triazacyclononane (**24**)

$LiAlH_4$ (22.2 mmol, 0.84 g) was stirred in dry ether under N_2(g), 1,4,7-tris(methylcarbamoylmethyl)-1,4,7-triazacyclononane (**22**) (1.28g, 3.7 mmol) in CH_2Cl_2 (15 cm^3) was added dropwise over 30 mins and the mixture then heated to reflux for 18 hours. The suspension was quenched successively with H_2O (2cm^3),15% KOH (5 cm^3), filtered through celite, washed with Et_2O (2 x 10cm^3) and evaporated to dryness leaving a clear oil. This was dissolved in 1M HCl (5cm^3), washed with Et_2O (2 x 10cm^3), basified with KOH and extracted with CH_2Cl_2 (4 x 10cm^3) to yield a clear oil (0.275g, 0.93 mmol, 25%); *m/z* (DCI) 301 (M^++1), 288, 244 and 58; ν_{max} (film) 3395vs, 2942, 2828, 1649, 1546, 1377, 1300, 1113, 1035, 876, 731 and 607cm^{-1}; δ_H ($CDCl_3$) 2.63 (12H, m, CH_2N), 2.56 (12H, t, *J* = 3Hz, ring CH_2N), 2.38 (9H, s, CH_3) and 2.17 (3H, s, NH); δ_C ($CDCl_3$) 59.0 (CH_2N), 57.3 (CH_2N ring), 50.6 (CH_2N) and 36.9 (CH_3).

1,4,7-Tris(N-benzyl-2-aminoethyl))-1,4,7-triazacyclononane (**25**)

1,4,7-Tris(benzylcarbamoylmethyl)-1,4,7-triazacyclononane (**23**) (1.07 mmol, 0.6129g) in CH_2Cl_2 (10 cm^3) was added dropwise to a suspension of $LiAlH_4$ (13 mmol, 0.5g) in Et_2O (10 cm^3) and heated to reflux for 18 hours. After quenching the suspension was basified (KOH), extracted into CH_2Cl_2 (5 x 10cm^3) and evaporated to yield a yellow oil (0.414g, 0.78 mmol, 73%); *m/z* (DCI) 529 (M^++1), 410, 396, 374; ν_{max} (oil) 3406 (NH), 3084, 3080, 3028 (Ar CH), 2923, 2823, 1647, 1603, 1549, 1453, 737 and 699cm^{-1}; δ_H ($CDCl_3$) 7.33 (15H, m, Ar), 3.78 (6H, s, CH_2Ar), 2.66 (12H, m, CH_2N), 2.63 (12H, m, CH_2N) and 2.05 (3H, br s, NH); δ_C ($CDCl_3$) 141.1 (Ar quat), 128.8, 128.7 (Ar), 127.3 (Ar), 59.1 (CH_2N), 57.2 (CH_2N ring), 54.6 (CH_2N) and 48.0 (CH_2Ar).

1,4,7-Tris(N-methyl-N-ethoxycarbonylmethyl-(2-aminoethyl))-1,4,7-triazacyclononane(**26**)

1,4,7-Tris(N-methyl-2-aminoethyl))-1,4,7-triazacyclononane (**24**) (0.27g, 0.93 mmol) was dissolved in dry EtOH (3cm^3) and stirred with dry Cs_2CO_3 (3.1mmol, 1.0g). Ethylbromoacetate (3.1mmol, 0.52g, 0.34cm^3) was added and the mixture heated to 65°C for 2 hours. A further portion of ethylbromoacetate was then added (0.2cm^3) and heated to reflux for a further 2 hours. The mixture was cooled, filtered and evaporated to yield a brown oil (0.746g) which was purified by gravitational alumina column chromatography (gradient elution 0-10% Pr^{i}OH in CH_2Cl_2) to yield a yellow oil (0.2g, 0.41mmol, 44%). R_f 0.45 (streaked) [Alumina, MeOH-CH_2Cl_2 (5:95)]; Found (M^++1) 559.418 $C_{27}H_{54}N_6O_6$ requires 559.418; *m/z* (DCI) 559 (M^++1), 532, 505, 475, 224 and 180; δ_H ($CDCl_3$) 4.22 (6H, q, *J* = 6Hz, $COCH_3$), 3.25 (6H, s, NCH_2CO), 3.2-2.55 (12H, br m, CH_2N), 2.43 (9H, s, NCH_3) and 1.25 (9H, t, *J* = 6Hz, CH_3); ν_{max} (film) 3440vs, 1737, 1638vs, 1560, 1466, 1412, 1380, 1206s, 1096, 1025 and 909cm^{-1}.

1,4,7-Tris(N-benzyl-N-ethoxycarbonylmethyl-(2-aminoethyl))-1,4,7-triazacyclononane (**27**)

1,4,7-Tris(N-benzyl-2-aminoethyl)-1,4,7-triazacyclononane (**25**) (0.78mmol, 0.414g) was stirred in dry MeCN (3cm^3) with K_2CO_3 (2.6mmol, 0.36g). Ethylbromoacetate (2.6mmol, 0.43g, 0.29cm^3) was added and the mixture heated to 40°C for 3 hours. The mixture was then cooled, filtered and solvent evaporated to give a brown/orange oil (0.48g) which was purified by gravitational alumina column chromatography (gradient elution 0-5% MeOH in CH_2Cl_2) to yield a yellow oil (0.315g, 0.4mmol, 77%). R_f 0.4 [Alumina MeOH-CH_2Cl_2, (95:5)]; Mass found 787.5121 $C_{45}H_{66}N_6O_6$ requires 787.5122; *m/z* (DCI) 787 (M^++1), 580, 263, 220, 194 and 148; δ_H ($CDCl_3$) 7.27 (15H, m, Ar), 4.13 (6H, q, *J* = 7.2Hz, $C\underline{H}_2CH_3$), 3.74 (6H, s, $C\underline{H}_2Ar$), 3.29 (6H, s, CH_2CO), 2.95 (12H, s, CH_2N), 2.83 (12H, s, CH_2N) and 1.24 (9H, t, *J* =7.1Hz, CH_3); δ_C ($CDCl_3$) 171.7 (CO), 138.8, 129.5, 128.9, 127.8 (Ar), 60.9, 50.1, 55.2, 54.9 (CH_2N), 53.0, 51.2 (CH_2Ar) and 14.7 (CH_3); ν_{max} (film) 3422vs, 3027, 2980, 2843, 1732vs (ester), 1650, 1556, 1453, 1194vs, 1028s, 739vs and 701 cm^{-1}.

1,4,7-Tris(N-benzyl-N-carboxymethyl-(2-aminoethyl))-1,4,7-triazacyclononane (**28**)

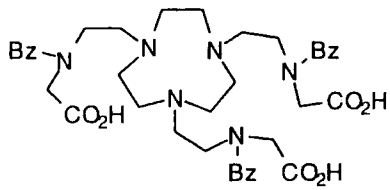

1,4,7-Tris(N-benzyl-N-ethoxycarbomylmethyl-(2-aminoethyl))-1,4,7-triazacyclononane (**27**) was heated to reflux with 6M HCl (5cm^3) overnight and monitored by TLC. The

solvent was removed under reduced pressure to yield a pale yellow glass (0.24g, quant); *m/z* (FAB) 702 (M^+), 565, 635, 185, 91 and 75; δ_H (D_2O) 7.27 (15H, m, Ar), 4.34 (6H, s, CH_2Ar), 3.93 (6H, s, CH_2CO), 3.55 (6H, br s, CH_2N), 3.40 (6H, br s, CH_2N) and 3.17 (12H, br s, CH_2N ring); δ_C (D_2O) 170.9 (CO), 134.4, 133.6, 132.4, 130.6 (Ar), 62.5, 56.3, 56.2, 53.6, 52.6, 52.2 and 52.1; ν_{max} (nujol) 1731 (CO acid), 747 and 700cm^{-1}.

Gadolinium Complex of 1,4,7-tris(N-benzyl-N-carboxymethyl-(2-aminoethyl))-1,4,7-triazacyclononane (**29**)

1,4,7-Tris(N-benzyl-N-acetate-(2-aminoethyl))-1,4,7-triazacyclononane (**25**) (0.1g, 0.14mmol) was dissolved in 0.1M HCl and Gd_2O_3 (s) (0.06g, 0.17mmol) was added, the pH was adjusted to 2 and the mixture was heated to 80°C until a clear brown solution was formed. The pH was adjusted to 6 using 0.1M NaOH and heating continued for a further 3 hours. The solvent was removed under reduced pressure and the product was purified by preparative TLC [Alumina MeOH - CH_2Cl_2 (10:90)] R_f 0.2 (streaked) to yield a white solid (0.018g, 0.021mmol, 15%); *m/z* (FAB) 858, 641, 551, 493, 462 and 435; ν_{max} (film) 3399 (vs, br), 1613vs, 1450, 1416, 1328, 750 and 702cm^{-1}.

6.2.5 SYNTHESIS OF 12N3 BASED LIGANDS FOR GADOLINIUM

1,5,9-Tris(methylcarbamoylmethyl)-1,5,9-triazacyclododecane (**30**)

1,5,9-Triazacyclododecane (0.5g, 2.9 mmol) in dry ethanol (10 cm^3) was heated to reflux with 2-chloro-N-methylethanamide (9.6 mmol, 1.1g) and K_2CO_3 (9.6 mmol, 1.32g) for 24 hours. The mixture was then cooled, filtered and evaporated giving a yellow oil. This was dissolved in 1M HCl (5cm^3), washed with CH_2Cl_2 (10cm^3), basified with KOH and extracted with $CHCl_3$ (5 x 10cm^3). Drying and evaporation gave a yellow oil, this was purified by gravitational alumina column chromatography (0.55g, 1.4 mmol, 50%); (eluant 2% MeOH in CH_2Cl_2) R_f 0.3 (streaked); Mass found 384.2828 $C_{18}H_{36}N_6O_3$ calculated 384.2849; *m/z* (DCI) 385 (M^++1), 127, 74; ν_{max} (oil) 3386 (NH), 2941, 2812, 1651 (amide) and 1547cm^{-1}; δ_H ($CDCl_3$) 7.08 (3H, br q, NH), 2.91 (6H, s, CH_2CO), 2.69 (9H, d, J =4Hz, CH_3), 2.45 (12H, t , J =6Hz, NCH_2) and 1.53 (6H, p, J = 6Hz, CH_2); δ_C ($CDCl_3$) 172.0 (CO), 58.9 (NCH_2CO), 50.8 (NCH_2), 26.3 (CH_3) and 23.4 (CH_2).

1,5,9-Tris(benzylcarbamoylmethyl)-1,5,9-triazacyclododecane (**31**)

1,5,9-Triazacyclododecane (0.5g, 2.9mmol) in dry ethanol (10cm^3) was heated to reflux with 2-chloro-N-benzylethanamide (1.8g, 9.6mmol) and K_2CO_3 (1.3g, 9.6mmol) for 18 hours and reaction was monitored by TLC. The mixture was cooled, filtered and evaporated giving a brown oil, this was treated with 1M KOH (5cm^3) and extracted into

CH_2Cl_2 (3 x 10cm^3) to yield a pale brown oil (1.32g, 2.2mmol, 74%); R_f 0.8 [Alumina TLC MeOH-CH_2Cl_2 (5:95)]; *m/z* (DCI) 613 (M^++1), 466, 203, 150 and 108; δ_H ($CDCl_3$) 7.21 (3H, t, NH), 7.15 (15H, m, Ar), 4.28 (6H, d, *J* =5.4Hz, CH_2Ar), 2.78 (6H, s, CH_2CO), 2.15 (12H, t, *J* = 5.4Hz, CH_2N ring) and 1.54 (6H, p, *J* = 5.4Hz, CH_2); δ_C ($CDCl_3$) 171.1 (CO), 138.6 (quat Ar), 129.2, 128.2, 128.4, 128.1 (Ar), 58.9 (CH_2Ar), 50.6, 43.7 (CH_2N) and 22.8 (CH_2); ν_{max} (film) 3305, 3062, 3029, 2927, 2817, 1658.7(vs, amide CO), 1520.9s, 1453.8m, 1427.3w, 1246m, 910.9m, 730.8s and 700.0s cm^{-1}.

1,5,9-Tris(N-methyl-2-aminoethyl)-1,5,9-triazacyclododecane **(32)**

1,5,9-Tris(methylcarbamoylmethyl)-1,5,9-triazacyclododecane **(30)** (0.5524g, 1.4 mmol) in CH_2Cl_2 (15 cm^3) was added dropwise to a suspension of $LiAlH_4$ (8.4 mmol, 0.32g) in Et_2O (15 cm^3) and heated under reflux overnight. Excess $LiAlH_4$ was quenched with H_2O (2cm^3) and 15% KOH (2 cm^3), washed with Et_2O (5cm^3) and evaporated to yield a yellow oil (0.3028g, 0.88 mmol, 63%); Mass found (M^++1) 343.3549 $C_{18}H_{42}N_6$ calculated 343.3549; *m/z* (DCI) 343 (M^++1), 298 and 286; ν_{max} (oil) 3398 (NH), 2956cm^{-1}; δ_H ($CDCl_3$) 2.47 (6H, t, *J* = 6Hz, CH_2N), 2.35-2.25 (27H, m, CH_2N, CH_3N) and 1.40 (6H, p, *J* = 6Hz, CH_2); δ_C ($CDCl_3$) 54.0, 50.0 (CH_2N), 37.0 (CH_3) and 21.8 (CH_2).

1,5,9-Tris(N-benzyl-2-aminoethyl)-1,5,9-triazacyclododecane **(33)**

1,5,9-Tris(benzylcarbamoylmethyl)-1,5,9-triazacyclododecane **(31)** (1.3g, 2.2mmol) in CH_2Cl_2 (10cm^3) was added dropwise to a suspension of $LiAlH_4$ (26.4mmol, 1g) in dry ether (10cm^3) and heated under reflux overnight. After quenching as described for **(24)**, the suspension was basified (KOH) and extracted into CH_2Cl_2 (5 x 10cm^3), and evaporated to yield a yellow oil (0.763g, 1.34mmol, 61%); *m/z* (DCI) 571 (M^++1), 482 and 438; δ_H ($CDCl_3$) 7.27 (15H, br s, Ar), 7.20 (3H, br m, NH), 3.73 (6H, s, CH_2Ar), 2.62 (6H, t, *J* = 5Hz, CH_2N), 2.42 (6H, t, *J* = 5Hz, CH_2N), 2.31 (12H, t, *J* = 5Hz, CH_2N) and 1.43 (6H, m, CH_2); δ_C ($CDCl_3$) 140.8 (Ar quat), 128.8, 128.6, 127.4 (Ar), 54.5 (CH_2N), 54.1 (CH_2N), 50.0 (CH_2N, ring), 47.1 (CH_2Ar) and 21.8 (CH_2); ν_{max} (film) 3300, 3084, 3060, 3025, 2955, 2800vs, 1666s, 1494, 1453vs, 1359, 1245, 1117s, 735vs and 698vs cm^{-1}.

1,5,9-Tris(N-methyl-N-ethoxycarbonylmethyl-(2-aminoethyl))-1,5,9-triazacyclododecane **(34)**

1,5,9-Tris(N-methyl-2-aminoethyl)-1,5,9-triazacyclododecane **(32)** (0.2g, 0.58mmol) was heated to 40°C for 5 hours in MeCN (3cm^3) with K_2CO_3 (1.9mmol, 0.26g) and ethylbromoacetate (1.9mmol, 0.32g, 0.21cm^3). Progress of the reaction was monitored by TLC. After filtration and evaporation of the solvent the resulting brown oil was

purified by gravitational alumina column chromatography (gradient elution fom 0-10% MeOH in CH_2Cl_2) to yield a yellow oil (0.322g, 0.54 mmol, 93%); R_f 0.6 (streaked) [alumina, MeOH - CH_2Cl_2 (5:95)]; (Found 601.4646 $C_{30}H_{60}N_6O_6$ requires 601.4652); *m/z* (DCI) 601 (M^++1), 544, 470, 413 and 213; δ_H ($CDCl_3$) 4.18 (6H, q, J = 7.2Hz, OCH_2), 3.27 (6H, s, CH_2CO), 3.00-2.45 (21H, m, CH_2N, CH_3N), 2.38 (12H, m, CH_2N), 1.6 (6H, br m, CH_2) and 1.28 (9H, t, J = 7Hz, CH_3); δ_C ($CDCl_3$) 171.3 (CO), 60.9 (OCH_2), 59.3 ($N\underline{C}H_2CO$), 55.3, 52.3, 49.8 (NCH_2), 43.3 (NCH_3), 21.7 (CH_2) and 14.7 (CH_3); ν_{max} (film) 3420vs, 2962, 2805, 1732vs, 1633s, 1565vs, 1454, 1409vs, 1250, 1192vs, 1116 and 1028cm^{-1}.

1,5,9-Tris(N-benzyl-N-ethoxycarbomylmethyl-(2-aminoethyl))-1,5,9-triazacyclododecane **(35)**

1,5,9-Tris(N-benzyl-2-aminoethyl)-1,5,9-triazacyclododecane (**33**) (0.368g, 0.65mmol) was stirred in dry MeCN (3cm^3) with K_2CO_3 (2.1mmol, 0.29g). Ethylbromoacetate (2.1mmol, 0.36g, 0.24cm^3) was added and the mixture heated to 50°C for 3 hours. It was then cooled, filtered and evaporated to give a yellow/orange oil (0.7g) which was purified by gravitational alumina column chromatography (gradient elution 0-5% MeOH in CH_2Cl_2) to yield a yellow oil (0.4g, 0.48mmol, 74%). R_f 0.35 (streaked) [Alumina MeOH-CH_2Cl_2, (95:5)]; *m/z* (DCI) 829 (M^++1), 754, 696, 610, 194, 116 and 58; δ_H ($CDCl_3$) 7.15 (15H, s, Ar), 3.97 (6H, q, J =7.1Hz, OCH_2), 3.55 (6H, s, $C\underline{H}_2Ar$), 3.10 (6H, s, NCH_2CO), 2.47 (12H, m, CH_2N), 2.10 (12H, m, CH_2N ring), 1.35 (6H, br m, CH_2 ring) and 1.10 (9H, t, J =7.1Hz, CH_3); δ_C ($CDCl_3$) 171.7 (CO), 138.5 (Ar quat), 129.6, 129.2, 128.0 (Ar), 60.7 (OCH_2), 58.8 ($N\underline{C}H_2CO$), 57.4, 55.0, 51.0 (CH_2N), 48.7 ($\underline{C}H_2Ar$), 20.1 (CH_2) and 14.3 (CH_3); ν_{max} (film) 3418vs, 2977, 2812, 1736vs, 1649.9, 1453, 1379, 1196vs, 1112, 1027, 745, and 701cm^{-1}.

1,5,9-Tris(N-benzyl-N-t-butylacetate-(2-aminoethyl))-1,5,9-triazacyclododecane **(36)**

1,5,9-Tris(N-benzyl-2-aminoethyl))-1,5,9-triazacyclododecane **(33)** (0.39g, 0.68mmol) was stirred in dry EtOH (2cm^3) with K_2CO_3 (2.26mmol, 0.31g) and t-butylbromoacetate (2.26mmol, 0.44g, 0.367cm^3) and heated to 40°C for 18 hours. The reaction was monitored by TLC, and further t-butylbromoacetate (0.07g, 0.34mmol, 0.06cm^3) was added and heated for a further 6 hours. The mixture was filtered and evaporated under reduced pressure to give a yellow oil (0.775g) which was purified by flash silica column chromatography [MeOH - CH_2Cl_2 (5:95)] to yield a pale yellow oil (0.50g, 0.548mmol, 81%). *m/z* (DCI) 915 (M^++1) 859, 801, 752, 422 and 191; δ_H ($CDCl_3$) 7.21 (15H, s, Ar), 3.64 (6H, s, NCH_2Ar), 3.28 (6H, s, NCH_2CO), 3.08 (6H, m, CH_2N), 2.92 (6H, m, CH_2N), 2.51 (12H, m, CH_2N ring), 2.04 (6H, m, CH_2 ring) and 1.37 (27H, s, CH_3); δ_C ($CDCl_3$) 170.9 (CO), 138.9 (Ar quat), 129.9, 128.9, 128.1 (Ar), 81.8 (quat), 59.0, 55.8, 51.9 (CH_2N), 48.9 ($\underline{C}H_2Ar$), 28.6 (CH_3) and 20.0 (CH_2); ν_{max} (film)

3854vs, 2975, 2811, 1732vs, 1660vs, 1495, 1367, 1250, 1220, 1153, 1077, 1028, 918 and 843cm^{-1}.

1,5,9-Tris(N-benzyl-N-acetate-(2-aminoethyl))-1,5,9-triazacyclododecane (**37**)

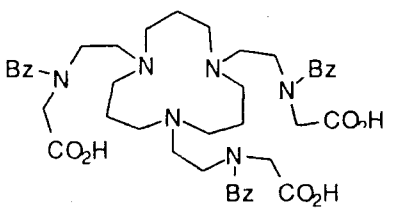

1,5,9-Tris(N-benzyl-N-ethylacetate-(2-aminoethyl))-1,5,9-triazacyclododecane (**35**) (0.1g, 0.12mmol) was treated with 6M HCl (20cm^3) and heated to 110°C for 48 hours. The solution was evaporated under reduced pressure and a sample was purified by preparative reverse phase HPLC (conditions stated above) R_t = 17.9 mins (0.006g, 1%). *m/z* (FAB) 727,115 and 91; ν_{max} (KBr disc) 3447vs, 1676vs, 1458, 1420, 1201vs and 1134s cm^{-1}; δ_H (D_2O, pD=1.5) 7.41 (15H, s, Ar), 4.30 (6H, s, C$\underline{H}_2$Ar), 3.79 (6H, t, *J* = 5Hz, CH_2CO), 3.62-2.60 (24H, m, CH_2N) and 1.95-1.65 (6H, br m, CH_2); δ_C (D_2O) 172.4, 172.3 (CO), 134.0, 133.4, 132.4, 132.0, 131.7, 131.2 (Ar), 62.5 (H_2Ar), 57.8 (CH_2CO), 52.8, 52.4, 52.1, 51.5, 50.9 (CH_2N) and 20.2 (CH_2).

6.2.6 SYNTHESIS OF PHOSPHINIC ACID ANALOGUES

Triethyl 1,4,7-tris(N-benzyl-N-methylenemethylphosphinate-2-aminoethyl)-1,4,7-triazacyclononane (**38**)

1,4,7-Tris(N-benzyl-2-aminoethyl)-1,4,7-triazacyclononane (**25**) (0.178g,0.34mmol) was dissolved in THF (30cm^3) and heated to reflux with paraformaldehyde (0.06g, 1.5mmol), methyldiethoxyphosphine (0.21g, 1.5mmol) in THF (5cm^3) was added and the mixture heated to reflux over 4Å molecular sieves for 18 hours. The mixture was filtered and the filtrate was evporated under reduced pressure to give a yellow oil (0.62g). This was purified by gravitational alumina column chromatography [gradient elution 0 -5% MeOH in CH_2Cl_2] to yield a pale yellow oil (0.201, 0.24mmol, 69%); R_f 0.4 [alumina MeOH - CH_2Cl_2 (10:90)]; Mass found 889.5044 $C_{45}H_{76}N_6O_6P_3$ requires 889.5039; *m/z* (DCI) 890, 769, 649, 226, 150, 109 and 91; δ_H ($CDCl_3$) 7.26 (15H, s, Ar), 4.02 (6H, q, OCH_2), 3.75 (6H, d, *J* = 13Hz, CH_2P), 2.79 (30H, m, CH_2N, ring, NCH_2P), 1.36 (9H, d, *J* =14Hz, PMe) and 1.27 (9H, t, *J* = 7Hz, CH_3); δ_C ($CDCl_3$) 139.0 (quat), 129.6, 128.8, 127.8 (Ar), 61.3 (d, *J* = 10Hz), 60.7 (d, *J* =6Hz), 56.3 , 55.2, 54.3 (d, ^1J = 91Hz, NCH_2P), 52.2 (CH_2N), 17.1 ($CH_2\underline{C}H_3$) and 14.2 (d, ^1J 92Hz, PCH_3); δ_P ($CDCl_3$) 52.6; ν_{max} (film) 3417.6vs, 2981, 2835, 1659.5, 1572, 1453, 1393, 1299, 1190vs, 1037vs, 950s, 720 and 701.5cm^{-1}.

1,4,7-Tris(2-aminoethyl-N-benzyl-N-methylenemethylphosphinic acid)-1,4,7-triazacyclononane **(39)**

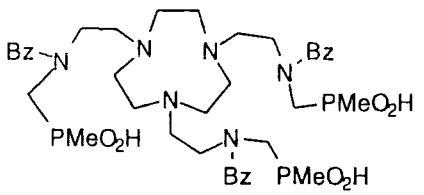

Triethyl 1,4,7-tris(N-benzyl-N-methylenemethylphosphinate-2-aminoethyl)-1,4,7-triazacyclononane (**38**) (0.045g, 0.053mmol) was heated to reflux in MeOH (2.5cm^3) with 1M KOH (2.5cm^3) for 16 hours. The solution was cooled, neutralised using 1M HCl (aq) and evaporated to dryness to yield a yellow oil and KCl(s). This was purified using semi-preparative reverse phase HPLC under standard conditions; R_t= 9.9 mins, to yield a pale yellow glass (0.02g, 0.0025mmol, 5%); *m/z* (FAB) 805.5 (M^++4H), 779.5, 741.5, 713.6, 687.5, 226.1, 175.1 and 134.1; δ_H (D_2O, pD = 14) 7.30 (15H, br, Ar), 3.73 (6H, s, CH_2Ar), 2.7-2.4 (30H, m, CH_2N, NCH_2P) and 1.23 (9H, d, J =13Hz, PMe); δ_C (D_2O) 184.4, 174.0, 139.4 (quat), 132.9, 131.8, 31.2 (Ar), 62.9, 62.7 ($\underline{C}H_2Ar$), 57.39 (d, J = 10Hz, $P\underline{C}H_2N$), 54.8 (CH_2N), 53.8, 53.7 (CH_2N), 52.5 (ring) and 18.79 (d, J = 9Hz, PMe); δ_P (D_2O, pD=7) 37.9; ν_{max} (film) 3424vs, 1639, 1135, 1031 and 739cm^{-1}.

Triethyl 1,5,9-tris(N-benzyl-N-methylenebenzylphosphinate-2-aminoethyl)-1,5,9-triazacyclododecane **(40)**

1,5,9-Tris(N-benzyl-2-aminoethyl)-1,5,9-triazacyclododecane (**33**) (0.172g, 0.3mmol) was heated to reflux in dry THF (30cm^3) over activated 4Å molecular sieves with paraformaldehyde (0.041g, 1.32mmol), benzyldiethoxyphosphine (0.282g, 1.32mmol) was added and the mixture heated to reflux for 16 hours. Reaction was judged to be complete when ^{31}P NMR showed the absence of any phosphine. The mixture was filtered and evaporated under reduced pressure and purified by gravitational alumina column chromatography [gradient elution 0 - 10% MeOH in CH_2Cl_2] to yield several mixed fractions and a pure pale yellow oil (0.0343g, 0.030mmol, 10%) R_f 0.15 (streaked) [alumina MeOH-CH_2Cl_2 (2:98)]; δ_H ($CDCl_3$) 7.30 (15H, Ar), 7.23 (15H, s, Ar), 4.05 (6H, q, OCH_2), 3.72 (6H, s, CH_2Ar), 3.15 (6H, d, J = 16Hz, PCH_2Ar), 2.9-2.2 (30H, m, CH_2N, NCH_2P), 1.35 (6H, br s, CH_2) and 1.25 (9H, t, J = 8Hz, CH_3); δ_C ($CDCl_3$) 138.5, 129.9, 129.1, 128.9, 128.5, 128.3, 127.2, 126.7 (Ar), 60.4 (d, ^2J = 8Hz, OCH_2), 60.7 (d, J =7Hz, CH_2Ar), 53.2 (d, ^3J 12Hz, CH_2N), 51.9 (d, ^1J = 95Hz, $P\underline{C}H_2$), 51.6 ($N\underline{C}H_2$), 49.4 (CH_2N), 35.0 (d, ^1J = 84Hz, $P\underline{C}H_2Ar$), 21.4 (CH_2 ring) and 16.5 (d, ^3J = 5Hz, $CH_2\underline{C}H_3$); δ_P ($CDCl_3$) 49.2; ν_{max} (film) 3486vs, 1634vs, 1495, 1454, 1404, 1296, 1262, 1160, 1046, 965 and 798cm^{-1}.

1,5,9-Tris(2-aminoethyl-N-benzyl-N-methylenebenzylphosphinic acid)-1,5,9-triazacyclododecane (**41**)

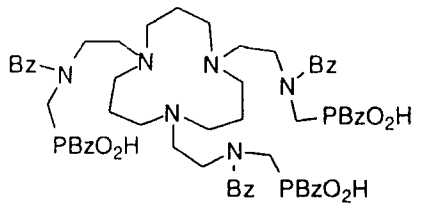

Triethyl 1,5,9-tris(N-benzyl-N-methylenebenzylphosphinate-2-aminoethyl))-1,5,9-triazacyclododecane (**40**) (0.039g, 0.036mmol) was heated to reflux in 6M HCl ($15cm^3$) for 20 hours. The solution was then cooled and the solvent removed under reduced pressure to yield a clear glass (0.036mmol, 0.041g); *m/z* (FAB) 1071 (M^+), 986, 908, 819 and 775; δ_H (D_2O, pD=0) 7.4-7.0 (30H, m, Ar), 4.31 (6H, s, CH_2Ar), 4.20 (6H, s, CH_2Ar), 3.59 (6H, m, CH_2N), 3.19 (12H, m, CH_2N), 2.93 (12H, m, CH_2N) and 1.81 (6H, br m, CH_2); δ_p (CD_3OD) 40.8; δ_P (D_2O) 30.7; ν_{max} (film) 3339vs, 3167, 3002, 2578s, 1690vs, 1654, 1495, 1455, 1202, 1170, 1068, 976, 832, 746 and $700cm^{-1}$.

6.2.7 YTTRIUM COMPLEXATION

Yttrium complex of 1,4,7,10-tetraazaclylododecane-N,N',N'',N'''-tetraacetic acid (**42**)
The ligand DOTA[3] (0.0268g, 0.066mol) was suspended in MeOH ($1cm^3$) and stirred and heated to 60°C. Yttrium triflate[2] (0.0355g, 0.066mmol) in MeOH ($0.5cm^3$) was added to the suspension and heating continued for 48 hours. The mixture was cooled and a white solid was collected, washed in MeOH and dried under reduced pressure. ^1H NMR confirmed that the product was Y-DOTA, by comparison with an authentic sample.[1,4]

Yttrium complex of 1,4,7-tris(2-aminoethyl-N-benzyl-N-methylenemethylphosphinic acid)-1,4,7-triazacyclononane (**43**)
1,4,7-Tris(2-aminoethyl-N-benzyl-N-methylenemethylphosphinic acid)-1,4,7-triazacyclononane (**39**) (0.02g, 0.025mmol) was heated to reflux in dry MeOH ($5cm^3$) with yttrium triflate[2] (0.0134g, 0.025mmol) for 24 hours. ^{31}P NMR of the crude reaction mixture gave a broad peak δ_P 40.7. Et_2O was added carefully and white precipitate began to appear. After 12 hours the suspension was centrifuged and washed with Et_2O and dried under reduced pressure to yield a white solid (0.019g, 0.021mmol, 84%); HPLC analytical R_t=10.7mins; ν_{max} (film) 3385, 1641, 1256, 1171, 1068 and $1031cm^{-1}$; δ_P (CD_3OD) 40.7; δ_H (CD_3OD) 9.78 (15H, br s, Ar), 5.6-5.0 (28H, br m, CH_2N) and 4.1-2.9 (9H, br m, PMe).

Yttrium complex of 1,5,9-tris(2-aminoethyl-N-benzyl-N-methylenebenzylphosphinic acid)-1,5,9-triazacyclododecane **(44)**

1,5,9-Tris(2-aminoethyl-N-benzyl-N-methylenebenzylphosphinic acid)-1,5,9-triazacyclododecane **(41)** (0.04g, 0.036mmol) in MeOH ($1cm^3$) was heated to 40°C. Yttrium triflate[2] (0.02g, 0.036mmol) in MeOH ($1cm^3$) was added and the solution heated for 16 hours. Upon cooling a white precipitate formed; this was centrifuged and washed in cold MeOH to yield a white solid (0.01g); δ_P (CD_3OD) 30.0 (broad); δ_H (CD_3OD) 7.5 (30H, m, Ar), 4.0-3.3 (30H, m, CH_2N, NCH_2P) and 1.22 (6H, m, CH_2 ring); ν_{max} (film) 3568, 3232vs, 1655s, 1458, 1252vs, 1176s, 1030vs and 640cm^{-1};

6.3 CHAPTER THREE EXPERIMENTAL

6.3.1. DTPA-NITROIMIDAZOLE-AMIDE

Diethylenetriamine-N,N''-di-N-(1-(3-aminopropyl)-2-nitroimidazole)-N,N',N''-triacetate **(48)**

DTPA-anhydride (0.155g, 0.43mmol) was stirred in dry pyridine ($5cm^3$) under N_2(g). 1-(3-Aminopropyl)-2-nitroimidazole **(53)**[5,6] (0.175g, 1.3mmol) in pyridine ($2cm^3$) was added slowly giving a yellow suspension this was heated to 50°C for 6 hours and monitored by HPLC. The pyridine was removed under reduced pressure to give a brown oil (0.27g, 0.383 mmol, 90%). This was purified using semi preparative reverse phase HPLC. Under analytical conditions R_t = 8.0 mins compared to the imidazole **(53)** with an R_t = 4.1 mins. Using the preparative conditions the main product peak was collected from 9.4-10.3 mins as a pale yellow oil. δ_H (D_2O) 7.32 (2H, s, Im-H), 7.01 (2H, s, Im-H), 4.33 (4H, t, *J* = 7Hz, CH_2-Im), 3.95 (8H, s, CH_2CO), 3.58 (2H, s, CH_2CO), 3.36 (4H, t, *J* = 4Hz, CH_2NH), 3.18 (4H, d, *J* = 6Hz, CH_2N), 3.10 (4H, d, *J* = 6Hz, CH_2N) and 1.94 (4H, m, CH_2); δ_C (D_2O) 175.3 (CO carboxylate), 173.4 (CO carboxylate), 170.3 (CO, amide), 170.0 (CNO_2), 130.8 (Im), 59.4 (CH_2N), 58.7 (CH_2N), 56.6 (CH_2COOH), 55.3 (CH_2COOH x 2), 53.3 (CH_2CONH), 50.4 ($NHCH_2$), 39.3 (CH_2Im) and 31.9 (CH_2); *m/z* (FAB) 698 (M^++1), 422, 337, 303, 271 and 225; ν_{max} 3275, 3100, 2930, 1720m, 1674vs, 1375m, 1200s, 1150, 850, 805 and 780cm^{-1}.

Gadolinium complex of diethylenetriamine-N,N''-di-N-(1-(3-aminopropyl)-2-nitroimidazole)-N,N',N''-triacetate. **(54)**

Diethylenetriamine-N,N''-di-N-(1-(3-aminopropyl)-2-nitroimidazole)-N,N',N''-triacetate **(48)** (0.03g, 0.043mmol) was dissolved in H_2O ($1cm^3$, pH2) and Gd_2O_3 (s) (0.043mmol, 0.016g) was added and the mixture heated to reflux for 30 mins. The pH was adjusted to 2 using dilute HCl and heated to reflux for a further 2 hours until all the

Gd_2O_3 had gone into solution. The pH was then adjusted to 6, using NaOH, and the mixture allowed to cool. This was purified using semi preparative reverse phase HPLC using standard conditions but no TFA was used in the solvents. Product was observed at λ=320nm, R_t=7.6mins and evaporation of the eluates gave a white solid (9.9mg, 0.012mmol, 27%); *m/z* (Electrospray) 891.5 (M^++K^+), 853 (M^+), 717.5, 701.5, 679.5, 491.2, 453 and 197.1; ν_{max} (KBr) 3420vs, 3256, 3100, 2944, 1636vs, 1540, 1490, 1362, 1202, 1164, 1096, 926, 837, 800 and 668cm^{-1}

Terbium complex of diethylenetriamine-N,N''-di-N-(1-(3-aminopropyl)-2-nitroimidazole)-N,N',N''-triacetate. **(55)**

Diethylenetriamine-N,N''-di-N-(1-(3-aminopropyl)-2-nitroimidazole)-N,N',N''-triacetate **(48)** (0.02g, 0.03mmol) was dissolved in H_2O (1cm^3) and heated to reflux with $Tb(OAc)_3$ (0.03mmol, 0.01g) for 2 hours. The pH was adjusted to 6 using NaOH and the mixture heated to reflux for 18 hours. The solution was cooled and purified by HPLC using the conditions described for **(54)**; R_t= 8.6mins. The eluates were freeze dried to yield a white solid (0.0062g, 0.0073mmol, 26%). ν_{max} (KBr) 3419vs, 2937, 1636vs, 1541, 1489, 1362, 1164, 1097, 928, 837 and 668cm^{-1}; *m/z* (Electrospray) 854.2, 841.1, 800.1, 583.2, 501.3, 301.3 and 272.3.

6.3.2 SYNTHESIS OF 12N3-NITROIMIDAZOLE CONJUGATE

(p-Cyanobenzyl)-9-(p-tolylsulphonyl)-1,5,9-triazacyclododecane-2,4-dione(**57**)[7]

To a solution of 3-(p-cyanobenzyl)-9-(p-tolylsulphonyl)-1,5,9-triazacyclododecane-2,4-dione(**56**)[7] (1.82g, 5.8 mmol) in dichloromethane (150 cm^3) was added triethylamine (1.17g, 1.61 cm^3, 11.6 mmol) and toluene-p-sulphonyl chloride (1.57g, 8.7 mmol) and the mixture was heated to reflux for 24 hours. Solvent was then evaporated under reduced pressure and the residue was purified by flash column chromatography on silica (5% MeOH in CH_2Cl_2) to yield a white solid (2.84g, 5.8 mmol, quantitative), m.p.258-260°C lit[7] 258-260°C; δ_H($CDCl_3$) 7.70 (2H, d, ArH), 7.55 (2H, d, ArH), 7.3 (4H, m, ArCN), 6.8 (2H, t, NH), 3.7-3.25 (9H, m), 2.85-3.15 (2H, m), 2.45 (3H, s, CH_3), 1.85 (2H, m) and 1.65 (2H, m).

(p-Aminomethylbenzyl)-9-(p-tolylsulphonyl)-1,5,9-triazacyclododecane **(58)**[7]

To a slurry of **(57)** (2.84g, 5.8 mmol) in tetrahydrofuran (10 cm^3) was added borane-THF (1M, 90 cm^3) and the mixture was heated to reflux for 48 hours. Excess of borane was destroyed with methanol (0°C) after which the mixture was evaporated under reduced pressure and the residue heated to reflux with 6M HCl (60 cm^3) for 3 hours. After removal of water from the mixture the residue was redissolved in aqueous base (pH> 13, KOH) and extracted with dichloromethane (4x 50 cm^3). The combined extracts

were dried (K_2CO_3) and evaporated to yield a colourless oil (2.15g, 4.84 mmol, 79%); *m/z* (DCI) 445 (M^+ +1), 419 and 291 (M^+-Ts); ν_{max} (film) 3400, 2250, 1640, 1600, 1450, 1330 and 1160 cm^{-1}; δ_H($CDCl_3$) 7.50 (2H, d), 7.12 (2H, d), 7.10 (2H, d), 6.90 (2H, d), 3.61 (2H, br s, $C\underline{H}_2NH_2$), 3.20-2.95 (4H, m, $C\underline{H}_2NTs$), 2.65-2.45 (4H, m, CH_2NH), 2.45-2.15 (4H, m, CH_2NH), 2.22 (2H, s, $C\underline{H}_2Ar$), 1.9-1.6 (5H, m, CH_2Ar) and 1.6-1.4 (4H, m, CH_2C).

3-Aminomethylbenzyl-1,5,9-triazacyclododecane (**59**)[7]

To a solution of (**58**) (1g, 2.21 mmol) in HBr-acetic acid (45% w/v; 80 cm^3) was added phenol (1g) and the mixture was heated to reflux for 24 hours. Upon cooling a precipitate formed and this was filtered off and washed with diethyl ether (3x 20 cm^3) to yield the trihydrobromide as a pink salt (0.73g, 1.36 mmol, 62%); δ_H (D_2O) 7.32 (4H, m, Ar), 4.11 (2H, s, CH_2N), 3.29-3.1 (12H, m, CH_2N), 2.77 (2H, d, $C\underline{H}_2Ar$), 2.55 (1H, m, CH) and 2.2-2.0 (4H, m, CH_2).

(2-Nitroimidazole-1-acetamidomethylbenzyl)-1,5,9-triazacyclododecane (**62**)

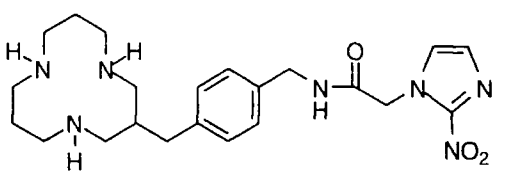

3-Aminomethylbenzyl-1,5,9-triazacyclododecane (**59**) (0.035g, 0.12 mmol) was dissolved in DMF (1cm^3) at 0°C. 2-Nitroimidazole-1-acetic acid (**60**)[8] (0.02g, 0.120 mmol) in DMF (0.5 cm^3) and triethylamine (0.026cm^3, 0.033g, 0.120 mmol) were added and then finally DPPA (0.05 cm^3, 0.0364g, 0.36 mmol). The mixture was stirred under N_2(g) at 0°C for 8 hours, then warmed to room temperature and allowed to stand for 4 days. After this period the DMF was removed under reduced pressure and the residue taken up in dichloromethane (20cm^3), washed with KOH (2x 10cm^3 of 1M), filtered, evaporated to give yellow oil (0.02g, 0.05 mmol, 41%); *m/z* (DCI) 523, 454, 445 (M^++1) and 444 (M^+); ν_{max} (soln in CH_2Cl_2) 1670 cm^{-1}; δ_H ($CDCl_3$) 7.18 (2H, d, Im), 7.1-6.9 (4H, m, Ar), 4.9-4.85 (2H, d, CH_2-Im), 4.25-4.15 (2H, s, $C\underline{H}_2NH$), 2.8-2.25 (12H, br m, CH_2N), 2.1-2.0 (1H, m, CH) and 1.6-1.4 (4H, br m, CH_2C).

(Acetamidomethylbenzyl)-1,5,9-triazacyclododecane (**66**)

To a solution of (**59**) (0.12g, 0.43 mmol) was added acetic acid (2cm^3), this was stirred and then the excess acetic acid was removed under reduced pressure. The acetic acid salt was dissolved in DMF (1 cm^3) and treated with triethylamine (0.10g, 0.14 cm^3, 1.03 mmol), acetic acid (0.020 cm^3, 0.020g, 0.35 mmol) and DPPA (0.074 cm^3, 0.095g, 0.35 mmol) under N_2(g) at R.T. for 2 weeks. After this period the DMF was removed under reduced pressure, the residue was redissolved in CH_2Cl_2 washed with 1M KOH (2

x10cm^3), LiCl (aq) (2 x 10cm^3), dried over potassium carbonate, filtered and evaporated to yield a pale yellow oil; δ_H ($CDCl_3$) 7.12 (4H, m, Ar), 4.30 (2H, d, CH_2NH), 2.8-2.3 (14H, m, CH_2N, CH_2Ar), 2.1-1.9 (1H, m, CH), 1.92 (3H, s, CH_3CO) and 1.6-1.4 (4H, m, CH_2C). It was confirmed that this was the desired compound by comparison with an authentic sample.[7]

DPPA route to 1-(Isobutylcarbamoylmethyl)-2-nitroimidazole (**65**)

The 2-nitroimidazole-1-acetic acid(**60**)[8] (0.161 g, 0.94 mmol) was stirred vigorously in dry DMF (1.5 cm^3) with $NaHCO_3$ (5 mmol, 0.42 g). Isobutylamine (0.94 mmol,0.069 g, 0.094 cm^3) was added and finally DPPA (1.4 mmol, 0.38 g, 0.3 cm^3) and the mixture was stirred at R.T for 18 hours. The DMF was removed under vacuum (0.1 mmHg) and the mixture washed with H_2O, 1M KOH and LiCl (aq) to yield a yellow oil (0.083 g, 36%). This was further purified by PLC R_f 0.45 (activated alumina, using 2% MeOH/ CH_2Cl_2 as eluant) to give a clear oil (0.023g, 0.1 mmol, 11 %). *m/z* (DCI) 227 (M^++1). ν_{max} (film) 1680 cm^{-1} (C=O). δ_H ($CDCl_3$) 7.11 (2H, s, Ar), 6.26 (1H, br t, NH), 4.95 (2H, s, CH_2CO), 3.05 (2H, t, J = 6Hz, $NC\underline{H_2}CH$), 1.72 (1H, m, CH) and 0.84 (6H, d, J = 7Hz, CH_3). δ_C ($CDCl_3$) 166.2 (CO), 128.7 (NCH), 127.8 (NCH), 125.5 (CNO_2), 52.5 (CH_2CO), 50.0 (NCH_2), 30.3 (CH) and 20.3 (CH_3).

PBOP route to 1-(Isobutylcarbamoylmethyl)-2-nitroimidazole (**65**)

To 2-nitroimidazole-1-acetic acid (**60**)[8] (0.1 g, 0.58 mmol) in dry acetonitrile (3cm^3) was added isobutylamine (0.58 mmol, 0.043 g, 0.06 cm^3), triethylamine (0.87 mmol, 0.088g, 0.12cm^3) and finally benzotriazol-1-yloxy- tripyrrolidinophosphonium hexafluorophosphate (PBOP) (0.58 mmol, 0.3g). The mixture was allowed to stir at R.T. for 18 hours and then the solvent was removed under reduced pressure leaving a pale yellow solid. The product was extracted into EtOAc, washed with brine and bicarbonate solution, dried and evaporated to give a yellow oil. This was purified by preparative alumina TLC. using 2% MeOH / CH_2Cl_2 as eluant (0.103g, 79%). The analysis of the product (**65**) was as described for previous experiment.

6.3.3 9N3 C-LINKED CONJUGATE

(+)-(2S)-Lysine methyl ester hydrochloride (**68**)[9]

L-Lysine (20g, 92 mmol) in dry MeOH (200cm^3) was heated to reflux under nitrogen in the presence of acetyl chloride (4cm^3) for 12 hours. The volume of solvent was reduced and the resulting white precipitate was filtered and dried under vacuum (18.44g, 81 mmol, 88%). δ_H(D_2O) 4.05 (1H, t, CH), 3.71 (3H, s, OCH_3), 2.92 (2H, t, CH_2NH_3), 1.85 (2H, m, CH_2CH), 1.61 (2H, m, CH_2CH_2CH) and 1.43 (2H, m, $CH_2CH_2NH_3$).

(2S)-N-(2-Aminoethyl)-2,6-diaminohexanamide (**69**)[9]

(+)-(*2S*)-Lysine methyl ester hydrochloride (7.09g, 30.4 mmol) was added in small batches over 2 hrs to ethylenediamine ($100cm^3$) at 90°C, with continuous stirring. The reaction mixture was heated to 120°C (6 hrs) and the ethylenediamine removed under reduced pressure. The residue was taken into aqueous sodium hydroxide (4M, 25 cm^3), the solvent was evaporated and the residue was dissolved in MeOH ($30cm^3$). The solution was filtered and the filtrate evaporated to leave a residue. This process was then repeated from the methanol stage. The subsequent residue was treated with dichloromethane (100 cm^3), filtered and the filtrate evaporated to give (**69**) as a yellow oil (5.41g, 28.8 mmol, 95%); $\delta_H(CDCl_3)$ 7.55 (1H, br s, CONH), 3.35 (1H, t, CH), 3.25 (2H, t, CH_2NHCO), 2.75 (2H, t, NCH_2), 2.62 (2H, t, NCH_2), 1.83 (2H, br, CH_2) and 1.38 (10H, m, NH_2CH_2); $\delta_C(CDCl_3)$ 23.0, 33.3, 34.8 (CH_2), 41.5, 41.7, 41.8, 44.8 (NCH_2), 55.1 (CH) and 175.3 (CO).

(5S)-3-Azanonane-1,5,9-triamine (**70**)[9]

The amide (**69**) (5.424g, 28.8 mmol) was heated to reflux in 1M borane-THF (180mmol, $180cm^3$) for 20 hours. Excess of borane was quenched with methanol ($100cm^3$) and solvents were evaporated to leave a residue which was heated to reflux in HCl (6M, 100 cm^3) for 3 hours. Evaporation of solvent followed by entraining in methanol (5 x 20 cm^3) gave the title compound as a white oily solid (7.04g, 22.0 mmol, 76%); δ_H (D_2O) 3.61 (1H, p, CH),3.5-3.2 (5H, m, NC<u>H</u>H, NCH_2), 3.01 (2H, t, NCH_2), 2.95-2.85 (1H, m, NC<u>H</u>H), 1.8-1.5 (4H, m, $C\underline{H}_2CH_2C\underline{H}_2$) and 1.5-1.3 (2H, m, $CH_2C\underline{H}_2CH_2$).

(5S)-N-(5,9-Diamino-7-azanonyl) benzamide (**71**)[9]

The tetraamine tetrahydrochloride (**70**) (1.92g, 6 mmol) was dissolved in water ($15cm^3$) and converted into the free tetraamine by addition of potassium hydroxide (0.96g, 24 mmol). Addition of copper carbonate (0.769g, 3.6 mmol) to the stirred solution at 50°C gave an intense blue colour. After continued stirring (40 mins, 50°C), benzoyl chloride (1.1g, 0.91 cm^3, 7.8 mmol) was added over 1 hour to the cooled solution (0°C), the pH being maintained above 9 with periodic addition of potassium hydroxide pellets. The solution was allowed to warm to room temperature and stirring continued for 1 hour. The dark solution was filtered and the filtrate treated with hydrogen sulphide over 15 minutes. Filtration followed by partial evaporation and exhaustive extraction with dichloromethane, with subsequent drying and evaporation of the combined extracts gave the title compound as a white solid. (0.89g, 3.2 mmol, 53%); ν_{max} (nujol) 3300 br (NH, NH_2, CONH), 1640 (CO) and 1600 cm^{-1}; δ_H ($CDCl_3$) 7.65 (2H, d, ArH), 7.25 (3H, m, ArH), 3.25 (2H, dt, $CONHCH_2$), 2.4-2.7 (6H, m, NCH_2) and 1.1-1.7 (11H, m+br s, CH_2, NH and NH_2).

(5S)-5,7,9-N',N'',N'''-Tris(p-methoxybenzenesulfonyl)-1-N-benzoyl-7-aza-1,5,9-triaminononane (**72**)

A solution of the benzamide (**71**) (0.89g, 3.2 mmol) in H_2O was stirred vigorously with K_2CO_3 (1.34g, 9.7mmol) and heated to 80°C, p-methoxybenzenesulphonyl chloride (2.5g, 12mmol) was added over a period of 2 hours. The resulting suspension was stirred for 15 hours before cooling. The solution was filtered and the solid was dissolved in hot CH_2Cl_2 (150 cm^3), this volume was reduced and the product recrystallised from CH_2Cl_2 to yield a white solid (0.96g, 1.14 mmol, 42%); R_f 0.4 [silica gel; CH_2Cl_2-MeOH (95:5)]; m.p. 159-160°C (Found:C, 54.76; H, 5.68; N,7.06. $C_{36}H_{44}N_4O_{10}S_3$ requires C, 54.8; H, 5.62; N, 7.10%); *m/z* (DCI): 788 (M^+ + 1), 617 and 446; δ_H [$(CD_3)_2SO$] 8.35 (1H, t, NHCO), 7.86 (1H, d, *J* = 6Hz, NHTs), 7.73 (4H, d, *J* = 9Hz, Ar), 7.53 (4H, q, *J* = 9Hz, Ar), 7.09 (4H, q, *J* = 9Hz, Ar), 3.87 (3H, s, OMe), 3.85 (3H, s, OMe), 3.80 (3H, s, OMe), 3.2-2.6 (9H, m, $C\underline{H}_2NHCO$, CH_2N, CHN), 1.5 (1H, m, CH_2C), 1.4-1.0 (3H, m, CH_2C) and 1.0-0.8 (2H, m, CH_2C); δ_C[$(CD_3)_2SO$] 166.2 (CO), 162.6, 162.2, 162.1 (ArOMe), 134.7, 133.4, 131.7, 131.0, 129.1, 129.1, 128.7, 128.2, 127.1, 127 (Ts), 114.5, 114.4, 114.2 (Ph), 112.7 (PhCO), 55.67, 55.61, 55.56, 53.6, 52.1, 48.8, 41.4 (CH, NCH_2), 30.8, 28.7 and 22.2 (CH_2); ν_{max} (Nujol) 3300br (NH), 1630 (CO), 1600 (aromatic ring), 1580, 1530 (NH), 1350 (SO_2) and 1150cm^{-1} (SO_2).

2-(4-Benzamidobutyl)-1,4,7-tris(p-methoxybenzenesulphonyl)-1,4,7-triazacyclononane (**73**).

Caesium carbonate (0.41g, 1.26 mmol) was added to a solution of the tri(p-methoxy benzenesulphonyl)amide (**72**) (0.5g, 0.63 mmol) in anhydrous DMF (25 cm^3) under dry nitrogen. A solution of ethylene glycol bis(toluene-p-sulphonate) (0.233g, 0.63 mmol) in anhydrous DMF (6.5cm^3) was added slowly over a period of 4 hours with efficient stirring. After the mixture had been stirred for 17 hours (20°C) its temperature was raised to 65°C for a further 6 hours. Solvent was removed under reduced pressure and the yellow residue was dissolved in chloroform (30cm^3) and washed with water (3x10cm^3). The organic layer was dried (K_2CO_3), filtered and evaporated under reduced pressure. The pale brown residue was purified by flash silica chromatography (gradient eluant 2-10% MeOH in CH_2Cl_2) to give a white glass (0.36g, 0.45 mmol, 72%); R_f 0.75 [silica gel; CH_2Cl_2-MeOH (95:5)]; m.p. 95-98°C; (Found: C, 55.71; H, 5.92; N, 6.97 $C_{38}H_{46}N_4O_{10}S_3$ requires C, 56.00; H, 5.69; N, 6.87%); $[\alpha]^{20}_D$ = +13.67 (CH_2Cl_2 c=0.13); *m/z* (DCI) 816 (M^++1), 815 (M^+), 810, 805, 803, 799, 793 and 791; (Found 815.2441 $C_{38}H_{47}N_4O_{10}S_3$ requires 815.2454); δ_H ($CDCl_3$) 7.78-7.69 (7H, m, Ar), 7.45-7.25 (4H, m, Ar), 7.0-6.85 (6H, m, Ar), 6.80 (1H, t, CONH), 4.15 (1H, br s), 3.81 (3H, s, OMe), 3.79 (3H, s, OMe), 3.78 (3H, s, OMe), 3.75-2.90 (13H, m,

CH_2N) and 1.6-1.15 (6H, m, CH_2); δ_C ($CDCl_3$) 168.0 (CO), 163.8, 163.61, 163.56 (CS), 135.1, 130.2, 129.5, 127.5, 132.0, 130.0, 129.3, 131.7, 129.9, 128.9 (aromatic C), 114.0, 114.95, 114.85 (OCH_3), 56.2, 53.0, 51.5 (CH_2N), 40.1 ($\underline{C}H_2NHCO$), 29.5 and 24.5 ($\underline{C}H_2C$); ν_{max} (film) 3400, 2944, 1650, 1633, 1595, 1538, 1495, 1462, 1301, 1257, 1149, 1090, 1022, 832 and 803cm^{-1}.

2-(4-Aminobutyl)-1,4,7-tris(p-methoxybenzenesulphonyl)-1,4,7-triazacyclononane (**74**)
The benzamide (**73**) (0.73g, 0.901 mmol) in hydrochloric acid (6M, 25cm^3) was heated to reflux for 4 days and stirred vigorously to overcome solubility problems. The reaction was monitored by TLC and when complete the mixture was cooled, washed with ether (3x10cm^3) and evaporated to dryness (0.01 mmHg) to yield the hydrochloride salt as a colourless glass. The product was obtained as the free amine by treatment with KOH (pH13) and extraction into dichlororomethane (0.227g, 0.304 mmol, 27%); *m/z* (DCI) 711 (M^++1), 707, 543, 385, 356, 291 and 155; δ_H ($CDCl_3$) 7.78-7.70 (6H, m, Ar), 7.31 (2H, m, Ar), 6.99-6.94 (6H, m, Ar), 3.86 (3H, s, OMe), 3.85 (3H, s, OMe), 3.85 (3H, s, OMe), 3.7-2.5 (13H, m, CH_2N) and 1.8-1.0 (6H, m, CH_2); ν_{max} 3400br s, 2950, 1640w, 1600s, 1575, 1500s, 1470, 1330, 1300, 1270vs, 1155vs and 1030cm^{-1}; δ_C ($CDCl_3$) 162.0 (CS), 130.9, 130.5, 129.2, 128.7, 126.0, 125.4 (aromatic C),116.0 (OCH_3), 59.5, 59.0, 58.8, 54.7, 53.0, 48.2, 46.1 (CH_2N), 28.7, 22.5 and 14.2 ($\underline{C}H_2C$).

2-(4-Benzamidobutyl)-1,4,7-triazacyclononane (**75**)[9]
2-(4-Benzamidobutyl)-1,4,7-tris(p-methoxybenzenesulphonyl)-1,4,7-triazacyclononane (**73**) (0.3g, 0.36mmol) was treated with concentrated sulphuric acid (5cm^3) at 115°C with stirring for 20 hours. To the cooled solution (0°C) was added NaOH (0.1M, 5cm^3). The precipitate was filtered and washed with distilled water (5cm^3). The combined filtrate and washings were extracted with CH_2Cl_2 (5 x 5cm^3) and the organic layer was dried (K_2CO_3), filtered and evaporated under reduced pressure to give a pale yellow oil (42mg, 0.14mmol, 38%); δ_H ($CDCl_3$) 7.82 (2H, dd, Ar H), 7.42 (3H, m, Ar), 3.51 (2H, m, $\underline{C}H_2NHCO$), 3.11 (3H, br s, NH), 2.74 (11H, m, CH_2N, CHN), 1.62 (2H, m, $\underline{C}H_2C$) and 1.38 (4H, m, $\underline{C}H_2C$).

2-(4-Aminobutyl)-1,4,7-triazacyclononane (**77**)
2-(4-Benzamidobutyl)-1,4,7-triazacyclononane (**75**) (0.12g, 0.395 mmol) was heated to reflux with HCl (6M, 20 cm^3) for 4 days and monitored by TLC. When reaction was complete the solution was washed with diethyl ether (3x10 cm^3) and evaporated to dryness (0.01 mmHg) to give the hydrochloride salt as a brown oil (0.139g, quant). The free amine was obtained by treating with KOH (pH13) and the aqueous phase was extracted exhaustively into dichloromethane (3 x 10cm^3) and chloroform (2 x 10cm^3) to

yield a pale yellow oil (0.106g, quant); *m/z* (DCI) 201 (M^++1), 118, 104, 84 and 46; δ_H ($CDCl_3$) 2.80-2.55 (11H, m, CH_2N), 2.35 (2H, m, CH_2N), 1.85-1.60 (5H, br s, NH), 1.35 (3H, m, CH_2C) and 1.25 (3H, m, CH_2C); δ_C (D_2O) 56.1 ($CH_2\underline{C}H_2NH_2$), 48.4 (CH), 45.2, 44.4, 44.2, 42.3, 42.0 (CH_2N), 33.9, 29.3 and 24.7 (CH_2C).

2-(4-Benzamidobutyl)-1,4,7,triazacyclononanetriyl triacetate (**78**)[9]

To a solution of 2-(4-Benzamidobutyl)-1,4,7-triazacyclononane (**75**) (0.11g, 0.362mmol) in dry ethanol (5cm^3) was added ethylbromoacetate (0.18g, 1.08mmol) and potassium carbonate (0.15g, 1.08mmol) and the mixture heated to 60°C for 3 hours. The mixture was cooled, filtered, and evaporated under reduced pressure and the residue was taken up in dichloromethane (50cm^3). The solution was washed with water (3 x15cm^3), dried (K_2CO_3) and evaporated and the residue was purified by gravitational alumina column chromatography [gradient eluant 0-3% MeOH in CH_2Cl_2] to yield a colourless oil (0.13g, 0.23g, 63%); *m/z* (DCI) 563 (M^++1), 477, 204 and 122; δ_H ($CDCl_3$) 7.83 (2H, d, ortho aromatic H), 7.40 (3H, m, m and p aromatic H), 7.27 (1H, m, NHCO), 4.12, 4.08, 4.07 (6H, q+q+q, CH_2O), 3.41 (8H, m, CH_2N and CHN), 1.61-1.42 (6H, m, CH_2C) and 1.20 (9H, t+t+t, CH_3); ν_{max} (film) 3330 br s (NHCO), 2980, 2930, 2840 (CH), 1742 (CO_2Et), 1649 (NHCO), 1538 (NH bend), 1190 and 1060 cm^{-1}.

2-(4-Aminobutyl)-1,4,7-triazacyclononane-1,4,7-triyltriacetic acid (**79**)[9]

The benzamide (**78**) (0.08g, 0.142 mmol) in hydrochloric acid (6M, 20 cm^3) was heated to reflux for 24 hours. After cooling, the solution was washed with diethyl ether (3x 10cm^3) and evaporated to dryness (0.01 mmHg) to yield the hydrochloride salt as a colourless glass (0.06g, 0.142 mmol, quantitative); δ_H (D_2O) 4.11 (6H, s, CH_2NCO_2), 3.8-3.0 (13H, br m, CH_2N and CHN), 2.90 (4H, t, CH_2NH_3), 1.62 (3H, br m, CH_2C) and 1.33 (3H, br m, CH_2C).

2-(4-Amidobutyl)-(p-nitrophenyl carboxyethyl)-1,4,7-triazacyclononane-1,4,7-triacetate (**83**)

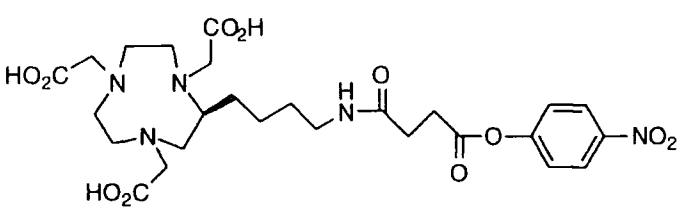

2-(4-Aminobutyl)-1,4,7-triazacyclononane-1,4,7-triacetate (**79**) (0.03g, 0.073mmol) was dissolved in 0.25cm^3 of DMSO with gentle warming. N-methylmorpholine (0.292 mmol, 0.029g, 0.032cm^3) and bis-p-nitrophenyl succinate (**81**) in 0.25cm^3 of DMSO were added with vigorous mixing under N_2(g) and the mixture was heated to 50°C. The reaction was monitored by analytical HPLC observing at 278nm at t=0 and t=30mins.

After 1 hour the product R_t= 8.4mins was purified using semi preparative reverse phase HPLC and the remaining reaction mixture was stored at -78°C. The product was checked for purity using analytical HPLC, examined by ^1H NMR and then used directly in the next step. δ_H (D_2O) 8.20 (2H, d, *J* = 12Hz, Ar), 7.23 (2H, d, *J* = 9Hz, Ar), 4.07-2.53 (19H, m, CH_2N ring, CH_2N, NCH_2CO_2H), 2.57 (4H, t, CH_2CO) and 1.37-1.18 (6H, m, CH_2).

2-(4-Amidobutyl carboxyethyl)-[1-(N-propyl)-2-nitroimidazole]-1,4,7-triazacyclononane-1,4,7-triacetate (**51**)

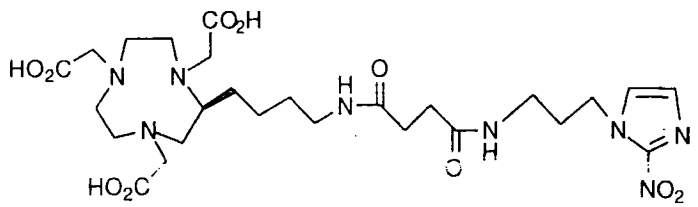

2-(4-Amidobutyl)-(p-nitrophenyl carboxyethyl)-1,4,7-triazacyclononane-1,4,7-triacetate (**83**) (0.02g, 0.034mmol) was dissolved in DMSO (0.5cm^3) and 1-(3-aminopropyl)-2-nitroimidazole (**53**) (0.24mmol, 0.032g) in DMSO (0.5cm^3) was added with mixing. The mixture was warmed in a water bath to 30°C overnight and monitored by analytical HPLC. The product was observed to appear at 10.4 mins and when formation was complete it was purified by semi preparative HPLC. After freeze drying a white solid was obtained (0.0072g) R_t 10.9mins; *m/z* (Electrospray) 616; δ_H (D_2O) 7.32 (1H, s, Ar), 7.04 (1H, s, Ar), 4.35 (2H, t, CH_2Im), 3.78-3.15 (13H, m, CH_2N), 3.10 (6H, br s, NCH_2COO), 3.01 (2H, t, CH_2N), 2.35 (4H, s, CH_2CO), 1.94 (2H, m, CH_2) and 1.35 (6H, m, CH_2); δ_C(D_2O) 176.2 (CO), 129.6 (Im), 58.6, 55.7, 49.4, 40.5, 38.0, 32.9, 30.6, 30.1 and 24.7; ν_{max} 3310, 2930, 1682, 1188 and 1082.

6.4 CHAPTER FOUR EXPERIMENTAL

6.4.1 12N4 - TUFTSIN

Molybdenum Tricarbonyl-1,4,7,10-tetraazacyclododecane Complex (**84**)[10]

1,4,7,10-Tetraazacyclododecane (1g, 5.8mmol) and molybdenum hexacarbonyl (1.53g, 5.8mmol) were heated to reflux in dibutylether (50cm^3) under Ar(g) for 3 hours, the bright yellow solid was filtered off under Ar(g) and dried under reduced pressure (1.8g, 5.2mmol, 90%). This was used immediately in the subsequent reaction.

[4-(4-Methoxyphenylsulfonamido)butylcarbomylmethyl]-1,4,7,10-tetraazacyclododecane (**87**)

The molybdenum tricarbonyl 12N4 complex (**84**) (1.84g, 5.22mmol) was stirred under Ar (g) in degassed DMF (50cm^3) with potassium carbonate (1g, 7.3mmol), N-(4-bromoacetamidobutyl)-4-methoxybenzenesulfonamide (**86**) (1.98g, 5.22mmol) was added and the solution heated to 80°C for 2 hours. The DMF was removed under reduced pressure and the resulting sticky brown mixture taken up in 10% HCl (50cm^3) and stirred in air overnight resulting in a dark brown solution containing a pale brown suspension. The pH was adjusted to 14 using KOH pellets and the black suspension filtered to remove decomplexed $Mo(CO)_3$. The yellow filtrate was extracted exhaustively with CH_2Cl_2 (6 x 20cm^3), the combined organic fractions were dried and evaporated to yield a yellow oil (1.51g, 3.23mmol, 62%). $\delta_H(CDCl_3)$ 7.95 (1H, t, $NHSO_2$), 7.71 (2H, d, J = 8.9Hz, $CHCOCH_3$), 6.90 (2H, d, J = 8.9Hz, $CHCSO_2$), 3.70 (3H, s, OMe), 3.2-2.4 (25H, CH_2 ring, NH ring, NCH_2CO, CH_2NHCO, CH_2NHSO_2) and 1.45 (4H, m, CH_2); $\delta_C(CDCl_3)$ 171.2 (CO), 162.2 ($\underline{C}OCH_3$), 131.9 (CSO_2), 128.8 ($\underline{C}HCOCH_3$), 113.9 ($\underline{C}HCSO_2$), 58.5 ($N\underline{C}H_2CO$), 55.4 (OCH_3), 52.8 ($\underline{C}H_2NCH_2CO$), 46.2, 44.6, 42.3 (ring C's), 42.2 ($\underline{C}H_2NHSO_2$), 38.1 ($\underline{C}H_2NHCO$), 26.2 and 26.1 (CH_2CH_2).

Triethyl 10-[4-(4-methoxyphenylsulphonamido)butylcarbomylmethyl]-1,4,7,10-tetraazacyclododecane-1,4,7-triyltrimethylenetri(methylphosphinate) (**88**)

To [4-(4-methoxyphenylsulfonamido) butylcarbomylmethyl]-1,4,7,10-tetraazacyclododecane (**87**) (1.07g, 2.27mmol) in THF (30cm^3) at 100°C were added paraformaldehyde (0.35g, 11.4mmol) and diethoxymethylphosphine (1.55g, 1.7cm^3, 11.4 mmol). The mixture was heated to reflux for 20 hours at 100°C with azeotropic removal of water by 4Å molecular sieves then cooled and filtered to remove excess paraformaldehyde and evaporated to give a pale yellow oil. Purification was carried out using alumina column chromatography (gradient elution 0-5% MeOH in CH_2Cl_2) to yield a pale yellow oil (0.997g, 1.2mmol, 53%); δ_H ($CDCl_3$) 7.72 (2H, d, $CHCOCH_3$), 6.90 (2H, d, $CHCSO_2$), 4.04 (6H, m, OCH_2), 3.82 (3H, s, OCH_3), 3.23 (2H, m, CH_2NHSO_2), 3.34-2.2 (26H, m, NCH_2), 1.47 (13H, m, CH_2, PCH_3) and 1.24 (9H, m, CH_2); δ_C ($CDCl_3$) 161.2 (CO)132.0, 128.2, 113.1 (Ar, 59 (OCH_2), 55.0 (OCH_3), 52.5-55.0 (12C), 42.1, 38.3, 26.0, 26.2, 15.9 and 13.1 (3C, d, PCH_3); δ_P ($CDCl_3$) 52.5 (br m).

10-[4-(4-Amino)butylcarbamoylmethyl]-1,4,7,10-tetraazacyclododecane-1,4,7-triyltrimethylenetri(methylphosphinic acid) (**89**)

To the phosphinate ester (**88**) (0.14g, 0.17mmol) was added phenol (140 mg) and 40% w/v HBr in glacial acetic acid (15 cm^3). The solution was heated to reflux at 110° C

overnight, and the solution allowed to cool to afford precipitation of the product. The reaction mixture was centrifuged, and the solvent decanted off leaving a pale white/brown solid which was washed with diethylether (3x15 cm^3), until the washings were colourless. The solids were taken up into water, filtered, and the solvents evaporated to yield the trihydrobromide salt as an off white solid. Overall yield (0.075mmol, 61 mg, 44%). $\delta_H(D_2O$; pD=0) 3.23 (2H, s, CH_2NHCO), 2.95-2.45 (26H, m, CH_2N ring, CH_2N, NCH_2P, CH_2NHCO, $CH_2NH_3^+$), 1.55 (4H, m, CH_2) and 1.3-1.2 (9H, d, J = 13Hz, CH_3P); δ_C (D_2O) 168.3 (CO), 58.2 (NCH_2CO), 51.1-55.5 (11C, CH_2N), 41.7, 41.4, 27.5, 26.5 and 17.3 (d, J =89Hz, PCH_3); δ_P (D_2O pD=13) 40.0.

N-Acetyl Tuftsin **(90)**

A sample of tuftsin (0.028mmol, 0.014g) was taken up in $(CD_3)_2SO$ (1cm^3) and the ^1H NMR spectrum obtained. Solid p-nitrophenyl acetate (0.003g, 0.014mmol) was added to this solution and stirred thoroughly at R.T. under N_2 (g). After 12 hours the ^1H NMR spectrum was obtained, having established that reaction was complete, the solution was purified on a Sephadex® G-25M column using PBS as eluant [PBS, pH7.2]. The desired product was detected on TLC [silica, 5% MeOH in CH_2Cl_2] R_f = 0.25 using ninhydrin spray as an indicator. *m/z* (FAB) 585 (100%, 2 acetates), 555 (17%), 543 (54%, 1 acetate), 499 (1%, tuftsin); δ_H [$(CD_3)_2SO$] 9.01, 8.12 (1H, d, J =8Hz, Thr NHCO), 7.93 (1H, t, J = 5Hz, Lys NHCO), 7.81, 7.47 (4H, m, Arg NH's), 7.39 (1H, d, J = 7.2 Hz, Arg NHCO) 4.60, 4.51 (1H, m, Lys α-CH), 4.34 (1H, m, Pro α-CH), 3.86 (1H, m, Arg α-CH), 3.82 (2H, m, Thr β-CH_2), 3.71 (2H, m, Pro δ+δ'-CH_2), 3.05 (1H, d, J = 4Hz, Thr α-CH), 3.02 (2H, m, Arg δ-CH_2), 2.98 (2H, m, Lys ε-CH_2-Tuftsin), 1.88 (3H, s, acetate), 1.75-1.25 (8H, m, Lys β-CH_2, Lys δ+δ'-CH_2, Lys γ-CH_2, Arg CH_2) and 1.05 (3H, d, J = 6Hz, Thr CH_3).

10-[4-((4-Amidobutyl)-4-nitrophenyl carboxyethyl)-carbamoylmethyl]-1,4,7,10-tetraazacyclododecane-1,4,7-triyltrimethylenetri(methylphosphinic acid) **(91)**

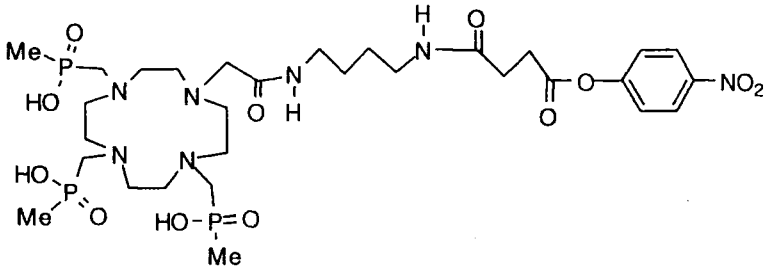

10-[(4-Aminobutyl)carbamoylmethyl]-1,4,7,10-tetraazacyclododecane-1,4,7-triyltrimethylenetri(methylphosphinic acid) **(89)** (0.14g, 0.16mmol) was stirred in DMSO (0.25cm^3) with N-methylmorpholine (0.113g, 0.123cm^3, 1.12mmol) and bis p-nitrophenyl succinate **(81)** (0.115g, 0.32mmol) at R.T. After 30 mins, HPLC revealed that the amount of the desired compound had begun to decrease so the reaction was

cooled to -78°C to stop it. The solution was purified using HPLC (standard conditions) R_t= 16 mins and any remaining p-nitrophenol was washed out with Et_2O (3 x 10cm3) to yield a yellow oil (0.0127g, 0.016mmol, 10%); *m/z* (Electrospray) 820.2 (M+Na), 798.3 (M^++1), 699.3 (M_1+Na), 677.3 (M_1=676.3); δ_H (D_2O) 8.31 (2H, d, *J* = 8.8Hz, Ar), 7.35 (2H, d, *J* = 8.8 Hz, Ar), 3.85 (2H, s, NCH_2CO), 3.5-3.1 (26H, m, CH_2N), 2.95 (2H, t, CH_2CO), 2.65 (2H, t, CH_2O), 1.52 (4H, m, CH_2) and 1.43 (9H, d, *J* = 14Hz, PMe); δ_P (D_2O, pD=4) 32.0 .

12N4-tuftsin conjugate (**92**)

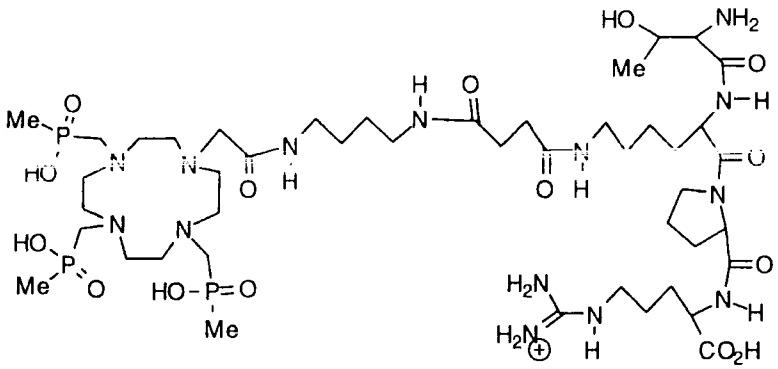

To 10-[4-((4-amidobutyl)-4-nitrophenyl succinate)-carbomylmethyl]-1,4,7,10-tetraazacyclododecane-1,4,7-triyltrimethylenetri(methylphosphinic acid) (**91**) (0.013g, 0.016mmol) in $(CD_3)_2SO$ (1cm^3) was added tuftsin (0.0192g, 0.038mmol) and the mixture was stirred thoroughly under N_2 (g) at R.T. and allowed to settle overnight. A fine brown precipitate in a yellow solution resulted. ^{1}H NMR revealed that the solution contained only p-nitrophenol and excess tuftsin. The solid was soluble in D_2O and a crude ^{1}H NMR was obtained before purification using a Sephadex column with PBS as eluant. The desired product was detected using TLC (silica 5% MeOH in CH_2Cl_2) R_f= 0.25; ν_{max} (KBr) 3404, 2455, 1653, 1406, 1265, 1121, 1054, 967, 890, 716, 642 and 516; δ_H (D_2O) 4.15 (m, Pro CH, Lys CH, Pro δ-CH_2, Arg α-CH), 3.91 (m, Thr β-CH_2), 3.7-2.9 (m, CH_2N, CH_2CO, CH_2P, Arg δ-CH_2, Thr α-CH), 2.52 (m, Pro β-CH_2), 2.23 (Lys β-CH_2), 2.1-1.5 (br m, CH_2, Lys δ-CH_2, Lys γ-CH_2, Arg γ-CH_2) and 1.50-1.15 (12H, m, CH_3P, Thr γ-CH_3); δ_P (D_2O) 39.8, 33.0.

Terbium complex of 10-[(4-amino)butylcarbamoylmethyl]-1,4,7,10-tetraazacyclododecane-1,4,7-triyltrimethylenetri(methylphosphinic acid) (**93**)

10-[(4-Amino)butylcarbamoylmethyl]-1,4,7,10-tetraazacyclododecane-1,4,7-triyltrimethylenetri(methylphosphinic acid) (**89**) (0.178g, 0.25mmol) was dissolved in H_2O (1cm^3) and the solution pH was found to be 1. Terbium (III) acetate hydrate (0.08g, 0.25cm^3) dissolved in H_2O (1.5cm^3) was added to the solution and heated to 90°C, the solution was adjusted from pH 2.5 to pH 6 using NaOH (aq) and heated for a further 5 hours. The complexation was monitored by analytical HPLC using the standard

conditions. Once complete the product was purified by preparative HPLC (reverse phase "Dynamax") observed at λ=254nm with gradient elution. 10.0 cm^3min^{-1}; t=0 min, 90% H_2O (0.1% trifluoroacetic acid), 10% MeCN (0.1 % trifluoroacetic acid); t=15 min, 40% H_2O, 60% MeCN; t=30 mins end time. This provided a pale yellow solid (0.261g, 0.32mmol, 64%) R_t = 6.3 mins. δ_P (D_2O, pD = 6) 628.4, 611.7, 521.8 (complex), 42.5, 39.9, 33.2 (ligand); ν_{max} (film) 3417, 2978, 2992, 2867, 1678 (amide), 1628, 1460, 1422, 1303, 1200 (PO), 1134, 1073, 972, 895, 800, 720 and 494cm^{-1}.

6.4.2 N AND N,N' FUNCTIONALISED 9N3 CONJUGATES

2-Bromo-N-benzoyl-5-aminopentyl ethanoate (**96**)

Synthesis was carried out in two steps starting from N-benzoyl-δ-amino valeric acid (**94**) (SIGMA). The bromination step was effected with red phosphorus and bromine according to the literature method.[11] Esterification was achieved by standard methods using ethanol and acetyl chloride and the product purified by 'flash' silica column chromatography eluting with ethyl acetate-hexane (1:1).

(2-(N-Benzoyl-3-aminopropyl)ethoxycarbonylmethyl)-1,4,7-triazacyclononane (**97**)

Potassium carbonate (0.138g, 1mmol) was added to a solution of 1,4,7-triazacyclononane (0.254g, 1.97mmol) in anhydrous DMF (5cm^3) under a nitrogen atmosphere and the mixture heated to 60°C. A solution of the α-bromo ester (**96**) (0.33g, 0.99mmol) in anhydrous DMF (5cm^3) was added dropwise over a period of 7 hours) and the mixture stirred for a further 24 hours at 60°C. The cooled reaction mixture was filtered and solvent removed under reduced pressure to give a pale brown oil. A small amount of the product (0.053g) was separated by semi preparative HPLC (Dynamax), but the remaining product was used without further purification. Purified material: HPLC: R_t = 11mins, observed at λ = 254 nm (Dynamax, reverse phase) with gradient elution. 10 cm^3min^{-1}; A = H_2O/0.1% TFA, B = MeCN/0.1% TFA from t=0 min; A = 90%, B = 10%; to t = 20 mins., A = 10%, B = 90%; Mass found 377.255 (M^++1) $C_{20}H_{32}N_4O_3$ requires 377.255; ν_{max} (film) 3306, 2984, 2865, 1676, 1545, 1448, 1309, 1202 and 1134cm^{-1}; *m/z* (DCI) 377 (M^++1), 291, 174, 130, 105, 97 and 85; δ_H (CD_3OD) 7.83 (2H, d, *J* =8.3Hz, Ar), 7.48 (3H, m, Ar), 4.23 (2H, q, *J* = 7.1Hz, OCH_2), 3.8-3.6 (3H, m, CH_2NCO, CHN), 3.6-3.2 (10H, m, ring CH_2N), 3.2-3.0 (2H, m, ring CH_2N), 2.0-1.7 (4H, m, CH_2) and 1.25 (3H, t, *J* = 6.2Hz, CH_3); δ_C (CD_3OD) 175.4 (CO), 170.5 (NHCO), 135.6, 132.7, 129.6, 128.2 (Ar), 64.7, 62.6 (CH_2O, CHCO), 48.1, 45.7, 44.3, 40.1 (CH_2N, CH_2N ring), 28.3, 27.8 (CH_2) and 14.5 (CH_3).

N,N'-Bis(2-(N-benzoyl-3-aminopropyl)ethoxycarbonylmethyl)-1,4,7-triazacyclononane (**98**)

Potassium carbonate (0.14g, 1mmol) was added to a solution of 1,4,7-triazacyclononane (0.26g, 2mmol) in anhydrous DMF (5cm^3) under a nitrogen atmosphere and the mixture heated to 60°C. A solution of the α-bromo ester (**96**) (0.33g, 0.99mmol) in anhydrous DMF (5cm^3) was added over a period of 7 hours and the mixture stirred at 60°C for 20 hours. The cooled mixture was filtered and solvent removed under reduced pressure to give a pale yellow oil. The di-alkylated product was separated by semi preparative HPLC (Dynamax, standard conditions) to give a yellow powder R_t = 16 mins, observed at λ = 254nm. Mass found (M^++1) 624.376 $C_{34}H_{50}N_5O_6$ requires 624.376; ν_{max} (film) 3280, 2930, 1675, 1543, 1458, 1311, 1202 and 136cm^{-1}; *m/z* (DCI) 624 (M^++1), 377, 291, 203, 174, 144, 122 and 105; δ_H ($CDCl_3$) 9.51 (2H, br m, NH), 7.79 (4H, m, Ar), 7.46 (6H, m, Ar), 4.12 (4H, q, *J* = 7.2Hz, OCH_2), 3.5-2.6 (18H, m, CH_2N), 1.64 (8H, m, CH_2C) and 1.22 (6H, m, CH_3); δ_C ($CDCl_3$) 172.3 (CO_2), 168.6 (NHCO), 133.4, 131.9, 128.6, 127.1 (Ar), 64.8, 64.1, 61.1 (CH_2O, CH_2CO), 44.4, 43.8, 39.7, 39.3 (CH_2N, ring CH_2N), 27.3, 27.1 (CH_2C) and 14.2 (CH_3).

(2-(N-Benzoyl-3-aminopropyl)ethoxycarbonylmethyl)-N'-N''-bis-(ethoxycarbonylmethyl)-1,4,7-triazacyclononane (**99**)

Caesium carbonate (0.114g, 0.35mmol) and ethylbromoacetate (0.041cm^3, 0.059g, 0.35mmol) were added to a solution of monoalkylated triamine (**97**) (0.053g, 0.14mmol) in dry MeCN (2cm^3) and the mixture stirred at 60°C for 20 hours. Solvent was removed under reduced pressure and the residue taken up in dichloromethane (5cm^3) and a fine white precipitate was removed by centrifuge. The solution was evapotated to dryness and the yellow oily residue (0.062g, 0.11mmol) purified by PLC [alumina: dichloromethane - methanol (98:2)] to yield a yellow oil (14.7mg, 0.027mmol, 17%); R_f 0.6 [alumina: CH_2Cl_2 - MeOH (98:2)]; HPLC: R_t = 5.5min. observed at λ = 254nm ("Synchropak" CM300 cation exchange) with gradient elution. 1.4 cm^{3}min^{-1}.; A= MeCN, B= H_2O, C= 1.0M NH_4OAc from t = 0min.; 20% A, 80% B, 0% C; to t =5 min. 20% A, 60% B, 20% C; to t = 10 min. 20% A, 0% B, 80% C; ν_{max} (film) 3409s, 2981, 1731s, 1692vs, 1650s, 1538, 1426, 1382,1303, 1203vs, 1127vs, 1027, 834, 802 and 721cm^{-1}; *m/z* (DCI) 549 (M^++1), 491, 463, 406, 250 and 105; δ_H ($CDCl_3$) 7.75 (2H, m, Ar), 7.38 (3H, m, Ar), 6.80 (1H, br s, NH), 4.08 (6H, m, CH_2O), 3.5-3.2 (7H, m, CH_2NCOPh, $CHCO_2$, CH_2CO_2), 3.0-2.5 (14H, m, CH_2N, ring), 2.0-1.5 (4H, m, CH_2) and 1.19 (9H, t, *J* = 7Hz, CH_3); δ_C ($CDCl_3$) 173.2, 172.2, 171.6, 167.5 (CO), 134.7, 131.2, 128.3, 127.0 (Ar), 66.1, 60.5, 60.3 (CH_2O, CH_2CO), 39.6 (CH_2N), 27.3, 26.3 (CH_2) and 14.2 (CH_3).

N,N'-Bis(2-(N-benzoyl-3aminopropyl)ethoxycarbonylmethyl)-N''-ethoxycarbonylmethyl-1,4,7-triazacyclononane **(100)**

Caesium carbonate (0.0166g, 0.051mmol) and ethylbromoacetate (0.0059cm^3, 0.0085g, 0.051mmol) were added to a solution of the dialkylated triamine **(98)** (0.0151g, 0.046mmol) in anhydrous MeCN (2cm^3). The mixture was stirred at 60°C for 20 hours after which the solution was filtered and the solvent removed under reduced pressure to yield a yellow oil (0.030g) which was purified by HPLC (Dynamax, reverse phase, standard conditions), and freeze dried to yield a yellow oil (0.0232g, 0.032mmol, 70%); R_t = 19min. observed at λ = 254nm; Mass found 710.4123 $C_{38}H_{55}N_5O_8$ Requires 710.4129 ; ν_{max} (film) 3336, 2982, 1732vs, 1644s, 1538, 1448, 1381, 1304, 1201vs, 1026, 800 and 709cm^{-1}; *m/z* (DCI) 710 (M^++1), 624, 277, 248, 174, 148 and 122; δ_H ($CDCl_3$) 7.81 (4H, m, Ar), 7.45 (6H, m, Ar), 4.20 (2H, q, *J* = 5Hz, CH_2CH_3), 4.17 (4H, q, *J* = 5Hz, CH_2CH_3), 4.0-2.9 (20H, m, CH_2N, CHN), 2.10-1.65 (8H, br m, CH_2) and 1.29 (9H, m, CH_3); δ_C ($CDCl_3$) 134.2, 131.6, 128.6, 127.1(Ar), 61.7, 60.5 (CH_2O), 39.5, 33.7, 28.9, 22.0 (CH_2N, CH_2CO_2), 14.2 and 14.1 (CH_2, CH_3).

N-(2-(3-Aminopropyl)carboxymethyl)-N'-N''-bis-(carboxymethyl)-1,4,7-triazacyclononane **(101)**

(2-(N-Benzoyl-3-aminopropyl)ethoxycarbonylmethyl)-N'-N''-bis-(ethoxycarbonylmethyl)-1,4,7-triazacyclononane **(99)** (0.1g, 0.18mmol) was heated to reflux in 6M HCl (15cm^3) for 3 days. The solvent was removed under reduced pressure, the resulting glass was taken up in H_2O and washed with Et_2O (3 x 5cm^3) and evaporated to yield a brown glassy solid (0.066g, 0.18mmol, quant.); *m/z* (FAB) 361 (M^++1), 303, 277, 246, 255 and 207; ν_{max} (film) 2922, 1725.8vs, 1413, 1210; δ_H (D_2O) 3.95 (4H, s, CH_2CO), 3.9-3.0 (15H, m, CH_2N, CHCO) and 2.1-1.7 (4H, m, CH_2); δ_C (D_2O) 178.1, 174.6 (CO), 69.6, 66.9, 62.1, 58.5, 53.8, 49.0, 41.9, 28.1 and 27.2.

N,N'-Bis(2-(3-aminopropyl)carboxymethyl)-N''-carboxymethyl-1,4,7-triazacyclononane **(102)**

N,N'-Bis(2-(N-benzoyl-3-aminopropyl)ethoxycarbonylmethyl)-N''-ethoxycarbonylmethyl-1,4,7-triazacyclononane **(100)** (0.023g, 0.027mmol) was treated using an analogous method to the synthesis of **(101)** to yield a brown glass (0.011g, 0.027mmol); ν_{max} (film) 2972s, 1731vs, 1415 and 1216; δ_H (D_2O) 4.17 (2H, s, CH_2CO), 3.91 (2H, m, $CHCO_2$), 3.25-2.9 (16H, m, CH_2N) and 2.1-1.6 (8H, m, CH_2).

N-[2-(3-Amidopropyl (p-nitrophenyl carboxyethyl) carboxymethyl)]-1,4,7-triazacyclononane **(103)**

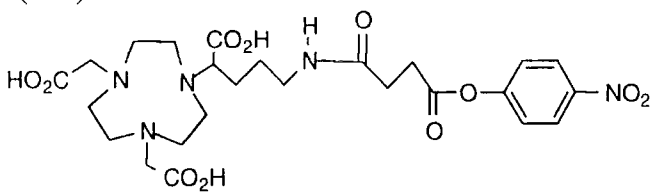

To N-(2-(3-aminopropyl)carboxymethyl)-N'-N''-bis-(carboxymethyl)-1,4,7-triazacyclononane **(101)** (0.0943g, 0.238mmol) in DMSO (0.5cm^3) was added solid bis-ester **(81)** (0.214g, 0.595mmol) and N-methyl morpholine (0.168g, 0.18cm^3, 1.6mmol). The mixture was stirred thoroughly at R.T. for 30mins and then purified using semi preparative HPLC: R_t=13.8mins, observed at λ = 278nm (Dynamax, reverse phase) with gradient elution 10 cm^{3}min^{-1}; A = H_2O/0.1% TFA, B = MeCN/0.1% TFA from t=0 min; A = 90%, B = 10%; to t = 20 mins., A = 25%, B = 75% to yield a yellow brown oil (0.1254g, 0.216mmol, 90%); ν_{max} (KBr disc) 3420, 2937, 2870, 1762vs, 1654vs, 1525s, 1349, 1204vs, 1132vs, 1010, 865, 798, 720 and 668; *m/z* (FAB) 582.4 (M^+); δ_H (D_2O) 8.30 (2H, d, *J* = 9.2, Ar), 7.33 (2H, d, *J* = 9.1Hz,Ar), 3.90-3.55 (9H, m, CH_2CO_2, CH_2CO), 3.55-2.80 (12H, m, CH_2N ring), 2.67 (2H, t, *J* = 5Hz, CH_2N) and 1.65 (4H, ,m, CH_2); δ_C (D_2O) 185.4, 177.2, 176.56, 175.9, 173.6 (CO), 158.0 (q), 148.4 (q), 128.5, 125.7 (Ar), 66.7, 58.7, 56.1, 53.1 (CH_2CO and CHCO), 52.1, 49.1, 41.7, 46.1 (CH_2N), 33.0 and 32.3 (CH_2).

N,N'-Bis-[2-(3-amidopropyl(p-nitrophenyl carboxyethyl)) carboxymethyl]-N''-carboxymethyl-1,4,7-triazacyclononane **(104)**

To N,N'-bis(2-(3-aminopropyl)carboxymethyl)-N''-carboxymethyl-1,4,7-triazacyclononane **(102)** (0.011g, 0.027mmol) in DMSO (0.5cm^3) was added solid bis ester **(81)** (0.025g, 0.068mmol) and N-methyl morpholine (0.019g, 0.02cm^3, 0.19mmol). The mixture was stirred thoroughly at room temperature for 30mins and then purified using HPLC: R_t=17mins, observed at λ = 278nm (Dynamax, reverse phase) with gradient elution 10 cm^{3}min^{-1}; A = H_2O/0.1% TFA, B = MeCN/0.1% TFA from t=0 min; A = 90%, B = 10%; to t = 20 mins., A = 25%, B = 75%. The resulting brown mixture was taken up in H_2O (3cm^3) and washed with Et_2O (3 x 5cm^3) to remove excess p-nitrophenol, the aqueous layer was freeze dried to yield a yellow brown oil (6.4mg, 0.0075mmol, 28%); ν_{max} (film) 3018vs, 1722vs, 1633s, 1593s, 1515, 1499, 1453vs, 1288, 1236, 1170, 1112, 1007, 853 and 754; δ_H (D_2O) 8.17 (4H, d, *J* = 8Hz, Ar), 7.2 (4H, d, *J* = 8Hz, Ar), 3.9-3.25 (12H, m, CH_2CO, CHCO, CH_2CONH), 3.25-2.8 (12H, m, ring), 2.5 (4H, t, *J* = 9Hz, CH_2N) and 1.9-1.4 (8H, m, CH_2).

9N3 tuftsin conjugate(**105**)

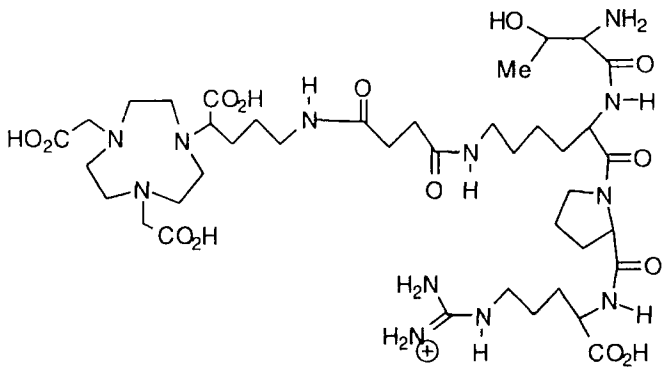

To the active ester (**103**) (0.062g, 0.11mmol) in $(CD_3)_2SO$ (1cm^3) was added a solid sample of tuftsin (0.13mmol, 70mg). The mixture was mixed thoroughly at R.T. for 3 hours, after this time some brown precipitate formed. ^{1}H NMR analysis revealed that the solution consisted of only p-nitrophenol and excess tuftsin. The solid was washed with DMSO (3x 1cm^3) and dried under reduced pressure to yield a brown oily solid (13.9mg, 0.015mmol, 13%); *m/z* (FAB) 944 (M+H), 922, 645, 459, 367, 275 and 186; *m/z* (Electrospray) 943.2 $(M+H)^+$; ν_{max} (film) 3405vs, 1633s, 1406, 1016, 952; δ_H (D_2O)4.6 (1H, br t, α-Lys), 4.35 (1H, br t, α-Pro), 4.05 (1H, br m, α-Arg, 4.00 (1H, t, β-Thr), 3.85 (1H, br m, δ-Pro), 3.65 (1H, br m, δ'-Pro), 3.6 (5H, m, CH_2CO_2), 3.54 (4H, m, CH_2CO), 3.5 (1H, m, α-Thr), 3.3-2.85 (12H, m, CH_2N ring; 2H, m, δ-Arg; 2H, m, ε-Lys), 2.65-2.4 (2H, m, CH_2N; 1H, m, β-Pro), 2.3 (1H, m, β'-Pro), 2.1-1.3 (2H, γ-Pro; 2H, β-Lys; 2H, β-Arg; 2H, δ-Lys; 2H, δ-Arg; 2H, γ-Lys; 4H, CH_2) and 1.21 (3H, d, J = 6Hz, γ-Thr).

6.5 CHAPTER FIVE EXPERIMENTAL

9-Acridine carbamoylethyl-2-[bis (2-aminoethyl)] amine(**113**)

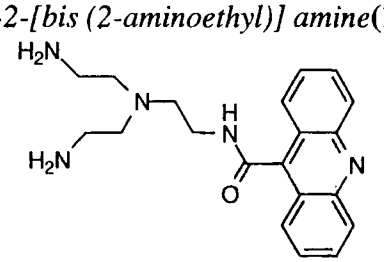

9-Acridine carboxylic acid (0.2g, 0.90mmol) was heated to reflux in thionyl chloride (1.5cm^3) for three hours until fully dissolved. The thionyl chloride was then removed under reduced pressure and the yellow acid chloride was dissolved in CH_2Cl_2 (2 x 1.5cm^3) and dried to remove all remaining $SOCl_2$. Tris (2-aminoethyl) amine (0.66g, 0.7cm^3, 4.5mmol) was stirred at 0°C and the freshly prepared acid chloride in CH_2Cl_2 (1cm^3) was added dropwise and allowed to stir and warm up to R.T. The resulting white suspension was basified (pH13) and extracted exhaustively into $CHCl_3$, the volume was reduced to give a yellow/brown solution which was purified using semi preparative

HPLC: R_t=8.8mins, observed at λ = 320nm ('Dynamax', reverse phase) with gradient elution. 10cm^{3}min^{-1}; A = H_2O/0.1% TFA, B = MeCN/0.1% TFA from t=0 min; A = 90%, B = 10%; to t = 20 mins., A = 10%, B = 90%; to yield a yellow oil (91.5mg, 0.26mmol, 23%); (Mass found 352.2121 $C_{20}H_{25}N_5O$ requires 352.2137); *m/z* (DCI) 352 (M^++1), 321, 180; ν_{max} (film) 3344, 2944, 1633, 1574, 1484, 1366, 1316, 1153, 868, 819 and 750cm^{-1}; δ_H (CD_3OD) 8.34 (6H, m, Ar), 7.94 (2H, t, *J* = 7Hz, Ar), 3.85 (2H, t, *J* = 7Hz, CH_2NHCO), 3.16 (4H, t, *J* = 5Hz, CH_2NH_2) and 2.95 (6H, m, CH_2N); δ_C (CD_3OD) 167.0(CO), 152.1 (CCO), 143.6, 138.0, 130.2, 130.1, 130.0, 124.3, 123.3 (Ar), 53.9, 52.6, 38.6 and 38.5 (CH_2N).

Bis [9-acridine carbomylethyl]- 2-(2-aminoethyl) amine **(114)**

Procedure as for **(113)**; purified using semi preparative HPLC: R_t=10mins, observed at λ = 320nm ('Dynamax', reverse phase) with gradient elution. 10 cm^{3}min^{-1}; A = H_2O/0.1% TFA, B = MeCN/0.1% TFA from t=0 min; A = 90%, B = 10%; to t = 20 mins., A = 10%, B = 90%; to yield a yellow oil (0.0533g, 0.096mmol, 10%); *m/z* (DCI) 559 (M^++1),516, 447, 354, 335, 321 and 180; ν_{max} (film) 3411, 3233, 3062, 1680vs, 1550, 1467, 1433, 1202vs, 1132vs, 836, 800, 756 and 722cm^{-1}; δ_H (CD_3OD) 8.25 (12H, m, Ar), 7.88 (4H, t, *J* = 7.5Hz, Ar), 3.91 (4H, t, *J* = 6Hz, CH_2NHCO), 3.17 (6H, t, *J* = CH_2N) and 2.85 (2H, t, CH_2NH_2); δ_C (CD_3OD) 167.8(CO), 152.8 (CCO), 143.8, 137.6, 130.0, 128.0, 124.1, 123.6 (Ar), 54.8, 52.6, 39.2 and 38.4 (CH_2N).

9-Acridine carbamoylethyl-2-(2-aminoethyl)-2-methyl amine **(117)**

9-Acridine carboxylic acid chloride was formed in the method of **(113)**. N^2-methyldiethylenetriamine (0.59g, 0.65cm^3, 5mmol) was stirred at 0°C with DMAP (5mg), a solution of the acid chloride (0.9mmol) in CH_2Cl_2 was added dropwise and then allowed to warm up to R.T overnight. The resulting white suspension was basified (pH13) and extracted exhaustively with $CHCl_3$, evaporated and the excess triamine removed by Kugelrohr distillation. The resulting brown oil was purified by HPLC: R_t=8.3 mins, observed at λ = 320nm ('Dynamax', reverse phase) with gradient elution. 10 cm^{3}min^{-1}; A = H_2O/0.1% TFA, B = MeCN/0.1% TFA from t=0 min; A = 90%, B = 10%; to t = 20 mins., A = 10%, B = 90%; to yield a yellow oil (0.182g, 0.57mmol, 63%); *m/z* (DCI) 530, 419, 323 (M^++1), 280, 223, 180 and 85; *m/z*(FAB) 324, 249, 180, 118 and 93; ν_{max} (film) 3424vs, 3046, 2925, 2524, 1692, 1666vs, 1568, 1466, 1434, 1270, 1199vs, 1130vs, 1023, 976, 837, 799, 758 and 722cm^{-1} ; δ_H (CD_3OD) 8.29 (4H, m, Ar), 8.23 (2H, t, *J* = 7Hz, Ar), 7.87 (2H, t, *J* = 8Hz, Ar), 4.14 (2H, t, *J* = 6Hz, CH_2NHCO), 3.68 (4H, m, CH_2NMe), 3.54 (2H, t, *J* = 6Hz, CH_2NH_2) and 3.11 (3H, s, NCH_3) ; δ_C (CD_3OD) 167.7 (CO), 150.7 (CCO), 143.9 (q Ar), 137.5 (Ar), 130.1, 128.0 (Ar), 124.1 (q Ar), 123.7 (Ar), 56.9, 54.6, 41.8, 36.7 and 35.9.

N,N'-Bis[9-acridine carbamoylethyl]-2-N-methyl amine (**118**)

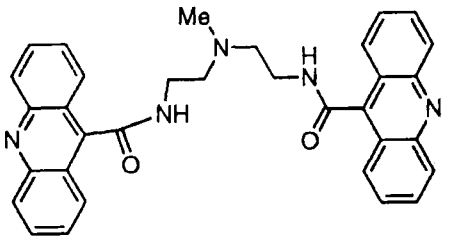

Procedure as for (**117**). The resulting mixture was purified by HPLC: R_t= 9.7 mins, observed at λ = 320nm ('Dynamax', reverse phase) with gradient elution. 10 cm^3min^{-1}; A = H_2O/0.1% TFA, B = MeCN/0.1% TFA from t=0 min; A = 90%, B = 10%; to t = 20 mins., A = 10%, B = 90%; to yield a yellow oil (0.0475g, 0.091mmol, 10%); *m/z* (DCI) 528 (M^++1), 323, 280, 249, 223, 205, 180 and 133; *m/z*(FAB) 528, 356, 249, 207, 180 and 93; ν_{max} (film) 3417, 1674vs, 1557, 1433, 1202vs, 1135vs, 800, 758 and 722cm^{-1}; δ_H (CD_3OD) 8.27 (8H, m, Ar), 8.10 (4H, t, *J* = 7Hz, Ar), 7.76 (4H, t, *J* = 7Hz, Ar), 4.20 (4H, t, *J* = 6Hz, CH_2N), 3.85 (4H, t, *J* = 6Hz, CH_2N) and 3.25 (3H, s, NMe); δ_C (CD_3OD) 168.5 (CO), 145.1 (CCO), 136.6, 129.9, 127.9, 124.9 (Ar), 56.9, 41.8 and 36.8 (CH_2N).

9-Acridine carbamoylethyl-2-(2-(p-nitrophenyl carboxyethyl) amidoethyl)-N-methyl amine (**119**)

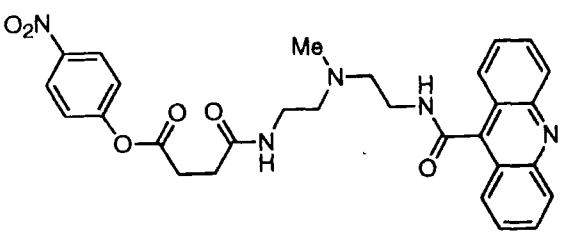

To acridine amine (**117**) (0.074g, 0.23mmol) in dry DMSO (0.5cm^3) was added bis p-nitrophenyl succinate (**81**) (0.247g, 0.69mmol) and N-methyl morpholine (0.046g, 0.05cm^3, 0.46 mmol) at R.T with vigorous mixing. Analytical HPLC revealed that reaction had taken place within a few minutes, the reaction mixture was then cooled to -78°C and only defrosted in portions for HPLC purification. R_t=13.7 mins, observed at λ = 353nm ('Dynamax', reverse phase) with gradient elution. 10 cm^3min^{-1}; A = H_2O/0.1% TFA, B = MeCN/0.1% TFA from t=0 min; A = 90%, B = 10%; to t = 20 mins., A = 25%, B = 75%; to t = 30 mins, A = 0%, B = 100%; to yield a yellow oil (0.0385g, 0.071mmol, 96%); *m/z* (Electrospray) 544, 437, 405, 280, 249, 180 and 126; ν_{max} (film) 3380, 1762, 1670vs, 1523s, 1430, 1348, 1202vs, 1129vs, 864, 834, 799, 753 and 720cm^{-1}; δ_H (CD_3OD) 8.17 (4H, m, Ar), 7.89 (2H+2H, m, Acridine + p-nitrophenol), 7.00 (2H, d,*J* = 9.2Hz, p-nitrophenol), 4.05 (2H, t, *J* = 5Hz, $CH_2NHCOAr$), 3.70 (4H, t, CH_2NMe), 3.51 (2H, t, CH_2NHCO), 3.11 (3H, s, NMe) and 2.69 (4H, m, CH_2O); δ_C (CD_3OD) 178.2 (CO), 175.4 (CO), 169.3 (CO), 157.3 (q

Ar), 151.7 (q Ar), 147.4 (q Ar), 142.7 (q Ar), 140.2 (q Ar), 131.8, 128.6, 127.6, 124.8 (2C), 122.8 (Ar), 59.2, 59.7, 43.3, 38.0, 37.3, 32.1 and 31.4.

6.6 REFERENCES

1. C.J. Broan, J.P.L. Cox, A.S. Craig, R. Kataky, D. Parker, A. Harrison, A. M. Randall and G. Ferguson, *J. Chem. Soc. Perkin Trans. 2*, 1991, 87.

2. J.H. Forsberg, V.T. Spaziano, T.M. Balasubramanian, G.K. Liu, S.A. Kinsley, C.A. Duckworth, J.J. Poteruca, P.S. Brown and J.L. Miller, *J. Org. Chem.*, 1987, **52**, 1017.

3. Synthesis carried out by P.K. Pulukkody.

4. D. Parker, P.K. Pulukkody, F.C. Smith, A. Batsanov and J.A.K. Howard, *J. Chem. Soc. Dalton. Trans.* 1994, 689.

5. I. Ahmed, I.J. Stratford and T.C. Jenkins, *Drug Res.*, 1985, **35(II)**, 1763

6. M.E. Perlman, J.A. Dunn, T.A. Piscitelli, J. Earle, W.C. Rose, G.L. Wampler, J.E. MacDiaarmid and T.J. Bardos, *J. Med. Chem.*, 1991, **34**, 1400.

7. I.M. Helps, D. Parker, K.J. Jankowski, J. Chapman and P.E. Nicholson, *J. Chem. Soc. Perkin Trans. 1*, 1989, 2079.

8. A.G. Beaman, W. Tautz and R. Duschinsky, *Antimicrobial Agents and Chemotherapy*, 1967, 520.

9. J.P.L. Cox, A.S. Craig, I.M. Helps, K.J.Jankowski, D. Parker, M.A.W. Eaton, A.T. Millican, K. Millar, N.R.A. Beeley and B.A. Boyce, *J. Chem. Soc. Perkin Trans. 1*, 1990, 2567.

10. K.P. Pulukkody, T.J. Norman, D. Parker, L. Royle and (in part) C.J. Broan, *J. Chem. Soc. Perkin Trans. 2*, 1993, 605.

11. J.C Eck and C.S. Marvel, *Org. Synth. Coll. Vol. 2*, 1943, 74.

Appendices

APPENDIX 1

FIRST YEAR COURSES

IONIC AND MOLECULAR RECOGNITION

MODERN NMR TECHNIQUES

NUCLEIC ACIDS

RESEARCH COLLOQUIA, SEMINARS AND LECTURES

Organised by the Department of Chemistry (August 1991 - July 1994)

1991

October 17th — Dr. J. A. Salthouse, University of Manchester.
Son et Lumière - A demonstration Lecture.

October 31st — Dr. R. Keeley, * Metropolitan Police Forensic Science.
Modern Forensic Science.

November 6th — Prof. B. F. G. Johnson,† University of Edinburgh.
Cluster - Surface Analogues.

November 7th — Dr. A. R. Butler, * University of St. Andrews.
Traditional Chinese Herbal drugs - a different way of treating disease.

November 13th — Prof. D. Gani,†* University of St. Andrews.
The chemistry of PLP-dependent Enzymes.

November 20th — Dr. M. More O' Ferrall,†* University College, Dublin.
Some Acid-Catalysed Rearrangements in Organic Chemistry.

November 28th — Prof. I. M. Ward, IRC in Polymer Science, University of Leeds.
The SCI Lecture - The Science and Technology of Orientated Polymers.

December 4th — Prof. R. Grigg,†* University of Leeds.
Palladium-Catalysed Cyclisation and Ion-Capture Process.

December 5th — Dr. A. L. Smith, ex Unilever.
Soap, Detergents and Black Puddings.

December 11th Dr. W. D. Cooper, Shell Research.
Colloid Science - Theory and Practice.

1992

January 22nd Dr. K. D. M. Harris,† * University of St. Andrews.
Understanding the Properties of Solid Inclusion Compounds.

January 29th Dr. A. Holmes,†* University of Cambridge.
Cycloaddition Reactions in the Service of the Synthesis of Piperidine and Indolizidine Natural Products.

January 30th Dr. M. Anderson, * Shell Research, Sittingborne.
Recent Advances in the Safe and Selective Control of Insect Pests.

February 12th Dr. D. E. Fenton,†* University of Sheffield.
Polynuclear Complexes of Molecular Clefts as Models for Copper Biosites.

February 13th Dr. J. Saunders, Glaxo Group Research Limited.
Molecular Modelling in Drug Discovery.

February 19th Prof. E. J. Thomas,†* University of Manchester.
Applications of Organostannanes to Organic Synthesis.

February 20th Prof. E. Vogel,* University of Cologne.
The Musgrave Lecture - Porphyrins - Molecules of Interdisciplinary Interest.

February 25th Prof. J. F. Nixon, University of Sussex.
The Tilden Lecture - Phosphaalkynes - New Building Blocks in Inorganic and Organometallic Chemistry.

February 26th Prof. M. L. Hitchmann,† University of Strathclyde.
Chemical Vapour Deposition.

March 5th Dr. N. C. Billingham, University of Sussex.
Degradable Plastics - Myth or Magic ?

March 5th Dr. S. E. Thomas,†* Imperial College.
Recent Advances in Organo-Iron Chemistry.

March 12th Dr. R. A. Hann, * ICI Imagedata.
Electronic Photography - An Image of the Future.

March 18th — Dr. H. Maskell,†* University of Newcastle.
Concerted or Stepwise Fragmentation in a Diamination Type Reaction.

April 7th — Prof D. M. Knight, Philosophy Department, University of Durham.
Interpreting Experiments - The Beginning of Electrochemistry.

May 13th — Dr. J-C. Gehret, * Ciba Geigy, Basel.
Some Aspects of Industrial Agrochemical Research.

October 15th — Dr. M. Glazer, Dr. S. Tarling, Oxford University & Birbeck College.
It Pays to be British ! - The Chemist's Role as an Expert Witness in Patent Litigation.

October 20th — Dr. H. E. Bryndza,* Du Pont Central Research.
Synthesis, Reactions and Thermochemistry of Metal (Alkyl) Cyanide Complexes and Their Impact on Olefin Hydrocyanation Catalysis.

October 22nd — Prof. A. Davies,* University College London.
The Ingold-Albert Lecture - The Behaviour of Hydrogen as a Pseudometal.

October 28th — Dr. J. K. Cockcroft, University of Durham.
Recent Developments in Powder Diffraction.

October 29th — Dr. J. Emsley, Imperial College, London.
The Shocking History of Phosphorus.

November 4th — Dr. T. P. Kee, University of Leeds.
Synthesis and Co-ordination Chemistry of Silylated Phosphites.

November 5th — Dr. C. J. Ludman,* University of Durham.
Explosions - A Demonstration Lecture.

November 11th — Prof. D. Robins,†* Glasgow University.
Pyrrolizidine Alkaloids - Biological Activity, Biosynthesis and Benefits.

November 12th — Prof. M. R. Truter, * University College, London.
Luck and Logic in Host - Guest Chemistry.

November 18th — Dr. R. Nix,† Queen Mary College, London.
Characterisation of Heterogeneous Catalysts.

November 25th — Prof. Y. Vallee. University of Caen.
Reactive Thiocarbonyl Compounds.

November 25th Prof. L. D. Quin,† University of Massachusetts, Amherst.
Fragmentation of Phosphorous Heterocycles as a Route to Phosphoryl Species with Uncommon Bonding.

November 26th Dr. D. Humber, Glaxo, Greenford.
AIDS - The Development of a Novel Series of Inhibitors of HIV.

December 2nd Prof. A. F. Hegarty, University College, Dublin.
Highly Reactive Enols Stabilised by Steric Protection.

December 2nd Dr. R. A. Aitken,†* University of St. Andrews.
The Versatile Cycloaddition Chemistry of $Bu_3P.CS_2$.

December 3rd Prof. P. Edwards, Birmingham University.
The SCI Lecture - What is Metal ?

December 9th Dr. A. N. Burgess,† ICI Runcorn.
The Structure of Perfluorinated Ionomer Membranes.

1993

January 20th Dr. D. C. Clary,† University of Cambridge.
Energy Flow in Chemical Reactions.

January 21st Prof. L. Hall, * Cambridge.
NMR - Window to the Human Body.

January 27th Dr. W. Kerr,* University of Strathclyde.
Development of the Pauson-Khand Annulation Reaction : Organocobalt Mediated Synthesis of Natural and Unnatural Products.

January 28th Prof. J. Mann,* University of Reading.
Murder, Magic and Medicine.

February 3rd Prof. S. M. Roberts, * University of Exeter.
Enzymes in Organic Synthesis.

February 10th Dr. D. Gillies, † University of Surrey.
NMR and Molecular Motion in Solution.

February 11th Prof. S. Knox,* Bristol University.
The Tilden Lecture - Organic Chemistry at Polynuclear Metal Centres.

February 17th Dr. R. W. Kemmitt,† University of Leicester.
Oxatrimethylenemethane Metal Complexes.

February 18th Dr. I. Fraser, * ICI Wilton.
Reactive Processing of Composite Materials.

February 22nd Prof. D. M. Grant, University of Utah.
Single Crystals, Molecular Structure, and Chemical-Shift Anisotropy.

February 24th Prof. C. J. M. Stirling,†* University of Sheffield.
Chemistry on the Flat-Reactivity of Ordered Systems.

March 10th Dr. P. K. Baker, University College of North Wales, Bangor.
Chemistry of Highly Versatile 7-Coordinate Complexes.

March 11th Dr. R. A. Y. Jones, University of East Anglia.
The Chemistry of Wine Making.

March 17th Dr. R. J. K. Taylor,†* University of East Anglia.
Adventures in Natural Product Synthesis.

March 24th Prof. I. O. Sutherland,†* University of Liverpool.
Chromogenic Reagents for Cations.

May 13th Prof. J. A. Pople, Carnegie-Mellon University, Pittsburgh, USA.
The Boys-Rahman Lecture - Applications of Molecular Orbital Theory.

May 21st Prof. L. Weber, University of Bielefeld.
Metallo-phospha Alkenes as Synthons in Organometallic Chemistry.

June 1st Prof. J. P. Konopelski, University of California, Santa Cruz.
Synthetic Adventures with Enantiomerically Pure Acetals.

June 2nd Prof. F. Ciardelli, University of Pisa.
Chiral Discrimination in the Stereospecific Polymerisation of Alpha Olefins.

June 7th Prof. R. S. Stein, University of Massachusetts.
Scattering Studies of Crystalline and Liquid Crystalline Polymers.

June 16th Prof. A. K. Covington, * University of Newcastle.
Use of Ion Selective Electrodes as Detectors in Ion Chromatography.

June 17th Prof. O. F. Nielsen, H. C. Ørsted Institute, Copenhagen University.
Low-Frequency IR and Raman Studies of Hydrogen Bonded Liquids.

September 13th Prof. Dr. A. D. Schlüter, Freie Universität Berlin.
Synthesis and Characterisation of Molecular Rods and Ribbons.

September 13th Dr. K. J. Wynne, Office of Naval Research, Washington.
Polymer Surface Design for Minimal Adhesion.

September 14th Prof. J. M. DeSimone, University of North Carolina, Chapel Hill.
Homogeneous and Heterogeneous Polymerisations in Environmentally Responsible Carbon Dioxide.

September 28th Prof. H. Ila,* North Eastern Hill University, India.
Synthetic Strategies for Cyclopentanoids via Oxoketene Dithioacetals.

October 4th Prof. F. J. Feher,† University of California, Irvine.
Bridging the Gap Between Surfaces and Solution with Sessilquioxanes.

October 14th Dr. P. Hubberstey, Nottingham University.
Alkali Metals - Alchemist's Nightmare, Biochemist's Puzzle and Technologist's Dream.

October 20th Dr. P. Quayle,†* University of Manchester.
Aspects of Aqueous ROMP Chemistry.

October 21st Prof. R. Adams,†* University of South Carolina.
Chemistry of Metal Carbonyl Cluster Complexes - Development of Cluster Based Alkyne Hydrogenation Catalysts.

October 27th Dr. R. A. L. Jones,†* Cavendish Laboratory.
Perambulating Polymers.

November 10th Prof. M. N. R. Ashfold,† University of Bristol.
High Resolution Photofragment Translational Spectroscopy : A New Way to Watch Photodissociation.

November 17th Dr. A. Parker,†*Laser Support Facility, RAL.
Applications of Time Resolved Resonance Raman Spectroscopy to Chemical and Biochemical Problems.

November 24th Dr. P. G. Bruce,†* University of St. Andrews.
Structure and Properties of Inorganic Solids and Polymers.

November 25th Dr. R. P. Wayne, Oxford University.
The Origin and Evolution of the Atmosphere.

December 1st Prof. M. A. McKervey,†* Queen's University, Belfast.
Synthesis and Applications of Chemically Modified Calixarenes.

December 8th Prof. O. Meth-Cohan,†* University of Sunderland.
Friedel's Folly Revisited - A Super Way to Fused Pyridines.

December 16th Prof. R. F. Hudson, University of Kent.
Close Encounters of the Second Kind.

1994

January 26th Prof. J. Evans,† University of Southampton.
Shining Light on Catalysts.

February 2nd Dr. A. Masters,† University of Manchester.
Modelling Water Without Using Pair Potentials.

February 9th Prof. D. Young,† University of Sussex.
Chemical and Biological Studies on the Coenzyme Tetrahydrofolic Acid.

February 16th Prof. K. H. Theopold, University of Delaware, USA.
Paramagnetic Chromium Alkyls - Synthesis and Reactivity.

February 23rd Prof. P. M. Maitlis,† University of Sheffield.
Across the Border : From Homogeneous to Heterogeneous Catalysis.

March 2nd Dr. C. Hunter,†* University of Sheffield.
Non Covalent Interactions Between Aromatic Molecules.

March 9th Prof. F. Wilkinson, Loughborough University of Technology.
Nanosecond and Picosecond Laser Flash Photolysis.

March 10th Prof. S. V. Ley,* University of Cambridge.
New Methods for Organic Synthesis.

March 25th Dr. J. Dilworth,* University of Essex.
Technetium and Rhenium Compounds with Applications as Imaging Agents.

Apil 28th Prof. R. J. Gillespie, * McMaster University, Canada.
The Molecular Structure of some Metal Fluorides and Oxofluorides - Apparent Exceptions to the VSEPR Model.

May 12th Prof. D. A. Humphreys, * McMaster University, Canada.
Bringing Knowledge to Life.

† Invited specially for the graduate training programme. *Author's attendance.

CONFERENCES ATTENDED

1. Stereochemistry at Sheffield, University of Sheffield. December 18th 1991

2. North East Graduate Symposium, University of Durham. April 3rd 1992

3. R.S.C. U.K. Macrocycles Group, University of Oxford. January 6th - 7th 1993

4. International Symposium on Metal Ions in Solution.* South Africa April 20th - 23rd 1993

5. North of England Cancer Research Campaign Meeting * University of Newcastle. July 21st 1993

6. Stereochemistry at Sheffield, University of Sheffield. December 15th 1993

7. North East Graduate Symposium, University of Northumberland. April 12th 1994

8. North of England Cancer Research Campaign Meeting * University of Newcastle. July 26th 1994

* Poster presented

PUBLICATIONS

1. D. Parker, K. Pulukkody, F.C. Smith, A. Batsanov and J.A.K. Howard, *J.Chem. Soc. Dalton Trans.*, 1994, 689.

2. T. J. Norman, F. C. Smith, D. Parker, A. Harrison, L. Royle, and C. A. Walker, *Supramolecular Chem.*, 1995, **4**, 305-308.

3. A. Harrison, C.A. Walker, K.A. Pereira, C. Counsell, D. Parker, L. Royle, R.C. Matthews, A.S. Craig and F.C. Smith, *Nucl. Med. Commun.*, 1995, in preparation.

APPENDIX 2

STRUCTURE DETERMINATION SUMMARY

CRYSTAL DATA

Empirical Formula

$C_{28}H_{34}N_5O_{12}Y$

Color; Habit

light-yellow bulk

Crystal Size (mm)	0.12 X 0.30 X 0.50
Crystal System	Triclinic
Space Group	$P\bar{1}$
Unit Cell Dimensions	$\underline{a}$ = 10.872(16) Å
	$\underline{b}$ = 11.200(16) Å
	$\underline{c}$ = 15.72(3) Å
	$\underline{\alpha}$ = 87.74(14)°
	$\underline{\beta}$ = 74.44(13)°
	$\underline{\gamma}$ = 61.67(10)°
Volume	1614(5) $Å^3$
Z	2
Formula Weight	721.5
Density(calc.)	1.484 Mg/m^3
Absorption Coefficient	1.875 mm^{-1}
F(000)	744

SOLUTION AND REFINEMENT

System Used	Siemens SHELXTL PLUS (VMS)
Solution	Direct Methods
Refinement Method	Full-Matrix Least-Squares
Quantity Minimized	$\Sigma w(F_o - F_c)^2$
Absolute Structure	N/A
Extinction Correction	N/A
Hydrogen Atoms	Riding model, fixed isotropic U
Weighting Scheme	$w^{-1} = \sigma^2(F) + 0.0010F^2$
Number of Parameters Refined	320
Final R Indices (obs. data)	R = 10.32 %, wR = 13.12 %
R Indices (all data)	R = 13.58 %, wR = 13.81 %
Goodness-of-Fit	3.19
Largest and Mean Δ/σ	0.008, 0.001
Data-to-Parameter Ratio	7.2:1
Largest Difference Peak	1.70 eA^{-3}
Largest Difference Hole	-1.99 eA^{-3}

DATA COLLECTION

Diffractometer Used	Siemens R3m/V
Radiation	MoKα (λ = 0.71073 Å)
Temperature (K)	120
Monochromator	Highly oriented graphite crystal
2θ Range	5.0 to 45.0°
Scan Type	2θ-θ
Scan Speed	Variable; 3.00 to 8.00°/min. in
Scan Range (ω)	1.60° plus Kα-separation
Background Measurement	Stationary crystal and stationary counter at beginning and end of scan, each for 25.0% of total scan time
Standard Reflections	3 measured every 150 reflections
Index Ranges	$-11 \leq h \leq 10$, $-10 \leq k \leq 0$ $-16 \leq l \leq 16$
Reflections Collected	3173
Independent Reflections	2965 (R_{int} = 6.67%)
Observed Reflections	2300 ($F \geq 4.0\sigma(F)$)
Absorption Correction	N/A

TABLE 1: Atomic coordinates ($x10^4$) and equivalent isotropic displacement coefficients ($Å^2 \times 10^3$)

	x	y	z	U(eq)
Y	2320(1)	1789(1)	2956(1)	20(1)
O(1)	-23(10)	2746(10)	2791(7)	30(5)
O(2)	3048(10)	178(10)	1787(7)	25(5)
O(3)	3052(11)	-1413(11)	970(7)	31(5)
O(4)	2864(10)	2698(9)	1614(6)	22(5)
O(5)	3600(10)	2325(10)	3710(7)	29(5)
O(6)	5592(10)	2281(10)	3888(6)	29(5)
O(7)	1140(10)	1936(10)	4462(6)	25(5)
O(8)	1326(10)	1499(10)	5833(7)	30(5)
O(1W)	1115(10)	4209(10)	3345(6)	28(5)
N(1)	3751(11)	-361(11)	3651(8)	23(6)
N(2)	1026(12)	167(12)	3210(8)	24(6)
N(3)	-2340(13)	3129(12)	3188(8)	31(7)
N(4)	5103(12)	746(11)	2119(7)	24(6)
N(5)	4052(13)	2310(12)	168(8)	28(6)
C(1)	3362(14)	-1388(14)	3525(10)	25(7)
C(2)	1695(15)	-873(14)	3766(10)	27(7)
C(3)	-524(16)	1094(14)	3624(11)	31(8)
C(4)	-962(16)	2382(15)	3146(11)	29(8)
C(5)	-2961(17)	4472(16)	2857(12)	45(9)
C(6)	5378(15)	-896(15)	3271(10)	29(7)
C(7)	5815(17)	-746(14)	2281(10)	30(8)
C(8)	5332(14)	854(14)	1147(9)	22(7)
C(9)	3980(16)	2035(14)	998(10)	24(8)
C(10)	2864(14)	3412(14)	-98(10)	25(7)
C(11)	-3801(10)	4493(12)	2245(6)	32(4)
C(12)	-5318	5185	2567	48(5)
C(13)	-6163	5258	2017	70(6)
C(14)	-5491	4640	1146	62(6)
C(15)	-3974	3949	824	61(5)
C(16)	-3129	3875	1374	49(5)

C(17)	1209(14)	-463(15)	2347(9)	26(7)
C(18)	2587(15)	-605(18)	1632(10)	30(8)
C(19)	3328(15)	56(14)	4627(9)	28(8)
C(20)	1823(15)	1255(14)	5011(10)	22(8)
C(21)	1827(10)	3009(10)	-332(6)	28(4)
C(22)	1588	1968	55	33(4)
C(23)	628	1634	-175	48(5)
C(24)	-93	2341	-793	51(5)
C(25)	145	3382	-1181	47(5)
C(26)	1106	3716	-951	42(4)
C(27)	5746(16)	1469(14)	2463(10)	27(8)
C(28)	4919(17)	2035(14)	3427(11)	30(8)
O(2W)	8532(18)	4265(17)	5416(10)	96(5)
O(3W)	1686(21)	3665(21)	6335(12)	122(6)
O(4W)A	3666(25)	4202(24)	5202(14)	71(7)
O(4W)B	4419(32)	4834(30)	4789(19)	53(8)

* Equivalent isotropic U defined as one third of the trace of the orthogonalized U_{ij} tensor

TABLE 2: Bond Lengths (Å)

Y-O(1)	2.334 (12)	Y-O(2)	2.320 (11)
Y-O(4)	2.360 (11)	Y-O(5)	2.332 (14)
Y-O(7)	2.341 (10)	Y-O(1W)	2.402 (11)
Y-N(1)	2.562 (12)	Y-N(2)	2.739 (16)
Y-N(4)	2.624 (12)	O(1)-C(4)	1.262 (23)
O(3)-C(18)	1.256 (26)	O(3)-C(18)	1.232 (20)
O(4)-C(9)	1.238 (14)	O(5)-C(28)	1.259 (20)
O(6)-C(28)	1.276 (25)	O(7)-C(20)	1.278 (19)
O(8)-C(20)	1.244 (18)	N(1)-C(1)	1.437 (24)
N(1)-C(6)	1.517 (18)	N(1)-C(19)	1.503 (19)
N(2)-C(2)	1.452 (19)	N(2)-C(3)	1.464 (16)
N(3)-C(17)	1.475 (21)	N(3)-C(4)	1.307 (19)
N(3)-C(5)	1.468 (20)	N(4)-C(7)	1.517 (18)
N(4)-C(8)	1.489 (18)	N(4)-C(27)	1.487 (26)
N(5)-C(9)	1.319 (19)	N(5)-C(10)	1.451 (18)
C(1)-C(2)	1.555 (21)	C(3)-C(4)	1.525 (22)
C(5)-C(11)	1.486 (25)	C(6)-C(7)	1.529 (21)
C(8)-C(9)	1.510 (19)	C(10)-C(21)	1.525 (23)
C(17)-C(18)	1.554 (21)	C(19)-C(20)	1.514 (16)
C(27)-C(28)	1.520 (21)		

TABLE 3: Bond Angles (°)

O(1)-Y-O(2)	87.3(4)	O(1)-Y-O(4)	84.8(4)
O(2)-Y-O(4)	71.7(4)	O(1)-Y-O(5)	138.7(3)
O(2)-Y-O(5)	133.0(3)	O(4)-Y-O(5)	98.6(4)
O(1)-Y-O(7)	84.3(4)	O(2)-Y-O(7)	130.8(4)
O(4)-Y-O(7)	154.2(3)	O(5)-Y-O(7)	75.1(4)
O(1)-Y-O(1W)	71.1(4)	O(2)-Y-O(1W)	141.7(4)
O(4)-Y-O(1W)	75.1(3)	O(5)-Y-O(1W)	70.2(4)
O(7)-Y-O(1W)	79.3(3)	O(1)-Y-N(1)	130.9(4)
O(2)-Y-N(1)	81.4(4)	O(4)-Y-N(1)	134.3(3)
O(5)-Y-N(1)	73.6(4)	O(7)-Y-N(1)	68.7(3)
O(1W)-Y-N(1)	136.6(4)	O(1)-Y-N(2)	63.3(4)
O(2)-Y-N(2)	63.5(4)	O(4)-Y-N(2)	124.8(4)
O(5)-Y-N(2)	135.4(4)	O(7)-Y-N(2)	69.5(4)
O(1W)-Y-N(2)	126.2(3)	N(1)-Y-N(2)	68.9(4)
O(1)-Y-N(4)	145.1(4)	O(2)-Y-N(4)	67.8(4)
O(4)-Y-N(4)	64.8(3)	O(5)-Y-N(4)	66.6(4)
O(7)-Y-N(4)	130.5(4)	O(1W)-Y-N(4)	113.6(4)
N(1)-Y-N(4)	71.1(4)	N(2)-Y-N(4)	120.0(4)
Y-O(1)-C(4)	125.5(9)	Y-O(2)-C(18)	133.5(8)
Y-O(4)-C(9)	122.3(9)	Y-O(5)-C(28)	126.1(11)
Y-O(7)-C(20)	122.3(8)	Y-N(1)-C(1)	110.5(9)
Y-N(1)-C(6)	110.8(9)	C(1)-N(1)-C(6)	111.0(10)
Y-N(1)-C(19)	106.4(7)	C(1)-N(1)-C(19)	109.3(12)
C(6)-N(1)-C(19)	108.7(12)	Y-N(2)-C(2)	108.5(11)
Y-N(2)-C(3)	105.1(10)	C(2)-N(2)-C(3)	113.3(11)
Y-N(2)-C(17)	109.9(9)	C(2)-N(2)-C(17)	110.6(11)
C(3)-N(2)-C(17)	109.3(13)	C(4)-N(3)-C(5)	124.3(16)
Y-N(4)-C(7)	106.6(9)	Y-N(4)-C(8)	110.9(8)
C(7)-N(4)-C(8)	109.4(10)	Y-N(4)-C(27)	110.4(7)
C(7)-N(4)-C(27)	110.8(12)	C(8)-N(4)-C(27)	108.8(13)
C(9)-N(5)-C(10)	123.6(10)	N(1)-C(1)-C(2)	114.7(11)

N(2)-C(2)-C(1)	111.0(13)	N(2)-C(3)-C(4)	107.9(13)
O(1)-C(4)-N(3)	122.4(14)	O(1)-C(4)-C(3)	119.6(14)
N(3)-C(4)-C(3)	117.7(16)	N(3)-C(5)-C(11)	109.7(16)
N(1)-C(6)-C(7)	112.6(13)	N(4)-C(7)-C(6)	110.5(10)
N(4)-C(8)-C(9)	108.9(9)	O(4)-C(9)-N(5)	121.8(13)
O(4)-C(9)-C(8)	122.3(13)	N(5)-C(9)-C(8)	115.9(11)
N(5)-C(10)-C(21)	114.4(13)	C(5)-C(11)-C(12)	117.5(6)
C(5)-C(11)-C(16)	122.5(6)	N(2)-C(17)-C(18)	111.8(15)
O(2)-C(18)-O(3)	127.8(15)	O(2)-C(18)-C(17)	115.2(13)
O(3)-C(18)-C(17)	116.9(18)	N(1)-C(19)-C(20)	115.9(12)
O(7)-C(20)-O(8)	124.5(10)	O(7)-C(20)-C(19)	117.2(12)
O(8)-C(20)-C(19)	118.3(13)	C(10)-C(21)-C(22)	121.8(7)
C(10)-C(21)-C(26)	118.2(7)	N(4)-C(27)-C(28)	110.3(14)
O(5)-C(28)-O(6)	123.6(14)	O(5)-C(28)-C(27)	119.4(17)
O(6)-C(28)-C(27)	116.8(15)		

TABLE 4: Anisotropic displacement coefficients ($Å^2 \times 10^3$)

	U_{11}	U_{22}	U_{33}	U_{12}	U_{13}	U_{23}
Y	13(1)	21(1)	39(1)	-16(1)	-12(1)	3(1)
O(1)	28(6)	30(6)	49(7)	-24(5)	-20(5)	9(5)
O(2)	32(6)	29(6)	46(7)	-36(5)	-21(5)	10(5)
O(3)	31(6)	43(7)	31(6)	-29(6)	-6(5)	-6(6)
O(4)	23(6)	24(6)	35(6)	-21(5)	-13(5)	7(5)
O(5)	14(6)	32(6)	47(7)	-12(5)	-14(5)	1(5)
O(6)	20(5)	38(7)	42(6)	-23(5)	-12(5)	8(5)
O(7)	21(5)	30(6)	30(6)	-16(5)	-8(5)	-10(5)
O(8)	24(6)	36(6)	31(6)	-18(5)	-3(5)	-9(6)
O(1W)	27(6)	31(6)	38(6)	-23(5)	-9(5)	7(5)
N(1)	11(6)	23(7)	39(7)	-12(6)	-8(6)	3(6)
N(2)	15(6)	29(7)	39(8)	-20(6)	-7(6)	7(6)
N(3)	24(7)	29(8)	52(8)	-21(7)	-13(6)	8(7)
N(4)	27(7)	24(7)	29(7)	-18(6)	-9(6)	-3(6)
N(5)	27(7)	34(8)	35(8)	-25(7)	-9(6)	6(7)
C(1)	21(8)	24(9)	36(9)	-18(8)	-4(7)	1(8)
C(2)	25(8)	19(9)	46(10)	-13(8)	-18(8)	1(8)
C(3)	31(9)	27(9)	53(10)	-28(8)	-11(8)	10(8)
C(4)	30(9)	31(10)	54(10)	-30(9)	-24(8)	11(8)
C(5)	35(10)	31(10)	88(14)	-24(9)	-34(10)	21(10)
C(6)	24(8)	18(8)	39(9)	-7(7)	-5(7)	-7(8)
C(7)	38(9)	18(9)	37(9)	-19(8)	-5(8)	10(8)
C(8)	17(8)	29(9)	37(9)	-21(7)	-13(7)	1(8)
C(9)	30(9)	25(9)	23(8)	-22(8)	6(7)	-15(8)
C(10)	19(8)	18(8)	48(9)	-9(7)	-20(7)	-9(7)
C(17)	12(7)	40(10)	32(8)	-16(8)	-6(7)	-6(8)
C(18)	18(8)	48(11)	21(9)	-16(9)	1(7)	6(9)
C(19)	27(8)	29(9)	40(9)	-21(8)	-13(7)	-3(8)
C(20)	23(8)	22(9)	43(10)	-23(8)	-19(8)	1(8)
C(27)	31(9)	17(8)	46(10)	-21(8)	-15(8)	7(8)
C(28)	30(10)	16(8)	62(11)	-17(8)	-29(9)	12(8)

The anisotropic displacement factor exponent takes the form:

$-2\pi^2(h^2a^{*2}U_{11} + \ldots + 2hka^*b^*U_{12})$

TABLE 5: H-atom coordinates (x 10^4) and isotropic displacement coefficients ($Å^2$ x 10^3)

	x	y	z	U
H(3)	-2954	2800	3428	80
H(5)	4874	1771	-257	80
H(1A)	3775	-2109	3881	80
H(1B)	3787	-1764	2914	80
H(2A)	1509	-1616	3698	80
H(2B)	1262	-496	4376	80
H(3B)	-692	1311	4243	80
H(3C)	-1091	672	3568	80
H(5B)	-2178	4637	2539	80
H(5C)	-3572	5173	3343	80
H(6A)	5886	-1838	3371	80
H(6B)	5666	-394	3581	80
H(7A)	6853	-1128	2056	80
H(7B)	5517	-1237	1969	80
H(8A)	5516	24	855	80
H(8B)	6155	997	902	80
H(10A)	3261	3770	-597	80
H(10B)	2314	4126	384	80
H(12)	-5780	5610	3166	80
H(13)	-7207	5734	2238	80
H(14)	-6073	4691	768	80
H(15)	-3512	3523	225	80
H(16)	-2086	3399	1153	80
H(17A)	361	85	2152	80
H(17B)	1289	-1350	2418	80
H(19A)	4022	286	4736	80
H(19B)	3391	-711	4946	80
H(22A)	2085	1481	481	80
H(23A)	464	917	92	80
H(24A)	-754	2111	-952	80
H(25A)	-351	3868	-1607	80
H(26A)	1270	4433	-1218	80
H(27A)	5716	2198	2111	80
H(27B)	6748	841	2418	80